



Universiteit
Leiden
The Netherlands

Glucocorticoid modulation of the immune response: Studies in zebrafish

Xie, Y

Citation

Xie, Y. (2020, November 26). *Glucocorticoid modulation of the immune response: Studies in zebrafish*. Retrieved from <https://hdl.handle.net/1887/138400>

Version: Publisher's Version

License: [Licence agreement concerning inclusion of doctoral thesis in the Institutional Repository of the University of Leiden](#)

Downloaded from: <https://hdl.handle.net/1887/138400>

Note: To cite this publication please use the final published version (if applicable).

Cover Page



Universiteit Leiden



The handle <http://hdl.handle.net/1887/138400> holds various files of this Leiden University dissertation.

Author: Xie, Y.

Title: Glucocorticoid modulation of the immune response: Studies in zebrafish

Issue Date: 2020-11-26

Glucocorticoid modulation of the immune response

Studies in zebrafish

Yufei Xie

ISBN: 978-94-6421-102-3

Thesis cover and layout: Yufei Xie

Thesis printing: IPSKAMP Printing

©2020 Yufei Xie. All right reserved. No part of this thesis may be reproduced, stored in retrieval systems, or transmitted in any form or by any means without prior written permission of the author.



Research funded by China Scholarship Council (CSC)

Glucocorticoid modulation of the immune response

Studies in zebrafish

Proefschrift

ter verkrijging van
de graad van Doctor aan de Universiteit Leiden,
op gezag van Rector Magnificus prof.mr. C.J.J.M. Stolker,
volgens besluit van het College voor Promoties
te verdedigen op donderdag 26 november 2020
klokke 10:00 uur

door

Yufei Xie

geboren te Pingxiang, Jiangxi, China
in 1990

Promotores: Dr. Marcel J.M. Schaaf

Prof. dr. Annemarie H. Meijer

Promotiecommissie:

Prof. dr. Gilles van Wezel

Prof. dr. Herman Spaink

Prof. dr. Alexander Kros

Prof. dr. Karolien De Bosscher (Ghent University)

Dr. Maria Forlenza (Wageningen University and Research)

Table of contents

Chapter 1: Introduction	6
Chapter 2: Modeling inflammation in zebrafish for the development of anti-inflammatory drugs.....	24
Chapter 3: Glucocorticoids inhibit macrophage differentiation towards a pro-inflammatory phenotype upon wounding without affecting their migration.....	56
Chapter 4: Glucocorticoid treatment exacerbates mycobacterial infection by reducing the phagocytic capacity of macrophages	96
Chapter 5: Liposome encapsulation of prednisolone phosphate improves its therapeutic ratio in a zebrafish model for inflammation.....	122
Chapter 6: Summary and Discussion	148
Samenvatting.....	160
Curriculum vitae	164
List of Publications.....	165

Chapter 1

Introduction

Glucocorticoids and the Glucocorticoid Receptor

Glucocorticoids (GCs) are a class of steroid hormones secreted by the adrenal gland. The main endogenous GC hormone in humans is cortisol. Under basal conditions, the level of cortisol keeps a circadian rhythm, peaking in the morning when the diurnal activity phase starts [1, 2]. However, in response to stress, the secretion of cortisol can increase rapidly and this secretion is mainly regulated by the hypothalamic-pituitary-adrenal (HPA) axis [3]. Upon stress, corticotropin releasing hormone (CRH) is secreted by the hypothalamus and promotes the secretion of adrenocorticotrophic hormone (ACTH) in the pituitary, while ACTH in turn stimulates the secretion of cortisol from the adrenal gland [3, 4].

In most vertebrate organisms, GCs such as cortisol exert their function through an intracellular receptor, the Glucocorticoid Receptor (GR) [5]. Like all other steroid receptors, GR belongs the nuclear receptor family and acts as a ligand-activated transcription factor. A schematic overview of the molecular mechanism of GR action is presented in Figure 1. GR usually forms a heterocomplex with a variety of chaperone proteins, including heat shock proteins (hsps) and immunophilins. Its affinity to GCs is dependent on the conformation of the receptor which is induced by the complex in an ATP-dependent manner [6, 7]. Upon ligand binding, the GR heterocomplex translocates to the nucleus, and alterations in the chaperone protein composition of the complex play a fundamental role in GR nuclear import. The recognition of the nuclear location signal (NLS) by importins mediates the translocation across the nuclear pore complex (NPC) with microtubules supporting the movement of the complex [8]. In the nucleus, GR can, as a dimer, bind directly to glucocorticoid response elements (GREs) in the DNA and recruit coregulators, mainly leading to transcriptional activation of various genes, which is the most typical mechanism of transactivation [9-11]. In addition, GR can repress gene transcription when it binds to negative GREs (nGREs) [12]. Moreover, monomeric GRs interact with other transcription factors (like STAT, AP-1) by binding to “composite” response elements, resulting in a positive or negative transcriptional regulation, or tether to other transcription factors (like AP-1, NF- κ B and STAT) and interfere with their activity, thereby positively or negatively modulating the transcription of the genes regulated by these transcription factors [13]. Apart from these genomic effects, GR can also exert immediate and reversible nongenomic effects, regulating signal transduction cascades and cell function through cytosolic GR and membrane-bound GR, by directly influencing the fluidity and composition of membrane, or by interacting with membrane receptors and kinases [14, 15]. As a result, through activation of GR, GCs regulates a wide variety of systems in our body, such as the immune, metabolic, reproductive, cardiovascular and central nervous system, helping the body to cope with stress and maintain homeostasis [16, 17].

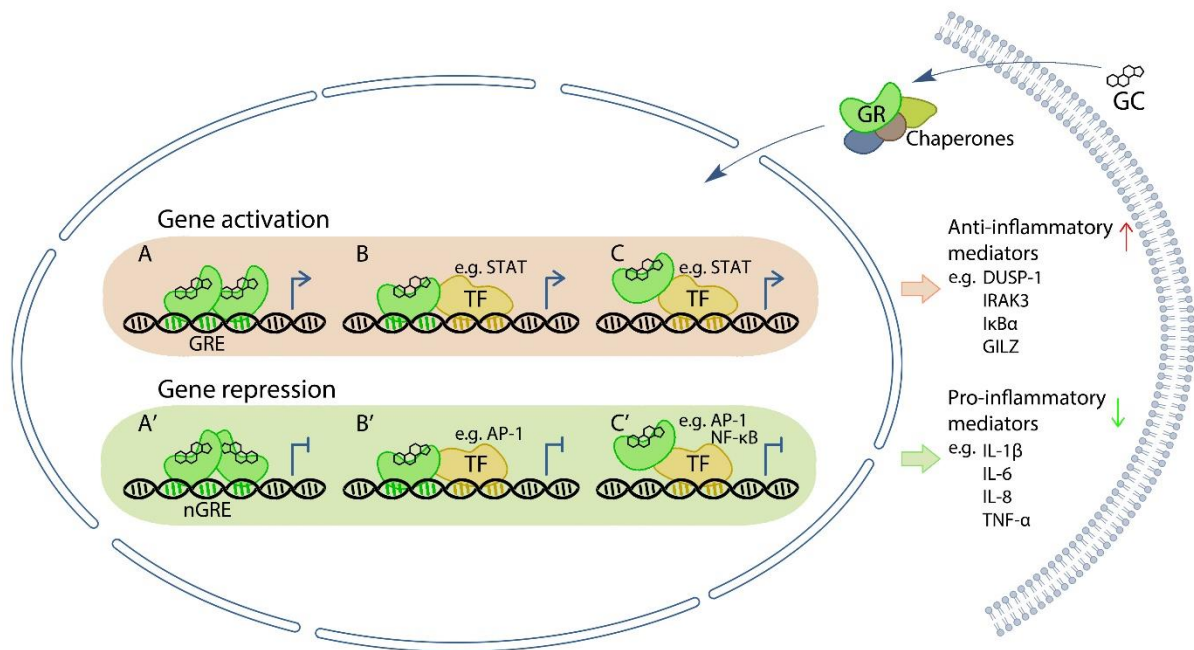


Figure 1. Molecular mechanisms underlying the anti-inflammatory action of glucocorticoids (GCs). GCs diffuse through the membrane freely and bind to the cytoplasmic glucocorticoid receptor (GR) complex, leading to a conformational change of the receptor and an alteration in the composition of the complex, allowing nuclear translocation. GR can activate and repress gene transcription through several mechanisms, including binding to glucocorticoid response elements (GREs) (A) or negative glucocorticoid response elements (nGREs) (A'), or by interaction with other TFs (B, B'), which may involve binding to composite elements or tethering (C, C'). As a result, the transcription of genes encoding anti-inflammatory proteins is upregulated, whereas the transcription of pro-inflammatory genes is downregulated.

Effects of GCs on the immune system

The vertebrate immune system consists of two major components. The first component is the innate immune system, which is composed of the surface barriers, innate leukocytes (such as phagocytes, mast cells, natural killer cells) and the complement system. The second component is the adaptive immune system, which is dependent on the recognition of specific antigens by T-cells and B-cells, and is able to generate memory cells [18]. When the body encounters harmful stimuli, such as invading pathogens, wounding or damage to cells, the immune system will be activated and an inflammatory response is triggered [19, 20]. This response is mainly induced by Pattern Recognition Receptors (PRRs) of the innate immune system, such as Toll-Like Receptors (TLRs), which recognize patterns in molecules frequently found in microbes (Pathogen-Associated Molecular Patterns (PAMPs)), or molecules released by damaged cells (Damage-Associated Molecular Patterns (DAMPs)). Subsequently, immune cells release pro-inflammatory cytokines, such as interleukin-1 β (IL-1 β) and tumor necrosis factor α (TNF- α), which in turn stimulate the synthesis and release of other inflammatory mediators, including chemokines and prostaglandins [19, 21]. Directed by the chemokine gradients, leukocytes migrate towards the inflamed site to deal with the damaged tissue or invading microbes [22, 23]. These

changes at the molecular level will lead to the five classical symptoms of inflammation: heat, pain, redness, swelling and loss of function. Normally, the inflammatory processes are actively terminated through functional reprogramming of the involved cells, which results in a restoration of homeostasis [19].

Generally, GCs exert anti-inflammatory effects on the immune system. Transcription factors downstream of the TLR signaling pathway, such as NF- κ B and AP-1, which are critical for the initiation of inflammation, can be inhibited by GCs, mainly through tethering mechanisms [13]. Moreover, GCs can upregulate the expression of inhibitors of TLR signaling, such as dual-specificity protein phosphatase 1 (DUSP1) [24], IL-1 receptor-associated kinase 3 (IRAK3) [25], and NF- κ B inhibitors [26, 27]. As a result, GCs inhibit the transcription of downstream pro-inflammatory cytokines and chemokines, which are important for the propagation of inflammation, like IL-1, IL-6, IL-8, TNF and CCL2 (also known as MCP-1) [28, 29]. Due to the decreased level of pro-inflammatory mediators, the extravasation and migration of leukocytes towards the inflamed site is reduced by GCs [30, 31]. In addition, GCs inhibit the antigen presentation by dendritic cells (DCs), T-cell activation, immunoglobulin production by B-cells, and suppress vascular permeability and dilation by repressing the expression of lipid mediators such as eicosanoids and prostaglandins [29]. In the resolution phase of inflammation, GCs induce the expression of Annexin-1, directing neutrophil apoptosis [32], and promote the differentiation of macrophages to an anti-inflammatory (M2) phenotype with high expression of scavenger receptors, which is essential for the clearance of apoptotic cells and debris [33-35]. These effects of GCs enhance the elimination of inflammation and restoration of homeostasis.

Although GCs are renowned for their repressive effects on the immune system, it has become clear that their effects are much more complicated than traditionally thought. Under specific conditions, GCs have been shown to play pro-inflammatory roles rather than the classical anti-inflammatory roles, which is thought to be dependent on the specific cell types, the phase of the immune response and the dose of GCs [36, 37]. For example, GCs can increase the level of TLR2, leading to an increased secretion of critical cytokines in HeLa cells (IL-1 β , IL-8, TNF- α) [38] and in a lung epithelial cell line (IL-6, IL-8) [39]. The expression of a member of the NOD-like receptor family (NLRP3) was also reported to be upregulated by GCs in macrophages, enhancing the secretion of IL-1 β , IL-6 and TNF- α [40]. GCs have also been shown to induce the expression of the purinergic receptor P2Y2R in a microvascular endothelial cell line, resulting in increased IL-6 secretion [41]. Apart from the cell-specificity of the effects, the timing of GC treatment also plays a role in determining the outcome. Prior exposure to GCs enhances the pro-inflammatory response to lipopolysaccharide (LPS) challenge, while post-exposure to GCs suppresses this response [42]. In addition, the dose of GCs can influence their effect since low-dose GC treatment was found to enhance inflammation, whereas a high dose of GCs resulted in

inhibition of inflammation in macrophages [43]. This GC-induced increase in inflammatory signaling may represent a sensitization of cells to inflammatory mediators to establish , a rapid inflammatory activation. In conclusion, the physiological and therapeutic outcomes of GCs result from the complex signaling mechanisms and the treatment conditions.

GCs as immunosuppressive drugs

In 1949, the GC 'Compound E' was used in the Mayo Clinic to treat rheumatoid arthritis (RA) patients and the symptoms of patients were found to be alleviated after treatment [44]. A year later, the Nobel Prize in Physiology or Medicine was awarded to Hench, Kendall and Reichstein for their research on 'hormones of the adrenal cortex' [45]. Since this 'Compound E' (which is generally referred to as cortisone nowadays) was described to alleviate RA, a lot of efforts have been made to synthesize and modify GCs for pharmaceutical purposes [44, 46]. Currently, a variety of synthetic GCs are used clinically, including prednisolone, dexamethasone and beclomethasone, which differ in their solubility, biological half-life and affinity to receptors, and can be administrated via different routes [47, 48]. Due to their well-established immunosuppressive effects, GCs are widely prescribed to treat various immune-related diseases, including asthma, dermatitis, several autoimmune diseases (e.g. multiple sclerosis, RA) and even some cancers (e.g. leukemia) [47, 49]. They have also been applied to treat inflammatory complications of infectious diseases, for example tuberculosis [50-52]. Recently, GCs, in particular dexamethasone, were adopted for treating patients with coronavirus disease 2019 (COVID-19), and were shown to decrease the mortality of patients with severe respiratory complications [53, 54].

Resistance and side effects of GCs

As effective anti-inflammatory drugs, the clinical use of GCs is largely limited by their side effects. Due to their intricate effects on various systems in the whole body, prolonged treatment with GCs may evoke osteoporosis, muscle weakness, hypertension, hyperglycemia and diabetes [55, 56]. The therapeutic immunosuppressive effect of GCs can also lead to infectious complications because of the inhibited function and lower number of immune cells [56-58]. In addition, patients under long-term GC therapy are at risk of developing adrenal insufficiency, which is mediated by the negative feedback loop in the HPA axis [47].

In order to improve the benefit/risk ratio of GC therapy, methods for delivering GCs locally have been adopted to reduce the systemic effects. For example, inhaled GCs may be used in asthma patients to achieve a maximal response in the lungs [59]. Similarly, intra-articular injection for RA, topical creams applied on the skin for dermatological problems and ocular drops for eye conditions induce mainly

local effects [47, 60]. However, side effects are not fully eliminated in these situations, since systemic distribution upon absorption into the bloodstream is often observed [47]. Another method to increase the efficacy of drug delivery at the target site can be achieved by encapsulation of GCs in nanoparticles like liposomes, which can accumulate specifically in the inflamed tissue, probably dependent on the enhanced permeability and retention (EPR) effect, or the phagocytosis by macrophages and their migration towards inflammatory sites [61-67]. A liposome-encapsulated prednisolone phosphate (PLP) formulation containing phospholipids linked to a polymer polyethylene glycol (PEG) chain has shown anti-inflammatory effects in a rabbit model of atherosclerosis [68]. However, when it was tested in a clinical trial, it failed to inhibit inflammation in atherosclerosis patients [69].

Traditionally, it is believed that the side effects of GCs are related to the transactivation activity of GCs, while therapeutic effects mainly result from transrepression [70]. Therefore, novel selective GR agonists or modulators (SEGRAMs) that favor transrepression over transactivation were developed, such as Compound A (CpdA), RU24858, mapracorat and fosdagrocorat [70-73]. It was reported that CpdA effectively suppresses inflammation in mouse models of arthritis and inflammatory polyneuropathies and does not induce hyperinsulinemia and hyperglycemia, which could be related to the CpdA-induced GR conformation that is different from classical GC-bound GR and does not allow receptor dimerization [74, 75]. Indeed, strong evidence exists that GR dimerization is indispensable for the treatment of acute inflammation [76, 77]. However, GR dimerization appears to be essential for the therapeutic effects in some conditions such as septic shock [78], contact allergy [79] and TNF-induced lethal inflammation [80].

Another possible way to establish a better therapeutic ratio for GCs is to modify the structure of existing GCs. For example, anti-CD163-dexamethasone conjugate, designed to target activated macrophages, showed a more potent effect in inhibiting LPS-induced acute phase response in rats compared to non-conjugated dexamethasone, and did not cause any systemic side effects [81]. Other modifications include the conjugation of prednisolone with hydrolysable polyethylene glycol (PEG) which increased the retention time in the lungs of rats [82]. Finally, the addition of γ -lactones and cyclic carbonates can make GCs easily inactivatable by specific enzymes once they enter the blood stream [83].

Besides the side effects of GC therapies, another issue limiting the usage of GCs is the occurrence of resistance to GCs, reflected by a decreased sensitivity and a reduced maximal response, which may be evoked in patients with different diseases, including chronic obstructive pulmonary disease (COPD), asthma and RA [84-86]. Multiple molecular mechanisms have been elucidated to account for this GC resistance. In GC-resistant asthma patients, defective GR ligand binding and nuclear translocation were

observed, which could have resulted from GR phosphorylation by mitogen-activated protein kinase (MAPK) or GR nitrosylation and could be reversed by using kinase inhibitors or nitric oxide (NO) synthase inhibitors [87-89]. Another mechanism of GC resistance is related to the increased expression of the alternative splice variant of GR, GR β , which acts as a dominant-negative inhibitor of the canonical GR α -isoform [90-92]. Increased activation or expression of some pro-inflammatory transcription factors, including AP-1, NF- κ B and STAT5, have also been reported to play a role in GR resistance [93-95]. Other possible mechanisms underlying GC resistance include decreased histone deacetylase 2 (HDAC2) activity which influences the repression of inflammatory gene expression by GCs, and increased expression of the efflux pump P-glycoprotein which transports foreign substances out of the cell [86, 96].

To overcome these problems regarding GC therapy and develop novel GC drugs, more research is required into the molecular and cellular mechanisms of the anti-inflammatory action, the side effects and the occurrence of resistance.

The zebrafish as an animal model for studying GC action

Over the last decades, the zebrafish has emerged as a useful animal model in diverse areas of biomedical research, including immunology, toxicology, cancer, and behavioral studies, adding to its traditional application in research on embryonic development [97, 98]. The zebrafish has a strong reproductive ability and can easily be maintained and bred under laboratory conditions. Moreover, the small size and the optically transparent embryonic and larval stages of the zebrafish make them suitable for microscopic imaging, and the successful sequencing of the zebrafish genome has enabled rapid screening of gene function. In recent years, more genetic tools and other experimental methods have been developed, which has results in the generation of numerous transgenic and mutant fish lines, and applications in drug screening [99, 100].

Like in humans, and in all other teleost fish species, the secretion of GCs in the zebrafish occurs upon stress and in a circadian rhythm. This process is regulated by the hypothalamus-pituitary-interrenal (HPI) axis, the fish equivalent of the HPA axis. The main GC in the zebrafish is also cortisol which acts through the zebrafish orthologue of the GR [101]. Most teleost fish contain two genes encoding a Gr due to a genome duplication that happened during their evolution, which has resulted in the presence of two different Gr proteins. However, in zebrafish only one *gr* gene has been identified [102-104]. The gene organization and protein structure of the zebrafish and human GR share a high level of similarity [104, 105]. Interestingly, both the human and zebrafish gene encode two GR splice variants, the α -isoform and the β -isoform. The canonical GR α -isoform of humans and zebrafish share an overall

similarity of 59.3 % at the amino acid level. The alternative splice variant of the zebrafish Gr, Gr β , which contains a different amino acid sequence at its C-terminal end than Gr α , also highly resembles the human GR β -isoform [104]. Like its human equivalent, the zebrafish Gr β was shown to act as a dominant-negative inhibitor of Gr α in cultured cells and is expressed at a significantly lower level compared to Gr α [104, 106]. However, the dominant-negative activity of Gr β could not be confirmed *in vivo* [106, 107]. All these advantages of the zebrafish model and similarities between the human and zebrafish GC signaling pathway make the zebrafish an excellent *in vivo* model system for GC-related research.

In recent years, many studies on GCs and GR have been performed in zebrafish, advancing our knowledge about their mode of action. Gene knockdown could be achieved in zebrafish by injecting morpholino (MO) antisense oligomers at the 1-cell stage, which inhibits translation or mRNA splicing of target genes [108]. Using a *gr* splice-blocking MO, it was demonstrated that the GC-induced inhibitory effect on zebrafish caudal fin regeneration was dependent on Gr activation [109] and that the induction of the *cripto-1* gene by Gr is involved in this process [110]. Interestingly, using transcriptome analysis it was observed in our laboratory that knockdown of the *gr* gene by a splice-blocking MO altered the expression of a distinct cluster of genes than treatment with the synthetic GC dexamethasone, suggesting that Gr regulates different sets of genes under basal conditions than upon increased activation, e.g. after stress [106]. Upon knockdown of *gr* with a translation blocking MO, multiple developmental defects were observed, demonstrating the crucial role of maternal *gr* transcripts [111], which is supported by the programming function of cortisol in the development of multiple organs including muscle, heart, bone and nervous system [112, 113]. Similarly, cortisol treatment during embryogenesis influences the cardiac performance [114] and the inflammatory responses [115], which mimics maternal stress.

The first *gr* mutant zebrafish line, *gr*^{s357}, was identified from a forward genetic screen based on behavioral assays [116]. This *gr*^{s357} mutant is characterized by a point mutation in the DNA binding domain, leading to defective GRE binding activity, and high cortisol levels [117, 118]. It has been used to study HPI hyperactivation related to depressive behavior and may provide a model to screen for potential anti-depressive drugs [118]. Furthermore, using this line, it has been established that Gr signaling increases the embryonic hematopoietic stem and progenitor cell production [119], affects the white skeletal muscle transcriptome [120], regulates the visual function of the retina [121] and increases anxiety-related behavior in adults [122], emphasizing the essential role of GC/Gr signaling during development. A zebrafish *gr*^{ia30} null mutant was produced using CRISPR/Cas9-mediated gene editing, which has a 5-nucleotide insertion in the *gr* gene, resulting in a frameshift that leads to a premature stop codon truncating the receptor upstream of its DNA binding domain. DBD. Larvae of

this mutant line show unresponsiveness to GCs, and have high cortisol levels, similar to the observations in the *gr^{s357}* line. Interestingly, *gr^{ia30}* larvae do not elicit an inflammatory response upon treatment with dextran sodium sulphate (DSS), whereas the *gr^{s357}* does show this response [123]. Using this mutant, it was revealed that GC regulates the amplitude of the circadian rhythm, the feeding behavior and the synchronization of feeding to circadian rhythm [124-126]. Recently, several mutant zebrafish lines targeting different positions of *gr* or blocking Gr synthesis have also been generated, such as *gr^{ca401}* [127], *gr^{sh543}* [128], *gr³⁶⁹⁻* [129] and *fdx1b^{uob205}* [130]. The generation of these different *gr* mutants helps to dissect the role of GC/Gr on the development, behavior, circadian rhythm, metabolism and inflammatory response. In addition, the generation of reporter zebrafish lines, such as the *Tg(GRE:Luciferase^{sb6})* and *Tg(GRE:GFP^{ia20})* lines, allows for *in vivo* visualization and monitoring of the transcriptional activity of the zebrafish Gr [131, 132].

Since the immune system and the response to inflammation are highly similar between zebrafish and humans, the zebrafish model is also extensively used for studies on the immune system [133-136]. The adaptive immune system matures after three to four weeks [137], which means that the innate immune system can be studied separately during early embryonic and larval stages. Various zebrafish models for human inflammatory diseases have been developed. In the embryo/larval tail amputation-induced inflammation model, GC treatment inhibits the migration of neutrophils towards the wounded site in a Gr-dependent manner, but does not affect macrophage migration [109, 138-140]. This inhibitory effect of GCs on inflammation is associated with a broad attenuation of the transcriptional response [138]. In addition, certain anti-inflammatory genes are upregulated. For example, Gr-induced MAPK phosphatase-1 (Mkp-1) gene expression was demonstrated to be involved, which inactivates JNK, resulting in reduced AP-1-induced transcriptional activation of pro-inflammatory genes [139]. In adult zebrafish, although GCs do not influence tail wounding-induced neutrophil recruitment [141], they were shown to inhibit the expression of pro-inflammatory genes like *il8*, *tnfa* and *il1b* and they do reduce the recruitment of leukocytes towards the wounded area upon brain and heart injuries [142, 143]. Inhibitory effects of GCs on the inflammatory response were also observed in embryonic and larval models for LPS-induced inflammation [144-147], CuSO₄-induced inflammation [148] and DSS-induced enterocolitis [149]. Furthermore, it has been shown that chronic stress-related increases in GC levels during early-life stages can cause a pro-inflammatory adult phenotype which is unable to exert appropriate regulation upon injury or immunological challenge [150]. In summary, zebrafish models for research on GC action are a valuable addition to help understanding the molecular and cellular mechanisms of their signaling pathway, which may accelerate the development of novel improved GC drugs.

Outline of the thesis

The side effects of GC therapy and the occurrence of resistance to this class of drugs are still major limitations for the clinical use of GCs. In addition, significant gaps remain in our understanding of the molecular and cellular mechanisms underlying the immunosuppressive and side effects of GCs. Therefore, more research into the mechanisms of GC action and the development of novel GC therapies is needed. In this thesis, we aim to study the mechanisms underlying the immune-suppressive effects of GCs in the context of wounding-induced inflammation and infection in the zebrafish model. In addition, we exploit this model to study liposome-mediated GC delivery as a therapeutic refinement.

This introductory chapter, **Chapter 1**, provides background information on the cellular and molecular mechanisms of GCs, specifically the actions of GCs in the immune system. As an anti-inflammatory drug, the application of GCs is limited by side effects and drug resistance, of which the mechanisms are discussed. Furthermore, this chapter highlights the recent contribution of zebrafish models to this field, which have been used to investigate the effects of GCs on development, metabolism and the inflammatory response.

Chapter 2 presents a comprehensive overview of the different inflammation models that have been established in zebrafish, including wounding-induced inflammation, chemical-induced inflammation, and mutation-induced inflammation models. The models are increasingly used to investigate the molecular mechanisms underlying the inflammatory response, contributing to our understanding of inflammation and inflammatory diseases. This review chapter also highlights the use of zebrafish inflammation models for screening and exploring novel anti-inflammatory drugs, including GC drugs.

In **Chapter 3**, a detailed analysis is performed on macrophage and neutrophil migration in the zebrafish larval tail amputation model, building further on our previous observation that GCs inhibit neutrophil migration but do not affect the migration of macrophages. Using quantitative PCR, we have dissected differential effects of GCs on chemokines that specifically attract neutrophil or macrophage migration. Based on RNA sequencing data of isolated macrophages, we determined the effect of GCs on wounding-induced transcriptional changes. By in vivo imaging, we have further substantiated the anti-inflammatory effects of GCs based on the morphology and differentiation status of macrophages, using a fluorescent reporter line for *tnfa*, a pro-inflammatory marker.

In **Chapter 4**, we have used the zebrafish *Mycobacterium marinum* (*Mm*) infection model for tuberculosis to study the functional consequences of the effects of GCs on the macrophage phenotype in relation to the defense response of the host. To this end, we studied the effects of GCs on the

severity of *Mm* infection (including the bacterial burden and dissemination in the zebrafish host) and the phagocytic and microbicidal capacity of macrophages. Having identified an inhibitory effect of GCs on phagocytosis, we further investigated this phenotype by assessing the intracellular/extracellular distribution of bacteria, the consequences for macrophage cell death, and the expression levels of genes involved in phagocytosis in macrophages.

The two previous chapters mainly focus on mechanisms of the immune-suppressive effects of GCs, while in **Chapter 5** we aim to set up a screening model for novel GC therapies, in particular the liposome delivery approach of GCs. Through confocal microscopy imaging, we studied the biodistribution of liposomes with different formulations, especially a new macrophage-targeting formulation. Using a laser wounding model in zebrafish larvae, we assessed the anti-inflammatory effect by comparing the effect of a liposome-encapsulated GC, prednisolone phosphate, on wounding-induced neutrophil migration to that of the free drug. Moreover, the drug effects on tail fin regeneration and GRE activation were studied as indications for the severity of side effects. The studies demonstrate the potential of liposome encapsulation of GCs to improve their therapeutic ratio.

Chapter 6 summarizes the results from the research chapters and discusses the findings in the context of current scientific literature.

References

1. Oster, H., et al., *The functional and clinical significance of the 24-h rhythm of circulating glucocorticoids*. *Endocrine Reviews*, 2016: p. er.2015-1080.
2. Son, G.H., et al., *Adrenal peripheral clock controls the autonomous circadian rhythm of glucocorticoid by causing rhythmic steroid production*. *Proceedings of the National Academy of Sciences*, 2008. **105**(52): p. 20970-20975.
3. Tsigos, C. and G.P. Chrousos, *Hypothalamic–pituitary–adrenal axis, neuroendocrine factors and stress*. *Journal of Psychosomatic Research*, 2002. **53**(4): p. 865-871.
4. Papadimitriou, A. and K.N. Priftis, *Regulation of the hypothalamic-pituitary-adrenal axis*. *Neuroimmunomodulation*, 2009. **16**(5): p. 265-271.
5. Evans, R.M., *The steroid and thyroid hormone receptor superfamily*. *Science*, 1988. **240**(4854): p. 889-895.
6. Pratt, W.B. and D.O. Toft, *Regulation of Signaling Protein Function and Trafficking by the hsp90/hsp70-Based Chaperone Machinery*. *Experimental Biology and Medicine*, 2003. **228**(2): p. 111-133.
7. Pratt, W.B. and D.O. Toft, *Steroid receptor interactions with heat shock protein and immunophilin chaperones*. *Endocrine reviews*, 1997. **18**(3): p. 306-360.
8. Vandevyver, S., L. Dejager, and C. Libert, *On the trail of the glucocorticoid receptor: into the nucleus and back*. *Traffic*, 2012. **13**(3): p. 364-374.
9. Schmid, W., et al., *Glucocorticoid receptor binds cooperatively to adjacent recognition sites*. *The EMBO journal*, 1989. **8**(8): p. 2257-2263.
10. Baschant, U. and J. Tuckermann, *The role of the glucocorticoid receptor in inflammation and immunity*. *The Journal of steroid biochemistry and molecular biology*, 2010. **120**(2-3): p. 69-75.

11. De Bosscher, K. and G. Haegeman, *Minireview: latest perspectives on antiinflammatory actions of glucocorticoids*. *Molecular endocrinology*, 2009. **23**(3): p. 281-291.
12. Surjit, M., et al., *Widespread negative response elements mediate direct repression by agonist-liganded glucocorticoid receptor*. *Cell*, 2011. **145**(2): p. 224-241.
13. Kassel, O. and P. Herrlich, *Crosstalk between the glucocorticoid receptor and other transcription factors: molecular aspects*. *Molecular and cellular endocrinology*, 2007. **275**(1-2): p. 13-29.
14. Johnstone III, W.M., et al., *Nongenomic glucocorticoid effects and their mechanisms of action in vertebrates*, in *International Review of Cell and Molecular Biology*. 2019, Elsevier. p. 51-96.
15. Panettieri, R.A., et al., *Non-genomic effects of glucocorticoids: an updated view*. *Trends in pharmacological sciences*, 2019. **40**(1): p. 38-49.
16. Greulich, F., et al., *There goes the neighborhood: Assembly of transcriptional complexes during the regulation of metabolism and inflammation by the glucocorticoid receptor*. *Steroids*, 2016. **114**: p. 7-15.
17. Sapolsky, R.M., L.M. Romero, and A.U. Munck, *How do glucocorticoids influence stress responses? Integrating permissive, suppressive, stimulatory, and preparative actions*. *Endocrine reviews*, 2000. **21**(1): p. 55-89.
18. Janeway Jr, C.A., *Immunobiology*. 2020.
19. Netea, M.G., et al., *A guiding map for inflammation*. *Nature immunology*, 2017. **18**(8): p. 826.
20. Chen, L., et al., *Inflammatory responses and inflammation-associated diseases in organs*. *Oncotarget*, 2018. **9**(6): p. 7204.
21. Takeuchi, O. and S. Akira, *Pattern recognition receptors and inflammation*. *Cell*, 2010. **140**(6): p. 805-820.
22. MacLeod, A.S. and J.N. Mansbridge, *The Innate Immune System in Acute and Chronic Wounds*. *Adv Wound Care (New Rochelle)*, 2016. **5**(2): p. 65-78.
23. Bonecchi, R., et al., *Chemokines and chemokine receptors: an overview*. *Frontiers in bioscience (Landmark edition)*, 2009. **14**: p. 540.
24. Abraham, S. and A. Clark, *Dual-specificity phosphatase 1: a critical regulator of innate immune responses*. 2006, Portland Press Ltd.
25. Miyata, M., et al., *Glucocorticoids suppress inflammation via the upregulation of negative regulator IRAK-M*. *Nature communications*, 2015. **6**(1): p. 1-12.
26. Scheinman, R.I., et al., *Role of transcriptional activation of I κ B α in mediation of immunosuppression by glucocorticoids*. *Science*, 1995. **270**(5234): p. 283-286.
27. Beaulieu, E. and E.F. Morand, *Role of GILZ in immune regulation, glucocorticoid actions and rheumatoid arthritis*. *Nature Reviews Rheumatology*, 2011. **7**(6): p. 340.
28. Newton, R., et al., *Glucocorticoid and cytokine crosstalk: feedback, feedforward, and co-regulatory interactions determine repression or resistance*. *Journal of Biological Chemistry*, 2017. **292**(17): p. 7163-7172.
29. Cain, D.W. and J.A. Cidlowski, *Immune regulation by glucocorticoids*. *Nature Reviews Immunology*, 2017. **17**(4): p. 233-247.
30. Coutinho, A.E. and K.E. Chapman, *The anti-inflammatory and immunosuppressive effects of glucocorticoids, recent developments and mechanistic insights*. *Molecular and Cellular Endocrinology*, 2011. **335**(1): p. 2-13.
31. Perretti, M. and A. Ahluwalia, *The microcirculation and inflammation: site of action for glucocorticoids*. *Microcirculation*, 2000. **7**(3): p. 147-161.
32. Perretti, M. and F. D'acquistio, *Annexin A1 and glucocorticoids as effectors of the resolution of inflammation*. *Nature Reviews Immunology*, 2009. **9**(1): p. 62-70.
33. Varga, G., et al., *Glucocorticoids induce an activated, anti - inflammatory monocyte subset in mice that resembles myeloid - derived suppressor cells*. *Journal of leukocyte biology*, 2008. **84**(3): p. 644-650.

34. Heasman, S., et al., *Glucocorticoid-mediated regulation of granulocyte apoptosis and macrophage phagocytosis of apoptotic cells: implications for the resolution of inflammation*. Journal of Endocrinology, 2003. **178**(1): p. 29-36.
35. Ehrchen, J., et al., *Glucocorticoids induce differentiation of a specifically activated, anti-inflammatory subtype of human monocytes*. Blood, 2007. **109**(3): p. 1265-1274.
36. Busillo, J.M. and J.A. Cidlowski, *The five Rs of glucocorticoid action during inflammation: ready, reinforce, repress, resolve, and restore*. Trends in Endocrinology & Metabolism, 2013. **24**(3): p. 109-119.
37. Galon, J., et al., *Gene profiling reveals unknown enhancing and suppressive actions of glucocorticoids on immune cells*. The FASEB journal, 2002. **16**(1): p. 61-71.
38. Imasato, A., et al., *Inhibition of p38 MAPK by glucocorticoids via induction of MAPK phosphatase-1 enhances nontypeable Haemophilus influenzae-induced expression of toll-like receptor 2*. Journal of Biological Chemistry, 2002. **277**(49): p. 47444-47450.
39. Homma, T., et al., *Corticosteroid and cytokines synergistically enhance toll-like receptor 2 expression in respiratory epithelial cells*. American journal of respiratory cell and molecular biology, 2004. **31**(4): p. 463-469.
40. Busillo, J.M., K.M. Azzam, and J.A. Cidlowski, *Glucocorticoids sensitize the innate immune system through regulation of the NLRP3 inflammasome*. Journal of Biological Chemistry, 2011. **286**(44): p. 38703-38713.
41. Ding, Y., et al., *Dexamethasone Enhances ATP-Induced Inflammatory Responses in Endothelial Cells*. Journal of Pharmacology and Experimental Therapeutics, 2010. **335**(3): p. 693-702.
42. Frank, M.G., et al., *Prior exposure to glucocorticoids sensitizes the neuroinflammatory and peripheral inflammatory responses to E. coli lipopolysaccharide*. Brain, Behavior, and Immunity, 2010. **24**(1): p. 19-30.
43. Lim, H.Y., et al., *Glucocorticoids exert opposing effects on macrophage function dependent on their concentration*. Immunology, 2007. **122**(1): p. 47-53.
44. Hench, P.S., et al., *The effect of a hormone of the adrenal cortex (17-hydroxy-11-dehydrocorticosterone: compound E) and of pituitary adrenocortical hormone in arthritis: preliminary report*. Ann Rheum Dis, 1949. **8**(2): p. 97-104.
45. Lindsten, J. and N. Ringertz, *The Nobel Prize in physiology or medicine, 1901-2000*. The Nobel prize: the first, 2001. **100**: p. 111-137.
46. Parente, L., *The development of synthetic glucocorticoids*, in *Glucocorticoids*, N.J. Goulding and R.J. Flower, Editors. 2001, Birkhäuser Basel: Basel. p. 35-51.
47. Paragliola, R.M., et al., *Treatment with Synthetic Glucocorticoids and the Hypothalamus-Pituitary-Adrenal Axis*. Int J Mol Sci, 2017. **18**(10).
48. Burns, C.M., *The history of cortisone discovery and development*. Rheumatic Disease Clinics, 2016. **42**(1): p. 1-14.
49. Barnes, P.J., *Glucocorticosteroids: current and future directions*. British Journal of Pharmacology, 2011. **163**(1): p. 29-43.
50. Kadiravan, T. and S. Deepanjali, *Role of corticosteroids in the treatment of tuberculosis: an evidence-based update*. Indian J Chest Dis Allied Sci, 2010. **52**(3): p. 153-8.
51. Evans, D.J., *The use of adjunctive corticosteroids in the treatment of pericardial, pleural and meningeal tuberculosis: Do they improve outcome?* Respiratory Medicine, 2008. **102**(6): p. 793-800.
52. Singh, S. and K. Tiwari, *Use of corticosteroids in tuberculosis*. The Journal of Association of Chest Physicians, 2017. **5**(2): p. 70-75.
53. Sterne, J.A.C., et al., *Association Between Administration of Systemic Corticosteroids and Mortality Among Critically Ill Patients With COVID-19: A Meta-analysis*. Jama, 2020.
54. Horby, P., et al., *Dexamethasone in Hospitalized Patients with Covid-19-Preliminary Report*. The New England journal of medicine, 2020.
55. Moghadam-Kia, S. and V.P. Werth, *Prevention and treatment of systemic glucocorticoid side effects*. International journal of dermatology, 2010. **49**(3): p. 239-248.

56. Gensler, L.S., *Glucocorticoids: complications to anticipate and prevent*. Neurohospitalist, 2013. **3**(2): p. 92-7.
57. Dixon, W., et al., *The influence of systemic glucocorticoid therapy upon the risk of non-serious infection in older patients with rheumatoid arthritis: a nested case-control study*. Annals of the rheumatic diseases, 2011. **70**(6): p. 956-960.
58. Fardet, L., I. Petersen, and I. Nazareth, *Common Infections in Patients Prescribed Systemic Glucocorticoids in Primary Care: A Population-Based Cohort Study*. PLoS Med, 2016. **13**(5): p. e1002024.
59. Boulet, L.P., S. Gupta, and J.M. FitzGerald, *Inhaled Glucocorticoids in Asthma*. N Engl J Med, 2018. **378**(21): p. 2050-1.
60. Yasir, M. and S. Sonthalia, *Corticosteroid adverse effects*. 2019.
61. Wong, C., et al., *Liposomal prednisolone inhibits vascular inflammation and enhances venous outward remodeling in a murine arteriovenous fistula model*. Sci Rep, 2016. **6**: p. 30439.
62. Van Alem, C.M., et al., *Local delivery of liposomal prednisolone leads to an anti-inflammatory profile in renal ischaemia-reperfusion injury in the rat*. Nephrology Dialysis Transplantation, 2018. **33**(1): p. 44-53.
63. Hofkens, W., et al., *Intravenously delivered glucocorticoid liposomes inhibit osteoclast activity and bone erosion in murine antigen-induced arthritis*. Journal of controlled release, 2011. **152**(3): p. 363-369.
64. Metselaar, J.M., et al., *Complete remission of experimental arthritis by joint targeting of glucocorticoids with long - circulating liposomes*. Arthritis & Rheumatism: Official Journal of the American College of Rheumatology, 2003. **48**(7): p. 2059-2066.
65. Schiffelers, R.M., et al., *Liposome-encapsulated prednisolone phosphate inhibits growth of established tumors in mice*. Neoplasia, 2005. **7**(2): p. 118-127.
66. Schmidt, J., et al., *Drug targeting by long - circulating liposomal glucocorticosteroids increases therapeutic efficacy in a model of multiple sclerosis*. Brain, 2003. **126**(8): p. 1895-1904.
67. Montes-Cobos, E., et al., *Targeted delivery of glucocorticoids to macrophages in a mouse model of multiple sclerosis using inorganic-organic hybrid nanoparticles*. Journal of Controlled Release, 2017. **245**: p. 157-169.
68. Lobatto, M.E., et al., *Multimodal clinical imaging to longitudinally assess a nanomedical anti-inflammatory treatment in experimental atherosclerosis*. Molecular pharmaceutics, 2010. **7**(6): p. 2020-2029.
69. van der Valk, F.M., et al., *Prednisolone-containing liposomes accumulate in human atherosclerotic macrophages upon intravenous administration*. Nanomedicine: nanotechnology, biology and medicine, 2015. **11**(5): p. 1039-1046.
70. Vandewalle, J., et al., *Therapeutic Mechanisms of Glucocorticoids*. Trends Endocrinol Metab, 2018. **29**(1): p. 42-54.
71. Sundahl, N., et al., *Selective glucocorticoid receptor modulation: New directions with non-steroidal scaffolds*. Pharmacol Ther, 2015. **152**: p. 28-41.
72. Baiula, M., et al., *Mapracorat, a selective glucocorticoid receptor agonist, causes apoptosis of eosinophils infiltrating the conjunctiva in late-phase experimental ocular allergy*. Drug design, development and therapy, 2014. **8**: p. 745.
73. Stock, T., et al., *Improved disease activity with fosdagrocorat (PF - 04171327), a partial agonist of the glucocorticoid receptor, in patients with rheumatoid arthritis: a Phase 2 randomized study*. International journal of rheumatic diseases, 2017. **20**(8): p. 960-970.
74. Dewint, P., et al., *A plant-derived ligand favoring monomeric glucocorticoid receptor conformation with impaired transactivation potential attenuates collagen-induced arthritis*. The Journal of Immunology, 2008. **180**(4): p. 2608-2615.
75. Zhang, Z., Z.-Y. Zhang, and H.J. Schliesener, *Compound A, a plant origin ligand of glucocorticoid receptors, increases regulatory T cells and M2 macrophages to attenuate experimental*

- autoimmune neuritis with reduced side effects*. The Journal of Immunology, 2009. **183**(5): p. 3081-3091.
76. Souffriau, J., et al., *A screening assay for Selective Dimerizing Glucocorticoid Receptor Agonists and Modulators (SEDIGRAM) that are effective against acute inflammation*. Scientific reports, 2018. **8**(1): p. 1-13.
 77. De Bosscher, K., et al., *Activation of the Glucocorticoid Receptor in Acute Inflammation: the SEDIGRAM Concept*. Trends in Pharmacological Sciences, 2016. **37**(1): p. 4-16.
 78. Kleiman, A., et al., *Glucocorticoid receptor dimerization is required for survival in septic shock via suppression of interleukin-1 in macrophages*. Faseb j, 2012. **26**(2): p. 722-9.
 79. Tuckermann, J.P., et al., *Macrophages and neutrophils are the targets for immune suppression by glucocorticoids in contact allergy*. J Clin Invest, 2007. **117**(5): p. 1381-90.
 80. Vandevyver, S., et al., *O044 Glucocorticoid receptor dimerization induces MKP1 to protect against TNF-induced inflammation*. Cytokine, 2012. **59**(3): p. 518.
 81. Thomsen, K.L., et al., *Anti-CD163-dexamethasone conjugate inhibits the acute phase response to lipopolysaccharide in rats*. World J Hepatol, 2016. **8**(17): p. 726-30.
 82. Bayard, F.J., et al., *Polyethylene glycol-drug ester conjugates for prolonged retention of small inhaled drugs in the lung*. J Control Release, 2013. **171**(2): p. 234-40.
 83. Biggadike, K., et al., *Selective plasma hydrolysis of glucocorticoid gamma-lactones and cyclic carbonates by the enzyme paraoxonase: an ideal plasma inactivation mechanism*. J Med Chem, 2000. **43**(1): p. 19-21.
 84. Barnes, P.J. and I.M. Adcock, *Glucocorticoid resistance in inflammatory diseases*. The Lancet, 2009. **373**(9678): p. 1905-1917.
 85. Barnes, P.J., K. Ito, and I.M. Adcock, *Corticosteroid resistance in chronic obstructive pulmonary disease: inactivation of histone deacetylase*. Lancet, 2004. **363**(9410): p. 731-3.
 86. Keenan, C.R., et al., *Glucocorticoid-resistant asthma and novel anti-inflammatory drugs*. Drug discovery today, 2012. **17**(17-18): p. 1031-1038.
 87. Irusen, E., et al., *p38 Mitogen-activated protein kinase-induced glucocorticoid receptor phosphorylation reduces its activity: Role in steroid-insensitive asthma*. Journal of Allergy and Clinical Immunology, 2002. **109**(4): p. 649-657.
 88. Galigniana, M.D., G. Piwien-Pilipuk, and J. Assreuy, *Inhibition of glucocorticoid receptor binding by nitric oxide*. Molecular pharmacology, 1999. **55**(2): p. 317-323.
 89. Ismaili, N. and M.J. Garabedian, *Modulation of glucocorticoid receptor function via phosphorylation*. Annals of the New York Academy of Sciences, 2004. **1024**(1): p. 86-101.
 90. Vazquez - Tello, A., et al., *Induction of glucocorticoid receptor - β expression in epithelial cells of asthmatic airways by T - helper type 17 cytokines*. Clinical & Experimental Allergy, 2010. **40**(9): p. 1312-1322.
 91. Goleva, E., et al., *Increased glucocorticoid receptor β alters steroid response in glucocorticoid-insensitive asthma*. American journal of respiratory and critical care medicine, 2006. **173**(6): p. 607-616.
 92. Kozaci, D., Y. Chernajovsky, and I. Chikanza, *The differential expression of corticosteroid receptor isoforms in corticosteroid-resistant and-sensitive patients with rheumatoid arthritis*. Rheumatology, 2007. **46**(4): p. 579-585.
 93. Loke, T.-K., et al., *Systemic glucocorticoid reduces bronchial mucosal activation of activator protein 1 components in glucocorticoid-sensitive but not glucocorticoid-resistant asthmatic patients*. Journal of allergy and clinical immunology, 2006. **118**(2): p. 368-375.
 94. Hakonarson, H., et al., *Profiling of genes expressed in peripheral blood mononuclear cells predicts glucocorticoid sensitivity in asthma patients*. Proceedings of the National Academy of Sciences, 2005. **102**(41): p. 14789-14794.
 95. Goleva, E., K.O. Kisich, and D.Y. Leung, *A role for STAT5 in the pathogenesis of IL-2-induced glucocorticoid resistance*. The Journal of Immunology, 2002. **169**(10): p. 5934-5940.
 96. Barnes, P.J., *Mechanisms and resistance in glucocorticoid control of inflammation*. The Journal of steroid biochemistry and molecular biology, 2010. **120**(2-3): p. 76-85.

97. Tavares, B. and S. Santos Lopes, *The Importance of Zebrafish in Biomedical Research*. Acta Medica Portuguesa, 2013. **26**(5): p. 583-592.
98. Lieschke, G.J. and P.D. Currie, *Animal models of human disease: zebrafish swim into view*. Nature Reviews Genetics, 2007. **8**(5): p. 353-367.
99. Barut, B.A. and L.I. Zon, *Realizing the potential of zebrafish as a model for human disease*. Physiological Genomics, 2000. **2**(2): p. 49.
100. Vogel, G., *Sanger Will Sequence Zebrafish Genome*. Science, 2000. **290**(5497): p. 1671.
101. Schaaf, M.J., A. Chatzopoulou, and H.P. Spaink, *The zebrafish as a model system for glucocorticoid receptor research*. Comp Biochem Physiol A Mol Integr Physiol, 2009. **153**(1): p. 75-82.
102. Alsop, D. and M.M. Vijayan, *Development of the corticosteroid stress axis and receptor expression in zebrafish*. American Journal of Physiology - Regulatory, Integrative and Comparative Physiology, 2008. **294**(3): p. R711-R719.
103. Bury, N.R., *The evolution, structure and function of the ray finned fish (Actinopterygii) glucocorticoid receptors*. Gen Comp Endocrinol, 2016.
104. Schaaf, M.J., et al., *Discovery of a functional glucocorticoid receptor beta-isoform in zebrafish*. Endocrinology, 2008. **149**(4): p. 1591-9.
105. Stolte, E.H., et al., *Evolution of glucocorticoid receptors with different glucocorticoid sensitivity*. J Endocrinol, 2006. **190**(1): p. 17-28.
106. Chatzopoulou, A., et al., *Transcriptional and metabolic effects of glucocorticoid receptor alpha and beta signaling in zebrafish*. Endocrinology, 2015. **156**(5): p. 1757-69.
107. Chatzopoulou, A., et al., *Functional analysis reveals no transcriptional role for the glucocorticoid receptor β -isoform in zebrafish*. Molecular and Cellular Endocrinology, 2017. **447**: p. 61-70.
108. Stainier, D.Y., et al., *Guidelines for morpholino use in zebrafish*. PLoS genetics, 2017. **13**(10): p. e1007000.
109. Mathew, L.K., et al., *Unraveling tissue regeneration pathways using chemical genetics*. J Biol Chem, 2007. **282**(48): p. 35202-10.
110. Garland, M.A., et al., *Glucocorticoid receptor-dependent induction of *cripto-1* (one-eyed pinhead) inhibits zebrafish caudal fin regeneration*. Toxicology Reports, 2019. **6**: p. 529-537.
111. Pikulkaew, S., et al., *The knockdown of maternal glucocorticoid receptor mRNA alters embryo development in zebrafish*. Developmental dynamics, 2011. **240**(4): p. 874-889.
112. Nesan, D. and M.M. Vijayan, *Role of glucocorticoid in developmental programming: evidence from zebrafish*. General and comparative endocrinology, 2013. **181**: p. 35-44.
113. Wilson, K.S., et al., *Early-life glucocorticoids programme behaviour and metabolism in adulthood in zebrafish*. J Endocrinol, 2016. **230**(1): p. 125-42.
114. Nesan, D. and M.M. Vijayan, *Embryo exposure to elevated cortisol level leads to cardiac performance dysfunction in zebrafish*. Molecular and cellular endocrinology, 2012. **363**(1-2): p. 85-91.
115. van den Bos, R., et al., *Early Life Glucocorticoid Exposure Modulates Immune Function in Zebrafish (*Danio rerio*) Larvae*. Frontiers in Immunology, 2020. **11**(727).
116. Muto, A., et al., *Forward genetic analysis of visual behavior in zebrafish*. PLoS Genet, 2005. **1**(5): p. e66.
117. Griffiths, B., et al., *A zebrafish model of glucocorticoid resistance shows serotonergic modulation of the stress response*. Frontiers in behavioral neuroscience, 2012. **6**: p. 68.
118. Ziv, L., et al., *An affective disorder in zebrafish with mutation of the glucocorticoid receptor*. Molecular psychiatry, 2013. **18**(6): p. 681-691.
119. Kwan, W., et al., *The central nervous system regulates embryonic HSPC production via stress-responsive glucocorticoid receptor signaling*. Cell stem cell, 2016. **19**(3): p. 370-382.
120. Palstra, A.P., et al., *Cortisol acting through the glucocorticoid receptor is not involved in exercise-enhanced growth, but does affect the white skeletal muscle transcriptome in zebrafish (*danio rerio*)*. Frontiers in physiology, 2019. **9**: p. 1889.

121. Muto, A., et al., *Glucocorticoid receptor activity regulates light adaptation in the zebrafish retina*. *Frontiers in neural circuits*, 2013. **7**: p. 145.
122. Sireeni, J., et al., *Profound effects of glucocorticoid resistance on anxiety-related behavior in zebrafish adults but not in larvae*. *General and Comparative Endocrinology*, 2020: p. 113461.
123. Facchinello, N., et al., *nr3c1 null mutant zebrafish are viable and reveal DNA-binding-independent activities of the glucocorticoid receptor*. *Scientific reports*, 2017. **7**(1): p. 1-13.
124. Mosser, E.A., et al., *Identification of pathways that regulate circadian rhythms using a larval zebrafish small molecule screen*. *Scientific reports*, 2019. **9**(1): p. 1-14.
125. Filosa, A., et al., *Feeding state modulates behavioral choice and processing of prey stimuli in the zebrafish tectum*. *Neuron*, 2016. **90**(3): p. 596-608.
126. Morbiato, E., et al., *Feeding Entrainment of the Zebrafish Circadian Clock Is Regulated by the Glucocorticoid Receptor*. *Cells*, 2019. **8**(11): p. 1342.
127. Faught, E. and M.M. Vijayan, *The mineralocorticoid receptor is essential for stress axis regulation in zebrafish larvae*. *Scientific Reports*, 2018. **8**(1): p. 1-11.
128. Marchi, D., et al., *Bidirectional crosstalk between Hypoxia-Inducible Factor and glucocorticoid signalling in zebrafish larvae*. *PLoS genetics*, 2020. **16**(5): p. e1008757.
129. Gans, I., et al., *Klf9 is a key feedforward regulator of the transcriptomic response to glucocorticoid receptor activity*. *bioRxiv*, 2020: p. 863555.
130. Griffin, A., et al., *Ferredoxin 1b (Fdx1b) is the essential mitochondrial redox partner for cortisol biosynthesis in zebrafish*. *Endocrinology*, 2016. **157**(3): p. 1122-1134.
131. Weger, B.D., et al., *A chemical screening procedure for glucocorticoid signaling with a zebrafish larva luciferase reporter system*. *JoVE (Journal of Visualized Experiments)*, 2013(79): p. e50439.
132. Benato, F., et al., *A living biosensor model to dynamically trace glucocorticoid transcriptional activity during development and adult life in zebrafish*. *Molecular and cellular endocrinology*, 2014. **392**(1-2): p. 60-72.
133. Lieschke, G.J., et al., *Morphologic and functional characterization of granulocytes and macrophages in embryonic and adult zebrafish*. *Blood*, 2001. **98**(10): p. 3087-3096.
134. Herbomel, P., B. Thisse, and C. Thisse, *Ontogeny and behaviour of early macrophages in the zebrafish embryo*. *Development*, 1999. **126**(17): p. 3735-3745.
135. Bennett, C.M., et al., *Myelopoiesis in the zebrafish, Danio rerio*. *Blood, The Journal of the American Society of Hematology*, 2001. **98**(3): p. 643-651.
136. Langenau, D.M. and L.I. Zon, *The zebrafish: a new model of T-cell and thymic development*. *Nature Reviews Immunology*, 2005. **5**(4): p. 307-317.
137. Lam, S.H., et al., *Development and maturation of the immune system in zebrafish, Danio rerio: a gene expression profiling, in situ hybridization and immunological study*. *Developmental & Comparative Immunology*, 2004. **28**(1): p. 9-28.
138. Chatzopoulou, A., et al., *Glucocorticoid-Induced Attenuation of the Inflammatory Response in Zebrafish*. *Endocrinology*, 2016. **157**(7): p. 2772-84.
139. Zhang, Y., et al., *In Vivo Interstitial Migration of Primitive Macrophages Mediated by JNK-Matrix Metalloproteinase 13 Signaling in Response to Acute Injury*. *The Journal of Immunology*, 2008. **181**(3): p. 2155-2164.
140. Hall, C.J., et al., *Epidermal cells help coordinate leukocyte migration during inflammation through fatty acid-fuelled matrix metalloproteinase production*. *Nat Commun*, 2014. **5**: p. 3880.
141. Geurtzen, K., et al., *Immune suppressive and bone inhibitory effects of prednisolone in growing and regenerating zebrafish tissues*. *Journal of Bone and Mineral Research*, 2017. **32**(12): p. 2476-2488.
142. Huang, W.C., et al., *Treatment of Glucocorticoids Inhibited Early Immune Responses and Impaired Cardiac Repair in Adult Zebrafish*. *PLoS One*, 2013. **8**(6): p. e66613.
143. Kyritsis, N., et al., *Acute inflammation initiates the regenerative response in the adult zebrafish brain*. *Science*, 2012. **338**(6112): p. 1353-1356.

144. Yang, L.-L., et al., *Endotoxin molecule lipopolysaccharide-induced zebrafish inflammation model: a novel screening method for anti-inflammatory drugs*. *Molecules*, 2014. **19**(2): p. 2390-2409.
145. Wijesinghe, W., et al., *Assessment of anti-inflammatory effect of 5 β -hydroxypalisadin B isolated from red seaweed *Laurencia snackeyi* in zebrafish embryo in vivo model*. *Environmental Toxicology and Pharmacology*, 2014. **37**(1): p. 110-117.
146. Sun, Q., et al., *Anti-inflammatory properties of extracts from *Chimonanthus nitens* Oliv. leaf*. *PloS one*, 2017. **12**(7).
147. Yang, L., et al., *Protective effect of phillyrin on lethal LPS-induced neutrophil inflammation in zebrafish*. *Cellular Physiology and Biochemistry*, 2017. **43**(5): p. 2074-2087.
148. d'Alençon, C.A., et al., *A high-throughput chemically induced inflammation assay in zebrafish*. *BMC biology*, 2010. **8**(1): p. 151.
149. Oehlers, S.H., et al., *Retinoic acid suppresses intestinal mucus production and exacerbates experimental enterocolitis*. *Disease models & mechanisms*, 2012. **5**(4): p. 457-467.
150. Hartig, E.I., et al., *Cortisol-treated zebrafish embryos develop into pro-inflammatory adults with aberrant immune gene regulation*. *Biol Open*, 2016. **5**(8): p. 1134-41.

Chapter 2

Modeling inflammation in zebrafish for the development of anti-inflammatory drugs

Yufei Xie, Annemarie H. Meijer, Marcel J.M. Schaaf

Abstract

Dysregulation of the inflammatory response in humans can lead to various inflammatory diseases, like asthma and rheumatoid arthritis. The innate branch of the immune system, including macrophage and neutrophil functions, plays a critical role in all inflammatory diseases. This part of the immune system is well conserved between humans and the zebrafish, which has emerged as a powerful animal model for inflammation, because it offers the possibility to image and study inflammatory responses *in vivo* at the early life stages. This review focuses on different inflammation models established in zebrafish, and how they are being used for the development of novel anti-inflammatory drugs. The most commonly used model is the tail fin amputation model, in which part of the tail fin of a zebrafish larva is clipped. This model has been used to study fundamental aspects of the inflammatory response, like the role of specific signaling pathways, the migration of leukocytes, and the interaction between different immune cells, and has also been used to screen libraries of natural compounds, approved drugs, and well-characterized pathway inhibitors. In other models the inflammation is induced by chemical treatment, such as lipopolysaccharide (LPS), leukotriene B4 (LTB4) and copper, and some chemical-induced models, such as treatment with trinitrobenzene sulfonic acid (TNBS), specifically model inflammation in the gastro-intestinal tract. Two mutant zebrafish lines, carrying a mutation in the hepatocyte growth factor activator inhibitor 1a gene (*hai1a*) and the cdp-diacylglycerolinositol 3-phosphatidyltransferase (*cdipt*) gene, show an inflammatory phenotype, and they provide interesting model systems for studying inflammation. These zebrafish inflammation models are often used to study the anti-inflammatory effects of glucocorticoids, to increase our understanding of the mechanism of action of this class of drugs and to develop novel glucocorticoid drugs. In this review, an overview is provided of the available inflammation models in zebrafish, and how they are used to unravel molecular mechanisms underlying the inflammatory response and to screen for novel anti-inflammatory drugs.

1. Introduction

1.1. Inflammation and inflammatory diseases

When the body encounters harmful stimuli, such as invading pathogens, wounding or damaged cells, the immune system will be activated and an inflammatory response is triggered [1, 2]. This response is induced by Pattern Recognition Receptors (PRRs) such as Toll-Like Receptors (TLRs) recognizing patterns in molecules characteristic for microbes (Pathogen-Associated Molecular Patterns (PAMPs)), or molecules released by damaged cells (Damage-Associated Molecular Patterns (DAMPs)). Subsequently, immune cells release pro-inflammatory cytokines, such as IL-1 β and TNF- α , which in

turn stimulate the synthesis and release of inflammatory mediators, including chemokines and prostaglandins [1, 3]. Directed by the chemokine gradients, leukocytes migrate towards the inflamed site to deal with the damaged tissue or invading microbes [4, 5]. These changes at the molecular level will lead to the five classical symptoms of inflammation: heat, pain, redness, swelling and eventually loss of function. Normally, the inflammatory processes are actively terminated through functional reprogramming of involved cells, which results in restored homeostasis [1].

A dysregulated inflammatory response is observed in various diseases. Abnormally and excessively activated inflammation plays an essential role in the pathogenesis of inflammatory disorders such as asthma, rheumatoid arthritis and allergic and autoimmune diseases [6, 7]. Chronic inflammation in the gastrointestinal tract can lead to inflammatory bowel disease (IBD), which may even cause non-digestive tract complications [8]. In addition, it has become apparent that chronic inflammation is involved in some diseases that were previously not considered to be inflammation-related, including cancer, type 2 diabetes, neurodegenerative diseases and atherosclerosis [9-12]. Finally, although inflammation serves primarily as a beneficial defence response against infections, acute or chronic overactivation of the inflammatory response is well known to exacerbate infectious disease pathologies, for example in COVID-19 and tuberculosis [13, 14].

Traditionally, the therapeutic regimen for inflammation includes the use of steroidal (glucocorticoid (GC)) and non-steroidal anti-inflammatory drugs [15]. However, the use of these drugs may provoke multiple side effects including osteoporosis, gastrointestinal disorders, cardiovascular or cerebrovascular events and infection [16, 17]. Moreover, drug resistance may occur in a subpopulation of patients [17]. In the past decades, successful monoclonal antibody therapies have dramatically improved the prognosis of patients with inflammatory disorders, for example rheumatoid arthritis [18] and novel inhibitors of critical components of inflammatory signaling pathways have been discovered [15, 19]. Despite this notable progress, there is still an unmet need for more effective and safer anti-inflammatory drugs. In this review, we discuss the usefulness of the zebrafish as an animal model for studying the mechanisms of inflammation and as a screening system to accelerate research aimed at the discovery of novel anti-inflammatory drugs (an overview is presented in Tables 1 and 2).

1.2. The zebrafish as an animal model for biomedical research

The use of zebrafish (*Danio rerio*) as a research model started in the 1950s and it was initially applied for studying embryonic development [20]. The zebrafish is a tropical fish that grows healthily in freshwater at temperatures around 24.6°C to 38.6°C [21]. When zebrafish find a shore of shallow water, they tend to spawn in the morning, which can be easily simulated in the laboratory with sliding

bottom inserts and lamp light at 28°C [22, 23]. The transparent embryonic and larval stages, the relatively short generation time, the small size and strong reproduction ability of zebrafish make it a highly versatile animal model. Over the years, more and more genetic tools and experimental methods have been applied, leading to the successful sequencing of the zebrafish genome, enabling rapid screening of gene function, and the generation of various transgenic or mutant fish lines and models for studying human diseases [24-26]. Due to the accumulation of knowledge and available tools for zebrafish, we are currently able to optimally exploit the advantages of this model.

Although initially used to study embryonic development, the zebrafish has emerged as a versatile animal model in diverse areas of biomedical research, including immunology, toxicology, cancer, and behavioral biology [27, 28]. In recent years, there have been many successful attempts modelling human diseases using zebrafish. For example, the characteristics of benign and malignant tumors that develop in zebrafish are similar to the histological symptoms of human tumors [29], zebrafish infected with *Mycobacterium marinum* adequately simulate hallmarks of human tuberculosis [30], and the phenotype of zebrafish carrying a mutation in the gene *sauternes* closely resembles the pathology of human X-linked congenital sideroblastic anemia [31]. In this review, we will discuss how the zebrafish is used as an animal model for inflammatory diseases and how the available models have been used for research on anti-inflammatory drugs.

An important advantage of the model is that the small size of zebrafish embryos and the development of automated techniques facilitate high-throughput screening [32-34]. Although *C. elegans* and *Drosophila* are also frequently used for high-throughput screening, their cuticles may act as a barrier for diffusion [35, 36]. Zebrafish embryos do not have cuticles, and most drugs can therefore be delivered by simply adding them to the culture medium at a relatively low dose. As a vertebrate, zebrafish are evolutionarily more closely related to mammals compared to worms and flies, so results can more easily be extrapolated to humans. Therefore, zebrafish models have a strong potential to serve as whole animal models to be used in preclinical bioassays during drug development.

The immune system of zebrafish is highly similar to that of humans. Important components of the innate immune system, macrophages, can be observed from 15 hours post fertilization (hpf) [37]. By the onset of blood circulation at 26 hpf, embryonic macrophages are already capable of phagocytosing particles, producing reactive oxygen species (ROS), and killing pathogens [37, 38]. The zebrafish neutrophils, which develop by 18 hpf and mature between 24-48 hpf, resemble human neutrophils regarding the segmented nuclei, granules, and expression of myeloperoxidase [39, 40]. Additionally, zebrafish show conserved critical parts of the adaptive immune system, including thymus development, thymocyte development and the function of T-cells and B-cells [41]. The adaptive

immune system matures after three to four weeks [42, 43], which means that the innate immune system can be studied separately during early embryonic and larval stages. The inflammatory response has also been found to be well conserved in zebrafish and this has been successfully exploited to increase our mechanistic understanding of the role of neutrophils in inflammatory diseases [44, 45]. The inflammatory response in zebrafish larvae can be induced using a variety of approaches. In this review we provide an overview of different methods to trigger inflammation (see Figure 2 for a schematic overview of these different methods), and we discuss how they are used for studies on the molecular mechanisms underlying the inflammatory response as well as for research aiming at the development of novel anti-inflammatory drugs, in particular novel GC drugs.

2. Inflammatory disease models in zebrafish

2.1. Wounding-induced inflammation

2.1.1. Introduction

Acute inflammation induced by tail wounding is a well-established model for inflammation and regeneration studies in zebrafish (Fig. 1, Fig. 2A). Tail wounding can be performed by amputation of part of the tail fin, or incision of the fin with a sterile scalpel or needle under a stereo microscope, which can be performed in zebrafish embryos, larvae and adults [46-48]. In embryos (stages up to 72 hpf) and larvae (72 hpf onwards), the amputation may include a distal part of the notochord, to induce a stronger response (Fig. 1A). Subsequently, an acute local inflammatory response can be observed, inducing accumulation of macrophages and neutrophils near the wounded area [46]. The visualization of leukocytes is possible through the use of transgenic fish in which the expression of autofluorescent proteins, such as GFP and mCherry, is driven by promoters which are specifically active in neutrophils (such as the myeloperoxidase (*mpx*) [46] and lysozyme (*lyz*) promoter [49]), or in macrophages (such as the macrophage-expressed gene-1 (*mpeg-1*) [50, 51] and *mfap4* promoter [52]), or by a promoter that marks both these cell types (*coro1a* [53]). Besides direct transection, the wounding can also be inflicted by laser irradiation of the epidermis on the trunk [54], the yolk sac [55], skeletal muscle tissue [56], or melanocytes over the yolk sac [57] and in the caudal hematopoietic tissue (CHT) [58]. Recently, thermal damage inflicted to the tail fin by a cautery pen has been shown to result in a dramatic loss of collagen fibers in the wound region (unlike tail fin transection), which was accompanied by a stronger inflammatory response and a delayed regeneration than observed after tail transection [59, 60].

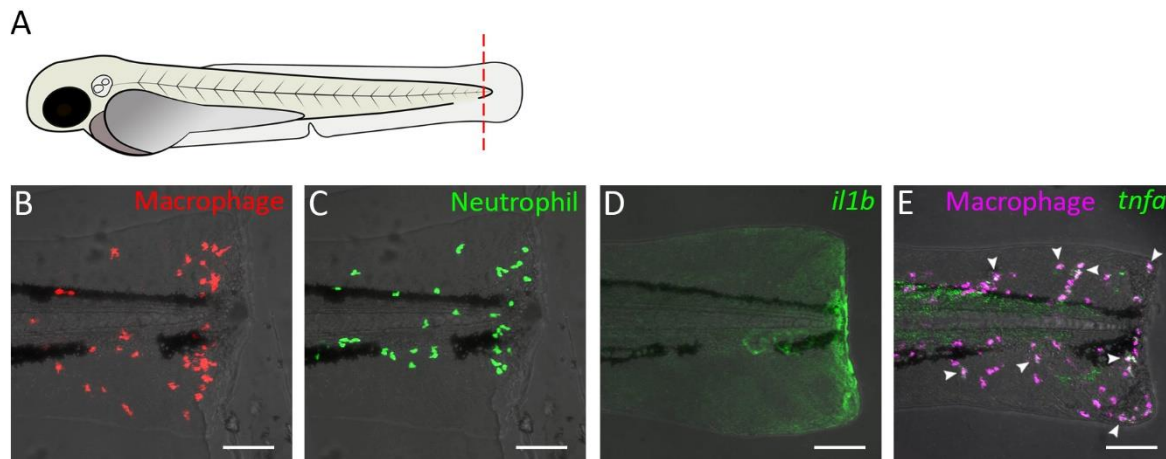


Figure 1. Tail transection in zebrafish larvae as a model for inflammation. A. Schematic drawing of a zebrafish larva at 3 dpf. The dashed red line shows a site of transection (in some studies, the transection site may not include a part of the notochord). B-E. Confocal microscopy images of tail from amputated larvae of the following transgenic lines: *Tg(mpeg1:mcherry-F)* (B), *Tg(mpx:GFP)* (C), *Tg(il1b:GFP)* (D), *Tg(mpeg1:mCherry-F/tnfa:eGFP-F)* (E). Images were taken at 4 hours post amputation using a Nikon Eclipse Ti-E microscope with a Plan Apo 20X/0.75 NA objective. Images show accumulation of macrophage (B) and neutrophils (C), activation of the *il1b* gene (D) and *tnfa* expression in macrophage (E) near the wound. In panel E, arrow heads indicate macrophages in which *tnfa* was activated.

2.1.2. Studies on molecular mechanisms underlying the inflammatory response

Using the zebrafish tail wounding model for inflammation, different molecular pathways of the inflammatory response have been unraveled. As a first response to wounding, the damaged epithelium generates a sustained hydrogen peroxide (H_2O_2 , a major reactive oxygen species (ROS)) gradient from the wounded site, through local activation of the epithelial NADPH oxidase Duox [61, 62]. This gradient initiates the recruitment of leukocytes to the wounded area, in particular neutrophils, which use the Src family kinase Lyn as a redox sensor to detect the H_2O_2 gradient [63]. In addition, epithelial cells have been shown to use fatty acid β -oxidation to increase their mitochondrial ROS production in response to wounding. This process requires the activity of a zebrafish homologue of the mammalian mitochondrial enzyme, Immunoresponsive gene 1 (IRG1), and was shown to contribute to neutrophil recruitment [64, 65].

In neutrophils, phosphoinositide 3-kinase (PI3K) was found to mediate migration by inducing actin polymerization and generating membrane protrusions at the leading edge through Rac activation and polarization of F-actin dynamics (in a Rac-independent way), which is required for actomyosin-mediated tail contraction [58]. Treatment with the microtubule-destabilizing drug nocodazole impairs neutrophil migration towards wounds, even though this process enhances the polarity of F-actin dynamics [66]. SHIP phosphatases limit neutrophil mobility and their migration towards a wound,

probably by inhibiting PI3K activity [67]. Neutrophil migration also appears to require the Wiskott-Aldrich syndrome protein (WASp) for their proper migratory behavior [68].

Macrophages migrate to a wounded area by extension of pseudopods and they are capable of phagocytosing tissue debris [57]. Microtubule disassembly by nocadazole inhibited macrophage migration towards a wound, through global activation of Rho kinase (ROK) and thus a loss of the polarity of ROK activity [55]. Two distinct subsets of zebrafish macrophages were identified using a *Tg(tnfa:GFP)* reporter line, similar to the differentiation processes that are observed in mammalian macrophages [69, 70]. GFP-positive macrophages could already be observed at 1 hour post-wounding, and they are characterized by a flattened and lobulated morphology, and expression of markers characteristic of classically activated, pro-inflammatory (M1) macrophages. Those GFP-positive macrophages could convert to negative ones, which dominate the population at later stages, showing features of alternatively activated, anti-inflammatory (M2) macrophages.

The migration of leukocytes upon tail wounding is dependent on *de novo* protein synthesis, since treatment with the protein synthesis inhibitor cycloheximide was shown to inhibit the migration of neutrophils and macrophages [71]. Both AP-1- and NF- κ B-induced transcription have been shown to be involved and the action of these transcription factor complexes is highly regulated by MAP kinase (MAPK) activity. One class of MAPKs, the c-Jun N-terminal Kinases (JNKs), are involved in the regulation of the AP-1-induced transcription, , whereas another class, the p38 MAPKs, appeared not to be alter the function of AP-1. Upon wounding, active JNKs were shown to activate c-Jun, which in turn induces the transcription of *mmp13* in neutrophils, which is required for the migration of these cells [72]. This JNK/c-Jun/Mmp13 pathway can be inhibited by Mkp-1 [72]. In addition, JNK-mediated c-Jun activation results in an increased expression of the *alox5* gene, encoding the 5-lipoxygenase Alox5, a key enzyme involved in the biosynthesis of leukotrienes, including LTB4 [73]. This pathway was also shown to be required for neutrophil migration upon tail wounding and could be inhibited by activation of the cannabinoid receptor type 2 (Cnr2) [73]. NF- κ B activation, characterized by p65 phosphorylation, was shown to be dependent on the phosphorylation of another class of MAPKs, the Extracellular signal-regulated kinases (ERKs) [74]. The activation of this pathway was shown to be dependent on the circadian gene *period1b* (*per1b*), and results in an increased expression of pro-inflammatory molecules like *tnfa*, *il1b*, *il6*, and *il8* [74].

The cytokine IL-8 (or CXCL8) is known to be a potent chemoattractant for neutrophils in mammalian systems [75, 76]. The zebrafish homologs Cxcl8a (Cxcl8-l1) and Cxcl8b.1 (Cxcl8-l2) have been shown to be upregulated upon tail wounding, mediating neutrophil recruitment through Cxcr2 [77, 78]. The chemokines Ccl2 and Cxcl11aa were demonstrated to be required for the wound-induced migration of

macrophages by knocking down the expression of the genes encoding their respective receptors, *Ccr2* and *Cxcr3.2* [79]. Suppressing the activation of the cytokine IL-1 β (by caspase-1 inhibitors and P2X7 antagonists) resulted in attenuated migration of neutrophils and macrophages [80]. In addition, knockdown of the gene encoding IL-1 β by morpholino treatment was shown to decrease the migration of neutrophils towards the wounded area in two studies (although IL-1 β appeared to be dispensable for random basal motility) [80, 81]. The migration of macrophages was not affected upon by *il1b* morpholino knockdown in one study [80], and decreased in another [81]. The IL-1 β pathway (also involving the adaptor protein Myd88) was shown to act independently of NADPH oxidase-mediated ROS production, since treatment with the NADPH oxidase inhibitor DPI did not affect *il1b* expression levels (and vice versa: *il1b* and *myd88* knockdown did not affect ROS production upon tail wounding) [81].

Several hours after the wounding, the response enters the resolution phase, and active Wnt/ β -catenin signaling has been suggested to play a role in this transition [82]. In the resolution phase of the inflammatory response, neutrophils leave the wounded area (a process called reverse migration) or undergo apoptosis [83]. The survival of neutrophils is regulated by Serum and Glucocorticoid Regulated Kinase 1 (SGK1), which is an anti-apoptotic protein downstream of the neutrophil survival factor GM-CSF [84]. The hypoxia-inducible factor-1 α (HIF-1 α) has been proven to be a critical factor for the regulation of myeloid cell function in mammals, and the activation of Hif-1 α delays the resolution of inflammation in zebrafish by inhibiting neutrophil apoptosis and reverse migration [85]. The reverse-migrating neutrophils were found to exhibit an activated morphology and to respond normally to a secondary challenge [86]. The *Cxcl12/Cxcr4* signaling axis plays a role in neutrophil retention and the knockdown of *cxcr4b* and *cxcl12a* or the pharmacological inhibition of this signaling increased the movement of neutrophils away from the wounded area [87].

For regeneration studies, the amputation is usually performed on 2 days post fertilization (dpf) zebrafish, after which tissue repair can be observed gradually and complete regeneration can be established 3 days later, at 5 dpf, which is within the time frame in which regulations of animal experimentation do not apply [88, 89]. It was demonstrated that the tissue regeneration of zebrafish embryos is dependent on ROS-induced vimentin production at the wound edge, and that the Stat3 and Tgf β signaling pathways are involved in this process [59, 60]. Furthermore, it was shown that regeneration was not affected after ablation of macrophages and neutrophils using morpholino knockdown of the *pu.1/spi1b* gene, which encodes a transcription factor required to permit myeloid cell development [88]. However in later studies, macrophages were shown to be crucial for cell proliferation and tissue regeneration, since ablation of macrophages by an *irf8* morpholino (which

drives myeloid cell fate toward neutrophil development) resulted in impairment of the fin regeneration, and the presence of large vacuoles in the regenerated tissue [53]. A specific subset of macrophages, peripheral tissue-resident macrophages, were shown to contribute to tail fin regeneration by ROS production and downregulation of inflammatory mediators such as $IL-1\beta$ at the damaged site [90]. In the adult zebrafish tail fin amputation model, macrophages have also been shown to enhance tail fin regeneration, by regulating tissue growth and bone ray patterning, which was demonstrated by depletion of macrophages in transgenic fish using the nitroreductase (NTR)/metronidazole(MTZ) cell ablation technology [82]. Mutation of the *runx1* gene reduced neutrophil numbers, but did not affect tail fin regeneration [53]. These findings suggest that the inflammatory response induced by wounding, in particular the recruitment of macrophages, is critical for tissue repair and regeneration.

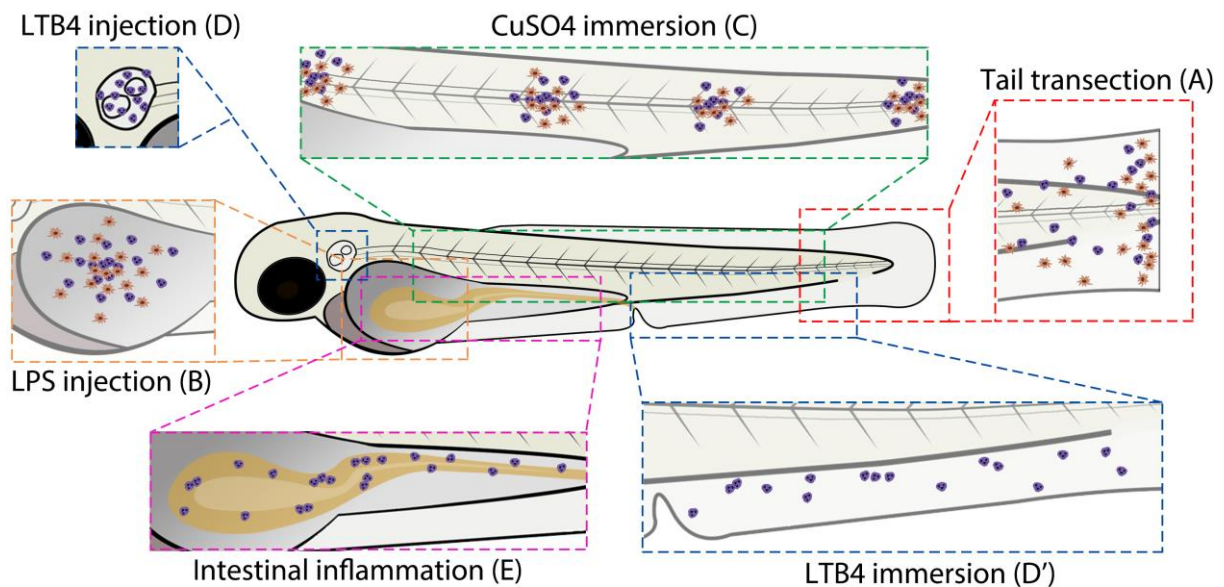


Figure 2. Schematic overview of commonly used zebrafish larval inflammation models. A. Transection of the tail fin. B. LPS injection in the yolk sac. C. CuSO₄ immersion causing damage to the neuromasts. D. LTB₄ injection in the otic vesicle. D'. LTB₄ immersion. E. Chemical-induced intestinal inflammation. All presented models induce leukocyte recruitment. Red cells represent macrophages and purple cells represent neutrophils (in some models, the macrophage infiltration is not shown because it has not been investigated in the studies cited in this review). Alternative zebrafish larval inflammation models, discussed in the text but not presented in this figure, include laser wounding-, tail fin incision-, LPS immersion- and mutation-induced inflammation. For the tail fin transection/incision, CuSO₄ immersion and intestinal inflammation models, adult zebrafish have been used as well.

2.1.3. 2Drug discovery studies

Tail wounding-induced inflammation in zebrafish has been used for anti-inflammatory drug testing and screening in numerous studies. Natural compounds, well-characterized drugs and defined pathway inhibitors have been tested and several libraries of such compounds have been screened in this model system. These studies contributed to the validation of this inflammation model and resulted in the identification of a number of novel anti-inflammatory compounds, requiring validation in other models and further optimization and testing.

In order to find new anti-inflammatory drugs from collections of existing or clinically approved drugs (drug repositioning [91]), a library of approved drugs that had not previously been characterized as anti-inflammatory compounds, were screened for their ability of suppressing neutrophil recruitment in the zebrafish tail wounding assay [92]. Interestingly, the ten most potent repositioned drugs from this zebrafish screen (including amodiaquin dihydrochloride, alfuzosin hydrochloride and clonidine hydrochloride) also displayed anti-inflammatory activity in a mouse model of skin inflammation. To discover novel analogs of an existing drug with reduced side effects, several analogs of thalidomide were screened using the zebrafish tail wounding model. A number of these analogs were shown to cause a reduction in neutrophil recruitment, without displaying the infamous teratogenic side effects of the original drug [93]. Important drug targets for accelerating the resolution of inflammation, ErbBs, were identified by screening kinase inhibitors in the zebrafish tail fin wounding model [94]. ErbB inhibitors and simultaneous gene knockdown of two genes that encode ErbB kinases (*egfra* and *erbb2*) resulted in suppression of neutrophil apoptosis and reduced the level of inflammation in zebrafish larvae.

In addition, structure-function studies have been performed using this model. For example, meisoindigo, which is a derivative of indirubin, a chemical constituent of the traditional Chinese herbal medicine Qing Dai was found to inhibit leukocyte migration induced by tail wounding without affecting reverse migration or Akt and Erk activity, whereas indirubin (which represents the core structure of meisoindigo) did not show an effect [95]. Moreover, a particular chemical group, consisting of fused benzene and pyran rings with an attached carbonyl group (1,4-benzopyrone) or its isomer 'coumarin' (1-benzopyran-2-one), was found to be present in four of the nine most-active pro-resolution compounds identified in a large screen of 2000 well-characterized and approved drugs. All four of these drugs accelerated the resolution of the inflammation and three of them also inhibited neutrophil migration towards the wound [96]. Other compounds containing this benzopyrone structure were shown to have similar effects and the most active one, isopimpinellin, was found to inhibit the

recruitment of leukocytes (by inhibiting PI3K), and to promote the resolution phase (by inducing neutrophil apoptosis) [97].

Natural compound libraries are rich sources for drug discovery. Various natural products have been demonstrated to have an inhibitory effect on the infiltration of leukocytes near the wounded area, including extracts from the medicinal herb ginseng (roots of plants in the genus *Panax*, such as *Panax ginseng*) [98]. One of the bioactive compounds in these extracts was shown to be the ginsenoside Rg1, a glycosylated steroid that exerts its anti-inflammatory activity through the glucocorticoid receptor (GR) [99]. Similar effects on leukocyte migration have been observed for an essential oil from *Thymus vulgaris* [100], for the coumarin-derivative bergapten isolated from *Ficus hirta* roots [101], for an extract from the green seaweed *Cymopolia barbata* and its major active component, cymopol [102], and for the compound *micrometam C* isolated from *Micromelum falcatum* trees, which are mangrove associates [103]. Downregulation of the expression of various pro-inflammatory genes and upregulation of the anti-inflammatory gene *il10* in the tail-wounding assay was found for an extract from *Clerodendrum cyrtophyllum* Turcz leaves [104]. Inhibition on tail wound-induced ROS generation was shown for a metabolite isolated from the red seaweed *Laurencia snackeyi*, 5 β -Hydroxypalisadin B [105], for bergapten [101] and for the polysaccharide fucoidan, extracted from the brown seaweed *Ecklonia cava* [106]. The latter two compounds also attenuated the inflammatory response by inhibiting the synthesis of Nitric Oxide (NO), which is an important inflammatory mediator. Enhancement of the resolution of the inflammation, by promoting neutrophil apoptosis and reverse migration, was demonstrated for tanshinone IIA, a compound extracted from the root of the plant species *Salvia miltiorrhiza* [96].

Table 1. Overview of zebrafish models for inflammation.

Inflammatory models	Age	Treatment	Inflammatory responses	References
Tail wounding-induced inflammation				
Transection	2-5 dpf	Amputation	Accumulation of macrophages and neutrophils; increased ROS production; upregulated inflammatory genes	[46, 61-63]
	2-4 dpf	Incision	Accumulation of macrophages and neutrophils; increased ROS production;	[47, 57, 62]
Laser	4 dpf	Epidermis	Accumulation of neutrophils	[54]
	22 hpf	Yolk sac	Accumulation of macrophages	[55, 57]
	1-2 dpf	Skeletal muscle	Myofibril damage	[56]
	2-3 dpf	Tail fin	Accumulation of macrophages and neutrophils; ROS signaling; upregulated inflammatory genes (<i>tnfa</i>)	[59, 60]
Chemical-induced inflammation				
LPS	1-3 dpf	Immersion	Increased ROS and NO production; upregulated inflammatory genes (<i>il1b, tnfa, il10, p65, nfkb1a</i>)	[107, 108]
	3 dpf	Yolk injection	Accumulation of macrophages and neutrophils; upregulated inflammatory genes (<i>il1b, tnfa, il6</i>)	[109]
CuSO ₄	2-7 dpf	Immersion	Hair cell death; infiltration of macrophages and neutrophils; oxidative stress	[110-114]
	Adult	Immersion	Oxidative damage and apoptosis in the gills; upregulated inflammatory genes (<i>tnfa, mmp9, myd88, il6, il8</i>)	[115-117]
LTB ₄	3 dpf	Otic vesicle injection	Neutrophil recruitment	[77, 118, 119]
	2 dpf	Hindbrain injection	Macrophage recruitment	[120]
	3 dpf	Immersion	Neutrophil accumulation in the fin	[33, 63]
Enterocolitis	3-8 dpf	TNBS immersion	Gut dilation; loss of villi and clefts; infiltration of neutrophils; increased number of goblet cells; upregulation of inflammatory genes (<i>il1b, tnfa, mmp9, ccl20, il8</i>)	[121, 122]
	3-6 dpf	DSS immersion	Mucus accumulation; infiltration of neutrophils; reduced proliferation; upregulation of inflammatory genes (<i>il1b, tnfa, mmp9, ccl20, il8, il23</i>)	[123]
	3-6 dpf	Glafenine immersion	Intestinal epithelial cell apoptosis and shedding; ER stress	[124, 125]
	Adult	TNBS intrarectal injection	Epithelial disruption; neutrophil infiltration; upregulation of inflammatory genes (<i>il1b, tnfa, il8, il10</i>)	[126]

	Adult	Oxazolone intrarectal injection	Epithelial damage; infiltration of granulocytes; goblet cell depletion; upregulation of inflammatory genes (<i>il1b</i> , <i>tnfa</i> , <i>il10</i>)	[127]
Mutation-induced inflammation				
<i>hai1a</i>	1-3 dpf		Epidermal defects (skin); leukocyte accumulation; enhanced keratinocytes apoptosis; upregulation of inflammatory genes (<i>mmp9</i>)	[128-130]
<i>cdipt</i>	5-6 dpf		Intestinal damage; reduced mucos ecretion; infiltration of macrophages and neutrophils; goblet cell apoptosis; impaired proliferation; ER stress; upregulation of inflammatory genes	[131, 132]

Table 2. Overview of drugs showing anti-inflammatory effects in zebrafish inflammation models

Inflammatory models	Drugs showing anti-inflammatory effect	References
Tail amputation	Extract from <i>Clerodendrum cyrtophyllum</i> Turcz	[104]
	Extract from <i>Cymopolia barbata</i> and its major active component cymopol	[102]
	Ginsenoside Rg1 from ginseng; beclomethasone	[99]
	ErbB kinase inhibitors	[94]
	Extracts from ginseng	[98]
	Bergapten from <i>Ficus hirta</i>	[101]
	Meisoindigo, a derivative of indirubin	[95]
	Analogs of thalidomide	[93]
	<i>Mircometam C</i> from <i>Micromelum falcatum</i>	[103]
	Isopimpinellin from the Apiaceae family, and other compounds containing a benzopyrone structure	[96, 97]
	Tanshinone IIA from <i>Salvia miltiorrhiza</i> ; dexamethasone	[96]
Approved drugs (eg: glipizide, tetracycline HCl, dexamethasone)	[92]	
5 β -Hydroxypalisadin B from <i>Laurencia snackeyi</i> ; dexamethasone	[105]	
Fucoidan from <i>Ecklonia cava</i>	[106]	
Tail incision	Essential oil from <i>Thymus vulgaris</i>	[100]
LPS immersion	Polyphyllin VII from <i>Paris polyphylla</i>	[133]
	Caffeine	[134]
	Oleuropein from <i>Olea europaea</i>	[135]
	Polyphenol-rich extract from <i>Ecklonia cava</i>	[136]
	5 β -Hydroxypalisadin B from <i>Laurencia snackeyi</i> ; dexamethasone	[105]
Fucoidan from <i>Ecklonia cava</i>	[106]	
LPS injection	Phillyrin from <i>Forsythia suspensa</i> Vahl; dexamethasone	[137]
	Extracts from <i>Chimonanthus nitens</i> Oliv.; dexamethasone	[138]
	Chlorogenic acid	[109]
CuSO ₄ immersion	Extract from <i>Clerodendrum cyrtophyllum</i> Turcz	[104]
	Enzymatic peptide from skipjack (<i>Katsuwonus pelamis</i>); indometacin	[139]
	Terpene glycoside from <i>Sanguisorba officinalis</i>	[140]
	Polyphyllin VII from <i>Paris polyphylla</i>	[133]
	Pituitary adenylate cyclase-activating polypeptide(PACAP)-38)	[141]
	Extract from Quzhou Fructus Aurantii; indometacin	[142]
Clinically approved drugs (eg: tenatoprazole, candesartan)	[143]	
TNBS immersion	Cholecystokinin; dopamine receptor agonists; dexamethasone	[144]
	5-aminosalicylic acid; prednisolone	[121, 122]
	NOS inhibitors; thalidomide; parthenolide;	[121]
DSS immersion	Cholecystokinin; dopamine receptor agonists	[144]
	Retinoic acid; dexamethasone	[123]

2.2. Chemical-induced inflammation

2.2.1. LPS-induced inflammation

Lipopolysaccharide (LPS) is an endotoxin in the cell walls of Gram-negative bacteria which acts as a PAMP that induces the innate immune response upon recognition by TLRs [145]. LPS-induced inflammation in zebrafish is generally established by non-invasive immersion of embryos in egg medium containing LPS [107, 146] or injection into the yolk [109] (Fig. 2B). In mammals, the immune response to LPS is characterized by TLR4-mediated induction of NF- κ B and the expression of various inflammatory mediators, including TNF α and IL-1 [147, 148]. However, the TLR4 paralogs identified in zebrafish do not recognize LPS, due to the differences in extracellular structures for recognition and the lack of essential costimulatory molecules [149-151].

Despite the poorly characterized recognition mechanism for LPS, a response similar to that observed in mammals has been observed, indicating a high degree of conservation between the zebrafish and mammalian transcription factors and signaling pathways in response to LPS stimulation [152, 153]. LPS stimulation enhanced the production of NO and ROS, increased the levels of iNos and Cox2 proteins, and the mRNA levels for *p65*, *nfkbiaa* and other genes encoding key pro-inflammatory cytokines including *tnfa* and *il1b* [107, 108]. Pre-treatment of zebrafish with a sublethal dose of LPS was shown to prevent mortality as a result of a subsequent lethal dose of LPS, which demonstrates that tolerance, generally observed in mammals, can be reproduced in zebrafish. *Cxcr4* signaling appeared to play an important role in the occurrence of LPS tolerance [146, 154].

LPS-induced inflammation in zebrafish has been used as a model for research on anti-inflammatory drugs. A lot of compounds and extracts from traditional medicinal or non-medicinal herbs were tested using this model, and several of these showed inhibition on LPS injection-induced inflammation. Chlorogenic acid, a polyphenolic compound which occurs in coffee and phillyrin (the main ingredient in *Forsythia suspensa* Vahl fruits) inhibited macrophage and neutrophil recruitment to the site where LPS was injected, and improved the survival rate [109, 137]. The latter compound inhibited the MyD88/NF- κ B signalling pathway by decreasing expression levels of genes encoding I κ B α , IL-1 β , IL-6, and Tnf- α [137]. Extracts from *Chimonanthus nitens* Oliv. leaves also inhibited recruitment of neutrophils (and not macrophages), reduced the LPS-induced upregulation of *il1b*, *il6* and *tnfa* expression [138].

In many studies, the ROS and/or NO production have been used as a readout for the anti-inflammatory effect. Polyphyllin VII (PP7) from *Paris polyphylla* inhibited NO generation, and also decreased the heartbeat and attenuated the yolk sac edema after LPS injection into the yolk sac [133]. Fucoïdan and

a polyphenol-rich fraction extracted from *Ecklonia cava* inhibited both NO and ROS formation [106, 136], just like the compound 5 β -Hydroxypalisadin B, which was also shown to be anti-inflammatory in the tail-wounding model [105]. The polyphenol-rich fraction extracted from *Ecklonia cava* also decreased cell death and improved survival [136]. In some reports, only the NO generation was used as an indicator for the anti-inflammatory effect of drugs, and this has been used to demonstrate the effects of caffeine [134] and oleuropein, a phenolic compound present in olives and leaves of the olive tree (*Olea europaea*) [135].

Apolipoprotein(apo)A-I is one of the major constituents of high-density lipoproteins (HDLs) which has been shown to have anti-inflammatory effects [155]. The role of apoA-I modification was tested in zebrafish embryos by co-injecting LPS and HDLs containing either native or glycated apoA-I. The results demonstrated a reduced mortality upon injection of HDLs with native apoA-I, probably due to its anti-inflammatory effect [156].

LPS treatment has also been used in combination with tail wounding to enhance leukocyte accumulation near the wound. This model was utilized to evaluate the bioactivity of structurally diverse natural products of an East African medicinal plant, *Rhynchosia viscosa*, resulting in the identification of both known and novel isoflavone derivatives with anti-inflammatory activity [157, 158].

2.2.2. Copper-induced inflammation

Copper is a trace element acting as a catalytic cofactor for various enzymes involved in energy and antioxidant metabolism [159]. Excessive inorganic copper from the environment could disturb the copper balance in zebrafish and lead to an inflammatory response mediated by damage from the oxidative stress [160]. In adults, soluble copper was reported to induce oxidative damage and apoptosis in the gills and showed dose-dependent lethality [115, 116]. Upon copper sulfate (CuSO₄) treatment, the neutrophils in the kidney marrow were found to be activated, and analysis of the proteome of neutrophils revealed regulation of proteins involved in cell cycle, NO signaling, regulation of cytoskeleton and immune-related processes [117].

Exposure of zebrafish embryos to CuSO₄ was reported to inhibit the survival and development of embryos [161, 162]. It induces an inflammatory status, which is related to exacerbated damage and oxidative stress, and the endogenous signaling molecule adenosine was shown to be involved [113]. Importantly, within two hours this treatment induces death of hair cells in the neuromasts of the lateral line, which regenerate and reach full functionality one day later [110, 111]. This damage to the neuromasts results in a localized robust inflammatory response in the neuromasts, including the

infiltration of macrophages and neutrophils [112] (Fig. 2C). The recruited macrophages play a critical role in the regeneration of damaged hair cells since ablation of macrophages significantly delays this process, while neutrophils are not required [114].

The accumulation of neutrophils in the neuromasts is one of the most frequently used indicators for the level of inflammation in this model and has been applied to assess the effect of known anti-inflammatory drugs [112]. Since the induction of inflammation by CuSO₄ can be established by just adding the compound into the culture medium, an automated high-throughput drug screening assay could be developed with this model based on leukocyte accumulation around neuromasts, using a double transgenic line with the neutrophils labelled in red and the neuromasts in green (using the claudin b (*cl دنب*) promoter driving GFP expression) [112, 163]. Using this automated system, various drugs from a library of clinically approved drugs were identified to have an anti-inflammatory effect, among which the NOS1 inhibitor 3-Bromo-7-nitroindazole. Further investigation revealed a novel pro-inflammatory role of NO signaling via soluble guanylate cyclase and in a soluble guanylate cyclase - independent manner through protein S-nitrosylation [143].

Furthermore, a neuropeptide, pituitary adenylate cyclase-activating polypeptide(PACAP)-38, known to be an anti-apoptotic and anti-inflammatory factor, was reported to inhibit neutrophil migration towards the neuromasts and expression of pro-inflammatory genes (*il8*, *il1b*, *il6* and *atf3*) [141]. Several natural products were reported to exert an inhibitory effect on the CuSO₄-induced neutrophil accumulation, including a new terpene glycoside extracted from the root of *Sanguisorba officinalis* [140], an enzymatic peptide (SEP) from skipjack (*Katsuwonus pelamis*) [139] and an extract from Quzhou Fructus Aurantii, an unripe fruit from the bitter orange tree (*Rutaceae Citrus changshan-huyou* Y.B. Chang) [142]. The compound PP7 (from *Paris polyphylla*) also showed an inhibition of the neutrophil migration upon CuSO₄ stimulation, similar to what was observed for this compound in the LPS-induced inflammation model [133]. An extract from leaves of *Clerodendrum cyrtophyllum* Turcz decreased the oxidative stress induced by CuSO₄ and inhibited inflammation by downregulating genes related to inflammatory processes (*cox2*, *pla2*, *c3a*, *mpx*) and cytokines (*il1b*, *il8*, *tnfa* and *il10*) [104].

2.2.3. LTB₄-induced inflammation

Leukotriene B₄ (LTB₄) is an eicosanoid released by leukocytes, acting as a pro-inflammatory mediator and enhancing leukocyte accumulation at sites of inflammation [164, 165]. In zebrafish, LTB₄ was demonstrated to attract both neutrophils and macrophages [119, 120]. Upon injection of LTB₄ into the otic vesicle of 3 dpf zebrafish larvae, neutrophil recruitment to the ear was observed at one hour after the injection, and this recruitment was not dependent on Cxcl8/Cxcr2 signaling [77, 118] (Fig. 2D). In addition, injection of LTB₄ into the hindbrain at 30 hpf recruited macrophages independent of

Cxcl11aa/Cxcr3.2 signaling [120]. Bath application of LTB₄ induced dissemination of neutrophils into fins, which can be quantitated by counting cells in the ventral fin (Fig. 2D'). This LTB₄-induced migration of neutrophils was not prevented by inhibition of the Cxcl8/Cxcr2 signaling pathway either [118], or by DPI or Lyn knockdown [63]. A Zebrafish Entrapment by Restriction Array (ZEBRA) microfluidic device was designed to quickly position zebrafish embryos and larvae in a predictable array, suitable for automated imaging. The effectiveness of this device was demonstrated by assessing the inhibitory effect of the PI3K inhibitor LY294002 on LTB₄-induced neutrophil migration [33]. The device can be designed with access ports to enable the administration of treatments, and it could potentially be used for other inflammation assays like tail wounding as well [33].

2.2.4. Chemical-induced intestinal inflammation

Inflammatory bowel disease (IBD) represents a group of intestinal disorders that are characterized by inflammation of the digestive tract [8]. IBD is modeled in zebrafish by treatment of fish with chemicals that induce an IBD-like enterocolitis [166] (Fig. 2E). In adult zebrafish, intrarectal administration of the hapten oxazolone was reported to induce enterocolitis, characterized by infiltration of granulocytes, epithelial damage, goblet cell depletion and upregulated expression of genes encoding cytokines (*il1b*, *tnfa*, *il-10*) [127]. Similar results were obtained upon intrarectal administration in adult zebrafish of another hapten, trinitrobenzene sulfonic acid (TNBS), which was also shown to increase the intestinal mRNA and peptide levels of melanin-concentrating hormone (Mch) and the mRNA levels encoding its receptor [126].

Immersion of larvae in egg water containing TNBS between 3 and 8 dpf induced an inflammatory response in the gut [121]. Using a fluorescent dye, which was swallowed by the fish, the gut architecture and motility could be assessed, showing TNBS-induced dilation of the gut, reduction in villus length, expansion of crypts, and a loss of peristalsis. Throughout the length of the gut, histological analysis showed an expansion of the lumen, a smoothening of the gut lining which was devoid of villi and clefts, and an increase in the number of goblet cells [121]. The reported changes in intestinal cell morphology were not observed in a different study in which different doses and durations of TNBS exposure were used [122]. In this study an increased number of neutrophils in the inflamed intestine and increased expression of *il1b*, *tnfa*, *mmp9*, *ccl20* and *il8* was observed upon TNBS treatment [122].

Exposure of zebrafish larvae to the detergent dextran sodium sulfate (DSS) has also been utilized to induce intestinal inflammation. This treatment recapitulates several aspects of TNBS-induced enterocolitis, inducing symptoms such as elevated expression of pro-inflammatory genes and neutrophil recruitment around the intestine [123]. However, the inflammatory phenotype was not identical to that induced by TNBS, and DSS treatment actually protects against TNBS-induced

enterocolitis [123]. The non-steroidal anti-inflammatory drug glafenine has also been used in zebrafish larvae to induce intestinal injury after 12 hours of exposure, which is characterized by profound intestine-specific pathological changes. Glafenine was shown to induce intestinal epithelial cell apoptosis and shedding, which resulted from ER stress and the induction of the unfolded protein response [124]. The inhibition of multidrug resistance (MDR) efflux pumps by glafenine appeared to play an important role in the intestinal epithelial cell shedding. This shedding plays a protective role by restricting inflammation and promoting survival [125].

Just like in humans suffering from IBD and in mouse models of IBD [167], the variable composition of the gut microbiota was demonstrated to be an important determinant of intestinal inflammation in zebrafish. Treatment of adult zebrafish with vancomycin or colistin sulphate differentially affected the components of the intestinal microbiota, which influenced the severity of the oxazolone-induced enterocolitis and the composition of the intestinal leukocyte infiltration [127]. In larvae, treatment with the broad-spectrum antibiotics kanamycin and ampicillin, which resulted in a severe loss of microbiota, decreased mortality after TNBS exposure, and inhibited the induction of pro-inflammatory gene expression and leukocyte migration to the intestine [122]. Using a protocol to generate germ-free zebrafish larvae, it was confirmed that the TNBS-induced pathology, including histological changes and an increased expression of genes encoding pro-inflammatory cytokines, entirely depended on the presence of resident microbiota [168]. TNBS-induced enterocolitis in larvae increased the proportion of *Proteobacteria* (especially *Burkholderia*) and decreased the relative number of Firmicutes (*Lactobacillus* group) in the composition of the larval microbiota, and these changes correlated with the severity of the enterocolitis [169]. Cotreatment with excretory-secretory products from the nematode *Anisakis* showed a suppression on TNBS-induced mortality and pro-inflammatory gene expression in adult zebrafish, suggesting that the exposure to the immunomodulatory effects of parasitic helminths could be protective against IBD [170].

Validation of the larval TNBS-induced enterocolitis model was further performed using known (steroidal and non-steroidal) anti-inflammatory and antibiotic drug treatments which ameliorated the response to TNBS [121, 122]. A small drug screen was performed using this model as well, in which NOS inhibitors and thalidomide and parthenolide were tested. Whereas all compounds showed a reduction of *tnfa* expression, only the NOS inhibitors rescued the *in vivo* disease phenotype, assessed by histological analysis [121]. Similarly, the DSS-induced model was validated by demonstrating the role of retinoic acid (RA) in suppressing the pathological intestinal mucin production [123]. In addition, the DSS- and TNBS-induced larval enterocolitis models have been used for screening small molecules from a large clinical compound library using the neutrophil accumulation in the intestine as a readout [144]. Most of the hits were known antibiotics or anti-inflammatory agents, confirming the validity of

the screening assay. Novel drug hits were also identified using this assay, such as cholecystokinin (CCK) and dopamine receptor agonists, and the involvement of these receptors was confirmed by using CCK and dopamine receptor antagonists, which were shown to exacerbate inflammation in these models [144].

2.3. Mutation-induced inflammation

2.3.1. The *hai1a* mutant

To identify genes with essential functions during zebrafish skin development, a screen of mutants generated by insertional mutagenesis was performed [171], and a mutant line was identified carrying an insertion in the hepatocyte growth factor activator inhibitor 1a gene (*hai1a*, also known as *spint11b*) [128, 129]. Hai1a is known to be an inhibitor of serine proteases, in particular of Matriptase 1a. The *hai1a* mutant zebrafish larvae display a phenotype reminiscent of the human condition psoriasis: the basal keratinocytes in the epidermis lose their regular polygonal shape and the tight contact to adjacent cells, form aggregates and display enhanced apoptosis. These epidermal defects induce an inflammatory response in the skin, which is illustrated by leukocytes strongly accumulating near aggregates of keratinocytes with apoptotic cells at 1 dpf [128, 129]. The mutant neutrophils display a more random motility, but retain their ability to respond to directional signals [129]. A microarray transcriptome analysis showed that the expression of pro-inflammatory genes was increased in the mutant fish [130]. Among those genes, matrix metalloproteinase 9 gene (*mmp9*) played a critical role. Morpholino knockdown of *mmp9* partially rescued the abnormal epithelial phenotype as well as the neutrophilic infiltration of the epithelium, and restored the organization of collagen fibers.

2.3.2. The *cdipt* mutant

Screening the same collection of insertional mutants, in which the *hai1a* mutant was found [171], for liver defects, a mutant with an insertion in the cdp-diacylglycerolinositol 3-phosphatidyltransferase (*cdipt*) gene was identified [131]. Cdipt, also known as Phosphatidylinositol synthase, has an indispensable role in the synthesis of a critical phospholipid, phosphatidylinositol (PtdIns). The mutant larvae displayed chronic endoplasmic reticulum (ER) stress which contributes to hepatic steatosis around 5 dpf, resembling features of nonalcoholic fatty liver disease in humans [131]. A mild inflammatory response was observed, reflected by the presence of macrophages adjacent to necrotic hepatocytes and increased expression of inflammatory genes. More recently, it was reported that the *cdipt* mutant shows a pathological phenotype in the gastro-intestinal tract reminiscent of IBD [132]. The PtdIns deficiency led to an ER stress-mediated cytopathology in intestinal epithelial cells, including vacuolation, microvillus atrophy and impaired proliferation, subsequently resulting in reduced mucus

secretion, goblet cell apoptosis, autophagy, and bacterial overgrowth. Eventually, this results in an inflammatory response, reflected by the infiltration of macrophages and neutrophils into the intestines. The inflammation could be suppressed by antibiotics and anti-inflammatory drugs, but these treatments failed to suppress the ER stress phenotype. Treatment of mutant larvae with phenylbutyric acid (PBA), a small chemical chaperone and a well-established drug proven to reduce ER stress, was shown to alleviate the mutant phenotype [132].

3. The use of zebrafish inflammation models for research on glucocorticoid drugs

Steroidal anti-inflammatory drugs, also referred to as GCs, have been studied extensively using zebrafish inflammation models. This research has focused on the molecular mechanisms underlying the anti-inflammatory action of these compounds and aims at the development of novel GC drugs. In addition, due to their well-characterized anti-inflammatory effects, GCs are frequently used as a positive control in anti-inflammatory drug screens and the golden standard for anti-inflammatory drugs, and therefore provide a useful method for validation of novel animal models for inflammation.

GCs are a class of steroid hormones secreted by the adrenal gland, regulating a wide variety of systems in the body, like the immune, metabolic, reproductive, cardiovascular and central nervous system [172-174]. In humans, the secretion of the main endogenous GC, cortisol, shows a diurnal pattern, is greatly enhanced upon stress, and is mainly regulated by the hypothalamic-pituitary-adrenal (HPA) axis [175, 176]. The immune-suppressive effects of GCs were first reported by Hench et al. (1949), who demonstrated that adrenocorticotrophic hormone (ACTH) and cortisone improved clinical features of rheumatoid arthritis patients [177]. Subsequently, GCs were soon applied in eye inflammation [178, 179], and currently GCs are frequently prescribed worldwide to treat various immune-related diseases, including asthma, rheumatoid arthritis, dermatitis, leukemia, several autoimmune diseases and even some cancers, due to their potent and well-established anti-inflammatory and immune-suppressive effects [180, 181]. These effects of GCs are mediated by an intracellular receptor, the glucocorticoid receptor (GR). GCs activate the translocation of this receptor from the cytoplasm to the nucleus, where it acts as a transcription factor, inducing the expression of anti-inflammatory genes and inhibiting the transcriptional activity of pro-inflammatory genes [180, 182].

Like in humans, the main endogenous GC hormone in fish is cortisol and its secretion is regulated by the hypothalamus-pituitary-interrenal (HPI) axis, the fish equivalent of the HPA axis [183, 184]. Zebrafish, similarly to humans, have a Gr that is encoded by a single *gr* gene [185, 186]. In addition, both zebrafish and humans express an alternative splice variant, Gr β , which is notably absent in mice

[186]. The zebrafish Gr is structurally and functionally highly similar to its mammalian equivalent, which includes the immune-suppressive action that is observed upon Gr activation in zebrafish [186, 187].

Upon tail amputation in embryos, treatment with several synthetic GCs has been shown to inhibit the migration of neutrophils towards the wounded site in a Gr-dependent manner. However, GCs leave the migration of macrophages unaffected [65, 71, 72, 79, 88]. The Gr-induced upregulation of the expression of the gene encoding MAPK phosphatase-1 (Mkp-1) was suggested to be involved in the inhibition of neutrophil migration, by inactivation of JNK, resulting in a reduced AP-1-induced transcriptional activation of pro-inflammatory genes [72]. Indeed, studying the transcriptome by microarray analysis showed that almost all wounding-induced changes in transcription were attenuated by GC treatment [71]. Although the chemotactic migration of macrophages is not affected by GCs, their differentiation towards a pro-inflammatory (M1) phenotype is inhibited upon GC treatment [79]. In a combined infection/tail wounding model, GCs were shown to inhibit the infection-induced expression in epidermal and/or epidermal cells of *irg1l*, thereby inhibiting the ROS production which is important for leukocyte migration [65]. In adult zebrafish, no effect of GC treatment on neutrophil recruitment upon tail wounding was detected [188]. In adult zebrafish models for brain and heart injuries, GCs were shown to inhibit the expression of pro-inflammatory genes like *il8*, *tnfa* and *il1b* and reduced the recruitment of leukocytes towards the wounded area [189, 190].

In the LPS-induced inflammation model, GC administration was reported to inhibit the production of ROS and NO, the expression of pro-inflammatory genes, the recruitment of leukocytes, and the mortality [105, 109, 137, 138]. In the Copper-induced inflammation model using CuSO₄ immersion of larvae, GCs also caused inhibition of neutrophil accumulation [112]. Similarly, utilizing the DSS-induced enterocolitis model, GCs were observed to inhibit the expression of pro-inflammatory genes and neutrophil infiltration [123]. Interestingly, in larvae from a CRISPR/Cas9-generated Gr mutant line, the DSS-induced increase in pro-inflammatory gene expression was abolished due to the deficiency in Gr signaling, suggesting a dual action, both pro- and anti-inflammatory, of GC signaling in the immune system [191].

The clinical use of GCs is severely limited by the severity of their side effects, which include diabetes and obesity, osteoporosis and impaired wound healing. Interestingly, these effects have been modeled in zebrafish as well, opening up the possibility to evaluate both the therapeutic anti-inflammatory effect and the adverse effects. GC effects on metabolism, including increased glucose concentrations, were observed in zebrafish embryos and the global transcriptional changes underlying these effects have been characterized [192]. GC-induced osteoporosis was modeled by treating larvae with GCs between 5 and 10 dpf and performing staining with alizarin red (which binds to calcified matrix) [193],

and studying extracellular matrix (ECM)-, osteoblast-, and osteoclast-related genes [194, 195]. Alternatively, regenerating scales that were removed from GC-treated adult fish have been used to model GC-induced osteoporosis [196]. Finally, inhibitory effects on tissue regeneration and wound healing have been shown in many zebrafish injury models. Inhibition of regeneration by GCs was observed after spinal motor neuron lesions in larvae [197], and in adult zebrafish after tail fin amputation, brain lesion, and cardiac injury, GCs were demonstrated to inhibit tissue regeneration [188-190, 198]. GC treatment of zebrafish embryos blocks the regeneration of the tail fin upon amputation through inhibition on blastemal formation and cell proliferation [88, 199]. Interestingly, the ginsenoside Rg1 was shown to inhibit neutrophil migration in a Gr-dependent manner, but did not show any effect on tissue regeneration. These data suggest that this compound may provide an interesting lead for the development of novel anti-inflammatory drugs with reduced side effects [99].

4. Concluding remarks

The use of animal models is a critical part of biomedical research and crucial for the development of novel drugs. A wide range of human disease models have been established in mammalian models such as rats and mice, which have largely contributed to the remarkable progress in our understanding of the mechanisms underlying these diseases and the development of novel therapies. However, the rodent systems have limitations such as the high cost of housing and breeding and they are not suited for large-scale automated screening. The development of the zebrafish animal model in the past decades has added a complementary system, which allows the performance of automated high through-put screening *in vivo*, mainly due to the small size and transparency of zebrafish larvae. The similarities of the immune system and inflammatory responses between zebrafish and mammals guarantee good translational value.

In order to model inflammatory diseases, three types of inflammation models have been developed in zebrafish: wounding-, chemical- and mutation-induced inflammation. These models have enabled a detailed investigation of the cellular and molecular mechanisms underlying the inflammatory response, adding to our knowledge of the mechanisms of leukocyte behavior and the identification of potential drug targets. For example, using the zebrafish model, it was observed for the first time that a tissue-scale H₂O₂ gradient is created during the onset of an inflammatory response which signals to leukocytes in the tissues [61], and that Lyn acts as a redox sensor to mediate the migration of leukocyte [63]. In addition, the described models have been used for the screening of compound libraries. This has led to the discovery of important novel targets for anti-inflammatory drugs, such as ErbBs [94]. Moreover, various drug candidates were tested or identified, such as natural extracts (e.g. fucoidan [106], tashinone IIA [96] and cymopol [102]), thalidomide analogs [93], and the PI3K inhibitor LY294002

[33]). In summary, these zebrafish inflammation models have been shown to be very useful to unravel the molecular and cellular aspects of the inflammatory response and for the discovery of novel drug targets. Besides, these models have proven to be effective screening tools for candidate drugs, providing an intermediate between in vitro assays and rodent experiments with great potential to accelerate the preclinical phase of anti-inflammatory drug development.

References

1. Netea, M.G., et al., *A guiding map for inflammation*. Nature immunology, 2017. **18**(8): p. 826.
2. Chen, L., et al., *Inflammatory responses and inflammation-associated diseases in organs*. Oncotarget, 2018. **9**(6): p. 7204.
3. Takeuchi, O. and S. Akira, *Pattern recognition receptors and inflammation*. Cell, 2010. **140**(6): p. 805-820.
4. MacLeod, A.S. and J.N. Mansbridge, *The Innate Immune System in Acute and Chronic Wounds*. Adv Wound Care (New Rochelle), 2016. **5**(2): p. 65-78.
5. Bonecchi, R., et al., *Chemokines and chemokine receptors: an overview*. Frontiers in bioscience (Landmark edition), 2009. **14**: p. 540.
6. Marrack, P., J. Kappler, and B.L. Kotzin, *Autoimmune disease: why and where it occurs*. Nature medicine, 2001. **7**(8): p. 899-905.
7. Ngoc, L.P., et al., *Cytokines, allergy, and asthma*. Current opinion in allergy and clinical immunology, 2005. **5**(2): p. 161-166.
8. Hanauer, S.B., *Inflammatory bowel disease: epidemiology, pathogenesis, and therapeutic opportunities*. Inflammatory bowel diseases, 2006. **12**(suppl_1): p. S3-S9.
9. Mathis, D. and S.E. Shoelson, *Immunometabolism: an emerging frontier*. 2011, Nature Publishing Group.
10. Grivennikov, S.I., F.R. Greten, and M. Karin, *Immunity, inflammation, and cancer*. Cell, 2010. **140**(6): p. 883-899.
11. DeLegge, M.H. and A. Smoke, *Neurodegeneration and inflammation*. Nutrition in clinical practice, 2008. **23**(1): p. 35-41.
12. Geovanini, G.R. and P. Libby, *Atherosclerosis and inflammation: overview and updates*. Clinical Science, 2018. **132**(12): p. 1243-1252.
13. Merad, M. and J.C. Martin, *Pathological inflammation in patients with COVID-19: a key role for monocytes and macrophages*. Nature Reviews Immunology, 2020: p. 1-8.
14. Kaufmann, S.H. and A. Dorhoi, *Inflammation in tuberculosis: interactions, imbalances and interventions*. Current opinion in immunology, 2013. **25**(4): p. 441-449.
15. Li, P., Y. Zheng, and X. Chen, *Drugs for Autoimmune Inflammatory Diseases: From Small Molecule Compounds to Anti-TNF Biologics*. Frontiers in Pharmacology, 2017. **8**(460).
16. Antman, E.M., et al., *Use of nonsteroidal antiinflammatory drugs: an update for clinicians: a scientific statement from the American Heart Association*. Circulation, 2007. **115**(12): p. 1634-1642.
17. Moghadam-Kia, S. and V.P. Werth, *Prevention and treatment of systemic glucocorticoid side effects*. International journal of dermatology, 2010. **49**(3): p. 239-248.
18. Senolt, L., *Emerging therapies in rheumatoid arthritis: focus on monoclonal antibodies*. F1000Research, 2019. **8**.
19. O'Neill, L.A., *Targeting signal transduction as a strategy to treat inflammatory diseases*. Nature reviews Drug discovery, 2006. **5**(7): p. 549-563.
20. Streisinger, G., et al., *Production of clones of homozygous diploid zebra fish (Brachydanio rerio)*. Nature, 1981. **291**(5813): p. 293-296.

21. Engeszer, R.E., et al., *Zebrafish in the wild: a review of natural history and new notes from the field*. *Zebrafish*, 2007. **4**(1): p. 21-40.
22. Eaton, R.C. and R.D. Farley, *Spawning Cycle and Egg Production of Zebrafish, Brachydanio rerio, in the Laboratory*. *Copeia*, 1974. **1974**(1): p. 195-204.
23. Avdesh, A., et al., *Regular care and maintenance of a zebrafish (Danio rerio) laboratory: an introduction*. *JoVE (Journal of Visualized Experiments)*, 2012(69): p. e4196.
24. Lieschke, G.J. and P.D. Currie, *Animal models of human disease: zebrafish swim into view*. *Nat Rev Genet*, 2007. **8**(5): p. 353-67.
25. Barut, B.A. and L.I. Zon, *Realizing the potential of zebrafish as a model for human disease*. *Physiological Genomics*, 2000. **2**(2): p. 49.
26. Vogel, G., *Sanger Will Sequence Zebrafish Genome*. *Science*, 2000. **290**(5497): p. 1671.
27. Tavares, B. and S. Santos Lopes, *The Importance of Zebrafish in Biomedical Research*. *Acta Medica Portuguesa*, 2013. **26**(5): p. 583-592.
28. Patton, E.E. and D.M. Tobin, *Spotlight on zebrafish: the next wave of translational research*. 2019, The Company of Biologists Ltd.
29. Amatruda, J.F., et al., *Zebrafish as a cancer model system*. *Cancer Cell*, 2002. **1**(3): p. 229-231.
30. Prouty, M.G., et al., *Zebrafish-Mycobacterium marinum model for mycobacterial pathogenesis*. *FEMS Microbiology Letters*, 2003. **225**(2): p. 177-182.
31. Brownlie, A., et al., *Positional cloning of the zebrafish sauterne gene: a model for congenital sideroblastic anaemia*. *Nat Genet*, 1998. **20**(3): p. 244-50.
32. Carvalho, R., et al., *A high-throughput screen for tuberculosis progression*. *PloS one*, 2011. **6**(2).
33. Bischel, L.L., et al., *Zebrafish Entrapment By Restriction Array (ZEBRA) device: a low-cost, agarose-free zebrafish mounting technique for automated imaging*. *Lab Chip*, 2013. **13**(9): p. 1732-6.
34. Meijer, A. and H. Spaik, *Host-pathogen interactions made transparent with the zebrafish model*. *Current drug targets*, 2011. **12**(7): p. 1000-1017.
35. Strecker, T.R., et al., *The effects of the glucocorticoid, dexamethasone, on the development of the Drosophila embryo*. *Roux's archives of developmental biology*, 1995. **204**(6): p. 359-368.
36. Burns, A.R., et al., *A predictive model for drug bioaccumulation and bioactivity in Caenorhabditis elegans*. *Nature chemical biology*, 2010. **6**(7): p. 549.
37. Herbomel, P., B. Thisse, and C. Thisse, *Ontogeny and behaviour of early macrophages in the zebrafish embryo*. *Development*, 1999. **126**(17): p. 3735-3745.
38. Hermann, A.C., et al., *Development of a respiratory burst assay using zebrafish kidneys and embryos*. *Journal of immunological methods*, 2004. **292**(1-2): p. 119-129.
39. Bennett, C.M., et al., *Myelopoiesis in the zebrafish, Danio rerio*. *Blood, The Journal of the American Society of Hematology*, 2001. **98**(3): p. 643-651.
40. Lieschke, G.J., et al., *Morphologic and functional characterization of granulocytes and macrophages in embryonic and adult zebrafish*. *Blood*, 2001. **98**(10): p. 3087-3096.
41. Langenau, D.M. and L.I. Zon, *The zebrafish: a new model of T-cell and thymic development*. *Nature Reviews Immunology*, 2005. **5**(4): p. 307-317.
42. Lam, S.H., et al., *Development and maturation of the immune system in zebrafish, Danio rerio: a gene expression profiling, in situ hybridization and immunological study*. *Developmental & Comparative Immunology*, 2004. **28**(1): p. 9-28.
43. Page, D.M., et al., *An evolutionarily conserved program of B-cell development and activation in zebrafish*. *Blood*, 2013. **122**(8): p. e1-11.
44. Henry, K.M., et al., *Zebrafish as a model for the study of neutrophil biology*. *Journal of leukocyte biology*, 2013. **94**(4): p. 633-642.
45. Shelef, M.A., S. Tauzin, and A. Huttenlocher, *Neutrophil migration: moving from zebrafish models to human autoimmunity*. *Immunological reviews*, 2013. **256**(1): p. 269-281.
46. Renshaw, S.A., et al., *A transgenic zebrafish model of neutrophilic inflammation*. *Blood*, 2006. **108**(13): p. 3976-8.

47. Mathias, J.R., et al., *Resolution of inflammation by retrograde chemotaxis of neutrophils in transgenic zebrafish*. Journal of leukocyte biology, 2006. **80**(6): p. 1281-1288.
48. Lee, Y., et al., *Fgf signaling instructs position-dependent growth rate during zebrafish fin regeneration*. Development, 2005. **132**(23): p. 5173-5183.
49. Hall, C., et al., *The zebrafish lysozyme C promoter drives myeloid-specific expression in transgenic fish*. BMC developmental biology, 2007. **7**(1): p. 42.
50. Bernut, A., et al., *Mycobacterium abscessus cording prevents phagocytosis and promotes abscess formation*. Proc Natl Acad Sci U S A, 2014. **111**(10): p. E943-52.
51. Ellett, F., et al., *mpeg1 promoter transgenes direct macrophage-lineage expression in zebrafish*. Blood, The Journal of the American Society of Hematology, 2011. **117**(4): p. e49-e56.
52. Walton, E.M., et al., *The macrophage-specific promoter mfap4 allows live, long-term analysis of macrophage behavior during mycobacterial infection in zebrafish*. PloS one, 2015. **10**(10): p. e0138949.
53. Li, L., et al., *Live imaging reveals differing roles of macrophages and neutrophils during zebrafish tail fin regeneration*. Journal of Biological Chemistry, 2012. **287**(30): p. 25353-25360.
54. Feng, Y., et al., *Live imaging of innate immune cell sensing of transformed cells in zebrafish larvae: parallels between tumor initiation and wound inflammation*. PLoS biology, 2010. **8**(12).
55. Redd, M.J., et al., *Imaging macrophage chemotaxis in vivo: studies of microtubule function in zebrafish wound inflammation*. Cell motility and the cytoskeleton, 2006. **63**(7): p. 415-422.
56. Otten, C. and S. Abdelilah-Seyfried, *Laser-inflicted injury of zebrafish embryonic skeletal muscle*. JoVE (Journal of Visualized Experiments), 2013(71): p. e4351.
57. Mathias, J.R., et al., *Characterization of zebrafish larval inflammatory macrophages*. Developmental & Comparative Immunology, 2009. **33**(11): p. 1212-1217.
58. Yoo, S.K., et al., *Differential regulation of protrusion and polarity by PI (3) K during neutrophil motility in live zebrafish*. Developmental cell, 2010. **18**(2): p. 226-236.
59. Miskolci, V., et al., *Distinct inflammatory and wound healing responses to complex caudal fin injuries of larval zebrafish*. Elife, 2019. **8**.
60. LeBert, D., et al., *Damage-induced reactive oxygen species regulate vimentin and dynamic collagen-based projections to mediate wound repair*. Elife, 2018. **7**: p. e30703.
61. Niethammer, P., et al., *A tissue-scale gradient of hydrogen peroxide mediates rapid wound detection in zebrafish*. Nature, 2009. **459**: p. 996.
62. Enyedi, B. and P. Niethammer, *H2O2: a chemoattractant?*, in *Methods in enzymology*. 2013, Elsevier. p. 237-255.
63. Yoo, S.K., et al., *Lyn is a redox sensor that mediates leukocyte wound attraction in vivo*. Nature, 2011. **480**: p. 109.
64. Hall, C.J., et al., *Immunoresponse gene 1 augments bactericidal activity of macrophage-lineage cells by regulating β -oxidation-dependent mitochondrial ROS production*. Cell Metab, 2013. **18**(2): p. 265-78.
65. Hall, C.J., et al., *Epidermal cells help coordinate leukocyte migration during inflammation through fatty acid-fuelled matrix metalloproteinase production*. Nat Commun, 2014. **5**: p. 3880.
66. Yoo, S.K., et al., *The role of microtubules in neutrophil polarity and migration in live zebrafish*. Journal of cell science, 2012. **125**(23): p. 5702-5710.
67. Lam, P.-y., et al., *The SH2-domain-containing inositol 5-phosphatase (SHIP) limits the motility of neutrophils and their recruitment to wounds in zebrafish*. Journal of cell science, 2012. **125**(21): p. 4973-4978.
68. Cvejic, A., et al., *Analysis of WASp function during the wound inflammatory response—live-imaging studies in zebrafish larvae*. Journal of cell science, 2008. **121**(19): p. 3196-3206.
69. Nguyen-Chi, M., et al., *Identification of polarized macrophage subsets in zebrafish*. Elife, 2015. **4**: p. e07288.
70. Mosser, D.M. and J.P. Edwards, *Exploring the full spectrum of macrophage activation*. Nat Rev Immunol, 2008. **8**(12): p. 958-69.

71. Chatzopoulou, A., et al., *Glucocorticoid-Induced Attenuation of the Inflammatory Response in Zebrafish*. *Endocrinology*, 2016. **157**(7): p. 2772-84.
72. Zhang, Y., et al., *In Vivo Interstitial Migration of Primitive Macrophages Mediated by JNK-Matrix Metalloproteinase 13 Signaling in Response to Acute Injury*. *The Journal of Immunology*, 2008. **181**(3): p. 2155-2164.
73. Liu, Y.-J., et al., *Cannabinoid receptor 2 suppresses leukocyte inflammatory migration by modulating the JNK/c-Jun/Alox5 pathway*. *Journal of Biological Chemistry*, 2013. **288**(19): p. 13551-13562.
74. Ren, D.-l., X.-b. Wang, and B. Hu, *Circadian gene period1b regulates proinflammatory cytokine expression through NF- κ B signalling in zebrafish*. *Fish & shellfish immunology*, 2018. **80**: p. 528-533.
75. Baggiolini, M. and I. Clark-Lewis, *Interleukin - 8, a chemotactic and inflammatory cytokine*. *FEBS letters*, 1992. **307**(1): p. 97-101.
76. Huber, A.R., et al., *Regulation of transendothelial neutrophil migration by endogenous interleukin-8*. *Science*, 1991. **254**(5028): p. 99-102.
77. de Oliveira, S., et al., *Cxcl8 (IL-8) Mediates Neutrophil Recruitment and Behavior in the Zebrafish Inflammatory Response*. *The Journal of Immunology*, 2013.
78. Sarris, M., et al., *Inflammatory chemokines direct and restrict leukocyte migration within live tissues as glycan-bound gradients*. *Current Biology*, 2012. **22**(24): p. 2375-2382.
79. Xie, Y., et al., *Glucocorticoids inhibit macrophage differentiation towards a pro-inflammatory phenotype upon wounding without affecting their migration*. *Dis Model Mech*, 2019. **12**(5).
80. Ogryzko, N.V., et al., *Zebrafish tissue injury causes upregulation of interleukin-1 and caspase-dependent amplification of the inflammatory response*. *Dis Model Mech*, 2014. **7**(2): p. 259-64.
81. Yan, B., et al., *IL-1 β and Reactive Oxygen Species Differentially Regulate Neutrophil Directional Migration and Basal Random Motility in a Zebrafish Injury-Induced Inflammation Model*. *The Journal of Immunology*, 2014. **192**(12): p. 5998-6008.
82. Petrie, T.A., et al., *Macrophages modulate adult zebrafish tail fin regeneration*. *Development*, 2014. **141**(13): p. 2581-2591.
83. de Oliveira, S., E.E. Rosowski, and A. Huttenlocher, *Neutrophil migration in infection and wound repair: going forward in reverse*. *Nature Reviews Immunology*, 2016. **16**(6): p. 378.
84. Burgon, J., et al., *Serum and glucocorticoid-regulated kinase 1 regulates neutrophil clearance during inflammation resolution*. *The Journal of Immunology*, 2014. **192**(4): p. 1796-1805.
85. Elks, P.M., et al., *Activation of hypoxia-inducible factor-1 α (Hif-1 α) delays inflammation resolution by reducing neutrophil apoptosis and reverse migration in a zebrafish inflammation model*. *Blood*, 2011. **118**(3): p. 712-722.
86. Ellett, F., et al., *Defining the phenotype of neutrophils following reverse migration in zebrafish*. *Journal of leukocyte biology*, 2015. **98**(6): p. 975-981.
87. Isles, H.M., et al., *The CXCL12/CXCR4 signaling Axis retains neutrophils at inflammatory sites in zebrafish*. *Frontiers in immunology*, 2019. **10**: p. 1784.
88. Mathew, L.K., et al., *Unraveling tissue regeneration pathways using chemical genetics*. *J Biol Chem*, 2007. **282**(48): p. 35202-10.
89. Kawakami, A., T. Fukazawa, and H. Takeda, *Early fin primordia of zebrafish larvae regenerate by a similar growth control mechanism with adult regeneration*. *Developmental dynamics: an official publication of the American Association of Anatomists*, 2004. **231**(4): p. 693-699.
90. Morales, R.A. and M.L. Allende, *Peripheral macrophages promote tissue regeneration in zebrafish by fine-tuning the inflammatory response*. *Frontiers in immunology*, 2019. **10**: p. 253.
91. Ashburn, T.T. and K.B. Thor, *Drug repositioning: identifying and developing new uses for existing drugs*. *Nature reviews Drug discovery*, 2004. **3**(8): p. 673-683.
92. Hall, C.J., et al., *Repositioning drugs for inflammatory disease-fishing for new anti-inflammatory agents*. *Disease models & mechanisms*, 2014. **7**(9): p. 1069-1081.

93. Beedie, S.L., et al., *In vivo screening and discovery of novel candidate thalidomide analogs in the zebrafish embryo and chicken embryo model systems*. *Oncotarget*, 2016. **7**(22): p. 33237.
94. Rahman, A., et al., *Inhibition of ErbB kinase signalling promotes resolution of neutrophilic inflammation*. *Elife*, 2019. **8**: p. e50990.
95. Ye, B., et al., *Meisoindigo, but not its core chemical structure indirubin, inhibits zebrafish interstitial leukocyte chemotactic migration*. *Pharm Biol*, 2017. **55**(1): p. 673-679.
96. Robertson, A.L., et al., *A zebrafish compound screen reveals modulation of neutrophil reverse migration as an anti-inflammatory mechanism*. *Sci Transl Med*, 2014. **6**(225): p. 225ra29.
97. Robertson, A.L., et al., *Identification of benzopyrone as a common structural feature in compounds with anti-inflammatory activity in a zebrafish phenotypic screen*. *Disease models & mechanisms*, 2016. **9**(6): p. 621-632.
98. Sun, M., et al., *Characterization of ginsenoside extracts by delayed luminescence, high-performance liquid chromatography, and bioactivity tests*. *Photochemical & Photobiological Sciences*, 2019. **18**(5): p. 1138-1146.
99. He, M., et al., *Ginsenoside Rg1 Acts as a Selective Glucocorticoid Receptor Agonist with Anti-Inflammatory Action without Affecting Tissue Regeneration in Zebrafish Larvae*. *Cells*, 2020. **9**(5).
100. Polednik, K.M., A.C. Koch, and L.K. Felzien, *Effects of essential oil from *Thymus vulgaris* on viability and inflammation in zebrafish embryos*. *Zebrafish*, 2018. **15**(4): p. 361-371.
101. Yang, Y., et al., *Anti-inflammatory and proresolution activities of bergapten isolated from the roots of *Ficus hirta* in an in vivo zebrafish model*. *Biochemical and biophysical research communications*, 2018. **496**(2): p. 763-769.
102. Bousquet, M.S., et al., *Seaweed natural products modify the host inflammatory response via *Nrf2* signaling and alter colon microbiota composition and gene expression*. *Free Radical Biology and Medicine*, 2020. **146**: p. 306-323.
103. Tang, H., et al., *Micrometam C protects against oxidative stress in inflammation models in zebrafish and RAW264. 7 macrophages*. *Marine drugs*, 2015. **13**(9): p. 5593-5605.
104. Nguyen, T.H., et al., *Anti-Inflammatory and Antioxidant Properties of the Ethanol Extract of *Clerodendrum Cyrtophyllum Turcz* in Copper Sulfate-Induced Inflammation in Zebrafish*. *Antioxidants*, 2020. **9**(3): p. 192.
105. Wijesinghe, W., et al., *Assessment of anti-inflammatory effect of 5 β -hydroxyppalisadin B isolated from red seaweed *Laurencia snackeyi* in zebrafish embryo in vivo model*. *Environmental Toxicology and Pharmacology*, 2014. **37**(1): p. 110-117.
106. Lee, S.-H., et al., *Anti-inflammatory effect of fucoïdan extracted from *Ecklonia cava* in zebrafish model*. *Carbohydrate polymers*, 2013. **92**(1): p. 84-89.
107. Watzke, J., K. Schirmer, and S. Scholz, *Bacterial lipopolysaccharides induce genes involved in the innate immune response in embryos of the zebrafish (*Danio rerio*)*. *Fish & shellfish immunology*, 2007. **23**(4): p. 901-905.
108. Ko, E.-Y., et al., *The roles of NF- κ B and ROS in regulation of pro-inflammatory mediators of inflammation induction in LPS-stimulated zebrafish embryos*. *Fish & shellfish immunology*, 2017. **68**: p. 525-529.
109. Yang, L.-L., et al., *Endotoxin molecule lipopolysaccharide-induced zebrafish inflammation model: a novel screening method for anti-inflammatory drugs*. *Molecules*, 2014. **19**(2): p. 2390-2409.
110. Hernández, P.P., et al., *Sub-lethal concentrations of waterborne copper are toxic to lateral line neuromasts in zebrafish (*Danio rerio*)*. *Hearing research*, 2006. **213**(1-2): p. 1-10.
111. Olivari, F.A., P.P. Hernández, and M.L. Allende, *Acute copper exposure induces oxidative stress and cell death in lateral line hair cells of zebrafish larvae*. *Brain research*, 2008. **1244**: p. 1-12.
112. d'Alençon, C.A., et al., *A high-throughput chemically induced inflammation assay in zebrafish*. *BMC biology*, 2010. **8**(1): p. 151.
113. Leite, C.E., et al., *Involvement of purinergic system in inflammation and toxicity induced by copper in zebrafish larvae*. *Toxicology and applied pharmacology*, 2013. **272**(3): p. 681-689.

114. Carrillo, S.A., et al., *Macrophage recruitment contributes to regeneration of mechanosensory hair cells in the zebrafish lateral line*. Journal of cellular biochemistry, 2016. **117**(8): p. 1880-1889.
115. Craig, P.M., C.M. Wood, and G.B. McClelland, *Oxidative stress response and gene expression with acute copper exposure in zebrafish (Danio rerio)*. American Journal of Physiology-Regulatory, Integrative and Comparative Physiology, 2007. **293**(5): p. R1882-R1892.
116. Griffitt, R.J., et al., *Exposure to copper nanoparticles causes gill injury and acute lethality in zebrafish (Danio rerio)*. Environmental science & technology, 2007. **41**(23): p. 8178-8186.
117. Singh, S.K., et al., *Proteome dynamics in neutrophils of adult zebrafish upon chemically-induced inflammation*. Fish & shellfish immunology, 2014. **40**(1): p. 217-224.
118. Deng, Q., et al., *Localized bacterial infection induces systemic activation of neutrophils through Cxcr2 signaling in zebrafish*. J Leukoc Biol, 2013. **93**(5): p. 761-9.
119. Tobin, D.M., et al., *The Ita4h locus modulates susceptibility to mycobacterial infection in zebrafish and humans*. Cell, 2010. **140**(5): p. 717-730.
120. Torraca, V., et al., *The CXCR3-CXCL11 signaling axis mediates macrophage recruitment and dissemination of mycobacterial infection*. Dis Model Mech, 2015. **8**(3): p. 253-69.
121. Fleming, A., J. Jankowski, and P. Goldsmith, *In vivo analysis of gut function and disease changes in a zebrafish larvae model of inflammatory bowel disease: a feasibility study*. Inflammatory bowel diseases, 2010. **16**(7): p. 1162-1172.
122. Oehlers, S.H., et al., *A chemical enterocolitis model in zebrafish larvae that is dependent on microbiota and responsive to pharmacological agents*. Developmental Dynamics, 2011. **240**(1): p. 288-298.
123. Oehlers, S.H., et al., *Retinoic acid suppresses intestinal mucus production and exacerbates experimental enterocolitis*. Disease models & mechanisms, 2012. **5**(4): p. 457-467.
124. Goldsmith, J.R., et al., *Glafenine-induced intestinal injury in zebrafish is ameliorated by μ -opioid signaling via enhancement of Atf6-dependent cellular stress responses*. Disease models & mechanisms, 2013. **6**(1): p. 146-159.
125. Espenschied, S.T., et al., *Epithelial delamination is protective during pharmaceutical-induced enteropathy*. Proceedings of the National Academy of Sciences, 2019. **116**(34): p. 16961-16970.
126. Geiger, B.M., et al., *Intestinal upregulation of melanin-concentrating hormone in TNBS-induced enterocolitis in adult zebrafish*. PloS one, 2013. **8**(12).
127. Brugman, S., et al., *Oxazolone-induced enterocolitis in zebrafish depends on the composition of the intestinal microbiota*. Gastroenterology, 2009. **137**(5): p. 1757-1767. e1.
128. Carney, T.J., et al., *Inactivation of serine protease Matriptase1a by its inhibitor Hai1 is required for epithelial integrity of the zebrafish epidermis*. Development, 2007. **134**(19): p. 3461-3471.
129. Mathias, J.R., et al., *Live imaging of chronic inflammation caused by mutation of zebrafish Hai1*. Journal of Cell Science, 2007. **120**(19): p. 3372-3383.
130. LeBert, D.C., et al., *Matrix metalloproteinase 9 modulates collagen matrices and wound repair*. Development, 2015. **142**(12): p. 2136-2146.
131. Thakur, P.C., et al., *Lack of de novo phosphatidylinositol synthesis leads to endoplasmic reticulum stress and hepatic steatosis in cdipt - deficient zebrafish*. Hepatology, 2011. **54**(2): p. 452-462.
132. Thakur, P.C., et al., *Dysregulated phosphatidylinositol signaling promotes endoplasmic-reticulum-stress-mediated intestinal mucosal injury and inflammation in zebrafish*. Disease models & mechanisms, 2014. **7**(1): p. 93-106.
133. Zhang, C., et al., *In vitro and in vivo anti-inflammatory effects of polyphyllin VII through downregulating MAPK and NF- κ B pathways*. Molecules, 2019. **24**(5): p. 875.
134. Hwang, J.-H., et al., *Caffeine prevents LPS-induced inflammatory responses in RAW264. 7 cells and zebrafish*. Chemico-biological interactions, 2016. **248**: p. 1-7.
135. Ryu, S.-J., et al., *Oleuropein suppresses LPS-induced inflammatory responses in RAW 264.7 cell and zebrafish*. Journal of agricultural and food chemistry, 2015. **63**(7): p. 2098-2105.

136. Kim, S.-Y., et al., *Polyphenol-rich fraction from Ecklonia cava (a brown alga) processing by-product reduces LPS-induced inflammation in vitro and in vivo in a zebrafish model*. *Algae*, 2014. **29**(2): p. 165.
137. Yang, L., et al., *Protective effect of phillyrin on lethal LPS-induced neutrophil inflammation in zebrafish*. *Cellular Physiology and Biochemistry*, 2017. **43**(5): p. 2074-2087.
138. Sun, Q., et al., *Anti-inflammatory properties of extracts from Chimonanthus nitens Oliv. leaf*. *PloS one*, 2017. **12**(7).
139. Wang, Z.-g., et al., *Anti-Inflammatory Activity of a Peptide from Skipjack (Katsuwonus pelamis)*. *Marine drugs*, 2019. **17**(10): p. 582.
140. Guo, D.-L., et al., *Terpene Glycosides from Sanguisorba officinalis and Their Anti-Inflammatory Effects*. *Molecules*, 2019. **24**(16): p. 2906.
141. Kasica-Jarosz, N., P. Podlasz, and J. Kaleczyc, *Pituitary adenylate cyclase-activating polypeptide (PACAP-38) plays an inhibitory role against inflammation induced by chemical damage to zebrafish hair cells*. *PloS one*, 2018. **13**(6).
142. Li, L., et al., *Role of Quzhou Fructus Aurantii extract in preventing and treating acute lung injury and inflammation*. *Scientific Reports*, 2018. **8**(1): p. 1-11.
143. Wittmann, C., et al., *A zebrafish drug-repurposing screen reveals sGC-dependent and sGC-independent pro-inflammatory activities of nitric oxide*. *PloS one*, 2015. **10**(10).
144. Oehlers, S.H., et al., *A whole animal chemical screen approach to identify modifiers of intestinal neutrophilic inflammation*. *Febs j*, 2017. **284**(3): p. 402-413.
145. Beutler, B. and E.T. Rietschel, *Innate immune sensing and its roots: the story of endotoxin*. *Nature Reviews Immunology*, 2003. **3**(2): p. 169-176.
146. Novoa, B., et al., *LPS response and tolerance in the zebrafish (Danio rerio)*. *Fish & shellfish immunology*, 2009. **26**(2): p. 326-331.
147. Chow, J.C., et al., *Toll-like receptor-4 mediates lipopolysaccharide-induced signal transduction*. *Journal of Biological Chemistry*, 1999. **274**(16): p. 10689-10692.
148. Akira, S. and K. Takeda, *Toll-like receptor signalling*. *Nature reviews immunology*, 2004. **4**(7): p. 499-511.
149. Sullivan, C., et al., *The gene history of zebrafish tlr4a and tlr4b is predictive of their divergent functions*. *The Journal of Immunology*, 2009. **183**(9): p. 5896-5908.
150. Sepulcre, M.P., et al., *Evolution of lipopolysaccharide (LPS) recognition and signaling: fish TLR4 does not recognize LPS and negatively regulates NF- κ B activation*. *The Journal of Immunology*, 2009. **182**(4): p. 1836-1845.
151. Iliev, D.B., et al., *Endotoxin recognition: in fish or not in fish?* *FEBS letters*, 2005. **579**(29): p. 6519-6528.
152. Forn-Cuní, G., et al., *Conserved gene regulation during acute inflammation between zebrafish and mammals*. *Scientific reports*, 2017. **7**: p. 41905.
153. Copeland, S., et al., *Acute inflammatory response to endotoxin in mice and humans*. *Clin. Diagn. Lab. Immunol.*, 2005. **12**(1): p. 60-67.
154. Dios, S., et al., *The involvement of cholesterol in sepsis and tolerance to lipopolysaccharide highlighted by the transcriptome analysis of zebrafish (Danio rerio)*. *Zebrafish*, 2014. **11**(5): p. 421-433.
155. McDonald, M.C., et al., *Reconstituted high-density lipoprotein attenuates organ injury and adhesion molecule expression in a rodent model of endotoxic shock*. *Shock*, 2003. **20**(6): p. 551-7.
156. Park, K.-H. and K.-H. Cho, *A zebrafish model for the rapid evaluation of pro-oxidative and inflammatory death by lipopolysaccharide, oxidized low-density lipoproteins, and glycated high-density lipoproteins*. *Fish & shellfish immunology*, 2011. **31**(6): p. 904-910.
157. Cordero-Maldonado, M.L., et al., *Optimization and pharmacological validation of a leukocyte migration assay in zebrafish larvae for the rapid in vivo bioactivity analysis of anti-inflammatory secondary metabolites*. *PloS one*, 2013. **8**(10).

158. Bohni, N., et al., *Integration of microfractionation, qNMR and zebrafish screening for the in vivo bioassay-guided isolation and quantitative bioactivity analysis of natural products*. PLoS One, 2013. **8**(5).
159. Linder, M.C. and M. Hazegh-Azam, *Copper biochemistry and molecular biology*. The American journal of clinical nutrition, 1996. **63**(5): p. 797S-811S.
160. Pereira, T.C.B., M.M. Campos, and M.R. Bogo, *Copper toxicology, oxidative stress and inflammation using zebrafish as experimental model*. Journal of Applied Toxicology, 2016. **36**(7): p. 876-885.
161. Dave, G. and R. Xiu, *Toxicity of mercury, copper, nickel, lead, and cobalt to embryos and larvae of zebrafish, Brachydanio rerio*. Archives of Environmental Contamination and Toxicology, 1991. **21**(1): p. 126-134.
162. Johnson, A., E. Carew, and K. Sloman, *The effects of copper on the morphological and functional development of zebrafish embryos*. Aquatic Toxicology, 2007. **84**(4): p. 431-438.
163. Wittmann, C., et al., *Facilitating drug discovery: an automated high-content inflammation assay in zebrafish*. JoVE (Journal of Visualized Experiments), 2012(65): p. e4203.
164. Yokomizo, T., T. Izumi, and T. Shimizu, *Leukotriene B4: metabolism and signal transduction*. Archives of biochemistry and biophysics, 2001. **385**(2): p. 231-241.
165. Peters-Golden, M., et al., *Leukotrienes: underappreciated mediators of innate immune responses*. The Journal of Immunology, 2005. **174**(2): p. 589-594.
166. Lee, J.A. and S.A. Renshaw, *Zebrafish screens for new colitis treatments – a bottom - up approach*. The FEBS Journal, 2017. **284**(3): p. 399-401.
167. Packey, C. and R. Sartor, *Interplay of commensal and pathogenic bacteria, genetic mutations, and immunoregulatory defects in the pathogenesis of inflammatory bowel diseases*. Journal of internal medicine, 2008. **263**(6): p. 597-606.
168. He, Q., et al., *Role of gut microbiota in a zebrafish model with chemically induced enterocolitis involving toll-like receptor signaling pathways*. Zebrafish, 2014. **11**(3): p. 255-264.
169. He, Q., et al., *Microbial fingerprinting detects intestinal microbiota dysbiosis in Zebrafish models with chemically-induced enterocolitis*. BMC microbiology, 2013. **13**(1): p. 289.
170. Haarder, S., et al., *Effect of ES products from Anisakis (Nematoda: Anisakidae) on experimentally induced colitis in adult zebrafish*. Parasite Immunology, 2017. **39**(10): p. e12456.
171. Amsterdam, A., et al., *A large-scale insertional mutagenesis screen in zebrafish*. Genes & development, 1999. **13**(20): p. 2713-2724.
172. Oakley, R.H. and J.A. Cidlowski, *The biology of the glucocorticoid receptor: New signaling mechanisms in health and disease*. Journal of Allergy and Clinical Immunology, 2013. **132**(5): p. 1033-1044.
173. Chrousos, G.P. and T. Kino, *Intracellular Glucocorticoid Signaling: A Formerly Simple System Turns Stochastic*. Science's STKE, 2005. **2005**(304): p. pe48-pe48.
174. Revollo, J.R. and J.A. Cidlowski, *Mechanisms generating diversity in glucocorticoid receptor signaling*. Ann N Y Acad Sci, 2009. **1179**: p. 167-78.
175. Wei, Y., et al., *Regulation of hypothalamic-pituitary-adrenal axis activity and immunologic function contributed to the anti-inflammatory effect of acupuncture in the OVA-induced murine asthma model*. Neuroscience Letters.
176. Tsigos, C. and G.P. Chrousos, *Hypothalamic–pituitary–adrenal axis, neuroendocrine factors and stress*. Journal of Psychosomatic Research, 2002. **53**(4): p. 865-871.
177. Hench, P.S., et al., *The effect of a hormone of the adrenal cortex (17-hydroxy-11-dehydrocorticosterone: compound E) and of pituitary adrenocortical hormone in arthritis: preliminary report*. Ann Rheum Dis, 1949. **8**(2): p. 97-104.
178. Duke-Elder, S. and N. Ashton, *Action of cortisone on tissue reactions of inflammation and repair with special reference to the eye*. Br J Ophthalmol, 1951. **35**(11): p. 695-707.
179. O'Rourke, J.F., G. Iser, and R.W. Ryan, *An initial evaluation of prednisone therapy in ocular inflammation*. AMA Arch Ophthalmol, 1956. **55**(3): p. 323-32.

180. Busillo, J.M. and J.A. Cidlowski, *The five Rs of glucocorticoid action during inflammation: ready, reinforce, repress, resolve, and restore*. Trends in Endocrinology & Metabolism, 2013. **24**(3): p. 109-119.
181. Barnes, P.J., *Glucocorticosteroids: current and future directions*. British Journal of Pharmacology, 2011. **163**(1): p. 29-43.
182. Baschant, U. and J. Tuckermann, *The role of the glucocorticoid receptor in inflammation and immunity*. J Steroid Biochem Mol Biol, 2010. **120**(2-3): p. 69-75.
183. Schreck, C.B., et al., *Biology of stress in fish*. 2016: Academic Press.
184. Wendelaar Bonga, S.E., *The stress response in fish*. Physiological reviews, 1997. **77**(3): p. 591-625.
185. Alsop, D. and M.M. Vijayan, *Development of the corticosteroid stress axis and receptor expression in zebrafish*. American Journal of Physiology - Regulatory, Integrative and Comparative Physiology, 2008. **294**(3): p. R711-R719.
186. Schaaf, M.J., et al., *Discovery of a functional glucocorticoid receptor beta-isoform in zebrafish*. Endocrinology, 2008. **149**(4): p. 1591-9.
187. Schaaf, M.J., A. Chatzopoulou, and H.P. Spaink, *The zebrafish as a model system for glucocorticoid receptor research*. Comp Biochem Physiol A Mol Integr Physiol, 2009. **153**(1): p. 75-82.
188. Geurtzen, K., et al., *Immune suppressive and bone inhibitory effects of prednisolone in growing and regenerating zebrafish tissues*. Journal of Bone and Mineral Research, 2017. **32**(12): p. 2476-2488.
189. Huang, W.C., et al., *Treatment of Glucocorticoids Inhibited Early Immune Responses and Impaired Cardiac Repair in Adult Zebrafish*. PLoS One, 2013. **8**(6): p. e66613.
190. Kyritsis, N., et al., *Acute inflammation initiates the regenerative response in the adult zebrafish brain*. Science, 2012. **338**(6112): p. 1353-1356.
191. Facchinello, N., et al., *nr3c1 null mutant zebrafish are viable and reveal DNA-binding-independent activities of the glucocorticoid receptor*. Scientific reports, 2017. **7**(1): p. 1-13.
192. Chatzopoulou, A., et al., *Transcriptional and metabolic effects of glucocorticoid receptor alpha and beta signaling in zebrafish*. Endocrinology, 2015. **156**(5): p. 1757-69.
193. Barrett, R., et al., *A rapid, high content, in vivo model of glucocorticoid - induced osteoporosis*. Biotechnology Journal: Healthcare Nutrition Technology, 2006. **1**(6): p. 651-655.
194. He, H., et al., *Possible mechanisms of prednisolone-induced osteoporosis in zebrafish larva*. Biomedicine & Pharmacotherapy, 2018. **101**: p. 981-987.
195. Huo, L., et al., *Prednisolone induces osteoporosis-like phenotypes via focal adhesion signaling pathway in zebrafish larvae*. Biology open, 2018. **7**(7): p. bio029405.
196. De Vrieze, E., et al., *Prednisolone induces osteoporosis-like phenotype in regenerating zebrafish scales*. Osteoporosis International, 2014. **25**(2): p. 567-578.
197. Ohnmacht, J., et al., *Spinal motor neurons are regenerated after mechanical lesion and genetic ablation in larval zebrafish*. Development, 2016. **143**(9): p. 1464-1474.
198. Geurtzen, K. and F. Knopf, *Adult zebrafish injury models to study the effects of prednisolone in regenerating bone tissue*. JoVE (Journal of Visualized Experiments), 2018(140): p. e58429.
199. Sengupta, S., et al., *Alternate glucocorticoid receptor ligand binding structures influence outcomes in an in vivo tissue regeneration model*. Comparative Biochemistry and Physiology Part C: Toxicology & Pharmacology, 2012. **156**(2): p. 121-129.

Chapter 3

Glucocorticoids inhibit macrophage differentiation towards a pro-inflammatory phenotype upon wounding without affecting their migration

Yufei Xie, Sofie Tolmeijer, Jelle M. Oskam, Tijs Tonkens,
Annemarie H. Meijer, Marcel J.M Schaaf

Published in Disease Models & Mechanisms, 2019, 12(5), dmm037887

Abstract

Glucocorticoid drugs are widely used to treat immune-related diseases, but their use is limited by side effects and by resistance, which especially occurs in macrophage-dominated diseases. In order to improve glucocorticoid therapies, more research is required into the mechanisms of glucocorticoid action. In the present study, we have used a zebrafish model for inflammation to study glucocorticoid effects on the innate immune response. In zebrafish larvae, the migration of neutrophils towards a site of injury is inhibited upon glucocorticoid treatment, while migration of macrophages is glucocorticoid resistant. We show that wounding-induced increases in expression of genes encoding neutrophil-specific chemoattractants (Il8 and Cxcl18b) are attenuated by the synthetic glucocorticoid beclomethasone, but that beclomethasone does not attenuate the induction of the genes encoding Ccl2 and Cxcl11aa, which are required for macrophage recruitment. RNA sequencing on Fluorescence-Activated Cell Sorting (FACS)-sorted macrophages shows that the vast majority of the wounding-induced transcriptional changes in these cells are inhibited by beclomethasone, whereas only a small subset is glucocorticoid-insensitive. As a result, beclomethasone decreases the number of macrophages that differentiate towards a pro-inflammatory (M1) phenotype, which we demonstrated using a *tnfa:eGFP-F* reporter line and analysis of macrophage morphology. We conclude that differentiation and migration of macrophages are regulated independently, and that glucocorticoids leave the chemotactic migration of macrophages unaffected, but exert their anti-inflammatory effect on these cells by inhibiting their differentiation to an M1 phenotype. The resistance of macrophage-dominated diseases to glucocorticoid therapy can therefore not be attributed to an intrinsic insensitivity of macrophages to glucocorticoids.

Introduction

Glucocorticoids (GCs) are a class of steroid hormones secreted by the adrenal gland, and the main endogenous glucocorticoid in our body is cortisol [1-3]. Glucocorticoids regulate a wide variety of systems in our body, including the immune, metabolic, reproductive, cardiovascular and central nervous system [4-7]. Due to their potent and well-established immunosuppressive effects, they are often prescribed to treat various immune-related diseases, including asthma, rheumatoid arthritis, dermatitis, leukemia, and several autoimmune diseases [8, 9]. However, their clinical use is limited by two issues. First, chronic glucocorticoid therapy can lead to severe side effects, like osteoporosis, muscle weakness, diabetes, infection, and hypertension [10]. Second, resistance to glucocorticoid drug treatment occurs in a large number (~10-30%) of patients [11, 12]. In order to develop novel glucocorticoid therapies that overcome these barriers and retain their therapeutic efficacy, more

insight into the molecular and cellular mechanisms of glucocorticoid modulation of the immune response is required.

Glucocorticoids exert their function through an intracellular receptor, the glucocorticoid receptor (GR) [13], which acts as a transcription factor, altering the transcription of a plethora of genes. The GR modulates the transcription of genes by several mechanisms [14]. It can bind directly to DNA, to glucocorticoid response elements (GRE) and enhance transcription upon recruitment of transcriptional cofactors. In contrast, binding to negative GREs (nGREs) has been shown to repress gene transcription [15]. Alternatively, the GR can bind indirectly to DNA through interaction with other transcription factors, like AP-1, NF- κ B or STAT3. Through this 'tethering', it modulates the activity of these factors.

The tethering mechanism of the GR, resulting in the inhibition of transcription of immune-activating genes, is generally considered to be the main mechanism by which glucocorticoids exert their anti-inflammatory actions [16]. For example, TNF- or LPS-induced transcriptional responses in cultured cells can be repressed through tethering of the NF- κ B subunit p65 [17-20]. Other mechanisms, like the activation of anti-inflammatory genes through GRE binding, and a reduction of NF- κ B recruitment, contribute to the anti-inflammatory actions of GR as well, but the exact role of these mechanisms has not been fully established [21, 22]. Through these mechanisms, glucocorticoids exert strong suppressive effects on the inflammatory response [23]. At the initial stage of this response, they dampen signaling pathways downstream from Toll-like receptors (TLRs), inhibit the induction of genes encoding cytokines, upregulate the expression of anti-inflammatory proteins, and inhibit the generation of prostaglandins and leukotrienes [8, 24]. In addition, they reduce the blood flow to the inflamed tissue and inhibit vascular leakage. At subsequent stages, glucocorticoids attenuate the production of chemokines and adhesion molecules, thereby reducing leukocyte extravasation and migration towards the inflamed site [23, 24].

It has become clear that glucocorticoid action on the immune system is highly complex and requires further investigation. A complicating factor is that the effects of glucocorticoids have been shown to be highly cell type-specific [25]. Whereas they induce apoptosis of eosinophils and basophils, they promote the survival and proliferation of neutrophils [26, 27]. In monocytes, they induce an anti-inflammatory phenotype with increased mobility and phagocytic capacity [28]. Macrophages are often divided into two functional phenotypes: a classically activated, pro-inflammatory (M1) phenotype which contributes to the inflammatory response, and an alternatively activated (M2) phenotype which can be subdivided in several different phenotypes which have been shown to be involved in the resolution of inflammation and wound healing [29, 30]. In animal models for arthritis and acute lung injury, glucocorticoids have been shown to inhibit the differentiation of macrophages towards an M1

phenotype, whereas the effect on M2 differentiation is less clear [31, 32]. In addition to the cell type-specificity of glucocorticoid actions, it has become clear that the transcriptional regulation of immune-activating genes by the GR is not strictly suppressive [33]. Upregulation of various pro-inflammatory genes after glucocorticoid treatment has been observed in several cell types [34-38], and GR has been shown to activate pro-inflammatory genes in synergy with other signaling pathways [39-41]. In addition, some genes that are induced upon TNF or LPS treatment appear to be insensitive to the repressive action of GR [17-20].

In the present study, we have used the zebrafish as an *in vivo* model to study glucocorticoid effects on the inflammatory response. The immune system of the zebrafish is highly similar to that of humans. Like humans, the zebrafish has a thymus, innate immune cells (macrophages, neutrophils) and adaptive immune cells (T cells and B cells), and cells that bridge innate and adaptive immunity (dendritic cells) [42-44]. Besides, the innate immune system of zebrafish develops within a few days after fertilization, while the adaptive immune system only matures after two weeks, which means the innate immune system can be studied separately in larvae [43, 45]. Zebrafish larvae are widely used as a model system to study the inflammatory response [46-48]. Tail wounding-induced inflammation in zebrafish larvae is a well-established model in which amputation of the tail triggers the expression of many pro-inflammatory molecules and the recruitment of innate immune cells (neutrophils and macrophages) towards the wounded area [49, 50]. This model enables the investigation of cell-type specific inflammatory responses *in vivo* and has been widely used for research on leukocyte migration and infiltration and anti-inflammatory drug screening [51-53].

The zebrafish Gr is highly similar to its human equivalent in structure and function [54-56]. This makes the zebrafish a valuable model to study the molecular mechanisms of glucocorticoid action *in vivo* [56-58]. In previous work, we have studied the anti-inflammatory effects of glucocorticoids using the tail amputation model and found that glucocorticoid treatment attenuates the vast majority amputation-induced changes in gene expression, which were measured in lysates from whole larvae [59]. In addition, we observed that the recruitment of neutrophils to the wounded area is inhibited by glucocorticoids, but that the migration of macrophages is resistant to glucocorticoid treatment [59-61].

It has been shown that glucocorticoids are less effective in the treatment of inflammatory diseases dominated by macrophages, like chronic obstructive pulmonary disease (COPD), but the mechanisms underlying the limited responsiveness to glucocorticoid treatment remain poorly understood [62]. Therefore, in the present study, we sought to find a mechanistic explanation for our finding that glucocorticoids do not inhibit amputation-induced macrophage migration. We demonstrate that the

induction of genes encoding chemo-attractants involved in macrophage recruitment is insensitive to glucocorticoid treatment, providing an explanation for the resistance of macrophage migration to glucocorticoids. In addition, we show that macrophages should not be considered a generally glucocorticoid-insensitive cell type. In these cells, glucocorticoids attenuate almost all wounding-induced changes in gene expression. Through this modulation of the transcriptional response, glucocorticoids inhibit the differentiation of macrophages to a pro-inflammatory (M1) phenotype.

Results

Glucocorticoids inhibit migration of neutrophils, but leave macrophage migration unaffected

Using tail amputation in 3 dpf zebrafish larvae as a model for inflammation, we studied the effect of four glucocorticoids (beclomethasone, dexamethasone, hydrocortisone, prednisolone) on the migration of leukocytes towards a site of injury. To quantitate the migration of neutrophils and macrophages, we counted the number of these innate immune cells in a defined area of the tail at 4 hours post amputation (hpa, Figure 1A). All four glucocorticoids had a highly significant inhibitory effect on the migration of neutrophils, as previously observed [63] (Figure 1C). Three glucocorticoids (beclomethasone, dexamethasone and prednisolone) did not affect the migration of macrophages significantly, and one (hydrocortisone) induced a slight decrease (~12.5%, Figure 1B). These data are in line with a previous study from our group, in which we demonstrated that beclomethasone inhibited the migration of neutrophils and not of macrophages, that this effect was mediated through Gr, and that beclomethasone did not affect the total leukocyte numbers in the larvae [59].

To study the effects of beclomethasone on leukocyte migration in more detail, larvae were imaged using confocal microscopy between 1.5 and 12 hpa, and the leukocyte numbers in the wounded area were automatically determined using dedicated software. The results of this analysis showed that for the control group the average number of macrophages present in the wounded area increased from 16.7 ± 2.6 to 32.3 ± 3.2 cells between 1.5 hpa and 12 hpa (Figure 2A). No significant effect of beclomethasone on macrophage migration was observed (from 16.2 ± 1.8 to 27.3 ± 2.2 for the beclomethasone-treated group). For neutrophils, in the control group, a number of 10.8 ± 1.8 was observed at 1.5 hpa, and their number reached a peak of 23.0 ± 2.8 at around 5 hpa, then decreased and reached a level of 19.4 ± 2.5 at 9 hpa which remained relatively constant until 12 hpa (Figure 2B). In the beclomethasone-treated group, a lower number of recruited neutrophils was observed in the wounded area at 5 hpa (15.9 ± 1.8).

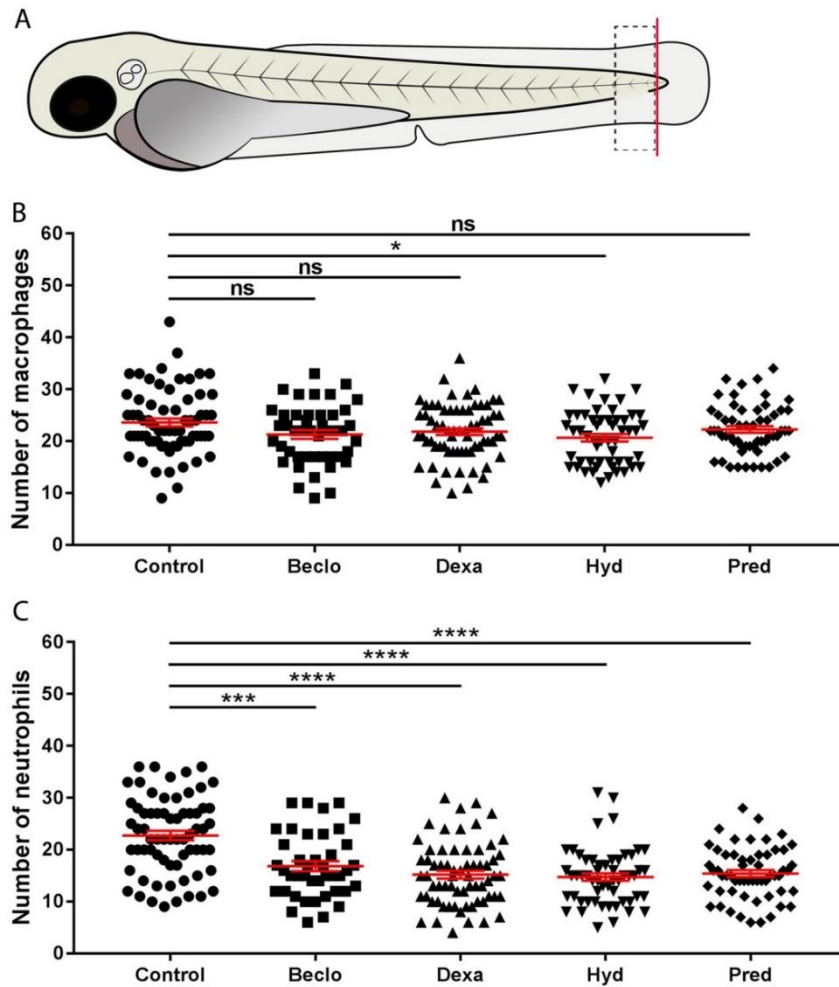


Figure 1. Effect of glucocorticoids on macrophage and neutrophil recruitment upon tail amputation in *Tg(mpx:GFP/mpeg1:mCherry-F)* larvae. A. Schematic drawing of a zebrafish larva at 3 dpf. The red line shows the site of amputation. The black dashed box shows the area in which cells were counted to quantitate the recruitment. B. The number of macrophages recruited to the wounded area at 4 hpa. In the Beclo (beclomethasone), Dexa (dexamethasone) and Pred (prednisolone) groups, no significant differences were observed compared the control group (vehicle-treated). In the Hyd (hydrocortisone) group, a significantly decreased number of macrophages was observed. C. The number of neutrophils recruited to the wounded area at 4 hpa. For all glucocorticoid-treated groups, a significantly reduced number of neutrophils was recruited compared to the control group. Statistical analyses were performed by ANOVA. Values shown are the means \pm s.e.m. of data from three independent experiments. Statistical significance is indicated by: ns, non-significant; * $P < 0.05$; *** $P < 0.001$; **** $P < 0.0001$.

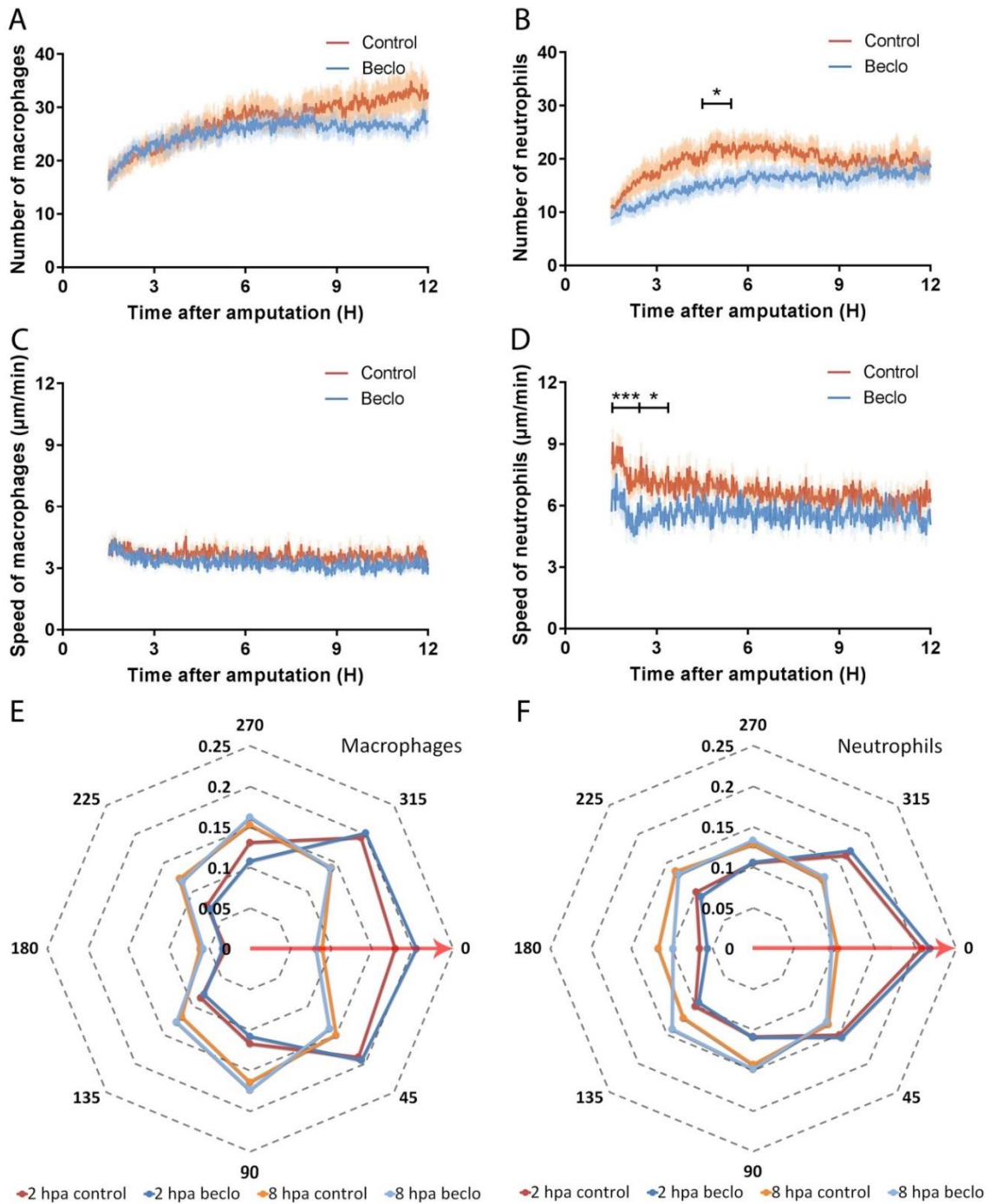


Figure 2. Live imaging and tracking of migrating macrophages and neutrophils upon tail amputation. A-B. The number of macrophages (A) and neutrophils (B) recruited to the wounded area from 1.5 hpa to 12 hpa in 3 dpf larvae in the vehicle-treated group (Control) and the beclomethasone-treated group (Becl). Data were averaged for each hour to proceed statistical analysis by ANOVA with a Fisher’s LSD post hoc test. No significant difference was observed for the number of recruited macrophages. A significantly reduced number of neutrophils were recruited in the beclomethasone treated group compared to the control group at 5 hpa. Values shown are the means \pm s.e.m. from 10 larvae. Statistical significance is indicated by: * $P < 0.05$. C-D. The velocity of macrophages (C) and neutrophils (D). Data were averaged for each hour to proceed statistical analysis by ANOVA with a Fisher’s LSD post hoc test. No significant difference was observed for the velocity of macrophages. At 2 and 3 hpa, the velocity of neutrophils in the beclomethasone-treated group was significantly lower than

the velocity in the control group. Values shown are the means \pm s.e.m. from 10 embryos. Statistical significance is indicated by: * $P < 0.05$; *** $P < 0.001$. E-F. The directionality of recruited macrophages (E) and neutrophils (F) at 2 hpa and 8 hpa. The circular x axis indicates the different angles made by cells, classified into 8 categories. Category 0 represents the direction towards the wound (including angles between 22.5 to -22.5 degrees, shown by the red arrows). The y axis indicates the size of the fraction of cells occurring within a category in that hour. Statistical analysis was performed by Kolmogorov-Smirnov test. No difference was observed between the control and beclomethasone treated groups. Values shown are the means from 10 embryos.

To further analyze the effects of beclomethasone, we used automated tracking of the leukocytes (see Movies 1-2 in Supplementary Information), and quantified the velocity and directionality of the migrating macrophages and neutrophils. The data showed that during the entire time frame, the velocity of the macrophages fluctuated around 3.5 $\mu\text{m}/\text{min}$ for both the control and the beclomethasone-treated group (Figure 2C). For neutrophils, the velocity peaked at 1.5 hpa (8.12 \pm 0.56 $\mu\text{m}/\text{min}$ for the control group and 5.70 \pm 0.72 $\mu\text{m}/\text{min}$ for the beclomethasone-treated group) and decreased slowly afterwards (Figure 2D). At 2 hpa and 3 hpa, the velocity of neutrophils in the beclomethasone-treated group was significantly lower compared to the control group.

In addition, we measured the direction in which the macrophages and neutrophils moved and plotted the distribution of these directions measured at 2 and 8 hours after amputation (Figures 2E-F). The results showed that at none of these time points beclomethasone affected the directionality of either macrophages or neutrophils. At 2 hpa, most of the macrophages (~60%) moved towards the wounded area (angles 292.5°- 360°, and 0°- 67.5°) (Figure 2E). Only less than 20% of them moved in the opposite direction (angles 112.5°- 247.5°). At 8 hpa, the percentage of macrophages that moved towards the wounded area in the control and beclomethasone-treated group decreased to ~40%. For the neutrophils, the directionality showed a similar trend (Figure 2F). At 2 hpa, over 50% of the neutrophils moved towards the wounded area in both the control group and the beclomethasone-treated group, while at 8 hpa, this percentage decreased to ~35%. In conclusion, beclomethasone does not affect any of the migration parameters of macrophages but reduces the number of recruited neutrophils and their velocity.

Beclomethasone inhibits the induction of chemoattractants for macrophages

To unravel the molecular mechanisms underlying the difference between the effect of beclomethasone on macrophage and neutrophil migration, we first studied the expression of chemoattractants that are known to be involved in the migration of these leukocytes. According to previous studies on leukocyte migration and infiltration, Ccl2 and Cxcl11aa are two of the key chemokines that stimulate the migration of macrophages, while Il8 and Cxcl18b are important for the stimulation of neutrophil migration [64-70]. Using qPCR on RNA samples from whole larvae, we determined the

expression levels of the genes encoding these four chemo-attractants (*ccl2*, *cxcl11aa*, *il8* and *cxcl18b*) at different time points after amputation, (Figure 3A-D). The results showed that at 4 hpa, the mRNA level of all four chemo-attractants was increased by amputation. At 2 hpa, the expression of *ccl2*, *cxcl11aa*, and *cxcl18b* was increased, and at 8 hpa the expression of *ccl2*, *il8* and *cxcl18b* showed an increase. In the presence of beclomethasone, amputation induced a smaller increase in *il8* and *cxcl18b* expression but the increase in the expression of *ccl2* and *cxcl11aa* was not inhibited. In addition, beclomethasone decreased the expression of *il8* independent of amputation. We previously observed a similar suppression under basal conditions by beclomethasone for *mmp3*, *mmp9* and *ilb* [59], indicating that for some immune-related genes, glucocorticoids downregulate the basal expression, in addition to attenuating their upregulation.

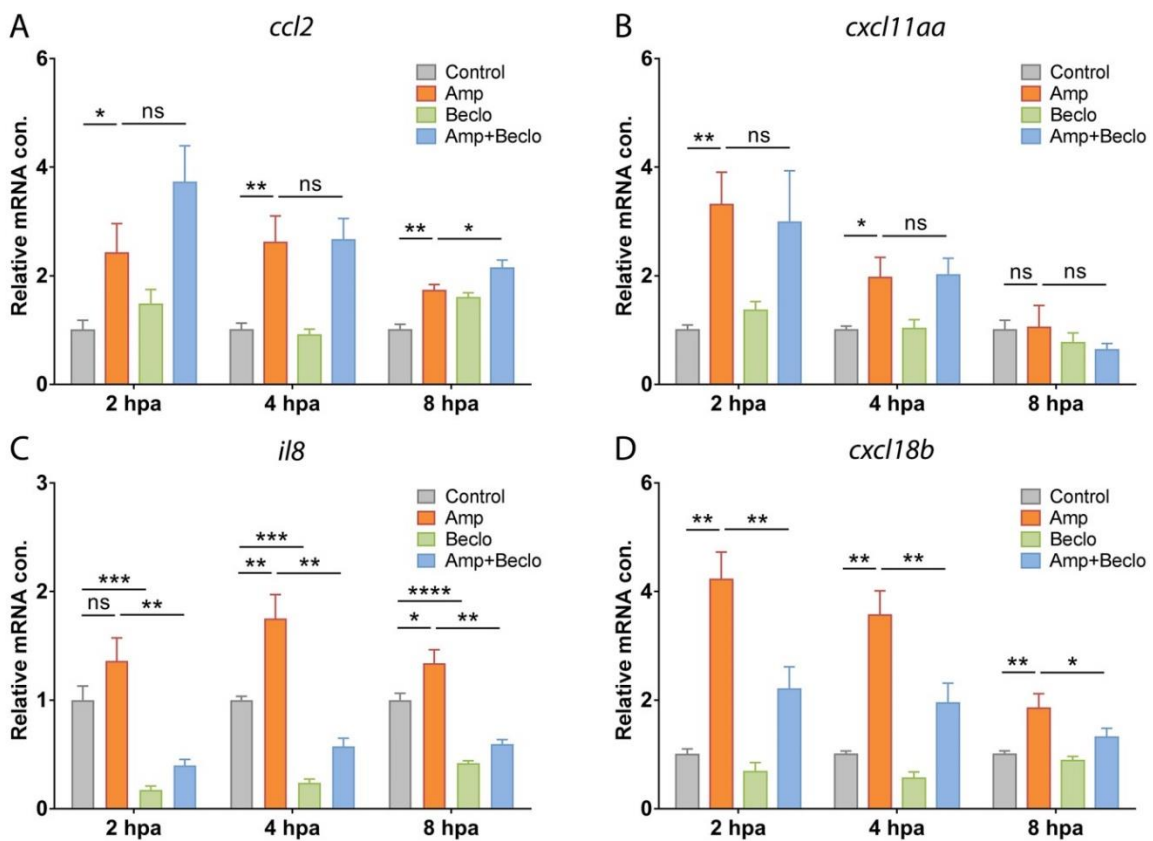


Figure 3. Expression levels of genes encoding chemo-attractants Ccl2 (A), Cxcl11aa (B), Il8 (C), and Cxcl18b (D) in whole larvae at 2hpa, 4hpa and 8hpa, determined by qPCR. Statistical analysis by ANOVA with a Fisher's LSD post hoc test showed that *ccl2* and *cxcl11aa* mRNA levels were significantly increased by amputation (Amp) and that the combined amputation/beclomethasone (Amp+Becl) treatment resulted in a similar level of regulation, relative to the non-amputated, vehicle-treated group (Control). Expression levels of *il8*, and *cxcl18b* showed a significant increase upon amputation, and this effect was lower upon the combined treatment. Expression level of *il8* was significantly suppressed by beclomethasone (Becl). Values shown are the means \pm s.e.m. of three independent experiments. Statistical significance is indicated by: ns, non-significant; * $P < 0.05$; ** $P < 0.01$; *** $P < 0.001$.

To demonstrate that the chemo-attractants Ccl2 and Cxcl11aa are required for macrophage recruitment in this tail amputation model, we analyzed their role in macrophage migration in our model. We used a previously described morpholino to create a knockdown of *Ccr2*, the receptor of Ccl2, in zebrafish larvae, which was shown not to affect the total number of leukocytes [65, 71]. In the *ccr2* morphants, a significantly decreased number of recruited macrophages was observed in the wounded area at 4 hpa (Figure 4A, C). However, the number of recruited neutrophils was identical to the number in the mock-injected controls (Figure 4B, D), the number of recruited neutrophils was unexpectedly high in these experiments (compared to data shown in Fig,1C, 2B and 4F), which we can only explain as an effect of the injections). For the receptor of Cxcl11aa, *Cxcr3.2*, we used a mutant fish line, and it was previously demonstrated that total numbers of leukocytes were not affected by the mutation [66]. The *cxcr3.2* *-/-* larvae showed significantly decreased numbers of both macrophages (Figure 4E, G) and neutrophils (Figure 4F, H) recruited to the wounded area compared to the *cxcr3.2* *+/+* controls (the number of recruited macrophages was slightly lower in these experiments (compared to data shown in Fig,1B, 2A and 4A), which may be due to the different genetic background of the used fish line).

These findings indicate that beclomethasone does not affect the amputation-induced increase in the expression of the genes encoding the chemo-attractants Ccl2 and Cxcl11aa, which are involved in macrophage recruitment upon tail amputation. This provides an explanation for the insensitivity of macrophage migration to glucocorticoid treatment.

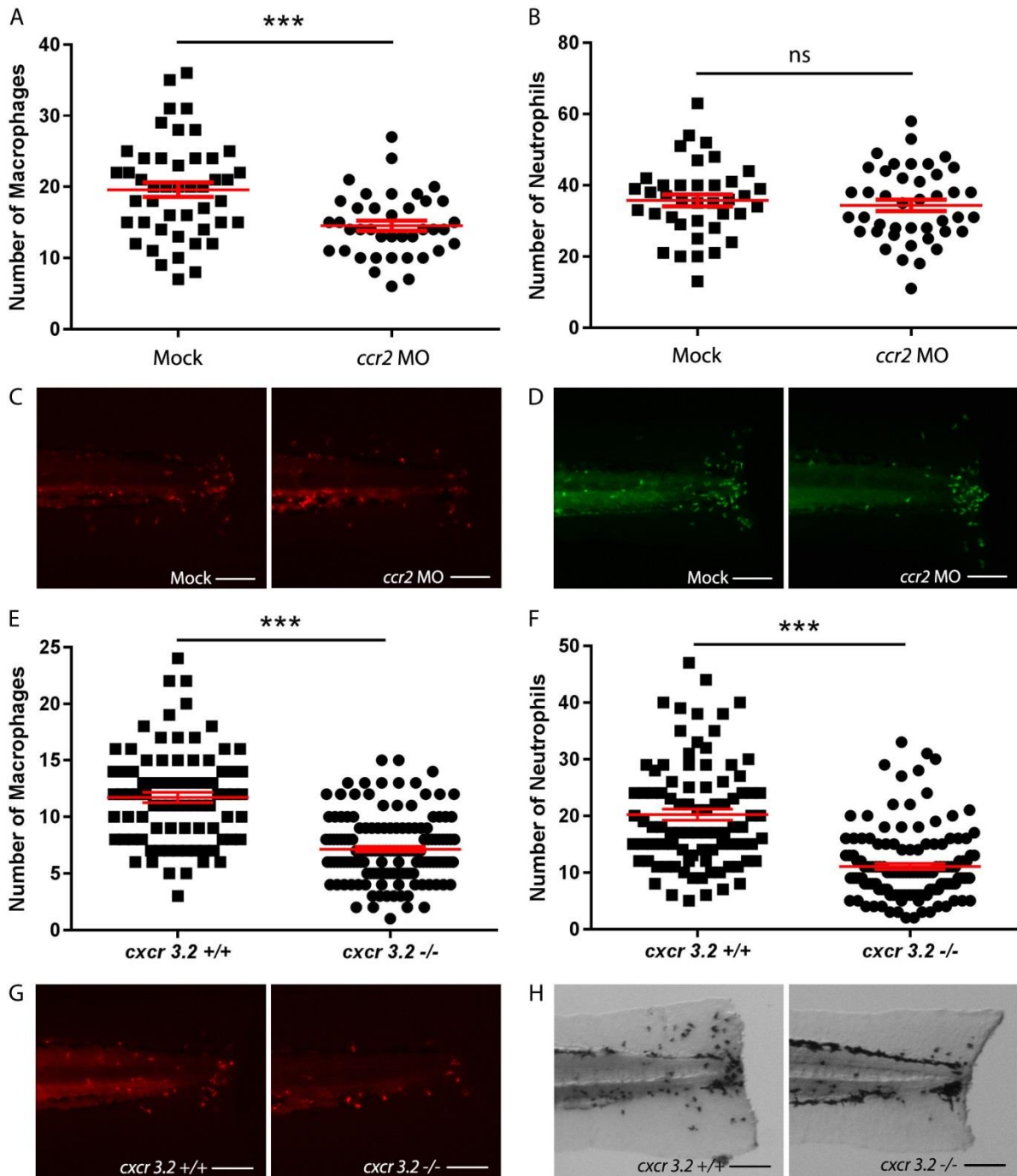


Figure 4. Effect of *ccr2* morpholino knockdown or *cxcr3.2* mutation on macrophage and neutrophil recruitment upon tail amputation in larvae. A-B. The number of macrophages (A) and neutrophils (B) recruited to the wounded area at 4 hpa in 3 dpf *Tg(mpx:GFP/mpeg1:mCherry-F)* larvae. In *ccr2* morpholino injected larvae, a significantly reduced number of macrophages were recruited compared to the number in mock(vehicle)-injected larvae. Statistical analysis were performed by two-tailed t-test. No significant difference was observed for the number of recruited neutrophils. Data were pooled from 3 independent experiments. Means \pm s.e.m. are indicated in red. Statistical significance is indicated by: ns, non-significant; *** $P < 0.001$. C-D. Representative images of the macrophages (fluorescently labeled by mCherry) (C) and the neutrophils (fluorescently labeled by GFP) (E) of mock-injected and *ccr2* morpholino-injected larvae at 4 hpa. Scale bar = 100 μ m. E-F. The number of macrophages (E) and neutrophils (F) that recruited to the wounded area at 4 hpa in 3 dpf *Tg(mpeg1:mCherry-F)*

larvae. Statistical analysis were performed by two-tailed t-test. A significantly reduced number of macrophages and neutrophils were recruited in *cxcr3.2* mutant larvae compared to the number in wild type controls. Data were pooled from 3 independent experiments. Means \pm s.e.m. are indicated in red. Statistical significance is indicated by: *** $P < 0.001$. G-H. Representative images of the macrophages (fluorescently labeled by mCherry) (G) and the neutrophils (stained using MPX assay) (H) of wild type and *cxcr3.2* mutant larvae at 4 hpa. Scale bar = 100 μ m.

Beclomethasone attenuates almost all amputation-induced changes in gene expression in macrophages

To study whether glucocorticoid treatment changes the transcriptional response of macrophages to wounding, we performed a transcriptome analysis on FACS-sorted macrophages derived from larvae at 4 hpa. We found that 620 genes were significantly regulated by amputation, of which 411 genes were upregulated and 209 genes were downregulated (Figure 5A, D, E). When the larvae had been amputated and treated with beclomethasone, only 327 significantly regulated genes were identified, of which 260 genes were upregulated and 67 genes were downregulated (Figure 5B, D, E). Apparently, amputation-induced gene regulation in macrophages is attenuated by beclomethasone administration. To study the effect of beclomethasone on the amputation-induced changes in gene expression in macrophages in more detail, we plotted the level of regulation by the combined amputation and beclomethasone treatment against the regulation by amputation in the absence of beclomethasone, for all genes that were significantly regulated by at least one of these treatments (Figure 5F). The resulting scatter plot shows that 75.37% of the genes regulated by amputation showed attenuation of this regulation when amputation was performed in the presence of beclomethasone. These results indicate that beclomethasone has a very general and strong dampening effect on the amputation-induced changes in gene expression in macrophages, which is in contrast with the lack of inhibition of the migration of these cells towards the wounded area.

Interestingly, only a small overlap was observed between the cluster of 620 amputation-regulated genes and the cluster of 327 genes regulated by the combined amputation and beclomethasone treatment (Figure 5A, C, D, E). Only 60 and 11 genes were present in the overlap between these clusters for up-regulation and down-regulation respectively (Figure 5 D, E). A large overlap was observed between the gene cluster regulated by the combination treatment and the cluster regulated by beclomethasone (without amputation) (134 genes in total, Figure 5B, C, D, E, Supplementary Figure 1A). This indicates that the cluster of genes regulated by the combination treatment mainly contains genes that are regulated as a result of the beclomethasone treatment. Apparently, amputation hardly affects beclomethasone-induced changes in gene expression, whereas beclomethasone has a very strong effect on amputation-induced transcriptional changes. The smallest overlap was observed between the cluster of amputation-regulated genes and the cluster of beclomethasone-regulated

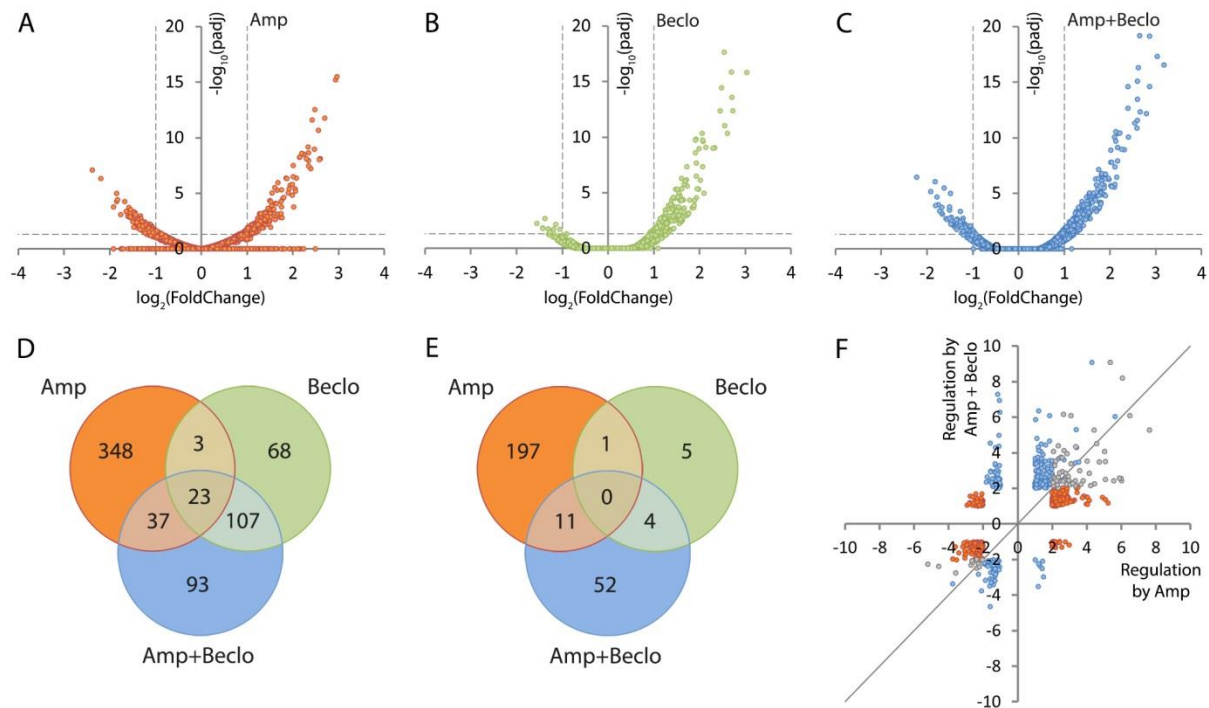


Figure 5. Macrophage-specific transcriptome analysis by RNA sequencing showing modulation of amputation-induced gene regulation by beclomethasone. A-C. Volcano plots indicating the fold change (x-axis) and p-value (y-axis) of the regulation for individual genes by amputation (A), beclomethasone (B) and the combined amputation/beclomethasone treatment (C), compared to the non-amputated, vehicle-treated control group. D-E. Venn diagrams showing overlaps between clusters of genes significantly upregulated (D) or downregulated (E) by amputation (Amp), beclomethasone (Becl) and the combined amputation/beclomethasone treatment (Amp+Becl). The diagrams show that there is a large number of genes regulated by amputation in macrophages. Beclomethasone affects the expression of a relatively small number of genes, but it decreases the number of genes significantly regulated upon amputation. F. Scatter plot showing the effect of beclomethasone treatment on amputation-regulated gene expression. For all genes showing significant regulation upon amputation (red and grey dots) or the combined beclomethasone and amputation treatment (blue and grey dots), the fold change due to beclomethasone and amputation treatment was plotted as a function of the fold change due to amputation. The grey dots represent the overlap between amputation and combination treatment. The grey line indicates the point at which beclomethasone treatment does not alter amputation-induced gene regulation. Of all the genes that were significantly regulated by amputation in macrophages, 75.37% showed attenuation in the presence of beclomethasone. Paired analysis were performed using DESeq (v1.26.0) R package by comparing each group to the control group (non-amputated/vehicle treated). Significantly regulated genes were selected by using a $p_{adj} < 0.05$ and $|\text{FoldChange}| > 2$ cutoff.

genes (Figure 5A, B, D, E, Supplementary Figure 1B), which suggests that upon amputation endogenous glucocorticoid signaling due to increased cortisol levels only regulates a small number of genes.

Using gene ontology analysis, we classified the regulated genes according to the KEGG-pathways they are involved in (Supplementary Figure 2, Supplementary Table 1). This analysis showed that the largest group of pathways regulated by amputation were involved in metabolism (16 pathways, 98 genes) and that 4 pathways (19 genes) involved in the immune system were altered. The combined amputation

and beclomethasone treatment affected a smaller number of pathways for both metabolism- and immune system-related pathways (12 pathways and 26 genes, and 1 pathway and 6 genes respectively). Only 5 of these pathways (Toll-like receptor signaling pathway, Insulin resistance, Biosynthesis of antibiotics, Galactose metabolism, Glycolysis/Gluconeogenesis) were both regulated by amputation and by the combination treatment. Beclomethasone treatment (without amputation) affected 7 pathways (5 metabolism-related), of which 6 were also regulated when the larvae were amputated in the presence of beclomethasone.

Among the significantly enriched metabolism-related KEGG pathways, we studied 3 specific pathways which are known to be associated with specific macrophage phenotypes: glycolytic metabolism which is increased in pro-inflammatory (M1) macrophages, and mitochondrial oxidative phosphorylation (OXPHOS) and tricarboxylic acid (TCA) cycle which are related to the anti-inflammatory (M2) phenotype [72]. We mapped the gene expression levels into these pathways (Supplementary Figure 3 A-C). The data showed that the vast majority of the mapped genes were up-regulated by amputation and this up-regulation was inhibited by beclomethasone treatment. We, therefore, conclude from the gene ontology analysis that amputation mainly up-regulates genes involved in metabolism and the immune system and that the vast majority of the amputation-induced changes in these gene ontology groups are attenuated by glucocorticoids.

Glucocorticoids inhibit the differentiation of macrophages towards a pro-inflammatory phenotype

Subsequently, we specifically analyzed the regulation of immune-related genes. For all immune-related genes that were significantly regulated by amputation, we plotted the regulation by amputation, by beclomethasone, and by the combination of amputation and beclomethasone (Figure 6). For the vast majority of these genes, the amputation-induced changes were attenuated by the administration of beclomethasone. Among those genes were 3 that are known to be associated with a pro-inflammatory (M1) phenotype of macrophages: *tnfa*, *il1b*, and *il6* [30, 73]. For 3 genes (*cd22*, *alox5ap*, and *tlr5b*), the amputation-induced regulation was enhanced by beclomethasone. These findings suggest that the differentiation of macrophages to a pro-inflammatory (M1) phenotype is sensitive to inhibition by glucocorticoids.

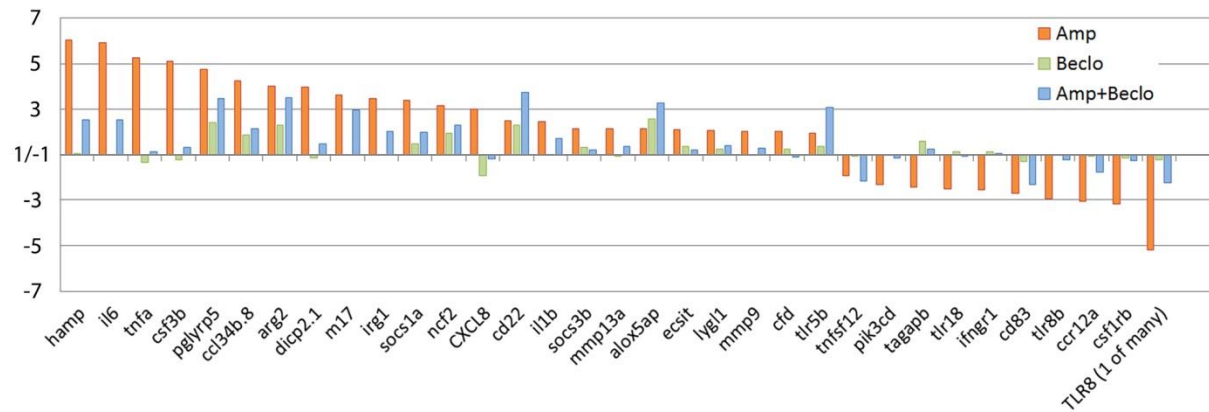


Figure 6. Regulation of immune-related genes in macrophages, determined by RNA sequencing analysis. For all genes significantly regulated upon amputation, the fold change due to amputation (Amp; red bars), beclomethasone (Beclomethasone; green bars), and the combined amputation/beclomethasone treatment (Amp+Beclomethasone; blue bars) is shown. The results show that beclomethasone dampens the amputation-induced expression of most genes, but for 4 genes (*cd22*, *alox5ap*, *tlr5b*) the combined treatment results in a higher fold change compared to the amputation treatment. Paired analysis were performed using DESeq (v1.26.0) R package by comparing each group to the control group (non-amputated/vehicle treated). Significantly regulated genes were selected by using a $p_{adj} < 0.05$ and $|\text{FoldChange}| > 2$ cutoff.

To study the glucocorticoid sensitivity of macrophage differentiation in more detail and validate some of the observed transcriptional changes, we performed qPCR on RNA samples isolated from FACS-sorted macrophages. At 4 hpa, the expression of 4 classic pro-inflammatory genes was measured: *il6*, *il1b*, *tnfa*, *mmp9*, of which the first 3 are markers for M1 macrophages and the 4th encodes a metalloproteinase that facilitates leukocyte migration by remodeling the extracellular matrix [30, 73, 74] (Figure 7A). The expression levels of *il6* and *il1b* showed an amputation-induced increase, and this increase was attenuated upon the combined beclomethasone and amputation treatment. The levels of *tnfa* and *mmp9* expression were not significantly increased by amputation, but the expression level of *tnfa* was significantly lower after the combination treatment compared to the amputation treatment.

In addition, we measured the expression levels of 4 markers for M2 macrophages, *arg2*, *cxcr4b*, *tgfb1* and *ccr2* [73, 75] (Figure 7B). The expression level of *arg2* was induced by amputation at 4 hpa, and this induction was similar upon the combination treatment. The other genes were not upregulated by amputation at this time point, but upon beclomethasone treatment the expression of *cxcr4b* was increased. Since the M2 macrophage markers are expected to show increased expression levels during the resolution phase of the inflammatory response [73], we measured the expression of those genes in macrophages at 24 hpa as well (Supplementary Figure 4 A). However, no significant upregulation by amputation was observed for any of these 4 genes. Thus, in this experiment on M2 markers, we only

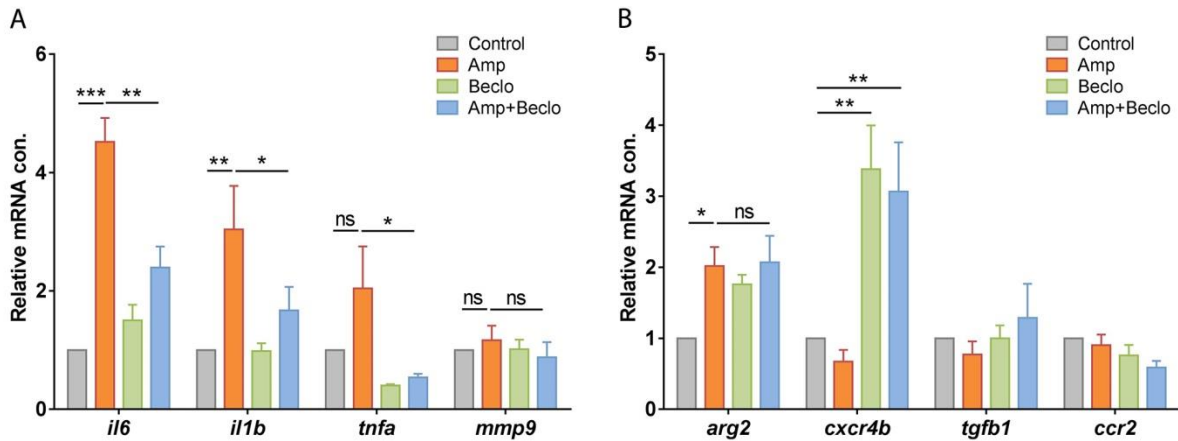


Figure 7. Expression levels of immune-related genes in FACS-sorted macrophages, determined by qPCR for *il6*, *il1b*, *tnfa*, *mmp9* (A) and for *arg2*, *cxcr4b*, *tgfb1*, *ccr2* (B) at 4hpa in 3 dpf larvae. Statistical analysis (ANOVA with a Fisher's LSD post hoc) showed the levels of *il6* and *il1b* expression were significantly increased by amputation, and this effect was inhibited by beclomethasone treatment. The expression level of *arg2* showed a significant increase upon amputation, and beclomethasone treatment did not affect this regulation. The expression level of *cxcr4b* was increased by beclomethasone treatment. Values shown are the means \pm s.e.m. of three independent experiments. Statistical significance is indicated by: ns, non-significant; * $P < 0.05$; ** $P < 0.01$; *** $P < 0.001$.

found an amputation-induced upregulation of the expression of *arg2* at 4 hpa, and this upregulation was insensitive to beclomethasone.

To further study the influence of beclomethasone on the differentiation of macrophages towards a pro-inflammatory (M1) phenotype, we used a reporter line for the expression of *tnfa*: the *Tg(mpeg1:mCherry-F/tnfa:eGFP-F)* fish line. Larvae from this line were amputated at 5 dpf, and at a more distal position than in the previous experiments to create a wound that recruits fewer macrophages which facilitates the visualization of individual *tnfa* expressing macrophages. We performed live confocal imaging at 2 and 4 hpa, and the GFP expression level in macrophages was used as a reporter for *tnfa* promoter activity *in vivo* (Figure 8 A-C). In the control group, an increase in the percentage of GFP-positive macrophages was observed between 2 and 4 hpa. During this time course, this percentage increased from $9.8 \pm 3.4\%$ to $23.8 \pm 4.0\%$. The images show that GFP expression does not exclusively occur in macrophages that have reached the wounded area. In the beclomethasone-treated group, at both time points, a lower percentage of *tnfa* expressing macrophages was recruited to the wounded area compared to the control group ($1.7 \pm 1.7\%$ and $1.4 \pm 1.4\%$ respectively).

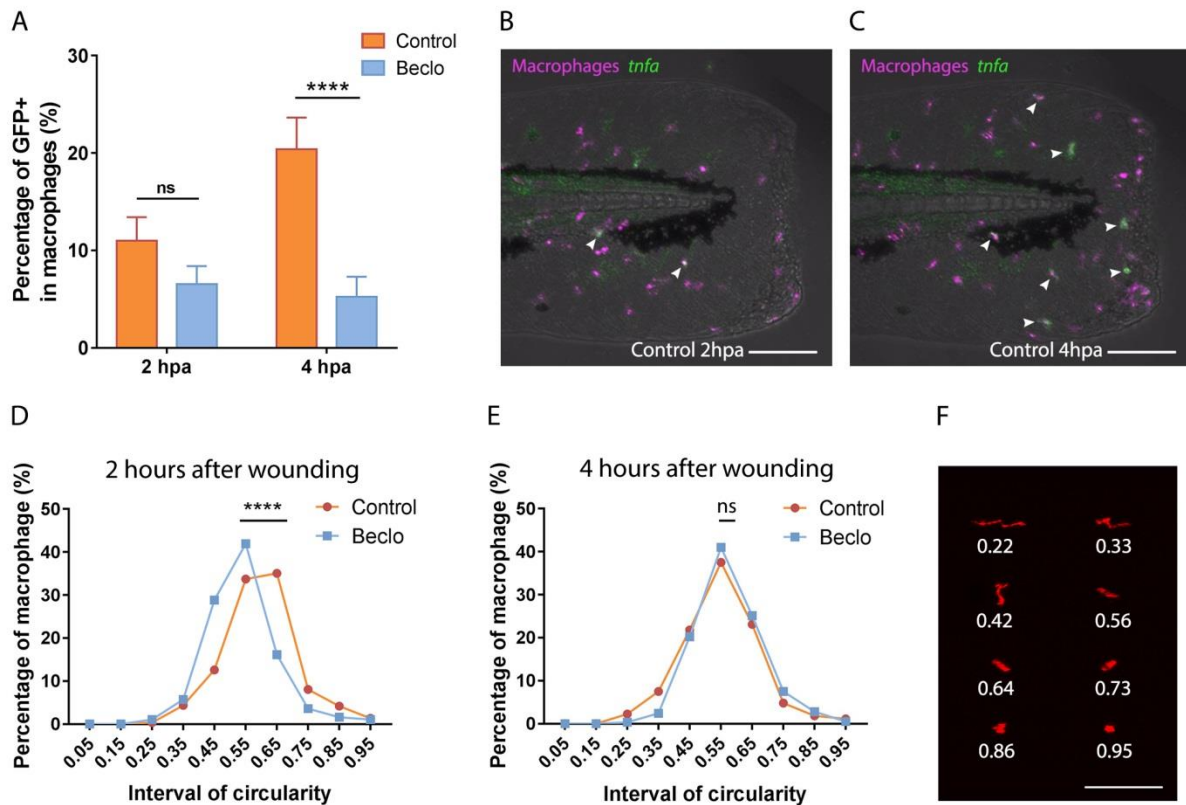


Figure 8. Effect of beclomethasone on the phenotype of macrophages. A. In *Tg(mpeg1:mCherry-F/tnfa:eGFP-F)* reporter larvae, the number of GFP-positive macrophages (as a percentage of the total number of macrophages) recruited to the wounded area were quantified at 2 and 4 hpa in 5 dpf larvae. Statistical analysis was performed by ANOVA with a Fisher's LSD post hoc. In the beclomethasone-treated group (Becl), at 4 hpa, a significantly reduced percentage of the recruited macrophages was GFP-positive compared to the vehicle-treated group (Control). Values shown are means \pm s.e.m. Statistical significance is indicated by: ns, non-significant; **** $P < 0.0001$. B-C. Representative images of macrophages (fluorescently labeled by mCherry) and GFP-positive macrophages (fluorescently labeled by both mCherry and GFP) in the control group at 2 hpa (B) and 4 hpa (C). Scale bar = 100 μ m. Arrow heads indicate macrophages displaying the GFP signal, which is a measure for activation of the *tnfa* promoter. D-E. The distribution of circularity of macrophages recruited to the wounded area at 2 h after wounding (a small hole was punched in the tail fin) (D) and at 4 h after wounding hpa (E) in 3 dpf *Tg(mpeg1:mCherry-F)* larvae. Statistical analysis were performed by Kolmogorov-Smirnov test. At 2 hpa, a significant difference of distribution pattern was observed between the two groups, with the beclomethasone-treated group (Becl) shifted towards lower circularity. At 4 hpa, no significant difference was observed. Statistical significance is indicated by: ns, non-significant; **** $P < 0.0001$. F. Representative images of macrophages analyzed in D and E and their corresponding circularity. Scale bar = 100 μ m.

Finally, we analyzed the influence of beclomethasone on the morphology of macrophages, since macrophage morphology has been shown to be an indicator for their differentiation: M1 macrophages are generally less elongated and dendritic than M2 macrophages [73]. Instead of amputation, a small hole was punched in the tail fins of the larvae with a glass microcapillary needle to recruit a reduced number of leukocytes, which facilitated the visualization of individual cells. We performed live confocal imaging at 3 dpf with the *Tg(mpx:GFP/mpeg1:mCherry-F)* fish line and the circularity of mCherry-

positive macrophages was used to quantitate the morphology (Figure 8 D-E). In the control group, at 2 hpa, the percentage of macrophages with a high circularity (0.5-1.0) was relatively high (67.6±4.0%) and gradually decreased to 47.9±3.2% at 12 hpa (Supplementary Figure 5 A). In the beclomethasone-treated group, at 2 hpa the percentage of macrophages with a high circularity was lower (51.7±3.5%) and remained relatively stable until 12 hpa (Supplementary Figure 5 B). The most obvious difference between the control and beclomethasone-treated group was observed at 2 hpa. At this time point, the plot showing the distribution of circularity shows a clear shift towards a lower circularity in the beclomethasone-treated group (Figure 8 D). At 4 hpa, this difference of circularity distribution between the control group and beclomethasone-treated group had disappeared (Figure 8 E). The highly transient nature of the increased circularity is probably due to the small size of the wound in this experiment. These data from the analysis of the circularity may suggest an inhibitory effect of beclomethasone on the differentiation of macrophages towards a pro-inflammatory (M1) phenotype, in line with the data obtained using the *tnfa:eGFP-F* reporter line.

Discussion

Although glucocorticoids have been used as anti-inflammatory drugs for decades, their mechanism of action and the specificity of their effects have not been fully unraveled yet. Using the zebrafish tail amputation model, we have shown that the inflammatory response comprises glucocorticoid-sensitive and glucocorticoid-insensitive pathways. Glucocorticoids inhibit the migration of neutrophils towards a site of inflammation by inhibiting the induction of chemoattractants for this cell type. However, the migration of macrophages is not affected by glucocorticoids, since the induction of two chemoattractants that are critical for macrophage recruitment, *ccl2* and *cxcl11aa*, is insensitive to treatment with the glucocorticoid beclomethasone. Using RNAseq analysis we show that beclomethasone attenuates most transcriptional responses to amputation in macrophages and inhibit their differentiation towards a pro-inflammatory (M1) phenotype.

Chemoattractants are important trafficking signals that direct the movement of immune cells into and out of specific tissues [76]. In this study, we have demonstrated that glucocorticoids exert a specific inhibitory effect on the induction of the expression of two chemoattractants involved in neutrophil recruitment (Il8 and Cxcl18b). Using *in vitro* and *in vivo* models, it has been demonstrated that human and mouse neutrophil migration is dependent on the induction of Il8 expression [68, 77, 78] and that this induction is inhibited by glucocorticoids [79-81]. In mammals, Il8 has been demonstrated to signal through the chemokine receptors Cxcr1 and Cxcr2, whereas in zebrafish only Cxcr2 has been shown to mediate the effects of Il8 [66, 82]. Interestingly, our RNAseq data show that amputation increased the expression of *il8* in macrophages, and that this increase was strongly attenuated by beclomethasone.

These data suggest that the glucocorticoid inhibition of the neutrophil migration results at least partly from the suppression of chemoattractant expression in macrophages. *Cxcl18b*, a chemokine specific for fish and amphibian species, has also been shown to act as a ligand for *Cxcr2* in zebrafish, thereby stimulating chemotaxis of neutrophils [67]. These findings suggest that *Cxcr2* activation is crucial for the migration of neutrophils and that glucocorticoids inhibit this migration by attenuating the induction of the expression of *Cxcr2* agonists like *Il8* and *Cxcl18b*.

In contrast to the inhibitory effect on neutrophil migration, our study revealed that glucocorticoids leave the induction of chemoattractants involved in macrophage recruitment (*Ccl2* and *Cxcl11aa*) unaffected. *Ccl2*, also known as monocyte chemoattractant protein-1 (MCP-1), and *Cxcl11aa* have been shown to be key chemokines implicated in macrophage migration and infiltration in humans and mice [64, 83-87]. In zebrafish, their role as chemoattractants for macrophages has been demonstrated during mycobacterial infection [65, 66, 71]. Our data show that these two chemoattractants also promote macrophage migration in the tail amputation model and that beclomethasone has no effect on the amputation-induced increase in their expression levels. The RNAseq analysis showed very low expression levels of *ccl2* and undetectable levels of *cxcl11aa* expression in macrophages, which suggests that the contribution of these cells to the increased expression of these chemokines is limited.

In line with our findings, it has been shown in bronchoalveolar lavage fluid of COPD patients that glucocorticoid treatment reduces neutrophil numbers, but that the number of macrophages was not decreased [88]. Contrary to our findings, in most of the studies carried out in humans and rats, the inflammation-induced *Ccl2* level has been found to be inhibited by glucocorticoids [83, 89, 90], and this inhibition is related to a decreased p38 MAPK phosphorylation [90, 91]. Similarly, glucocorticoids have been shown to inhibit *Cxcl11* upregulation in fluticasone propionate-stimulated peripheral blood monocytes, and in IFN- γ - or LPS-stimulated RAW 264.7 macrophages, as well as in multiple tissues of endotoxemia mice [28, 92]. Nevertheless, some studies do show an insensitivity of the mammalian *Ccl2* or *Cxcl11aa* induction to glucocorticoid treatment. In a breast cancer cell line (T47D), glucocorticoid treatment has no effect on *Il1*-stimulated *Ccl2* production [93], and in A549 epithelial cells, IFN γ -induced *Cxcl11* is insensitive to glucocorticoid treatment [94]. These data suggest that the observed insensitivity of the *ccl2* and *cxcl11a* induction to glucocorticoids, which underlies the glucocorticoid insensitivity of macrophage migration, requires a specific context, which may involve factors like the activating signal, the glucocorticoid treatment regime, or the cell type and tissue involved.

Although glucocorticoids did not affect the migration of macrophages in our study, they did have a big impact on the transcriptional changes in these cells upon amputation. We showed by RNAseq analysis

in FACS-sorted macrophages that, similarly to our previous findings from a microarray analysis carried out on RNA isolated from whole larvae [59], most of the amputation-induced transcriptional changes are decreased by beclomethasone, whereas a small subset of transcriptional responses is insensitive to glucocorticoid treatment. Focusing on the regulation of immune-related genes, we found that, in line with our previous findings in whole larvae [59], beclomethasone suppressed the induction of almost all pro-inflammatory, M1 associated, genes, like *il6*, *tnfa*, *il1b*, *il8* and *mmp9*. In line with these data, many genes involved in glycolysis, a metabolic pathway often associated with an M1 phenotype [72, 95, 96], were upregulated upon amputation and this upregulation was mostly inhibited by beclomethasone. This inhibitory effect of glucocorticoids on the induction of pro-inflammatory genes in macrophages is in agreement with *in vitro* results obtained in LPS-stimulated primary mouse macrophages [17, 18, 97]. In addition, *in vivo* data obtained in mouse models for arthritis and acute lung injury demonstrated an inhibitory effect of glucocorticoids on the differentiation of macrophages towards a pro-inflammatory M1 phenotype [31, 32]. In the present study, we observed a reduction in the number of macrophages with activation of a *tnfa:eGFP-F* reporter gene upon beclomethasone administration, and a morphology characterized by a low circularity, which demonstrates that the macrophage differentiation to an M1 phenotype was inhibited by the glucocorticoid treatment. Taken together, these data strongly support the idea that glucocorticoids inhibit the differentiation of macrophages to an M1 phenotype by interfering at the level of transcription.

This glucocorticoid effect on macrophages may have great clinical relevance, since this cell type has been identified as the main target for glucocorticoid action in several animal models for inflammatory diseases [98-100]. In murine models for contact allergy and septic shock it has been shown that the anti-inflammatory effect of glucocorticoids depends on the presence of GR in macrophages, suppressing the induction of pro-inflammatory mediators like IL-1 β [99, 101]. These glucocorticoid effects are absent in a mouse line with a deficiency in GR dimerization, suggesting that activation of anti-inflammatory gene transcription through GRE binding may be the main GR mechanism of action [99, 101]. Furthermore we conclude that the glucocorticoid resistance observed in macrophage-dominated inflammatory diseases like COPD cannot be attributed to a general insensitivity of macrophages to the immune-suppressive effects of glucocorticoids.

In addition to the effect of glucocorticoids on M1 differentiation, we investigated their effect on the differentiation of macrophages to an M2 phenotype. Previous studies in a mouse arthritis model showed that the induction of an M2 phenotype was not affected by glucocorticoids [31] and in an acute lung injury model [32] it was shown to be enhanced. In our RNAseq and qPCR analysis, the M2 marker *arg2* [30, 73, 75] was among the small subset of amputation-induced genes that were insensitive to beclomethasone, suggesting that the differentiation to an M2 phenotype is insensitive

to glucocorticoids. However, genes involved in the TCA cycle and OXPHOS, metabolic pathways associated with an M2 phenotype [72, 95, 96], were upregulated upon amputation and this upregulation was inhibited by beclomethasone, which would suggest that M2 differentiation is blocked by glucocorticoid treatment. In our qPCR analysis, we showed that the expression of various other M2 markers (*cxcr4b*, *tgfb1*, *ccr2*) was not increased upon amputation. The variation in responses of M2 markers to amputation and /or glucocorticoid treatment in our assay supports the idea that the M2 phenotype of macrophages may occur as various alternative differentiation states [29, 30]. Independent of the amputation, beclomethasone increased the expression of *cxcr4b* (and to a lesser extent *ccr2*), in line with previous observations that glucocorticoids induce the differentiation of human macrophages to an M2 phenotype *in vitro* [28, 102]. In summary, whereas the amputation-induced increases in the expression levels of M1 markers are consistently inhibited by beclomethasone, increased expression of M2 markers (when present in our assay) can be either insensitive or suppressed by glucocorticoid treatment.

In our tail amputation model for inflammation, the vast majority of macrophage transcriptional responses was suppressed by glucocorticoids and only a small subset of these responses was not affected. Studies in murine models for inflammatory diseases suggest that the anti-inflammatory GR action in macrophages depends on GRE-dependent transcriptional regulation, probably reducing the activation of a subset of pro-inflammatory transcription factors [98, 99, 101]. Alternatively, our data may indicate an important role for GR interaction ('tethering') with the transcription factor NF- κ B, since in many studies it has been shown that the NF- κ B-mediated transcriptional activation can be suppressed by GR or remains unaffected [17-20]. Recruitment of IRF3 to the transcription initiation complex has been shown to be associated with sensitivity to GR suppression [17, 97].

In conclusion, our *in vivo* study of the glucocorticoid modulation of the transcriptional responses to wounding using the zebrafish tail amputation model shows that the vast majority of these responses are sensitive to glucocorticoids, and only a small subset are insensitive. These insensitive responses play a role in the migration of macrophages and possibly their differentiation to an M2 phenotype, whereas the sensitive responses are involved in the migration of neutrophils and the differentiation of macrophages to an M1 phenotype. Our data demonstrate that these processes can be regulated independently, and that glucocorticoids exert their immunosuppressive effects on macrophages by modulating differentiation rather than migration.

Materials and methods

Zebrafish lines and maintenance

Zebrafish were maintained and handled according to the guidelines from the Zebrafish Model Organism Database (<http://zfin.org>) and in compliance with the directives of the local animal welfare committee of Leiden University. They were exposed to a 14 hours light and 10 hours dark cycle to maintain circadian rhythmicity. Fertilization was performed by natural spawning at the beginning of the light period. Eggs were collected and raised at 28°C in egg water (60 µg/ml Instant Ocean sea salts and 0.0025% methylene blue).

The following fish lines were used in this work: wild type (wt) strain AB/TL, the double transgenic lines *Tg(mpx:GFP/mpeg1:mCherry-F)* [49, 103] and *Tg(mpeg1:mCherry-F/tnfa:eGFP-F)* [73], and the combination of *Tg(mpeg1:mCherry-F)* and the homozygous mutants (*cxcr3.2^{-/-}*) or wt siblings (*cxcr3.2^{+/+}*) of the *cxcr3.2^{hu6044}* mutant strain [66].

Tail amputation and chemical treatments

After anesthesia with 0.02% aminobenzoic acid ethyl ester (tricaine, Sigma Aldrich), the tails of 3 days post fertilization (dpf) embryos were partially amputated (Figure 1A) with a 1mm sapphire blade (World Precision Instruments) on 2% agarose-coated Petri dishes under a Leica M165C stereomicroscope [49, 59]. In the experiment on larvae from the *Tg(mpeg1:mCherry-F/tnfa:eGFP-F)* line, the site of amputation was more distal, so the wound attracted a lower number of leukocytes, which facilitated the imaging of individual cells (Figure 8A-C). In the experiment in which we determined the morphology of the macrophages (Figure 8D-F), a hole was punched in the tail fin with a glass microcapillary needle (Harvard Apparatus, preparation of needles with 10-20 µm outer diameter described in [104]), in order to make an even smaller wound and attract an even lower number of leukocytes. Wounded and non-wounded (control) embryos were pretreated for 2 hours with 25 µM beclomethasone (Sigma Aldrich) or vehicle (0.05% dimethyl sulfoxide (DMSO)) in egg water prior to amputation/wounding and received the same treatment after the amputation/wounding.

Imaging and image quantification

Images of fixed or live larvae were captured using a Leica M205FA fluorescence stereomicroscope, equipped with a Leica DFC 345FX camera. In all fish lines used, the macrophages were detected based on the fluorescence of their mCherry label. Neutrophils were detected based on either their fluorescent GFP label or their mpx staining. To quantify the number of macrophages and/or neutrophils recruited to the wounded area, the cells in a defined area of the tail (Figure 1A) were

counted manually. Data were pooled from two or three independent experiments, and the means \pm s.e.m. of the pooled data are indicated.

Confocal microscopy and image analysis

For time lapse imaging and automated tracking of the leukocyte migration, the amputated larvae were mounted in 1.2% low melting agarose in egg water containing 0.02% tricaine and 25 μ M beclomethasone or 0.05% DMSO on 40 mm glass bottom dishes (Willco-Dish) and covered with 1.5 ml egg water containing tricaine and the corresponding chemicals. Confocal microscopy was performed using a Nikon Eclipse Ti-E microscope with a Plan Apo 20X/0.75 NA objective. A 488 nm laser was used for excitation of GFP and a 561 nm laser was used for excitation of mCherry. Time-lapse microscopy was performed at 28 °C with an interval of approximately one minute. From the obtained z-stacks, aligned maximum projection images were generated using NIS-Elements, which were further analyzed using Image J with custom-made plugins, developed by Dr. Joost Willemse (Leiden University), for localizing and tracking of cells ('Local Maxima Stack' and 'Track Foci', algorithms described previously in [105] and determining their circularity (calculated as $(\text{area} \times 4\pi)/(\text{circumference})^2$).

Morpholino injection

A morpholino targeting the translational start site of the *ccr2* gene (5'AACTACTGTTTTGTGTCGCCGAC3', purchased from Gene Tools) [71] was prepared and stored according to the manufacturer's instructions. Injection of 1 nl (0.5 mM) of the morpholino solution was performed into the yolk of fertilized eggs at the 1-2 cell stage.

RNA isolation, cDNA synthesis and quantitative PCR (qPCR)

At different time points after amputation, larvae were collected (15-20 per sample) in QIAzol lysis reagent (QIAGEN) for RNA isolation, which was performed using the miRNeasy mini kit (Qiagen), according to the manufacturer's instructions. Extracted total RNA was reverse-transcribed using the iScript™ cDNA Synthesis Kit (Bio-Rad). QPCR was performed on a MyiQ Single-Color Real-Time PCR Detection System (Bio-Rad) using iTaq™ Universal SYBR® Green Supermix (Bio-Rad). The sequences of the primers used are provided in Supplementary Table 2. Cycling conditions were pre-denaturation for 3 min at 95°C, followed by 40 cycles of denaturation for 15 s at 95°C, annealing for 30 s at 60°C, and elongation for 30 s at 72°C. Fluorescent signals were detected at the end of each cycle. Cycle threshold values (Ct values, i.e. the cycle numbers at which a threshold value of the fluorescence intensity was reached) were determined for each sample. For each sample, the Ct value was subtracted from the Ct value of a control sample, and the fold change of gene expression was calculated and adjusted to the

expression levels of a reference gene (*peptidylprolyl isomerase Ab (ppiab)*). Data shown are means \pm s.e.m. of three independent experiments.

Myeloperoxidase (Mpx) staining

Larvae were fixed in 4% paraformaldehyde (PFA, Sigma Aldrich) at 4°C overnight, and rinsed with PBS containing 0.05% Tween20. The myeloperoxidase (mpx) staining for the *cxcr3.2* mutant line was performed using the Peroxidase (Myeloperoxidase) Leukocyte kit (Sigma Aldrich), according to the manufacturer's instructions. To visualize both macrophages and neutrophils in the same larvae, the mpx staining was always performed after imaging of the fluorescent signal of the macrophages.

Fluorescence-Activated Cell Sorting (FACS) of macrophages

Macrophages were sorted from *Tg(mpeg1.4:mCherry-F)* embryos as previously described [106, 107]. Dissociation was performed with 100-150 embryos for each sample at 4 hours post amputation (hpa) using Liberase TL (Roche) and stopped by adding Fetal Calf Serum (FCS) to a final concentration of 10%. Isolated cells were resuspended in Dulbecco's PBS (DPBS), and filtered through a 40 μ m cell strainer. Actinomycin D (Sigma Aldrich) was added (final concentration of 1 μ g/ml) to each step to inhibit transcription. Macrophages were sorted based on their red fluorescent signal using a FACSaria III cell sorter (BD Biosciences). The sorted cells were collected in QIAzol lysis reagent (Qiagen) for RNA isolation. Extracted total RNA was either reverse-transcribed for qPCR or amplified using the SMART-seq V4 kit (Clontech) for sequencing.

Transcriptome analysis

A total of 12 samples (four experimental groups obtained from three replicate experiments) were processed for transcriptome analysis using cDNA sequencing. The RNA seq libraries generated with the SMART-seq V4 kit were sequenced using an Illumina HiSeq 2500 instrument according to the manufacturer's instructions with a read length of 50 nucleotides. Image analysis and base calling were done by the Illumina HCS version 2.2.68, and RTA version 1.18.66. cDNA sequencing data were analyzed by mapping the reads to the *Danio rerio* GRCz10 reference genome with annotation version 80 using Tophat (v2.1.0). Subsequently, the DESeq (v1.26.0) R package was used to test for differential expression. Before each analysis, the genes with low reads were removed (i.e. those genes for which the sum of reads from three replicates of the analyzed two groups was lower than 30). The output data were used for transcriptome analysis. Significant gene regulation was defined by using $p_{adj} < 0.05$ and $|\text{FoldChange}| > 2$ cutoffs. The raw data are available at Gene Expression Omnibus database under accession number GSE122643.

Gene ontology analysis was performed using the online functional classification tool Database for Annotation, Visualization, and Integrated Discovery (DAVID; <http://david.abcc.ncifcrf.gov/summary.jsp>). Further analysis of the macrophage transcriptomes was performed in R v3.4.3 using *Bioconductor* v3.6. Zebrafish Ensembl gene IDs were converted to Entrez Gene IDs using the R package *org.Dr.eg.db* v3.5.0. The enriched pathways in different groups were determined by comparing the statistically differentially expressed genes against the KEGG zebrafish database using the *kegga()* function from the *edgeR* package v3.20.7. Finally, gene expression data were mapped into significantly enriched KEGG pathways using *pathview* v1.18.0.

Statistical analysis

Statistical analysis was performed using GraphPad Prism 7 by one-way or two-way ANOVA (Figure 1, Figure 2, Figure 3, Figure 7, Figure 8A, Supplementary Figure 4), Kolmogorov-Smirnov test (Figure 8D, E) or two-tailed t-test (Figure 4). Significance was accepted at $p < 0.05$ and different significance levels are indicated: * $p < 0.05$; ** $p < 0.01$; *** $p < 0.001$; **** $p < 0.0001$.

Acknowledgements

We thank Dr. Tomasz Prajsnar and Dr. Gabriel Forn-Cuní for their assistance during the analysis of the transcriptomic data, and Frida Sommer for her help during the experiments with the *cxcr3.2* mutant line.

References

1. Chrousos, G.P., *The Hypothalamic–Pituitary–Adrenal Axis and Immune-Mediated Inflammation*. New England Journal of Medicine, 1995. **332**(20): p. 1351-1363.
2. Tsigos, C. and G.P. Chrousos, *Hypothalamic–pituitary–adrenal axis, neuroendocrine factors and stress*. Journal of Psychosomatic Research, 2002. **53**(4): p. 865-871.
3. Oakley, R.H. and J.A. Cidlowski, *The biology of the glucocorticoid receptor: New signaling mechanisms in health and disease*. Journal of Allergy and Clinical Immunology, 2013. **132**(5): p. 1033-1044.
4. Heitzer, M.D., et al., *Glucocorticoid receptor physiology*. Reviews in Endocrine and Metabolic Disorders, 2007. **8**(4): p. 321-330.
5. Revollo, J.R. and J.A. Cidlowski, *Mechanisms generating diversity in glucocorticoid receptor signaling*. Ann N Y Acad Sci, 2009. **1179**: p. 167-78.
6. Chrousos, G.P. and T. Kino, *Intracellular Glucocorticoid Signaling: A Formerly Simple System Turns Stochastic*. Science's STKE, 2005. **2005**(304): p. pe48-pe48.
7. Ramamoorthy, S. and J.A. Cidlowski, *Exploring the Molecular Mechanisms of Glucocorticoid Receptor Action from Sensitivity to Resistance*. Endocrine development, 2013. **24**: p. 41-56.
8. Busillo, J.M. and J.A. Cidlowski, *The five Rs of glucocorticoid action during inflammation: ready, reinforce, repress, resolve, and restore*. Trends in Endocrinology & Metabolism, 2013. **24**(3): p. 109-119.

9. Barnes, P.J., *Glucocorticosteroids: current and future directions*. British Journal of Pharmacology, 2011. **163**(1): p. 29-43.
10. Moghadam-Kia, S. and V.P. Werth, *Prevention and treatment of systemic glucocorticoid side effects*. International journal of dermatology, 2010. **49**(3): p. 239-248.
11. Barnes, P.J., K. Ito, and I.M. Adcock, *Corticosteroid resistance in chronic obstructive pulmonary disease: inactivation of histone deacetylase*. The Lancet, 2004. **363**(9410): p. 731-733.
12. Barnes, P.J. and I.M. Adcock, *Glucocorticoid resistance in inflammatory diseases*. The Lancet, 2009. **373**(9678): p. 1905-1917.
13. Bamberger, C.M., H.M. Schulte, and G.P. Chrousos, *Molecular Determinants of Glucocorticoid Receptor Function and Tissue Sensitivity to Glucocorticoids*. Endocrine Reviews, 1996. **17**(3): p. 245-261.
14. Ratman, D., et al., *How glucocorticoid receptors modulate the activity of other transcription factors: A scope beyond tethering*. Molecular and Cellular Endocrinology, 2013. **380**(1): p. 41-54.
15. Surjit, M., et al., *Widespread Negative Response Elements Mediate Direct Repression by Agonist- Liganded Glucocorticoid Receptor*. Cell, 2011. **145**(2): p. 224-241.
16. Reichardt, H.M., et al., *Repression of inflammatory responses in the absence of DNA binding by the glucocorticoid receptor*. The EMBO Journal, 2001. **20**(24): p. 7168-7173.
17. Ogawa, S., et al., *Molecular Determinants of Crosstalk between Nuclear Receptors and Toll-like Receptors*. Cell, 2005. **122**(5): p. 707-721.
18. Sacta, M.A., et al., *Gene-specific mechanisms direct glucocorticoid-receptor-driven repression of inflammatory response genes in macrophages*. Elife, 2018. **7**.
19. Rao, N.A., et al., *Coactivation of GR and NFKB alters the repertoire of their binding sites and target genes*. Genome Res, 2011. **21**(9): p. 1404-16.
20. Kuznetsova, T., et al., *Glucocorticoid receptor and nuclear factor kappa-b affect three-dimensional chromatin organization*. Genome Biology, 2015. **16**(1): p. 264.
21. Hubner, S., et al., *The glucocorticoid receptor in inflammatory processes: transrepression is not enough*. Biol Chem, 2015. **396**(11): p. 1223-31.
22. Oh, K.S., et al., *Anti-Inflammatory Chromatinscape Suggests Alternative Mechanisms of Glucocorticoid Receptor Action*. Immunity, 2017. **47**(2): p. 298-309 e5.
23. Smoak, K.A. and J.A. Cidlowski, *Mechanisms of glucocorticoid receptor signaling during inflammation*. Mechanisms of Ageing and Development, 2004. **125**(10): p. 697-706.
24. Coutinho, A.E. and K.E. Chapman, *The anti-inflammatory and immunosuppressive effects of glucocorticoids, recent developments and mechanistic insights*. Molecular and Cellular Endocrinology, 2011. **335**(1): p. 2-13.
25. Franco, L.M., et al., *Immune regulation by glucocorticoids can be linked to cell type-dependent transcriptional responses*. J Exp Med, 2019. **216**(2): p. 384-406.
26. Meagher, L.C., et al., *Opposing effects of glucocorticoids on the rate of apoptosis in neutrophilic and eosinophilic granulocytes*. The Journal of Immunology, 1996. **156**(11): p. 4422-4428.
27. Yoshimura, C., et al., *Glucocorticoids induce basophil apoptosis*. Journal of Allergy and Clinical Immunology, 2001. **108**(2): p. 215-220.
28. Ehrchen, J., et al., *Glucocorticoids induce differentiation of a specifically activated, anti-inflammatory subtype of human monocytes*. Blood, 2007. **109**(3): p. 1265-1274.
29. Mosser, D.M. and J.P. Edwards, *Exploring the full spectrum of macrophage activation*. Nat Rev Immunol, 2008. **8**(12): p. 958-69.
30. Martinez, F.O. and S. Gordon, *The M1 and M2 paradigm of macrophage activation: time for reassessment*. F1000Prime Reports, 2014. **6**: p. 13.
31. Hofkens, W., et al., *Liposomal targeting of prednisolone phosphate to synovial lining macrophages during experimental arthritis inhibits M1 activation but does not favor M2 differentiation*. PLoS One, 2013. **8**(2): p. e54016.
32. Tu, G.W., et al., *Glucocorticoid attenuates acute lung injury through induction of type 2 macrophage*. J Transl Med, 2017. **15**(1): p. 181.

33. Cruz-Topete, D. and J.A. Cidlowski, *One Hormone, Two Actions: Anti- and Pro-Inflammatory Effects of Glucocorticoids*. *Neuroimmunomodulation*, 2015. **22**(1-2): p. 20-32.
34. Galon, J., et al., *Gene profiling reveals unknown enhancing and suppressive actions of glucocorticoids on immune cells*. *Faseb j*, 2002. **16**(1): p. 61-71.
35. Chinenov, Y. and I. Rogatsky, *Glucocorticoids and the innate immune system: Crosstalk with the Toll-like receptor signaling network*. *Molecular and Cellular Endocrinology*, 2007. **275**(1-2): p. 30-42.
36. Busillo, J.M., K.M. Azzam, and J.A. Cidlowski, *Glucocorticoids sensitize the innate immune system through regulation of the NLRP3 inflammasome*. *J Biol Chem*, 2011. **286**(44): p. 38703-13.
37. Lannan, E.A., et al., *Proinflammatory Actions of Glucocorticoids: Glucocorticoids and TNF α Coregulate Gene Expression In Vitro and In Vivo*. *Endocrinology*, 2012. **153**(8): p. 3701-3712.
38. Ding, Y., et al., *Dexamethasone Enhances ATP-Induced Inflammatory Responses in Endothelial Cells*. *Journal of Pharmacology and Experimental Therapeutics*, 2010. **335**(3): p. 693-702.
39. Langlais, D., et al., *Regulatory network analyses reveal genome-wide potentiation of LIF signaling by glucocorticoids and define an innate cell defense response*. *PLoS Genet*, 2008. **4**(10): p. e1000224.
40. Anna, D., et al., *Glucocorticoids increase interleukin-6-dependent gene induction by interfering with the expression of the suppressor of cytokine signaling 3 feedback inhibitor*. *Hepatology*, 2012. **55**(1): p. 256-266.
41. Langlais, D., et al., *The Stat3/GR interaction code: predictive value of direct/indirect DNA recruitment for transcription outcome*. *Mol Cell*, 2012. **47**(1): p. 38-49.
42. Sullivan, C., et al., *Infectious disease models in zebrafish*. *Methods Cell Biol*, 2017. **138**: p. 101-136.
43. Masud, S., V. Torraca, and A.H. Meijer, *Modeling Infectious Diseases in the Context of a Developing Immune System*. *Curr Top Dev Biol*, 2017. **124**: p. 277-329.
44. Lewis, K.L., N. Del Cid, and D. Traver, *Perspectives on antigen presenting cells in zebrafish*. *Dev Comp Immunol*, 2014. **46**(1): p. 63-73.
45. Trede, N.S., et al., *The use of zebrafish to understand immunity*. *Immunity*, 2004. **20**(4): p. 367-79.
46. Powell, D., et al., *Chemokine Signaling and the Regulation of Bidirectional Leukocyte Migration in Interstitial Tissues*. *Cell Rep*, 2017. **19**(8): p. 1572-1585.
47. Oehlers, S.H., et al., *A whole animal chemical screen approach to identify modifiers of intestinal neutrophilic inflammation*. *Febs j*, 2017. **284**(3): p. 402-413.
48. Enyedi, B., M. Jelcic, and P. Niethammer, *The Cell Nucleus Serves as a Mechanotransducer of Tissue Damage-Induced Inflammation*. *Cell*, 2016. **165**(5): p. 1160-1170.
49. Renshaw, S.A., et al., *A transgenic zebrafish model of neutrophilic inflammation*. *Blood*, 2006. **108**(13): p. 3976-8.
50. Roehl, H.H., *Linking wound response and inflammation to regeneration in the zebrafish larval fin*. *Int J Dev Biol*, 2018. **62**(6-7-8): p. 473-477.
51. Robertson, A.L., et al., *Identification of benzopyrone as a common structural feature in compounds with anti-inflammatory activity in a zebrafish phenotypic screen*. *Dis Model Mech*, 2016. **9**(6): p. 621-32.
52. Niethammer, P., et al., *A tissue-scale gradient of hydrogen peroxide mediates rapid wound detection in zebrafish*. *Nature*, 2009. **459**: p. 996.
53. Yoo, S.K., et al., *Lyn is a redox sensor that mediates leukocyte wound attraction in vivo*. *Nature*, 2011. **480**: p. 109.
54. Stolte, E.H., et al., *Evolution of glucocorticoid receptors with different glucocorticoid sensitivity*. *J Endocrinol*, 2006. **190**(1): p. 17-28.
55. Chatzopoulou, A., et al., *Transcriptional and metabolic effects of glucocorticoid receptor alpha and beta signaling in zebrafish*. *Endocrinology*, 2015. **156**(5): p. 1757-69.

56. Schaaf, M.J., et al., *Discovery of a functional glucocorticoid receptor beta-isoform in zebrafish*. *Endocrinology*, 2008. **149**(4): p. 1591-9.
57. Schaaf, M.J., A. Chatzopoulou, and H.P. Spaink, *The zebrafish as a model system for glucocorticoid receptor research*. *Comp Biochem Physiol A Mol Integr Physiol*, 2009. **153**(1): p. 75-82.
58. Alsop, D. and M.M. Vijayan, *Development of the corticosteroid stress axis and receptor expression in zebrafish*. *American Journal of Physiology-Regulatory, Integrative and Comparative Physiology*, 2008. **294**(3): p. R711-R719.
59. Chatzopoulou, A., et al., *Glucocorticoid-Induced Attenuation of the Inflammatory Response in Zebrafish*. *Endocrinology*, 2016. **157**(7): p. 2772-84.
60. Mathew, L.K., et al., *Unraveling tissue regeneration pathways using chemical genetics*. *J Biol Chem*, 2007. **282**(48): p. 35202-10.
61. Zhang, Y., et al., *In Vivo Interstitial Migration of Primitive Macrophages Mediated by JNK-Matrix Metalloproteinase 13 Signaling in Response to Acute Injury*. *The Journal of Immunology*, 2008. **181**(3): p. 2155-2164.
62. Hakim, A., I.M. Adcock, and O.S. Usmani, *Corticosteroid resistance and novel anti-inflammatory therapies in chronic obstructive pulmonary disease: current evidence and future direction*. *Drugs*, 2012. **72**(10): p. 1299-312.
63. Hall, C.J., et al., *Epidermal cells help coordinate leukocyte migration during inflammation through fatty acid-fuelled matrix metalloproteinase production*. *Nat Commun*, 2014. **5**: p. 3880.
64. Deshmane, S.L., et al., *Monocyte chemoattractant protein-1 (MCP-1): an overview*. *J Interferon Cytokine Res*, 2009. **29**(6): p. 313-26.
65. Cambier, C.J., et al., *Phenolic Glycolipid Facilitates Mycobacterial Escape from Microbicidal Tissue-Resident Macrophages*. *Immunity*, 2017. **47**(3): p. 552-565 e4.
66. Torraca, V., et al., *The CXCR3-CXCL11 signaling axis mediates macrophage recruitment and dissemination of mycobacterial infection*. *Dis Model Mech*, 2015. **8**(3): p. 253-69.
67. Torraca, V., et al., *The inflammatory chemokine Cxcl18b exerts neutrophil-specific chemotaxis via the promiscuous chemokine receptor Cxcr2 in zebrafish*. *Dev Comp Immunol*, 2017. **67**: p. 57-65.
68. Huber, A.R., et al., *Regulation of Transendothelial Neutrophil Migration by Endogenous Interleukin-8*. *Science*, 1991. **254**(5028): p. 99-102.
69. de Oliveira, S., et al., *Cxcl8 (IL-8) Mediates Neutrophil Recruitment and Behavior in the Zebrafish Inflammatory Response*. *The Journal of Immunology*, 2013.
70. de Oliveira, S., E.E. Rosowski, and A. Huttenlocher, *Neutrophil migration in infection and wound repair: going forward in reverse*. *Nature Reviews Immunology*, 2016. **16**: p. 378.
71. Cambier, C.J., et al., *Mycobacteria manipulate macrophage recruitment through coordinated use of membrane lipids*. *Nature*, 2014. **505**(7482): p. 218-222.
72. Van den Bossche, J., J. Baardman, and M.P. de Winther, *Metabolic Characterization of Polarized M1 and M2 Bone Marrow-derived Macrophages Using Real-time Extracellular Flux Analysis*. *J Vis Exp*, 2015(105).
73. Nguyen-Chi, M., et al., *Identification of polarized macrophage subsets in zebrafish*. *Elife*, 2015. **4**: p. e07288.
74. Rohani, M.G. and W.C. Parks, *Matrix remodeling by MMPs during wound repair*. *Matrix Biology*, 2015. **44-46**: p. 113-121.
75. Yang, Z. and X.-F. Ming, *Functions of Arginase Isoforms in Macrophage Inflammatory Responses: Impact on Cardiovascular Diseases and Metabolic Disorders*. *Frontiers in Immunology*, 2014. **5**: p. 533.
76. Luster, A.D., R. Alon, and U.H. von Andrian, *Immune cell migration in inflammation: present and future therapeutic targets*. *Nat Immunol*, 2005. **6**(12): p. 1182-90.

77. Godaly, G., et al., *Transepithelial Neutrophil Migration Is CXCR1 Dependent In Vitro and Is Defective in IL-8 Receptor Knockout Mice*. *The Journal of Immunology*, 2000. **165**(9): p. 5287-5294.
78. Kaunisto, A., et al., *NFAT1 promotes intratumoral neutrophil infiltration by regulating IL8 expression in breast cancer*. *Molecular Oncology*, 2015. **9**(6): p. 1140-1154.
79. Keelan, J.A., T. Sato, and M.D. Mitchell, *Interleukin (IL)-6 and IL-8 Production by Human Amnion: Regulation by Cytokines, Growth Factors, Glucocorticoids, Phorbol Esters, and Bacterial Lipopolysaccharide1*. *Biology of Reproduction*, 1997. **57**(6): p. 1438-1444.
80. Huang, G., et al., *Low dose of glucocorticoid decreases the incidence of complications in severely burned patients by attenuating systemic inflammation*. *Journal of Critical Care*, 2015. **30**(2): p. 436.e7-436.e11.
81. Yano, A., et al., *Glucocorticoids Suppress Tumor Angiogenesis and *in vivo* Growth of Prostate Cancer Cells*. *Clinical Cancer Research*, 2006. **12**(10): p. 3003-3009.
82. Brugman, S., *The zebrafish as a model to study intestinal inflammation*. *Developmental & Comparative Immunology*, 2016. **64**: p. 82-92.
83. Wada, T., et al., *MIP-1alpha and MCP-1 contribute to crescents and interstitial lesions in human crescentic glomerulonephritis*. *Kidney Int*, 1999. **56**(3): p. 995-1003.
84. Lee, G.T., et al., *WNT5A induces castration-resistant prostate cancer via CCL2 and tumour-infiltrating macrophages*. *Br J Cancer*, 2018.
85. Szebeni, G.J., et al., *Inflammation and Cancer: Extra- and Intracellular Determinants of Tumor-Associated Macrophages as Tumor Promoters*. *Mediators Inflamm*, 2017. **2017**: p. 9294018.
86. Shen, J.Z., et al., *CCL2-dependent macrophage recruitment is critical for mineralocorticoid receptor-mediated cardiac fibrosis, inflammation, and blood pressure responses in male mice*. *Endocrinology*, 2014. **155**(3): p. 1057-66.
87. Gunn, M.D., et al., *Monocyte chemoattractant protein-1 is sufficient for the chemotaxis of monocytes and lymphocytes in transgenic mice but requires an additional stimulus for inflammatory activation*. *The Journal of Immunology*, 1997. **158**(1): p. 376-383.
88. Jen, R., S.I. Rennard, and D.D. Sin, *Effects of inhaled corticosteroids on airway inflammation in chronic obstructive pulmonary disease: a systematic review and meta-analysis*. *Int J Chron Obstruct Pulmon Dis*, 2012. **7**: p. 587-95.
89. Kim, J.S., M. Chopp, and S.C. Gautam, *High dose methylprednisolone therapy reduces expression of JE/MCP-1 mRNA and macrophage accumulation in the ischemic rat brain*. *J Neurol Sci*, 1995. **128**(1): p. 28-35.
90. Little, A.R., K. Sriram, and J.P. O'Callaghan, *Corticosterone regulates expression of CCL2 in the intact and chemically injured hippocampus*. *Neurosci Lett*, 2006. **399**(1-2): p. 162-6.
91. Baldassare, J.J., Y. Bi, and C.J. Bellone, *The Role of p38 Mitogen-Activated Protein Kinase in IL-1 β Transcription*. *The Journal of Immunology*, 1999. **162**(9): p. 5367-5373.
92. Widney, D.P., et al., *The Murine Chemokine CXCL11 (IFN-Inducible T Cell α Chemoattractant) Is an IFN- γ - and Lipopolysaccharide- Inducible Glucocorticoid-Attenuated Response Gene Expressed in Lung and Other Tissues During Endotoxemia*. *The Journal of Immunology*, 2000. **164**(12): p. 6322-6331.
93. Kelly, R.W., G.G. Carr, and S.C. Riley, *The Inhibition of Synthesis of a β -Chemokine, Monocyte Chemotactic Protein-1 (MCP-1) by Progesterone*. *Biochemical and Biophysical Research Communications*, 1997. **239**(2): p. 557-561.
94. O'Connell, D.M., B. Bouazza, and O. Tliba, *Time-Dependent Sensitivity Of IFN γ -Induced Genes To Glucocorticoids In Airway Epithelial Cells*, in *A108. RESPIRATORY BIOLOGY: AT A CROSSROAD BETWEEN INFECTION, INJURY, AND REPAIR*. 2015, Am Thoracic Soc. p. A2369-A2369.
95. Saha, S., I.N. Shalova, and S.K. Biswas, *Metabolic regulation of macrophage phenotype and function*. *Immunol Rev*, 2017. **280**(1): p. 102-111.
96. Kelly, B. and L.A.J. O'Neill, *Metabolic reprogramming in macrophages and dendritic cells in innate immunity*. *Cell Research*, 2015. **25**(7): p. 771-784.

97. Uhlenhaut, N.H., et al., *Insights into Negative Regulation by the Glucocorticoid Receptor from Genome-wide Profiling of Inflammatory Cistromes*. *Molecular Cell*, 2013. **49**(1): p. 158-171.
98. Bhattacharyya, S., et al., *Macrophage glucocorticoid receptors regulate Toll-like receptor 4-mediated inflammatory responses by selective inhibition of p38 MAP kinase*. *Blood*, 2007. **109**(10): p. 4313-4319.
99. Kleiman, A., et al., *Glucocorticoid receptor dimerization is required for survival in septic shock via suppression of interleukin-1 in macrophages*. *FASEB J*, 2012. **26**(2): p. 722-9.
100. Vettorazzi, S., et al., *Glucocorticoids limit acute lung inflammation in concert with inflammatory stimuli by induction of SphK1*. *Nat Commun*, 2015. **6**: p. 7796.
101. Tuckermann, J.P., et al., *Macrophages and neutrophils are the targets for immune suppression by glucocorticoids in contact allergy*. *J Clin Invest*, 2007. **117**(5): p. 1381-90.
102. Heideveld, E., et al., *Glucocorticoids induce differentiation of monocytes towards macrophages that share functional and phenotypical aspects with erythroblastic island macrophages*. *Haematologica*, 2018. **103**(3): p. 395-405.
103. Bernut, A., et al., *Mycobacterium abscessus cording prevents phagocytosis and promotes abscess formation*. *Proc Natl Acad Sci U S A*, 2014. **111**(10): p. E943-52.
104. Benard, E.L., et al., *Infection of zebrafish embryos with intracellular bacterial pathogens*. *J Vis Exp*, 2012(61).
105. Celler, K., G.P. van Wezel, and J. Willemse, *Single particle tracking of dynamically localizing TatA complexes in Streptomyces coelicolor*. *Biochem Biophys Res Commun*, 2013. **438**(1): p. 38-42.
106. Zakrzewska, A., et al., *Macrophage-specific gene functions in Spi1-directed innate immunity*. *Blood*, 2010. **116**(3): p. e1-11.
107. Rougeot, J., et al., *RNA sequencing of FACS-sorted immune cell populations from zebrafish infection models to identify cell specific responses to intracellular pathogens*. *Methods Mol Biol*, 2014. **1197**: p. 261-74.

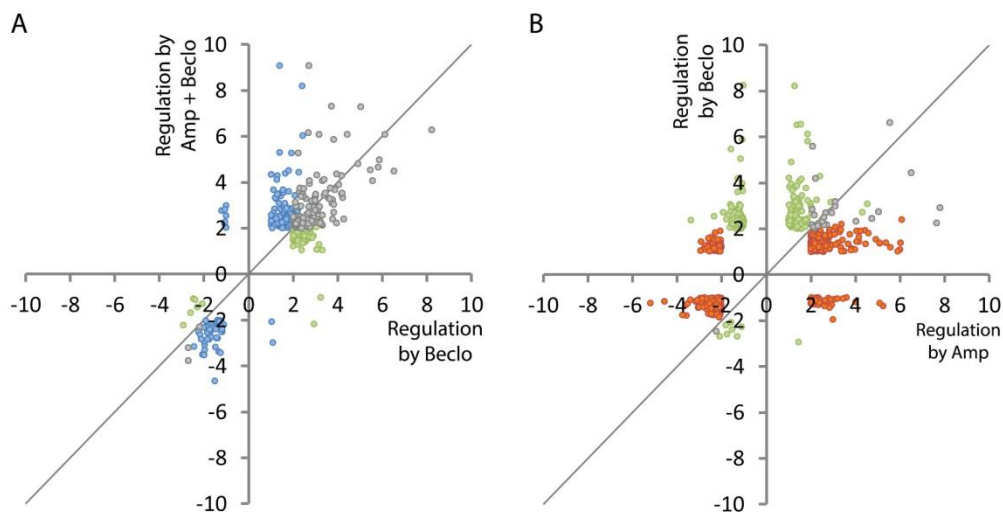
Supplementary Material

Online Movie 1 can be found at: <http://movie.biologists.com/video/10.1242/dmm.037887/video-1>

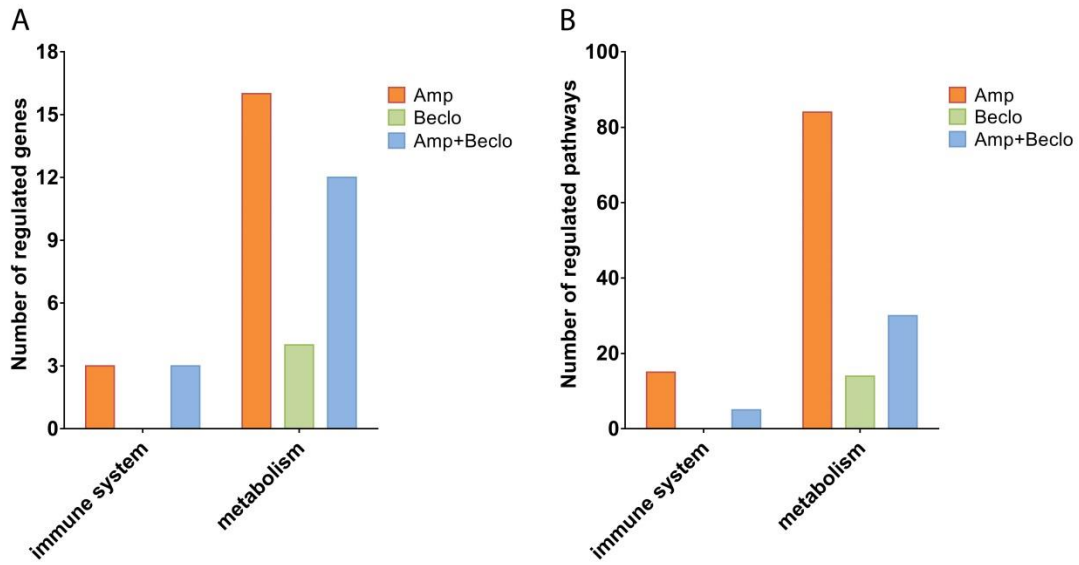
Online Movie 1. Macrophage migration upon tail amputation. Tracks of macrophages migrating between 1.5 and 5.5 hpa in 3 dpf larvae in the vehicle-treated group. Confocal microscopy images were analyzed using ImageJ with custom-made plugins, developed by Dr. Joost Willemsse (Leiden University), for localization and tracking of cells.

Online Movie 2 can be found at: <http://movie.biologists.com/video/10.1242/dmm.037887/video-2>

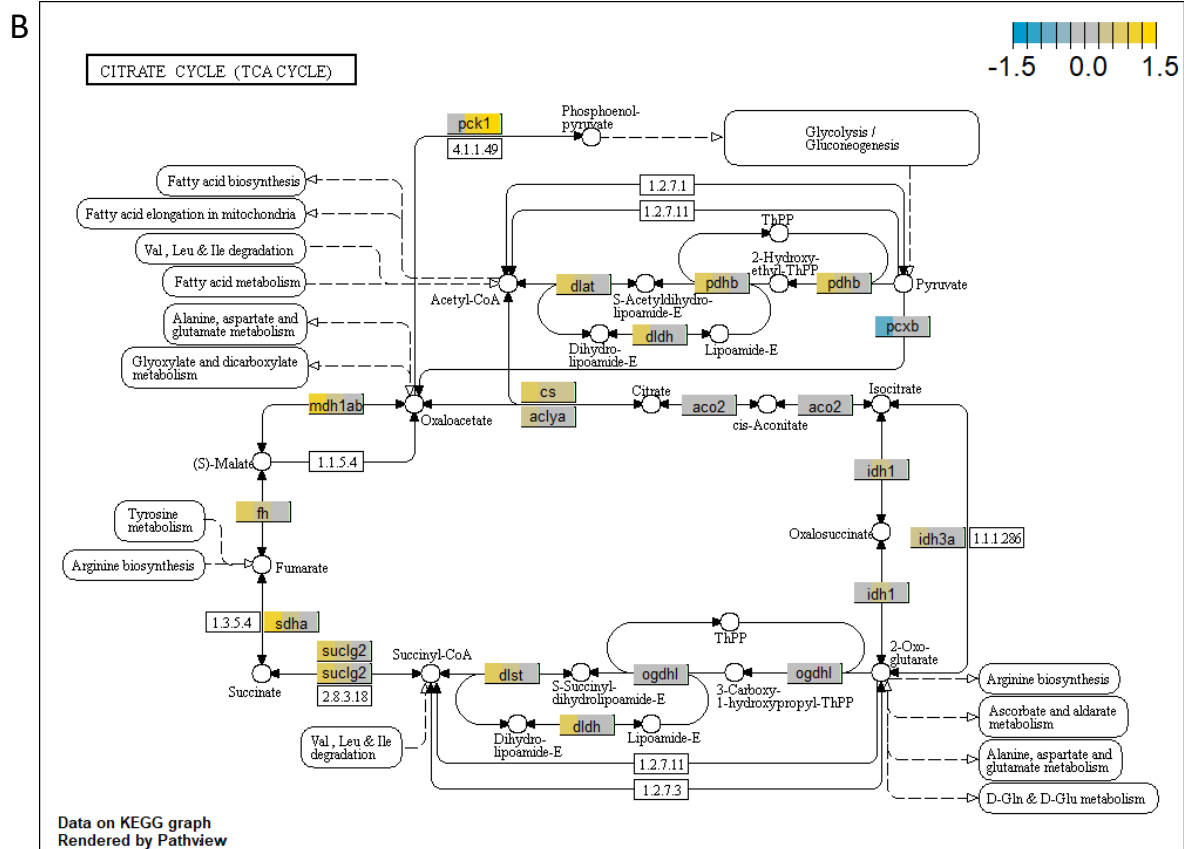
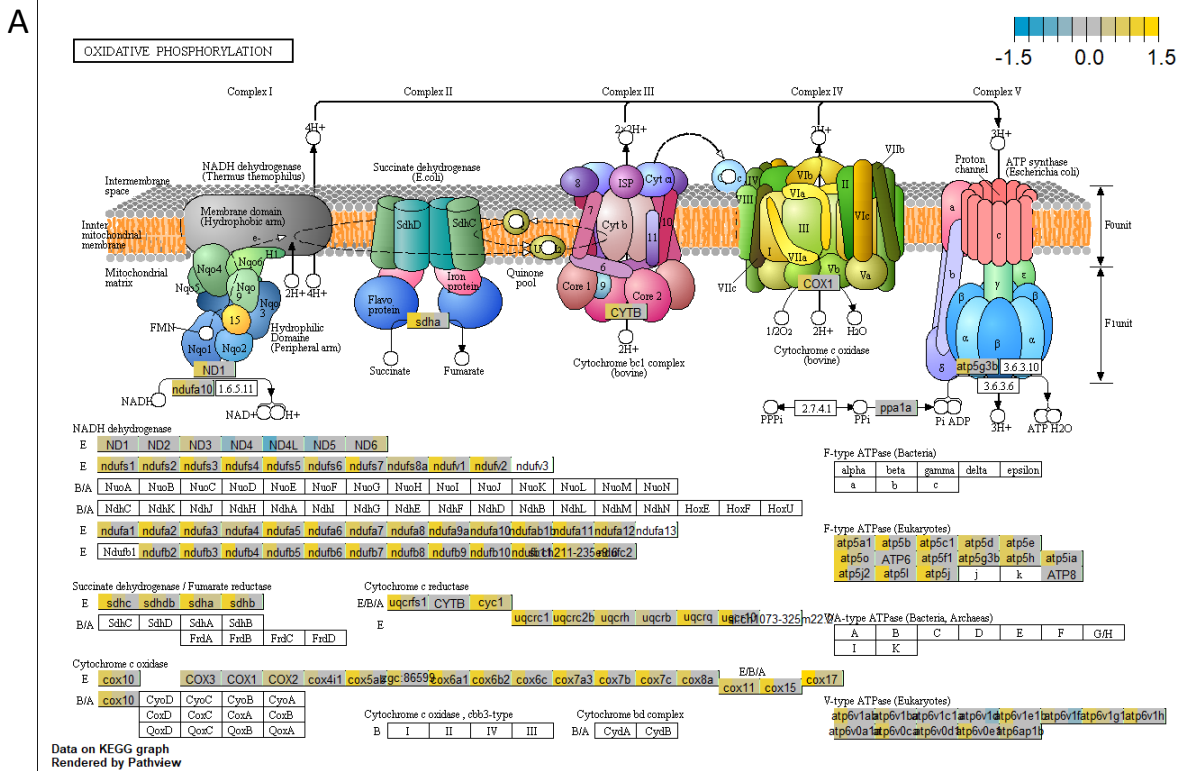
Online Movie 2. Neutrophil migration upon tail amputation. Tracks of neutrophils migrating between 1.5 and 5.5 hpa in 3 dpf larvae in the vehicle-treated group. Confocal microscopy images were analyzed using ImageJ with custom-made plugins, developed by Dr. Joost Willemsse (Leiden University), for localization and tracking of cells.

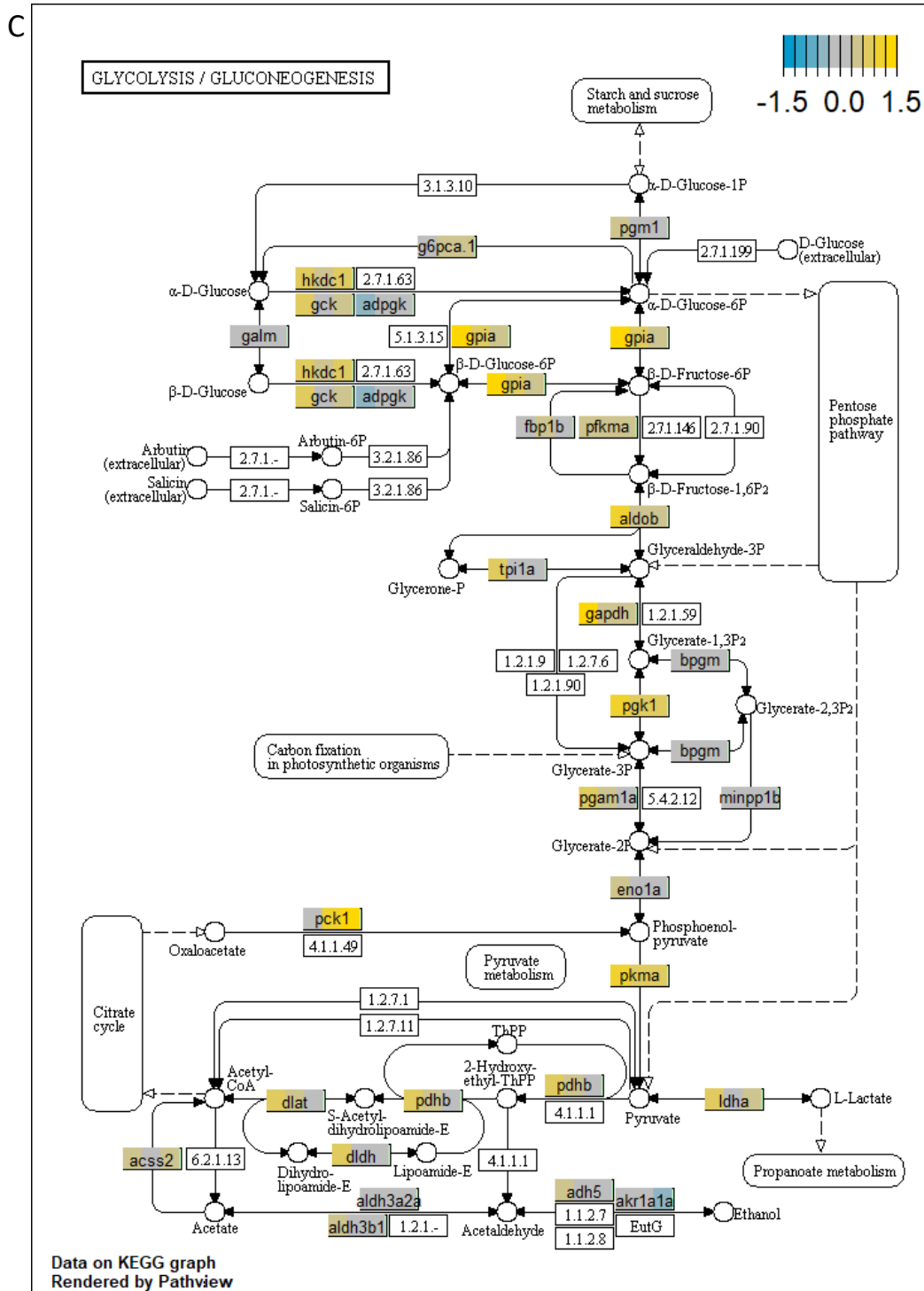


Supplementary Figure 1. Scatter plot showing the difference and overlaps in gene regulation between different treatments. A. Comparison between beclomethasone and combined beclomethasone and amputation treatment. For all genes showing significant regulation upon beclomethasone (green and grey dots) or the combined beclomethasone and amputation treatment (blue and grey dots), the fold change due to beclomethasone and amputation treatment was plotted as a function of the fold change due to beclomethasone. The plot shows a large group of genes (grey dots) regulated by both treatments. B. Comparison between amputation and beclomethasone treatment. For all genes showing significant regulation upon amputation (red and grey dots) or beclomethasone treatment (green and grey dots), the fold change due to beclomethasone treatment was plotted as a function of the fold change due to amputation. The plot shows a very small group of genes (grey dots) regulated by both treatments. The grey line indicates the point at which the two different treatment have the same effect. Significantly regulated genes were selected by using a $p_{adj} < 0.05$ and $|\text{FoldChange}| > 2$ cutoff.

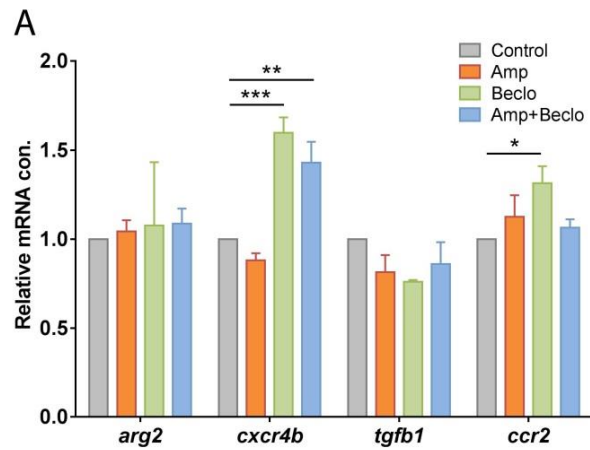


Supplementary Figure 2. Gene ontology analysis of RNA sequencing experiment. A. The number of KEGG pathways overrepresented in clusters of genes significantly regulated by amputation, beclomethasone, and amputation+beclomethasone. Amputation regulated pathways involved in the immune system and in metabolism. Amputation+beclomethasone treatment regulated a lower number of regulated pathways involved in both the immune system and metabolism. B. The number of regulated genes involved in the overrepresented pathways. Amputation regulated genes involved in immune- and metabolism-related pathways. Amputation+beclomethasone regulated a lower number of genes involved in these pathways.

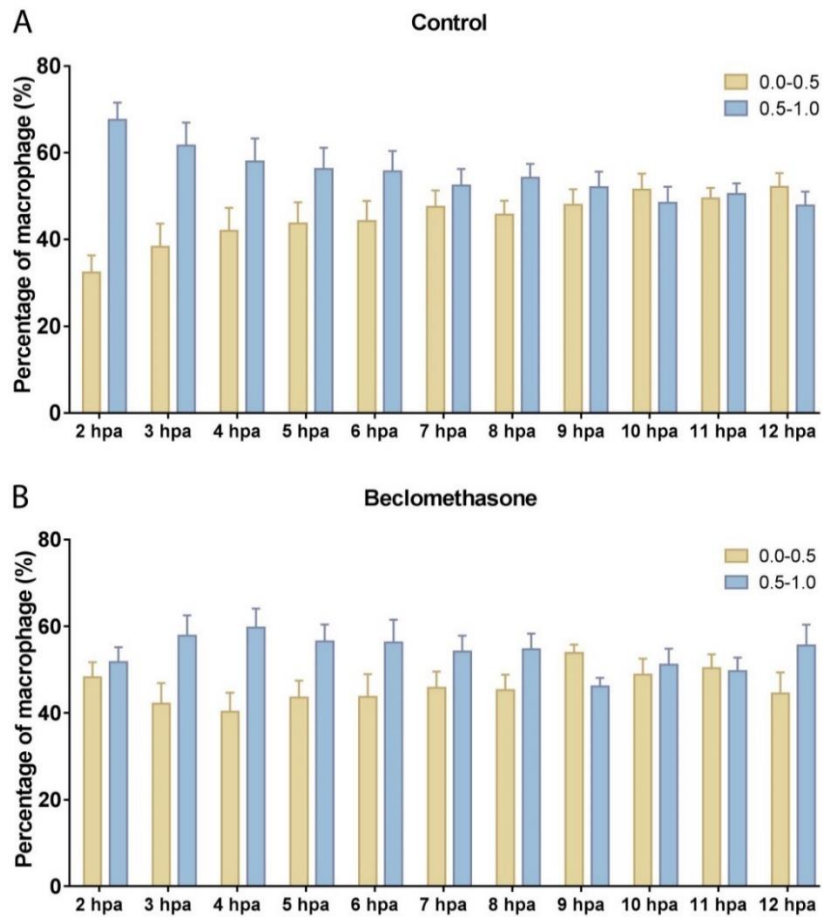




Supplementary Figure 3. Significantly enriched KEGG pathways mapped with gene expression level. In the oxidative phosphorylation (A), Citrate cycle (TCA cycle) (B) and Glycolysis/ Gluconeogenesis (C) pathways, the fold change of the genes is indicated by different colour and the intensity of the colour as shown in the scale. The three colour shown in one gene indicated the logarithm fold change of amputation, beclomethasone and amputation+beclomethasone treatment respectively. The maps show that the vast majority of the amputation-induced changes in gene expression are inhibited by beclomethasone treatment in these pathways.



Supplementary Figure 4. Expression levels of immune-related genes in FACS-sorted macrophages, determined by qPCR for *arg2*, *cxcr4b*, *tgfb1*, *ccr2* (A) at 24hpa in 3 dpf larvae. The expression level of *cxcr4b* was increased by beclomethasone treatment. Statistical analysis were performed by ANOVA with a Fisher's LSD post hoc. Values shown are the means \pm s.e.m. of three independent experiments. Statistical significance is indicated by: * $P < 0.05$; ** $P < 0.01$; *** $P < 0.001$.



Supplementary Figure 5. Effect of beclomethasone on the morphology of macrophages. The percentage of macrophages with different levels of circularity (0.0-0.5 and 0.5-1.0) were determined over time for the control group (A) and beclomethasone-treated group (B). In the control group, an increase in the percentage of macrophages with a circularity level between 0.0 and 0.5 and a decrease in the percentage of macrophages with a level between 0.5 and 1.0 was observed. In the beclomethasone-treated group, these changes were not observed. Values shown are means \pm s.e.m..

Supplementary Table 1. KEGG-pathways, based on RNA sequencing analysis.**Amputation**

Term	Count	%	P-value	Fold Enrichment
Immune system				
NOD-like receptor signaling pathway	6	1.03	2.89E-02	3.43
Toll-like receptor signaling pathway	8	1.37	6.13E-02	2.26
Cytokine-cytokine receptor interaction	11	1.89	6.58E-02	1.88
Jak-STAT signaling pathway	8	1.37	9.53E-02	2.04
Metabolism				
Oxidative phosphorylation	28	4.81	2.08E-13	5.60
Carbon metabolism	23	3.95	2.72E-10	5.15
Biosynthesis of antibiotics	31	5.33	4.11E-10	3.73
Metabolic pathways	83	14.26	1.20E-09	1.84
Glycolysis / Gluconeogenesis	17	2.92	3.07E-09	6.52
Biosynthesis of amino acids	13	2.23	3.87E-05	4.28
Arginine and proline metabolism	10	1.72	1.33E-04	5.00
Pentose phosphate pathway	7	1.20	6.51E-04	6.32
Citrate cycle (TCA cycle)	6	1.03	5.67E-03	5.09
Fructose and mannose metabolism	6	1.03	1.42E-02	4.10
Pyruvate metabolism	6	1.03	1.73E-02	3.91
Galactose metabolism	5	0.86	2.82E-02	4.24
Insulin resistance	10	1.72	4.62E-02	2.11
Glycine, serine and threonine metabolism	5	0.86	7.43E-02	3.11
Propanoate metabolism	4	0.69	7.54E-02	4.00
RNA degradation	7	1.20	8.06E-02	2.31
Others				
Cardiac muscle contraction	13	2.23	1.30E-04	3.79

Amputation & Beclomethasone

Term	Count	%	P-value	Fold Enrichment
Immune system				
Toll-like receptor signaling pathway	6	1.97	8.62E-03	4.64
Metabolism				
Insulin signaling pathway	10	3.28	3.19E-04	4.45
Starch and sucrose metabolism	5	1.64	6.92E-04	11.96
Insulin resistance	8	2.62	1.49E-03	4.60
Steroid hormone biosynthesis	4	1.31	1.16E-02	8.27
FoxO signaling pathway	7	2.30	2.16E-02	3.15
Biosynthesis of antibiotics	8	2.62	2.94E-02	2.63
Arginine biosynthesis	3	0.98	3.76E-02	9.57
Glyoxylate and dicarboxylate metabolism	3	0.98	6.69E-02	6.96
Galactose metabolism	3	0.98	6.69E-02	6.96
Glycolysis / Gluconeogenesis	4	1.31	6.72E-02	4.19
Retinol metabolism	3	0.98	8.94E-02	5.89
Alanine, aspartate and glutamate metabolism	3	0.98	9.33E-02	5.74
Others				
Adipocytokine signaling pathway	5	1.64	2.43E-02	4.45

Beclomethasone

Term	Count	%	P-value	Fold Enrichment
Metabolism				
FoxO signaling pathway	8	4.08	1.48E-03	4.57
Insulin signaling pathway	8	4.08	1.59E-03	4.51
Insulin resistance	6	3.06	1.06E-02	4.38
Glyoxylate and dicarboxylate metabolism	3	1.53	4.35E-02	8.82
Steroid hormone biosynthesis	3	1.53	5.35E-02	7.87
Others				
Focal adhesion	7	3.57	3.80E-02	2.74
Adipocytokine signaling pathway	4	2.04	5.57E-02	4.51

Supplementary Table 2. Sequences of Primers used in qPCR reactions.

Gene name	Gene accession	Sequence (5'-3')
<i>ppail</i>	ENSDARG00000103994	Fw: CATCCACAACCTTCCCGAACAC Rv: AACTGAAACACGGAGGCAAAG
<i>ccl2</i>	ENSDARG00000041835	Fw: GTCTGGTGTCTTTCGCTTTC Rv: TGCAGAGAAGATGCGTCGTA
<i>cxcl11aa</i>	ENSDARG00000100662	Fw: ACTCAACATGGTGAAGCCAGTGCT Rv: CTTCAGCGTGGCTATGACTTCCAT
<i>il8</i>	ENSDARG00000104795	Fw: TGTGTTATTGTTTTCTGGCATTTC Rv: GCGACAGCGTGGATCTACAG
<i>cxcl18b</i>	ENSDARG00000075045	Fw: TCTTCTGCTGCTGCTTGC GG T Rv: GGTGTCCCTGCGAGCACGAT
<i>il6</i>	ENSDARG00000102318	Fw: CGCTAAGGCAACTGGAAGAC Rv: CCAGACCACTGGGAAACACT
<i>il1b</i>	ENSDARG00000098700	Fw: TGTGTGTTTGGGAATCTCCA Rv: CTGATAAACCAACCGGGACA
<i>tnfa</i>	ENSDARG00000009511	Fw: ACCAGGCCTTTTCTTCAGGT Rv: TTTGCCTCCGTAGGATTCAG
<i>mmp9</i>	ENSDARG00000042816	Fw: CATTAAAGATGCCCTGATGTATCCC Rv: AGTGGTGGTCCGTGGTTGAG
<i>arg2</i>	ENSDARG00000039269	Fw: AAGGCCATTCTCAGCAGTGT Rv: AGGTTTCCCGAAGGTGAAGT
<i>cxcr4b</i>	ENSDART00000061499	Fw: GCGACCTCTCAGTCAGCAAT Rv: TCACAAGCACCACAAGTCCA
<i>tgfb1</i>	ENSDARG00000041502	Fw: CAACCGCTGGCTCTCATTTGA Rv: ACAGTCGCAGTATAACCTCAGCT
<i>ccr2</i>	ENSDARG00000079829	Fw: TGGCAACGCAAAGGCTTTCAGTGA Rv: AGGTTTCCCGAAGGTGAAGT

Chapter 4

Glucocorticoid treatment exacerbates mycobacterial infection by reducing the phagocytic capacity of macrophages

Yufei Xie, Annemarie H. Meijer, Marcel J.M. Schaaf

Abstract

Glucocorticoids are effective drugs for treating immune-related diseases, but prolonged therapy is associated with an increased risk of various infectious diseases, including tuberculosis. In this study, we have used a larval zebrafish model for tuberculosis, based on *Mycobacterium marinum* (*Mm*) infection, to study the effect of glucocorticoids. Our results show that the synthetic glucocorticoid beclomethasone increases the bacterial burden and the dissemination of a systemic *Mm* infection. The exacerbated *Mm* infection was associated with a decreased phagocytic activity of macrophages, higher percentages of extracellular bacteria, and a reduced rate of infected cell death, whereas the bactericidal capacity of the macrophages was not affected. The inhibited phagocytic capacity of macrophages was associated with suppression of the transcription of genes involved in phagocytosis in these cells. The decreased bacterial phagocytosis by macrophages was not specific for *Mm*, since it was also observed upon infection with *Salmonella* Typhimurium. In conclusion, our results show that glucocorticoids inhibit the phagocytic activity of macrophages, which may increase the severity of bacterial infections like tuberculosis.

Introduction

Glucocorticoids (GCs) are a class of steroid hormones that are secreted upon stress. The main endogenous GC in our body, cortisol, helps our bodies adapt to stressful situations and for this purpose it regulates a wide variety of systems, like the immune, metabolic, reproductive, cardiovascular and central nervous system. These effects are mediated by an intracellular receptor, the glucocorticoid receptor (GR), which acts as a ligand-activated transcription factor. Synthetic GCs are widely prescribed to treat various immune-related diseases due to their potent suppressive effects on the immune system. However, prolonged therapy with these pleiotropic steroids evokes severe side effects, such as osteoporosis and diabetes mellitus [1, 2]. Importantly, the therapeutic immunosuppressive effect of GCs may lead to infectious complications because of the compromised immune system [3-5]. Similarly, after chronic stress an increased susceptibility to infectious diseases has been observed, due to the high circulating levels of cortisol. In order to better understand these complex effects of GCs, more research is required into how GCs influence the susceptibility to infections and the course of infectious diseases.

Tuberculosis (TB) is the most prevalent bacterial infectious disease in the world, caused by the pathogen *Mycobacterium tuberculosis* (*Mtb*). Despite the efforts made to reach the “End TB Strategy” of the World Health Organization, *Mtb* still infects approximately one-quarter of the world's population and caused an estimated 1.5 million deaths in 2018, which makes it one of the top 10 causes

of death globally [6, 7]. The major characteristic of *Mtb* infection is the formation of granulomas containing infected and non-infected immune cells [8]. Most *Mtb*-infected people develop a latent, noncontagious infection and do not show any symptoms, with the bacteria remaining inactive, while contained within granulomas [9, 10]. About 5-10% of the carriers develop a clinically active TB disease associated with a loss of granuloma integrity [9, 11]. Among those TB patients, the majority manifest a lung infection and around 20% shows infection in other organs like the central nervous system, pleura, urogenital tracts, bones and joints, and lymph nodes [12]. Antibiotics are currently the mainstay for TB treatment, but since antibiotic resistance is rising and an effective vaccine against latent or reactivated TB is still lacking, alternative therapies to control TB are needed [13].

GCs are known to modulate the pathogenesis of TB, but their effects are highly complicated. The use of GCs is considered as a risk factor for TB. Patients who are being treated with GCs have an approximately 5-fold increased risk for developing new TB [14], and treatment with a moderate or high dose of GCs is associated with an increased risk of activation of latent TB [15-17]. Consequently, a tuberculin skin test (TST) for screening latent TB is recommended before starting GC therapy [14]. Moreover, chronic stress which is associated with increased circulating levels of the endogenous GC cortisol, has been shown to be associated with a higher incidence of TB [18].

Despite the generally detrimental effects of GCs on TB susceptibility and progression, certain types of TB patients are treated with GCs. Chronic TB patients may require GCs for treatment of other disorders, and it has been shown that adjunctive GC therapy may have beneficial effects. Traditionally, adjunctive GC with standard anti-TB therapy has been used for prevention of inflammatory complications in patients with tuberculous meningitis, pericarditis, and pleurisy [19-22]. It has been reported that adjunctive GC therapy could improve the probability of survival in tuberculous meningitis and pericarditis [23-26]. In case of pulmonary TB, the most common form of TB, adjunctive GC therapy is recommended in advanced tuberculosis since broad and significant clinical benefits have been demonstrated [27, 28].

Although GCs are being used for adjunctive therapy, the beneficial effects of GC treatment are still under debate. For tuberculous pleurisy TB, the efficacy of GCs is still controversial and for meningitis and pericarditis, information on the GC effects is still incomplete [22, 26, 29, 30]. A review regarding clinical trials for pulmonary TB showed that, although adjunctive GC therapy appears to have short-term benefits, it is not maintained in the long-term [31]. An explanation for the complexity of the effects of GC therapy in TB has been offered by Tobin et al. (2012). They showed that patients suffer from TB as a result of either a failed or an excessive immune response to the mycobacterial infection, and that only the subset of TB meningitis patients with an excessive response, showing a

hyperinflammatory phenotype (in their study as a result of a polymorphism in the *LTA4H* gene), benefited from adjunctive GC therapy. It was suggested that GCs may also be beneficial for similar subgroups of patients suffering from other forms of TB [32].

The complex interplay between GC actions and TB underscores the need for a better understanding of the effects of GCs on mycobacterial infection. In the present study we have studied these effects using *Mycobacterium marinum* (*Mm*) infection in zebrafish as a model system. *Mm* is a species closely related to *Mtb* that can infect zebrafish and other cold-blooded animals naturally, causing a TB-like disease [33]. Infection of zebrafish larvae with *Mm* provides an animal model system that mimics hallmark aspects of *Mtb* infection in humans and is widely used for research into mechanisms underlying the course of this disease [34-36]. Like *Mtb*, *Mm* is able to survive and replicate within macrophages and, in later stages of infection, induces the formation of granulomas [37]. The transparency of zebrafish at early life stages makes it possible to perform non-invasive long-term live imaging, which has been used to reveal the earliest stages of granuloma formation [38]. In addition, the availability of different transgenic and mutant zebrafish lines and the efficient application of molecular techniques allow us to exploit this zebrafish *Mm* infection model optimally to study both the host factors and bacterial factors involved in mycobacterial infection processes [33, 34, 39]. For example, zebrafish studies revealed that infected macrophages can detach from a granuloma and facilitate dissemination to new locations [38]. Moreover, the study of an *Ita4h* mutant zebrafish line showed that the polymorphism in the *LTA4H* gene is associated with the susceptibility to mycobacterial diseases and the response to adjunctive GC therapy in human, representing a prime example of translational research [32, 40].

The zebrafish has proven to be a suitable model for studying the effects of GCs, since the GC signaling pathway is very well conserved between zebrafish and humans. Both humans and zebrafish have a single gene encoding the GR, and the organization of these genes is highly similar [41-43]. Both the human and the zebrafish gene encodes two splice variants, the α -isoform, the canonical receptor, and the β -isoform, which has no transcriptional activity [42]. The DNA binding domain (DBD) and ligand binding domain (LBD) of the canonical α -isoform of the human and zebrafish GR share similarities of 98.4% and 86.5% respectively [42]. The zebrafish GR α -isoform, hereafter referred to as Gr, mediates GC effects that have traditionally been observed in humans and other mammals as well, like the effects on metabolism [44] and the suppression of the immune system [45]. This makes the zebrafish an ideal model to study the mechanisms of GC action *in vivo* [46, 47]. In a recent study, we have demonstrated that GC treatment inhibits the activation of the immune system in zebrafish larvae upon wounding [48]. The migration of the neutrophils and the differentiation of macrophages was attenuated upon treatment with the synthetic GC.

In the present study, to investigate the functional consequences of the previously observed GC effects on immune cells, we have investigated how GCs modulate the course of an *Mm* infection in zebrafish larvae. We demonstrate that beclomethasone increases the level of *Mm* infection and tissue dissemination. This increased *Mm* infection can be explained by an inhibition of the phagocytic activity of macrophages by beclomethasone, which did not affect the microbicidal capacity of these cells. The inhibitory effect of beclomethasone on phagocytosis, which most likely results from Gr interfering with the transcription of genes required for phagocytosis, results in a higher percentage of extracellular bacteria, which eventually leads to an exacerbation of the *Mm* infection.

Results

Beclomethasone increases mycobacterial infection through Glucocorticoid receptor (Gr) activation

To study the effect of GC treatment on *Mm* infection in zebrafish, we pretreated zebrafish embryos with beclomethasone and infected them intravenously with fluorescently labelled *Mm*. At 4 days post infection (dpi), the bacterial burden was assessed by quantification of pixel intensities of fluorescence microscopy images. We found that the bacterial burden increased by 2.3 fold when embryos were treated with 25 μ M beclomethasone compared with the vehicle-treated group (Figure 1 A, C). Beclomethasone treatment at lower concentrations of 0.04, 0.2, 1 and 5 μ M did not affect the bacterial burden. Therefore, a concentration of 25 μ M beclomethasone was used in subsequent experiments. We have previously shown that this concentration effectively reduces wound-induced leukocyte migration in zebrafish as well [48].

To demonstrate that the beclomethasone-induced increase in bacterial burden was not due to a general toxicity of beclomethasone but mediated specifically by the Gr, we used the GR antagonist RU-486. The results of these experiments showed that the beclomethasone-induced increase in bacterial burden at 4 dpi was abolished when co-treatment with RU-486 was applied (Figure 1 B, D), which indicates that the effect of beclomethasone requires activation of Gr. No significant difference was observed when the RU-486-treated larvae were compared to the vehicle-treated group. In conclusion, beclomethasone increases the level of *Mm* infection in zebrafish larvae and this effect is mediated by Gr.

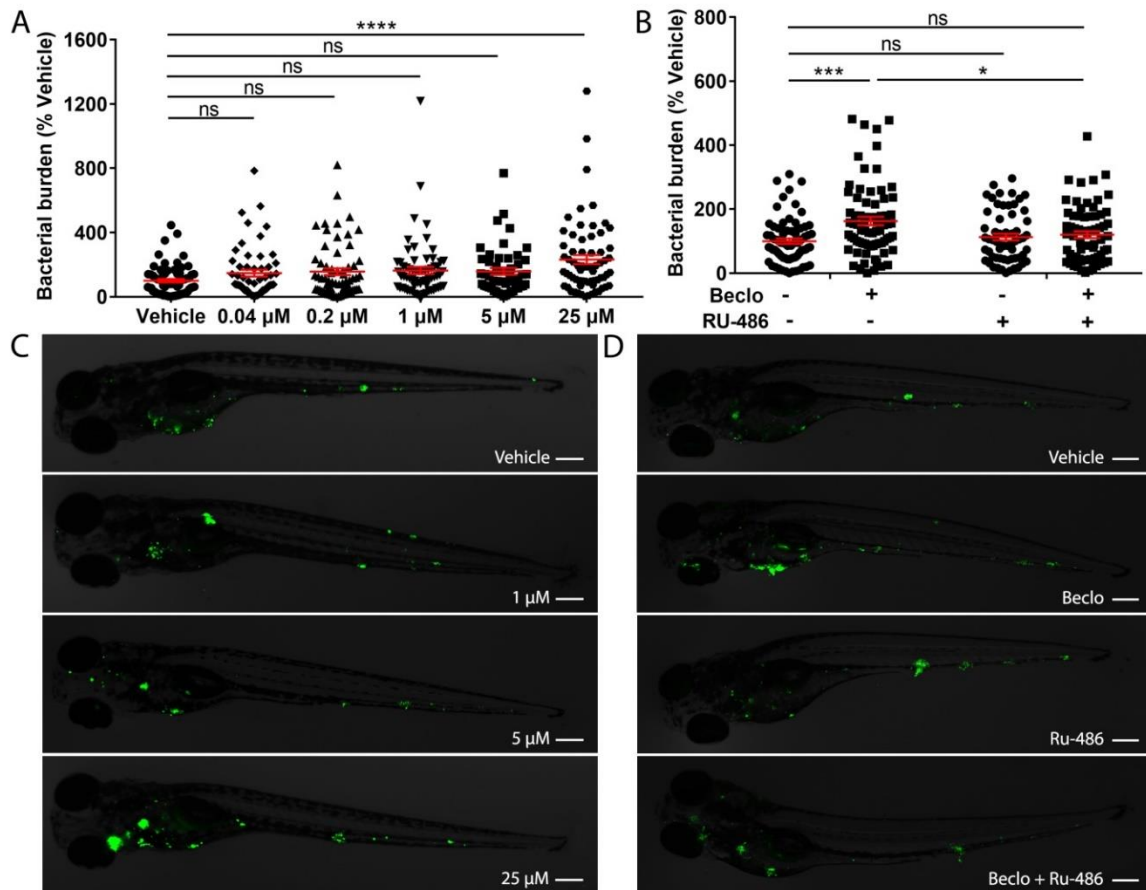


Figure 1. Effect of beclomethasone on *Mm* infection burden in zebrafish. A. Bacterial burden of zebrafish larvae at four days after intravenous injection (at 28 hpf) of *Mm* and treatment with vehicle or different concentrations of beclomethasone (beclo), started at 2 h before infection. Statistical analysis by one-way ANOVA with Bonferroni's post hoc test revealed that the bacterial burden was significantly increased in the group treated with 25 μ M beclomethasone, compared to the burden of the vehicle-treated group. B. Effect of the GR antagonist RU-486 on the beclomethasone-induced increase of the bacterial burden at 4 dpi. The bacterial burden was significantly increased by beclomethasone (25 μ M) treatment and this increase was abolished in the presence of RU-486. Statistical analysis was performed by two-way ANOVA with Tukey's post hoc test. In panels A and B, each data point represents a single larva and the means \pm s.e.m. of data accumulated from three independent experiments are shown in red. Statistical significance is indicated by: ns, non-significant; * $P < 0.05$; *** $P < 0.001$; **** $P < 0.0001$. C-D. Representative fluorescence microscopy images of *Mm*-infected larvae at 4 days post infection (dpi), representing experimental groups presented in panels A and B. Bacteria are shown in green. Scale bar = 200 μ m.

Beclomethasone treatment leads to a higher infection and dissemination level without influencing the microbicidal capacity of macrophages

Subsequently, we analyzed the effect of beclomethasone on *Mm* infection in more detail. The total bacterial burden (Figure 2 A), the number of bacterial clusters per individual (Figure 2 B) and the average size of the bacterial clusters (Figure 2 C) were quantified at 1, 2, 3 and 4 dpi. The results showed that the difference in bacterial burden between the beclomethasone-treated group and the vehicle group was not significant at 1-3 dpi, but that a significant difference was observed at 4 dpi (6186.1 ± 626.5 vs 2870.5 ± 235.0). However, a significant increase in the number of bacterial clusters in the beclomethasone-treated group was already detected at 3 dpi (28.3 ± 1.9 vs 18.1 ± 1.5 in the vehicle group) which was sustained at 4 dpi (64.2 ± 3.5 vs 35.4 ± 2.6). The size of the bacterial clusters at 4 dpi was also increased in the beclomethasone-treated group compared to the cluster size in the vehicle-treated group (741.6 ± 58.3 vs 498.3 ± 45.7). The increase in the number of bacterial clusters indicates an increased dissemination of the infection due to beclomethasone treatment. We confirmed this effect of beclomethasone on bacterial dissemination using hindbrain infection (Figure 2 D, E). Following *Mm* injection into the hindbrain ventricle, $66.1 \pm 2.0\%$ of embryos in the vehicle-treated group showed disseminated infection in tissues of the head and tail at 24 hours post infection (hpi), while a significantly higher number ($76.4 \pm 2.6\%$) showed this dissemination in the beclomethasone-treated group.

To study whether the increased infection and dissemination was related to the microbicidal capacity of macrophages, we injected *Mm* Δerp bacteria which are deficient for growth inside macrophages [49]. No significant difference was observed for the number of *Mm* clusters (Figure 3A) and the percentage of *Mm* inside macrophage (Figure 3B) between the beclomethasone-treated group and the vehicle-treated group. To assess the ability of macrophages to kill bacteria, we quantitated the percentage of bacteria-containing macrophages that contained only 1-10 bacteria in the tail region at 44 hpi [50]. There was no significant difference in this percentage between the vehicle-treated group ($82.0 \pm 4.9\%$) and the beclomethasone-treated group ($81.6 \pm 5.0\%$) (Figure 3C-E). Taken together, these findings indicate that beclomethasone treatment leads to a higher overall *Mm* infection level and increased dissemination, and that these effects are not related to an altered microbicidal capacity of macrophages.

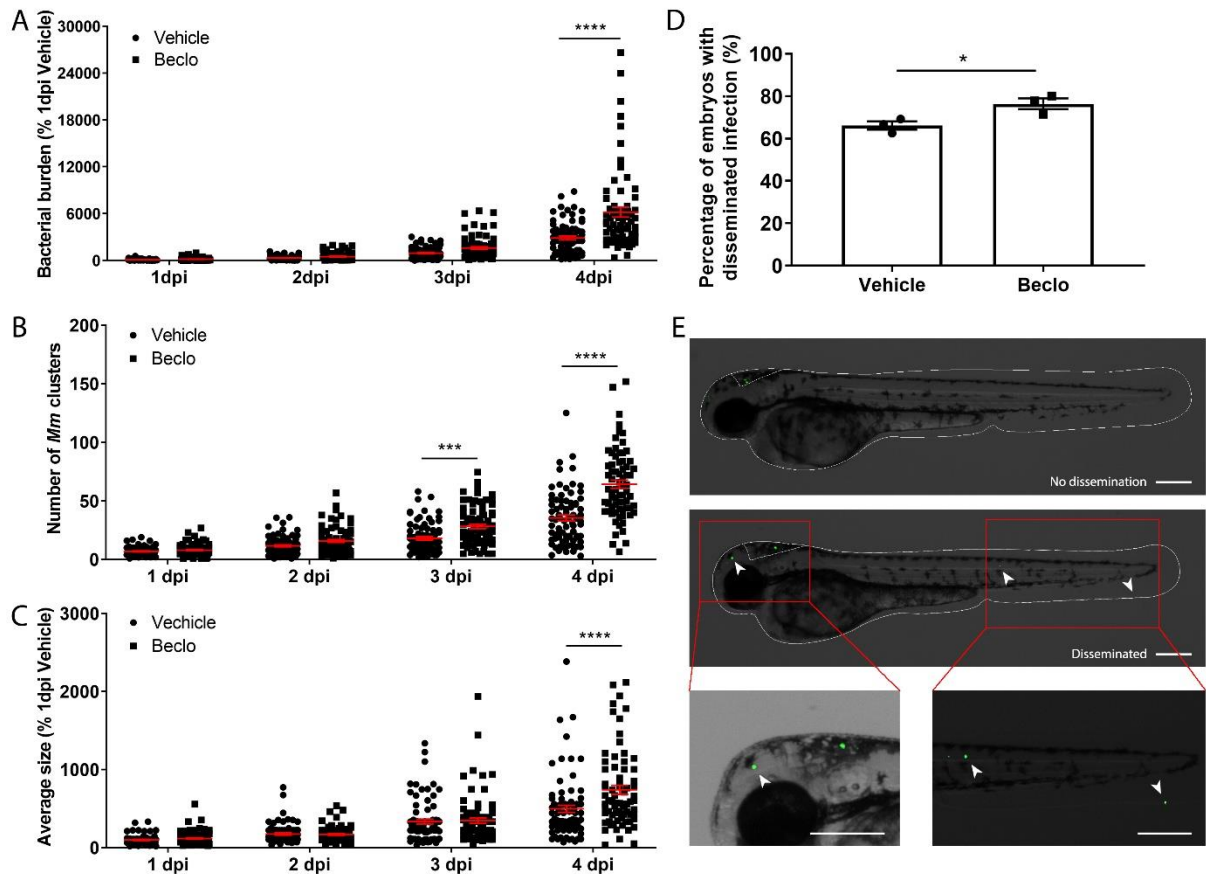


Figure 2. Beclomethasone effects on *Mm* infection progression and bacterial dissemination. A-C. Bacterial burden (A), number of bacterial clusters (B) and the average size of bacterial clusters (C) were determined at 1, 2, 3 and 4 dpi following intravenous *Mm* injection (28 hpf) and treatment with vehicle or 25 μ M beclomethasone, started at 2 h before infection. Significant increases due to the beclomethasone treatment were observed for all parameters at 4 dpi. For the number of bacterial clusters, the increase was also significant at 3 dpi. Statistical analysis was performed by two-way ANOVA with Tukey's post hoc test. Each data point represents a single larva and the means \pm s.e.m. of data accumulated from three independent experiments are shown in red. Statistical significance is indicated by: *** $P < 0.001$; **** $P < 0.0001$. D. Effect of beclomethasone on dissemination of *Mm* by hindbrain ventricle injection. Hindbrain infections were performed at 28 hpf, and at 24 hours post infection (hpi), a significantly increased percentage of larvae with disseminated *Mm* infection was detected in the beclomethasone-treated group compared to the vehicle group. Statistical analysis was performed by two-tailed t-test. Values shown are the means \pm s.e.m. of three independent experiments with a total sample size of 27 in the vehicle-treated group and 31 in the beclomethasone-treated group. Statistical significance is indicated by: * $P < 0.05$. E. Representative images of embryos with and without dissemination of the infection upon hindbrain injection of *Mm*. Scale bar = 200 μ m.

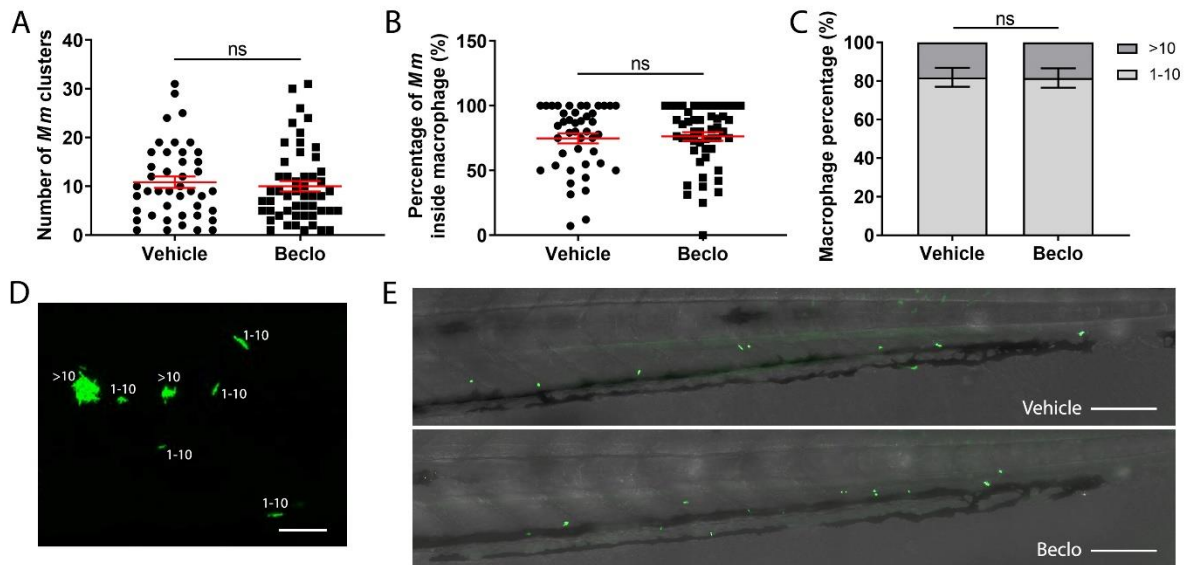


Figure 3. Effect of beclomethasone on *Mm* Δ *erp* mutant bacterial growth. A-C. The *Mm* Δ *erp* mutant strain was injected intravenously at 28 hpf, and at 44 hpi the number of *Mm* clusters (A) and the percentage of *Mm* inside macrophages (B), and the percentage of macrophages that contained 1-10 or more than 10 bacteria (of all macrophages containing bacteria) (C) were determined. No significant difference was observed between the vehicle- and beclomethasone-treated groups. Statistical analysis was performed using two-tailed t-tests. Values shown are the means \pm s.e.m. of three independent experiments, with each data point representing a single embryo. Statistical significance is indicated by: ns, non-significant. D. Representative confocal microscopy image of *Mm* Δ *erp* bacterial clusters (bacteria in green), indicated are clusters containing 1-10 bacteria and clusters containing more than 10 bacteria. Scale bar = 20 μ m. E. Representative images of the tail regions of a vehicle- and a beclomethasone-treated embryo infected with *Mm* Δ *erp* bacteria. Scale bar = 100 μ m.

Beclomethasone activation of Gr inhibits macrophage phagocytic activity

Since previous studies showed that increased *Mm* infection could be related to decreased phagocytic activity of macrophages in zebrafish [51], we studied the effect of beclomethasone on phagocytosis. We used the *Tg(mpeg1:mCherry-F)* line in which macrophages are fluorescently labeled, and assessed phagocytic activity of macrophages by determining the percentage of *Mm* that were internalized by macrophages in the yolk sac area [51] (Figure 4 A-C). In the vehicle-treated group, the percentage of phagocytosed *Mm* was $17.4 \pm 3.5\%$ at 5 minutes post infection (mpi) and gradually increased to $41.9 \pm 4.9\%$ and $52.8 \pm 5.2\%$ at 15 and 25 mpi respectively. At each of these time points, a lower percentage of *Mm* were phagocytosed in the beclomethasone-treated group ($4.6 \pm 1.6\%$ at 5 mpi, $25.7 \pm 4.7\%$ at 15 mpi and $34.0 \pm 5.2\%$ at 25 mpi). In addition, we studied the involvement of Gr in the beclomethasone-induced inhibition of phagocytosis at 5 mpi, by co-treatment with the GR antagonist RU-486 (Figure 4 D). We found that the decreased phagocytic activity that was observed upon beclomethasone treatment was abolished when larvae were co-treated with RU-486, indicating that the inhibition of phagocytosis by beclomethasone is mediated by Gr.

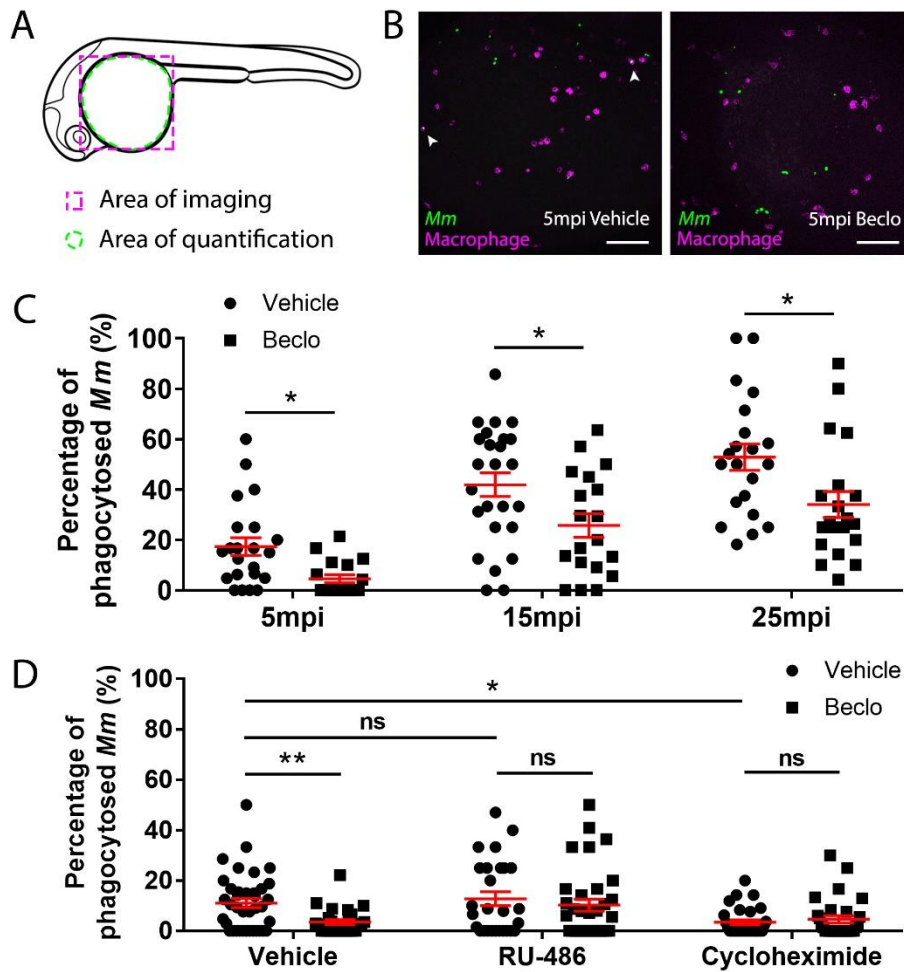


Figure 4. Effect of beclomethasone on phagocytic activity of macrophages and its dependency on Gr and *de novo* protein synthesis. A. Schematic drawing of a zebrafish embryos at 28 hpf indicating the areas of imaging (purple dashed box, used for representative images) and quantification (green dashed circle) of *Mm* phagocytosis. B. Representative confocal microscopy images of embryos of the *Tg(mpeg1:GFP)* line injected with *Mm* at 28 hpf. Images were taken of infected embryos that were vehicle- or beclomethasone-treated at 5 minutes post infection (mpi). Macrophages are shown in magenta, bacteria in green. Scale bar = 100 μ m. Arrowheads indicate bacterial clusters phagocytosed by macrophages. C. Percentages of phagocytosed *Mm* clusters (of total number of *Mm* clusters) at 5, 15 and 25 mpi. Statistical analysis, performed by fitting data to a beta inflated regression with Tukey's post hoc test, showed that beclomethasone decreased this percentage at all three time points. D. Effects of RU-486 and cycloheximide on the beclomethasone-inhibited phagocytic activity. Embryos were treated with vehicle or beclomethasone and received either a vehicle, RU-486 or cycloheximide co-treatment two hours before injection of *Mm* at 28 hpf, and phagocytic activity was determined at 5 mpi. The significant inhibitory effect of beclomethasone on phagocytosis was not observed in the presence of RU-486. Cycloheximide, just like beclomethasone, significantly inhibited the phagocytic activity, and the combined cycloheximide/beclomethasone treatment showed the same level of inhibition. Statistical analysis was performed by fitting data to a beta inflated regression with Tukey's post hoc test. In panels C and D, each data point represents a single embryo and the means \pm s.e.m. of data accumulated from three independent experiments are shown in red. Statistical significance is indicated by: ns, non-significant; * $P < 0.05$; ** $P < 0.01$.

Gr generally acts as a transcription factor, modulating the transcription rate of a wide variety of genes. To study whether phagocytosis could be modulated by altering the process of protein synthesis, we blocked *de novo* protein synthesis by treatment with cycloheximide (Figure 4 D). We observed that the phagocytic activity of macrophages at 5 mpi was decreased by the cycloheximide treatment ($3.4\pm 1.0\%$ vs $11.1\pm 1.8\%$ in the vehicle group). These data demonstrate that phagocytosis depends on *de novo* protein synthesis, and suggest that modulating transcription could be the mechanism underlying the inhibition of phagocytosis by Gr.

Beclomethasone treatment results in fewer intracellular bacteria and limits infected cell death

To further analyze the possible mechanisms underlying the beclomethasone-induced increase in the *Mm* infection level, we assessed the percentage of bacteria that are present inside and outside macrophages in the caudal hematopoietic tissue (CHT) at 48 hpi using *Mm* infection in the *Tg(mpeg1:GFP)* line. The results showed that beclomethasone treatment resulted in a decreased percentage of intracellular bacteria ($23.8\pm 3.0\%$) compared to the percentage in the vehicle-treated group ($36.5\pm 3.6\%$) (Figure 5 A, C). This result was in line with the observed decrease in phagocytosis at earlier stages of infection. Finally, we used terminal deoxynucleotidyl transferase dUTP nick end labelling (TUNEL) staining to detect cell death, and we performed this staining at 48 hpi [52]. In the beclomethasone-treated group, the percentage of *Mm* that were colocalized with TUNEL staining ($9.4\pm 1.6\%$) was significantly lower compared to the percentage of the vehicle group ($17.2\pm 2.3\%$) (Figure 5 B, D). These data suggest that the observed inhibition of phagocytosis upon beclomethasone treatment causes a decrease in the percentage of intracellular bacteria, which underlies the lower numbers of macrophages undergoing cell death as a result of the *Mm* infection.

Beclomethasone inhibits phagocytosis-related gene expression in macrophages

To unravel the molecular mechanisms underlying the beclomethasone-induced inhibition of the phagocytic activity of macrophages, we performed qPCR analysis on FACS-sorted macrophages derived from 28 hpf larvae after 2 h of beclomethasone treatment. To determine the phenotype of the sorted macrophages, the expression of a classic pro-inflammatory gene, *tnfa*, was measured [53, 54]. The levels of *tnfa* expression were significantly lower after beclomethasone treatment (Figure 6 A), in agreement with previously reported transcriptome analysis [48]. In addition, we measured the expression levels of seven phagocytosis-related genes, *sparcl1*, *uchl1*, *ube2v1*, *marcksa*, *marcksb*, *bsg* and *tubb5* [55-57] (Figure 6 B-H). The expression levels of four of these genes, *sparcl1*, *uchl1*, *marcksa*

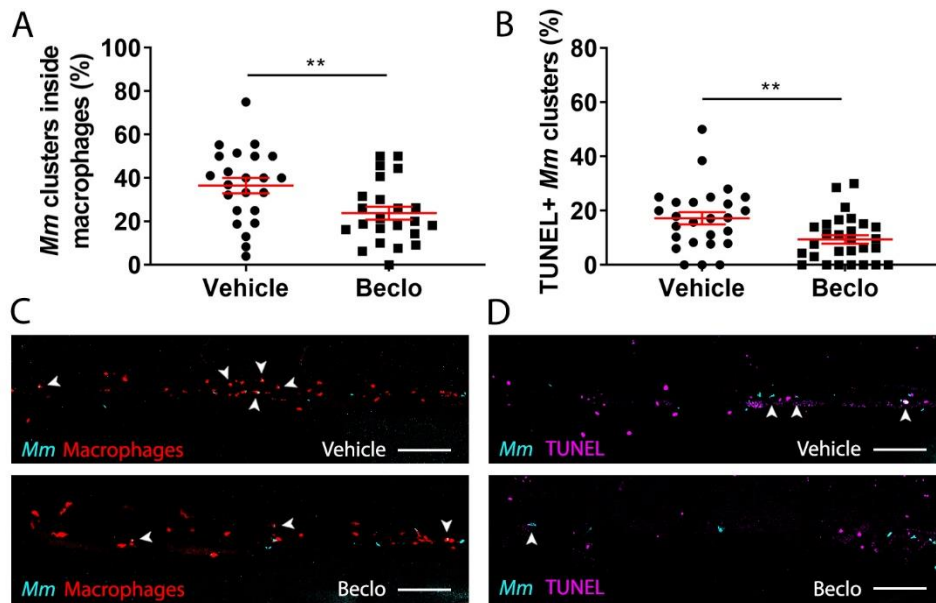


Figure 5. Effect of beclomethasone on intracellular bacterial growth and cell death. Infection was performed in *Tg(mpeg1:mCherry-F)* embryos at 28 hpf, a TUNEL assay was performed at 48 hpi, and the CHT region of the embryos was imaged using confocal microscopy. A. The percentage of *Mm* clusters that were inside macrophages based on colocalization with the red fluorescent signal from mCherry. Statistical analysis was performed by two-tailed t-test. In the beclomethasone-treated group, the percentage of *Mm* clusters inside macrophages was significantly lower compared to the vehicle-treated group. B. The percentage of TUNEL-positive *Mm* clusters. Statistical analysis by two-tailed t-test showed that the beclomethasone-treated group had a significantly lower percentage of TUNEL+ *Mm* clusters. In panels A and B, each data point represents a single embryo and the means \pm s.e.m. of data accumulated from three independent experiments are shown in red. Statistical significance is indicated by: ** P<0.01. C. Representative confocal microscopy images of macrophage phagocytosis. Bacteria are shown in blue and macrophages in red. Arrowheads indicate intracellular bacterial clusters. Scale bar = 100 μm. D. Representative confocal microscopy images of cell death (TUNEL+ cells in magenta) and *Mm* infection (bacteria in blue). Arrowheads indicate bacterial clusters overlapping with TUNEL+ cells. Scale bar = 100 μm.

and *marcksb*, were inhibited by beclomethasone treatment, while the levels of the other three (*ube2v1*, *bsg* and *tubb5*) were not affected. These data suggest that beclomethasone inhibits the phagocytic activity of macrophages by suppressing the transcription of phagocytosis-related genes in these cells.

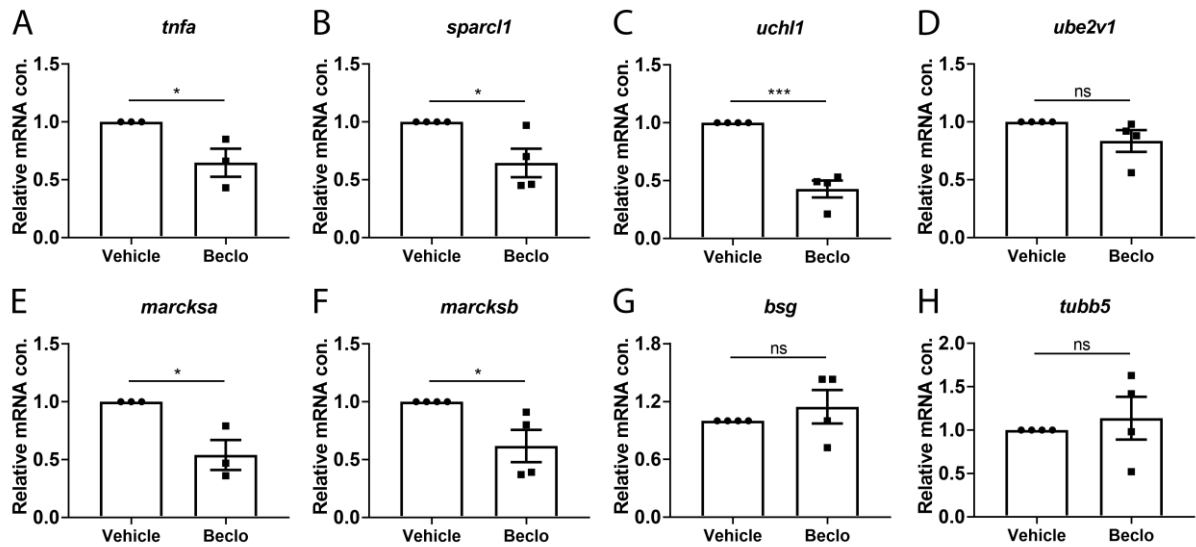


Figure 6. Effect of beclomethasone on gene expression levels in FACS-sorted macrophages. At 28 hpf, *Tg(mpeg1:mCherry-F)* embryos were treated with vehicle or beclomethasone for two hours, after which macrophages were isolated by FACS sorting. Gene expression levels were determined in the sorted cells by qPCR for *tnfa* (A), *sparcl1* (B), *uchl1* (C), *ube2v1* (D), *marcksa* (E), *marcksb* (F), *bsg* (G) and *tubb5* (H). Statistical analysis by two-tailed t-test showed that the levels of *tnfa*, *sparcl1*, *uchl1*, *marcksa* and *marcksb* expression were significantly inhibited by beclomethasone treatment. Data shown are the means \pm s.e.m. of three or four independent experiments, and markers show averages of individual experiments. Statistical significance is indicated by: ns, non-significant; * $P < 0.05$; *** $P < 0.001$.

Effect of Beclomethasone on the phagocytosis of *Salmonella* Typhimurium

To study whether the beclomethasone-induced inhibitory effect on macrophage phagocytosis of *Mm* can be generalized to other bacterial infections, we analyzed the effect of beclomethasone on infection with *Salmonella* Typhimurium, which is also an intracellular pathogen, but belongs to the gram-negative class. We quantified the percentages of bacteria phagocytosed by macrophages at different time points after infection in the *Tg(mpeg1:GFP)* fish line (Figure 7). In the vehicle group, the percentage of phagocytosed *Salmonella* Typhimurium increased from $5.7 \pm 0.7\%$ at 10 mpi to $9.0 \pm 1.2\%$ at 30 mpi and $17.9 \pm 1.7\%$ at 60 mpi, and these percentages were significantly lower in the beclomethasone-treated group at all time points ($3.1 \pm 0.5\%$ at 10 mpi, $6.5 \pm 1.0\%$ at 30 mpi and $10.0 \pm 1.4\%$ at 60 mpi). These data demonstrate that the inhibitory effect of beclomethasone on the phagocytic activity of macrophages is not specific for *Mm*, but can also be observed for a distantly related *Salmonella* species.

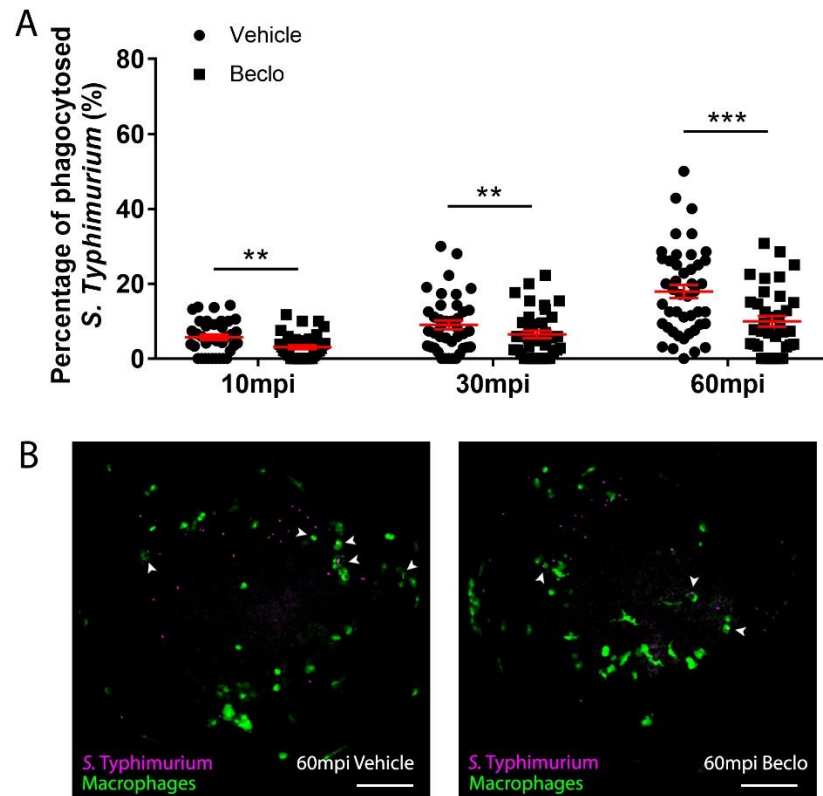


Figure 7. Effect of beclomethasone on phagocytosis of *Salmonella Typhimurium*. At 28 hpf *Tg(mpeg1:GFP)* embryos (vehicle- or beclomethasone-treated) were infected with *S. Typhimurium* through intravenous injection. At 10, 30, and 60 mpi, confocal microscopy images were taken of the yolk area, as indicated in Figure 4A, and the macrophage phagocytic capacity was determined. A. Percentage of phagocytosed *S. Typhimurium* at 10, 30 and 60 mpi. Statistical analysis, performed by fitting data to a beta inflated regression with Tukey's post hoc test, showed that the phagocytic activity of macrophages was significantly inhibited by beclomethasone treatment at 60 mpi, and not at other time points. Each data point represents a single embryo and the means \pm s.e.m. of data accumulated from three independent experiments are shown in red. Statistical significance is indicated by: ns, non-significant; **** $P < 0.0001$. B. Representative confocal microscopy images of infected vehicle- and beclomethasone-treated individuals at 60 mpi. Bacteria are shown in magenta, macrophages in green. Arrowheads indicate bacteria phagocytosed by macrophages. Scale bar = 100 μ m.

Discussion

Synthetic GCs are widely prescribed to treat various immune-related diseases, but their clinical use is limited by the severe side effects evoked by prolonged therapy, including a higher susceptibility to TB [5, 14]. In order to gain more insight into the mechanism underlying this GC effect, we used the zebrafish *Mm* infection model, which mimics human TB, and studied the effect of GC treatment on the development of the infection. We showed that GC treatment increased the level of *Mm* infection, which was reflected in the overall bacterial burden, the size and number of bacterial clusters and the level of dissemination. Since we found that GC treatment inhibited the phagocytic activity but not the microbicidal capacity of macrophages, we propose that the GC-induced increase in infection

susceptibility is due to the inhibition on phagocytosis. Analysis of the transcription level of phagocytosis-related genes in macrophages suggested that the inhibition of phagocytic activity by GCs is mediated by Gr interfering with phagocytosis-related gene transcription. As a result of the lower phagocytic activity of the macrophages, the percentage of intracellular bacteria is decreased, which results in a lower level of cell death due to the *Mm* infection and exacerbated growth of the extracellular bacterial fraction. Finally, we showed that GC treatment not only limited phagocytosis of mycobacteria, but also of a *Salmonella* species, which suggests that the decrease in phagocytic activity may also explain the increased susceptibility to other bacterial infections that is commonly observed in patients receiving GC therapy [3-5].

Upon bacterial infections, macrophages are the first responders of the immune system. In humans, *Mtb* generally infects lungs due to its air transmission properties and in the lungs it is taken up by alveolar macrophages within the first few days. In later stages, *Mtb* replicates, translocates to secondary loci and aggregates into granulomas with other attracted immune cells [58-60]. Consistently, in the zebrafish model, *Mm* is predominantly phagocytosed by macrophages within 30-60 min after intravenous infection in embryos, leading to initial stages of granuloma formation in the next few days [37, 51]. The phagocytosis activity and microbicidal capacity of macrophages have both been shown to be important for dealing with *Mm* infection [51, 61]. Interestingly, in our study we found that the microbicidal capacity of macrophages was not affected by GC treatment, which suggests that the inhibition of macrophage phagocytosis is a specific effect of GCs targeted at the uptake of pathogens rather than a global suppression of anti-microbial processes in macrophages.

Our study in the zebrafish model provides *in vivo* evidence for GC interference with macrophage phagocytosis that confirms results from various other studies. In line with our results, it has previously been shown that GCs decrease the phagocytosis of several *Escherichia coli* strains by human monocyte-derived (THP-1) macrophages and by murine bone marrow-derived macrophages (BMDMs) [62]. Similarly to our results, in this study the reduced phagocytosis activity was accompanied by a decreased expression of genes involved in phagosome formation including *MARCKS* and pro-inflammatory genes like *TNF* [62]. In earlier studies, decreased macrophage phagocytosis of carbon particles was observed *in vivo*, in GC-treated rats and rheumatoid arthritis patients [63, 64].

In contrast to our results on phagocytosis of mycobacteria, in other studies GC treatment has been shown to enhance the phagocytosis activity of macrophages. Upon GC exposure, increased phagocytosis of human monocyte-derived macrophages was observed for *Haemophilus influenzae* and *Streptococcus pneumoniae* [65], and *Staphylococcus aureus* [66]. This increased phagocytic activity would be in line with the well-established GC-induced enhancement of the phagocytosis of apoptotic

neutrophils, which has been observed in, differentiated THP-1 macrophages, through stimulation of a protein S/Mer tyrosine kinase dependent pathway [67-69], and in mouse alveolar macrophages [70]. This effect is considered to play an important role in GCs actively promoting the resolution of inflammation and reflects the GC-enhanced differentiation of macrophages to an anti-inflammatory phenotype [71, 72]. Interestingly, GC treatment does not enhance the phagocytosis capacity in differentiated THP-1 macrophages of latex beads or apoptotic cells [69]. Most likely, the effects of GCs on the phagocytic activity of macrophages are highly dependent on the differentiation status of the cells, the particles they encounter and the tissue environment.

Our study revealed an inhibitory effect of GCs on four phagocytosis-related genes in FACS-sorted macrophages: *sparcl-1*, *uchl-1*, *marcksa* and *marcksb*. Among those genes, the human and mouse homologs of *sparcl-1* and *uchl-1* were reported to have a phagocytosis-promoting activity [55, 57]. In human THP-1-derived macrophages, MARCKS plays a role in cytoskeletal remodeling and phagosome formation, and in line with our study the *MARCKS* gene expression was found to be inhibited by dexamethasone treatment [56, 62]. Together with our observation that phagocytosis is dependent on *de novo* protein synthesis, these results support the idea that GC treatment inhibits the phagocytosis activity of macrophages through interfering with transcription of genes that stimulate the phagocytic activity.

After internalization by macrophages, *Mm* are exposed to a bactericidal environment [73]. Some bacteria may be killed by macrophages, while others may proliferate mediated by virulence determinants like Erp and RD1 [49, 73, 74]. When the macrophages are incapable of containing the bacteria, they undergo cell death leading to recruitment of more macrophages [38]. In our study, GC treatment led to a lower percentage of intracellular *Mm* at later stages, consistent with the decreased phagocytosis at early time points, and consequently less *Mm*-related cell death. The GC treatment may also directly affect cell death, since in a recent study it was demonstrated that GCs inhibit necrosis of various *Mtb* infected mouse and human cell types by activating MKP-1, which suppresses a pathway involving p38 MAPK activation ultimately leading to a loss of mitochondrial integrity [75]. The increased numbers of extracellular bacteria could traverse endothelial barriers directly and grow more rapidly in a less restrictive environment outside macrophages, which may explain our observation of a higher bacterial burden induced by GC treatment.

Based on our results, it may seem surprising that adjunctive GC therapy is often beneficial to TB patients, and even increases survival among tuberculous meningitis and pericarditis patients [24-26]. However, many of these observed beneficial effects are either minor or under debate. This may be due to GC therapy benefiting only a subset of patients whose disease has mainly progressed as a result

of an excessive inflammatory response (which can be controlled with GC therapy), rather than a failed reaction to the infection, which was demonstrated for GC-treated TB meningitis patients with specific polymorphisms in the *LTA4H* gene (Tobin et al., 2012). We therefore suggest that in a subset of patients at later stages of infection, the anti-inflammatory effects of a GC treatment may outweigh a possible inhibitory effect on the phagocytic activity of the macrophages. Further research using the zebrafish model may shed light on a possible interplay between these effects, since the *Mm* infection model has been shown to have excellent translational value for human TB, including the effects of GC treatment (Tobin 2010, Tobin 2012).

In conclusion, our *in vivo* study on the effect of GC treatment in the zebrafish *Mm* infection model shows that GCs, through activation of Gr, inhibit the phagocytic activity of macrophages, which results in more extracellular bacterial growth and a higher infection level. These results may explain why clinically prolonged GC treatment is associated with an increased risk of TB and other bacterial infections.

Materials and methods

Zebrafish lines and maintenance

Zebrafish were maintained and handled according to the guidelines from the Zebrafish Model Organism Database (<http://zfin.org>) and in compliance with the directives of the local animal welfare body of Leiden University. They were exposed to a 14 hours light and 10 hours dark cycle to maintain circadian rhythmicity. Fertilization was performed by natural spawning at the beginning of the light period. Eggs were collected and raised at 28°C in egg water (60 µg/ml Instant Ocean sea salts and 0.0025% methylene blue). The following fish lines were used: wild type strain AB/TL, and the transgenic lines *Tg(mpeg1:mCherry-F^{umsF001})* [76] and *Tg(mpeg1:eGFP^{g122})* [77].

Bacterial culture and infection through intravenous injections

Bacteria used for this study were *Mycobacteria marinum*, strain M, constitutively fluorescently labelled with Wasabi or mCrimson [78, 79], *Mm* mutant Δ *erp* labelled with Wasabi [80], and *Salmonella enterica serovar* Typhimurium (*S. Typhimurium*) wild type (wt) strain SL1344 labelled with mCherry [81, 82]. The *Mm* strain M and *S. Typhimurium* wt strain were cultured at 28°C and 37°C respectively and the bacterial suspensions were prepared with phosphate buffered saline (PBS) with 2% (w/v) polyvinylpyrrolidone-40 (PVP40, Sigma-Aldrich), as previously described [83]. The suspension of *Mm* Δ *erp*-Wasabi was prepared directly from -80°C frozen aliquots.

After anesthesia with 0.02% aminobenzoic acid ethyl ester (tricaine, Sigma-Aldrich), 28 hours post fertilization (hpf) embryos were injected with *Mm* or *S. Typhimurium* into the blood island (or hindbrain if specified) under a Leica M165C stereomicroscope, as previously described [83]. The injection dose was 200 CFU for *Mm* and 50 CFU for *S. Typhimurium*.

Chemical treatments and bacterial burden quantification

The embryos were treated with 25 μ M (or different if specified) beclomethasone (Sigma-Aldrich) or vehicle (0.05% dimethyl sulfoxide (DMSO)) in egg water from 2 hours before injection to the end of an experiment. RU-486 (Sigma-Aldrich) was administered at a concentration of 5 μ M (0.02% DMSO), and cycloheximide (Sigma-Aldrich) at 100 μ g/ml (0.04% DMSO). If the treatment lasted longer than 1 day, the medium was refreshed every day.

For bacterial burden quantification, the embryos from the vehicle- and beclomethasone-treated groups were imaged alive using a Leica M205FA fluorescence stereomicroscope equipped with a Leica DFC 345FX camera (Leica Microsystems). The images were analyzed using custom-designed pixel quantification software (previously described by Benard et al. (2015)), and Image J (plugin 'Analyze Particles').

Hindbrain infection and analysis of dissemination

To assess the dissemination efficiency, the embryos were injected with 50 CFU *Mm* into the hindbrain at 28 hpf. At 2 dpi, the embryos were imaged with a Leica M205FA fluorescence stereomicroscope equipped with a Leica DFC 345FX camera. The embryos were classified into two categories: with or without disseminated infection. An embryo was considered without disseminated infection if all the bacteria were still contained in the hindbrain ventricle and considered with dissemination if bacteria were present in any other part of the embryo.

Analysis of microbicidal activity

After infection at 28 hpf with *Mm* Δ *erp*-Wasabi, *Tg(mpeg1:mCherry-F)* embryos were fixed at 44 hpi with 4% paraformaldehyde (PFA, Sigma-Aldrich) and imaged using a Leica TCS SP8 confocal microscope with 40X objective (NA 1.3). All macrophages that contained *Mm* Δ *erp*-Wasabi in the tail region were analyzed. The level of infection inside macrophages was classified into two categories based on the number of bacteria: 1-10 bacteria or >10 bacteria, following established protocols [49, 50].

Analysis of phagocytic activity

After infection at 28 hpf with *Mm*-Wasabi or *S. Typhimurium*-mCherry, *Tg(mpeg1:mCherry-F)* or *Tg(mpeg1:GFP)* embryos were fixed with 4% PFA at different time points and imaged using a Leica TCS SP8 confocal microscope with 20X objective (NA 0.75). The yolk sac area was selected as the quantification area (Figure 4A). The number of fluorescently labelled *Mm* or *S. Typhimurium* in this area, and those present inside a macrophage, were counted in a manual and blinded way.

TUNEL assay

After infection at 28 hpf, *Tg(mpeg1:mCherry-F)* embryos were fixed with 4% PFA at 48 hpi and stained using terminal deoxynucleotidyl transferase dUTP nick end labelling (TUNEL) with the In Situ Cell Death Detection Kit, TMR red (Sigma-Aldrich), as previously described by Zhang et al. (2019). For this TUNEL staining, the embryos were first dehydrated and then rehydrated gradually with methanol in PBS, and permeabilized with 10 µg/ml Proteinase K (Roche). The embryos were subsequently fixed with 4% PFA for another 20 min and stained with reagent mixture overnight at 37°C. After the reaction was stopped by washing with PBS containing 0.05% Tween-20 (PBST), the CHT region of the embryos was imaged using a Leica TCS SP8 confocal microscope with 40X objective (NA 1.3). The total number of fluorescently labelled *Mm* clusters and the number of these clusters overlapping with TUNEL staining were counted in a manual and blinded way.

Fluorescence-Activated Cell Sorting (FACS) of macrophages

Macrophages were sorted from *Tg(mpeg1:mCherry-F)* embryos as previously described [84, 85]. Dissociation was performed with 150-200 embryos for each sample after 2 hours beclomethasone or vehicle treatment (started at 28 hpf) using Liberase TL (Roche) and stopped by adding Fetal Calf Serum (FCS) to a final concentration of 10%. Isolated cells were resuspended in Dulbecco's PBS (DPBS), and filtered through a 40 µm cell strainer. Actinomycin D (Sigma-Aldrich) was added (final concentration of 1 µg/ml) to each step to inhibit transcription. Macrophages were sorted based on their red fluorescent signal using a FACS Aria III cell sorter (BD Biosciences). The sorted cells were collected in QIAzol lysis reagent (Qiagen) for RNA isolation.

RNA isolation, cDNA synthesis and quantitative PCR (qPCR) analysis

RNA isolation from FACS-sorted cells was performed using the miRNeasy mini kit (Qiagen), according to the manufacturer's instructions. Extracted total RNA was reverse-transcribed using the iScript™ cDNA Synthesis Kit (Bio-Rad). QPCR was performed on a MyiQ Single-Color Real-Time PCR Detection System (Bio-Rad) using iTaq™ Universal SYBR® Green Supermix (Bio-Rad). The sequences of the

primers used are provided in Supplementary Table 1. Cycling conditions were pre-denaturation for 3 min at 95°C, followed by 40 cycles of denaturation for 15 s at 95°C, annealing for 30 s at 60°C, and elongation for 30 s at 72°C. Fluorescent signals were measured at the end of each cycle. Cycle threshold values (Ct values, i.e. the cycle numbers at which a threshold value of the fluorescence intensity was reached) were determined for each sample. To determine the gene regulation due to beclomethasone treatment in each experiment, the average Ct value of the beclomethasone treated samples was subtracted from the average Ct value of the vehicle-treated samples, and the fold change of gene expression was calculated, which was subsequently adjusted to the expression levels of a reference gene (*peptidylprolyl isomerase Ab (ppiab)*).

Statistical analysis

Statistical analysis was performed using GraphPad Prism by one-way ANOVA with Bonferroni's post hoc test (Figure 1A) or two-way ANOVA with Tukey's post hoc test (Figure 1B, Figure 2 A-C) or two-tailed t-test (Figure 2D, Figure 3, 5, 6) or using R Statistical Software by fitting data to a beta inflated regression (from 'gamlss' package) [86] with Tukey's post hoc test (Figure 4, 7).

Acknowledgements

We thank Frida Sommer for her advice on *Mm Δerp* assays, Ralf Boland, Salomé Munoz Sanchez, Dr. Michiel van der Vaart and Aleksandra Fesliyska for their assistance with bacterial infections, Dr. Rui Zhang and Dr. Monica Varela Alvarez for their suggestions concerning TUNEL assays and Patrick van Hage for his help with the statistical analysis. We thank the fish facility team, in particular Ulrike Nehrdich, Ruth van Koppen, Karen Bosma and Guus van der Velden for zebrafish maintenance. We thank Dr. Georges Lutfalla and Dr. Graham Lieschke for providing transgenic zebrafish lines.

References

1. Buckley, L. and M.B. Humphrey, *Glucocorticoid-Induced Osteoporosis*. N Engl J Med, 2018. **379**(26): p. 2547-2556.
2. Suh, S. and M.K. Park, *Glucocorticoid-Induced Diabetes Mellitus: An Important but Overlooked Problem*. Endocrinol Metab (Seoul), 2017. **32**(2): p. 180-189.
3. Dixon, W., et al., *The influence of systemic glucocorticoid therapy upon the risk of non-serious infection in older patients with rheumatoid arthritis: a nested case-control study*. Annals of the rheumatic diseases, 2011. **70**(6): p. 956-960.
4. Fardet, L., I. Petersen, and I. Nazareth, *Common Infections in Patients Prescribed Systemic Glucocorticoids in Primary Care: A Population-Based Cohort Study*. PLoS Med, 2016. **13**(5): p. e1002024.
5. Caplan, A., et al., *Prevention and management of glucocorticoid-induced side effects: A comprehensive review: A review of glucocorticoid pharmacology and bone health*. J Am Acad Dermatol, 2017. **76**(1): p. 1-9.

6. World Health Organization, *Global tuberculosis report 2019*. 2019, Geneva: World Health Organization.
7. Houben, R.M. and P.J. Dodd, *The global burden of latent tuberculosis infection: a re-estimation using mathematical modelling*. PLoS medicine, 2016. **13**(10): p. e1002152.
8. Furin, J., H. Cox, and M. Pai, *Tuberculosis*. The Lancet, 2019. **393**(10181): p. 1642-1656.
9. Lin, P.L. and J.L. Flynn, *Understanding latent tuberculosis: a moving target*. The Journal of Immunology, 2010. **185**(1): p. 15-22.
10. Drain, P.K., et al., *Incipient and Subclinical Tuberculosis: a Clinical Review of Early Stages and Progression of Infection*. Clin Microbiol Rev, 2018. **31**(4).
11. Parikka, M., et al., *Mycobacterium marinum causes a latent infection that can be reactivated by gamma irradiation in adult zebrafish*. PLoS Pathog, 2012. **8**(9): p. e1002944.
12. Kulchavenya, E., *Extrapulmonary tuberculosis: are statistical reports accurate?* Therapeutic Advances in Infectious Disease, 2014. **2**(2): p. 61-70.
13. Hawn, T.R., et al., *Host-directed therapeutics for tuberculosis: can we harness the host?* Microbiol. Mol. Biol. Rev., 2013. **77**(4): p. 608-627.
14. Jick, S.S., et al., *Glucocorticoid use, other associated factors, and the risk of tuberculosis*. Arthritis Rheum, 2006. **55**(1): p. 19-26.
15. Kim, H., et al., *Mycobacterium tuberculosis infection in a corticosteroid-treated rheumatic disease patient population*. Clinical and experimental rheumatology, 1998. **16**(1): p. 9-13.
16. Bovornkitti, S., et al., *Reversion and Reconversion Rate of Tuberculin Skin Reactions in Correlation with the Use of Prednisone*. Diseases of the Chest, 1960. **38**(1): p. 51-55.
17. Schatz, M., et al., *The prevalence of tuberculosis and positive tuberculin skin tests in a steroid-treated asthmatic population*. Ann Intern Med, 1976. **84**(3): p. 261-5.
18. Lerner, B.H., *Can stress cause disease? Revisiting the tuberculosis research of Thomas Holmes, 1949-1961*. Ann Intern Med, 1996. **124**(7): p. 673-80.
19. Kadiravan, T. and S. Deepanjali, *Role of corticosteroids in the treatment of tuberculosis: an evidence-based update*. Indian J Chest Dis Allied Sci, 2010. **52**(3): p. 153-8.
20. Alzeer, A.H. and J.M. FitzGerald, *Corticosteroids and tuberculosis: risks and use as adjunct therapy*. Tuber Lung Dis, 1993. **74**(1): p. 6-11.
21. Evans, D.J., *The use of adjunctive corticosteroids in the treatment of pericardial, pleural and meningeal tuberculosis: Do they improve outcome?* Respiratory Medicine, 2008. **102**(6): p. 793-800.
22. Singh, S. and K. Tiwari, *Use of corticosteroids in tuberculosis*. The Journal of Association of Chest Physicians, 2017. **5**(2): p. 70-75.
23. Torok, M.E., et al., *Dexamethasone and long-term outcome of tuberculous meningitis in Vietnamese adults and adolescents*. PLoS One, 2011. **6**(12): p. e27821.
24. Strang, J.I., et al., *Management of tuberculous constrictive pericarditis and tuberculous pericardial effusion in Transkei: results at 10 years follow-up*. Qjm, 2004. **97**(8): p. 525-35.
25. Thwaites, G.E., et al., *Dexamethasone for the treatment of tuberculous meningitis in adolescents and adults*. N Engl J Med, 2004. **351**(17): p. 1741-51.
26. Wiysonge, C.S., et al., *Interventions for treating tuberculous pericarditis*. Cochrane Database Syst Rev, 2017. **9**(9): p. Cd000526.
27. Smego, R.A. and N. Ahmed, *A systematic review of the adjunctive use of systemic corticosteroids for pulmonary tuberculosis*. Int J Tuberc Lung Dis, 2003. **7**(3): p. 208-13.
28. Muthuswamy, P., et al., *Prednisone as adjunctive therapy in the management of pulmonary tuberculosis: report of 12 cases and review of the literature*. Chest, 1995. **107**(6): p. 1621-1630.
29. Ryan, H., J. Yoo, and P. Darsini, *Corticosteroids for tuberculous pleurisy*. Cochrane Database of Systematic Reviews, 2017(3).
30. Prasad, K., M.B. Singh, and H. Ryan, *Corticosteroids for managing tuberculous meningitis*. Cochrane Database of Systematic Reviews, 2016(4).

31. Critchley, J.A., L.C. Orton, and F. Pearson, *Adjunctive steroid therapy for managing pulmonary tuberculosis*. Cochrane Database Syst Rev, 2014(11): p. Cd011370.
32. Tobin, D.M., et al., *Host genotype-specific therapies can optimize the inflammatory response to mycobacterial infections*. Cell, 2012. **148**(3): p. 434-446.
33. Tobin, D.M. and L. Ramakrishnan, *Comparative pathogenesis of Mycobacterium marinum and Mycobacterium tuberculosis*. Cellular microbiology, 2008. **10**(5): p. 1027-1039.
34. Meijer, A.H., *Protection and pathology in TB: learning from the zebrafish model*. Semin Immunopathol, 2016. **38**(2): p. 261-73.
35. Ramakrishnan, L., *The zebrafish guide to tuberculosis immunity and treatment*. Cold Spring Harb Symp Quant Biol, 2013. **78**: p. 179-92.
36. Cronan, M.R. and D.M. Tobin, *Fit for consumption: zebrafish as a model for tuberculosis*. Disease models & mechanisms, 2014. **7**(7): p. 777-784.
37. Davis, J.M., et al., *Real-Time Visualization of Mycobacterium-Macrophage Interactions Leading to Initiation of Granuloma Formation in Zebrafish Embryos*. Immunity, 2002. **17**(6): p. 693-702.
38. Davis, J.M. and L. Ramakrishnan, *The Role of the Granuloma in Expansion and Dissemination of Early Tuberculous Infection*. Cell, 2009. **136**(1): p. 37-49.
39. van Leeuwen, L.M., A.M. van der Sar, and W. Bitter, *Animal models of tuberculosis: zebrafish*. Cold Spring Harbor perspectives in medicine, 2015. **5**(3): p. a018580.
40. Tobin, D.M., et al., *The Ita4h locus modulates susceptibility to mycobacterial infection in zebrafish and humans*. Cell, 2010. **140**(5): p. 717-730.
41. Stolte, E.H., et al., *Evolution of glucocorticoid receptors with different glucocorticoid sensitivity*. Journal of Endocrinology, 2006. **190**(1): p. 17-28.
42. Schaaf, M., A. Chatzopoulou, and H. Spaink, *The zebrafish as a model system for glucocorticoid receptor research*. Comparative Biochemistry and Physiology Part A: Molecular & Integrative Physiology, 2009. **153**(1): p. 75-82.
43. Alsop, D. and M.M. Vijayan, *Development of the corticosteroid stress axis and receptor expression in zebrafish*. Am J Physiol Regul Integr Comp Physiol, 2008. **294**(3): p. R711-9.
44. Chatzopoulou, A., et al., *Transcriptional and metabolic effects of glucocorticoid receptor α and β signaling in zebrafish*. Endocrinology, 2015. **156**(5): p. 1757-1769.
45. Chatzopoulou, A., et al., *Glucocorticoid-induced attenuation of the inflammatory response in zebrafish*. Endocrinology, 2016. **157**(7): p. 2772-2784.
46. Faught, E. and M.M. Vijayan, *Loss of the glucocorticoid receptor in zebrafish improves muscle glucose availability and increases growth*. Am J Physiol Endocrinol Metab, 2019. **316**(6): p. E1093-e1104.
47. Facchinello, N., et al., *nr3c1 null mutant zebrafish are viable and reveal DNA-binding-independent activities of the glucocorticoid receptor*. Scientific reports, 2017. **7**(1): p. 1-13.
48. Xie, Y., et al., *Glucocorticoids inhibit macrophage differentiation towards a pro-inflammatory phenotype upon wounding without affecting their migration*. Disease models & mechanisms, 2019. **12**(5): p. dmm037887.
49. Clay, H., H.E. Volkman, and L. Ramakrishnan, *Tumor necrosis factor signaling mediates resistance to mycobacteria by inhibiting bacterial growth and macrophage death*. Immunity, 2008. **29**(2): p. 283-94.
50. Sommer, F., et al., *Frontline Science: Antagonism between regular and atypical Cxcr3 receptors regulates macrophage migration during infection and injury in zebrafish*. Journal of Leukocyte Biology, 2020. **107**(2): p. 185-203.
51. Benard, E.L., et al., *Phagocytosis of mycobacteria by zebrafish macrophages is dependent on the scavenger receptor Marco, a key control factor of pro-inflammatory signalling*. Dev Comp Immunol, 2014. **47**(2): p. 223-33.
52. Zhang, R., et al., *Deficiency in the autophagy modulator Dram1 exacerbates pyroptotic cell death of Mycobacteria-infected macrophages*. bioRxiv, 2019: p. 599266.
53. Nguyen-Chi, M., et al., *Identification of polarized macrophage subsets in zebrafish*. Elife, 2015. **4**: p. e07288.

54. Martinez, F.O. and S. Gordon, *The M1 and M2 paradigm of macrophage activation: time for reassessment*. F1000Prime Rep, 2014. **6**: p. 13.
55. Jeon, H., et al., *Functional selection of phagocytosis-promoting genes: cell sorting-based selection*. J Biomol Screen, 2010. **15**(8): p. 949-55.
56. Carballo, E., et al., *Phagocytic and macropinocytic activity in MARCKS-deficient macrophages and fibroblasts*. American Journal of Physiology-Cell Physiology, 1999. **277**(1): p. C163-C173.
57. Banerjee, H., et al., *Differential expression of efferocytosis and phagocytosis associated genes in tumor associated macrophages exposed to African American patient derived prostate cancer microenvironment*. J Solid Tumors, 2019. **9**(2): p. 22-27.
58. Srivastava, S., J.D. Ernst, and L. Desvignes, *Beyond macrophages: the diversity of mononuclear cells in tuberculosis*. Immunol Rev, 2014. **262**(1): p. 179-92.
59. Cambier, C.J., S. Falkow, and L. Ramakrishnan, *Host evasion and exploitation schemes of Mycobacterium tuberculosis*. Cell, 2014. **159**(7): p. 1497-509.
60. Russell, D.G., *Mycobacterium tuberculosis and the intimate discourse of a chronic infection*. Immunological reviews, 2011. **240**(1): p. 252-268.
61. Clay, H., et al., *Dichotomous role of the macrophage in early Mycobacterium marinum infection of the zebrafish*. Cell Host Microbe, 2007. **2**(1): p. 29-39.
62. Olivares-Morales, M.J., et al., *Glucocorticoids Impair Phagocytosis and Inflammatory Response Against Crohn's Disease-Associated Adherent-Invasive Escherichia coli*. Frontiers in Immunology, 2018. **9**.
63. Jessop, J., B. Vernon-Roberts, and J. Harris, *Effects of gold salts and prednisolone on inflammatory cells. I. Phagocytic activity of macrophages and polymorphs in inflammatory exudates studied by a "skin-window" technique in rheumatoid and control patients*. Annals of the rheumatic diseases, 1973. **32**(4): p. 294.
64. Vernon-Roberts, B., J. Jessop, and J. Dore, *Effects of gold salts and prednisolone on inflammatory cells. II. Suppression of inflammation and phagocytosis in the rat*. Annals of the rheumatic diseases, 1973. **32**(4): p. 301.
65. Taylor, A., et al., *Defective macrophage phagocytosis of bacteria in COPD*. European Respiratory Journal, 2010. **35**(5): p. 1039-1047.
66. van der Goes, A., et al., *Dexamethasone promotes phagocytosis and bacterial killing by human monocytes/macrophages in vitro*. Journal of leukocyte biology, 2000. **67**(6): p. 801-807.
67. McColl, A., et al., *Glucocorticoids induce protein S-dependent phagocytosis of apoptotic neutrophils by human macrophages*. J Immunol, 2009. **183**(3): p. 2167-75.
68. Liu, Y., et al., *Glucocorticoids Promote Nonphlogistic Phagocytosis of Apoptotic Leukocytes*. The Journal of Immunology, 1999. **162**(6): p. 3639-3646.
69. Zahuczky, G., et al., *Differentiation and Glucocorticoid Regulated Apopto-Phagocytic Gene Expression Patterns in Human Macrophages. Role of Mertk in Enhanced Phagocytosis*. PLOS ONE, 2011. **6**(6): p. e21349.
70. McCubbrey, A.L., et al., *Glucocorticoids relieve collectin-driven suppression of apoptotic cell uptake in murine alveolar macrophages through downregulation of SIRP α* . The Journal of Immunology, 2012. **189**(1): p. 112-119.
71. Ehrchen, J.M., J. Roth, and K. Barczyk-Kahlert, *More Than Suppression: Glucocorticoid Action on Monocytes and Macrophages*. Front Immunol, 2019. **10**: p. 2028.
72. Busillo, J.M. and J.A. Cidlowski, *The five Rs of glucocorticoid action during inflammation: ready, reinforce, repress, resolve, and restore*. Trends Endocrinol Metab, 2013. **24**(3): p. 109-19.
73. Lesley, R. and L. Ramakrishnan, *Insights into early mycobacterial pathogenesis from the zebrafish*. Curr Opin Microbiol, 2008. **11**(3): p. 277-83.
74. Lewis, K.N., et al., *Deletion of RD1 from Mycobacterium tuberculosis mimics bacille Calmette-Guerin attenuation*. J Infect Dis, 2003. **187**(1): p. 117-23.
75. Gräb, J., et al., *Corticosteroids inhibit Mycobacterium tuberculosis-induced necrotic host cell death by abrogating mitochondrial membrane permeability transition*. Nature communications, 2019. **10**(1): p. 1-14.

76. Bernut, A., et al., *Mycobacterium abscessus* cording prevents phagocytosis and promotes abscess formation. *Proceedings of the National Academy of Sciences*, 2014. **111**(10): p. E943-E952.
77. Ellett, F., et al., *mpeg1* promoter transgenes direct macrophage-lineage expression in zebrafish. *Blood*, 2011. **117**(4): p. e49-e56.
78. Takaki, K., et al., *Evaluation of the pathogenesis and treatment of Mycobacterium marinum infection in zebrafish*. *Nature protocols*, 2013. **8**(6): p. 1114.
79. Ramakrishnan, L. and S. Falkow, *Mycobacterium marinum* persists in cultured mammalian cells in a temperature-restricted fashion. *Infection and Immunity*, 1994. **62**(8): p. 3222-3229.
80. Cosma, C.L., et al., *Mycobacterium marinum* Erp is a virulence determinant required for cell wall integrity and intracellular survival. *Infection and immunity*, 2006. **74**(6): p. 3125-3133.
81. Burton, N.A., et al., *Disparate impact of oxidative host defenses determines the fate of Salmonella during systemic infection in mice*. *Cell host & microbe*, 2014. **15**(1): p. 72-83.
82. Hoiseth, S.K. and B. Stocker, *Aromatic-dependent Salmonella typhimurium are non-virulent and effective as live vaccines*. *Nature*, 1981. **291**(5812): p. 238-239.
83. Benard, E.L., et al., *Infection of zebrafish embryos with intracellular bacterial pathogens*. *J Vis Exp*, 2012(61).
84. Zakrzewska, A., et al., *Macrophage-specific gene functions in Spi1-directed innate immunity*. *Blood*, 2010. **116**(3): p. e1-11.
85. Rougeot, J., et al., *RNA sequencing of FACS-sorted immune cell populations from zebrafish infection models to identify cell specific responses to intracellular pathogens*. *Methods Mol Biol*, 2014. **1197**: p. 261-74.
86. Stasinopoulos, D.M. and R.A. Rigby, *Generalized additive models for location scale and shape (GAMLSS) in R*. *Journal of Statistical Software*, 2007. **23**(7): p. 1-46.

Supplementary material

Supplementary Table 1. Sequences of Primers used in qPCR reactions.

Gene name	Gene accession	Sequence (5'-3')
<i>ppiab</i>	ENSDARG00000103994	Fw: CATCCACAACCTTCCCGAACAC Rv: ACACTGAAACACGGAGGCAAAG
<i>tnfa</i>	ENSDARG00000009511	Fw: ACCAGGCCTTTTCTTCAGGT Rv: TTTGCCTCCGTAGGATTCAG
<i>sparcl1</i>	ENSDARG00000074989	Fw: AACGAGGCTGAGAGCAAGGA Rv: GCTGTGGCTGTGGGGATTAC
<i>uchl1</i>	ENSDARG00000026871	Fw: GGCCAACAACCAGGACAGTA Rv: CCTCATCAGCAACAGCATCA
<i>ube2v1</i>	ENSDARG00000041875	Fw: GGTCAGAAGGGTGTGGAGA Rv: TCGTCACAAAACGGACAAAA
<i>marcksa</i>	ENSDARG00000004049	Fw: ATGAAGCCAAGACGGATGGA Rv: GCCACTGCTGGCTCAGTTTT
<i>marcksb</i>	ENSDARG00000008803	Fw: CAAGCTGAGCGGTTTCTCCT Rv: CCTCGGGTTCAGCATCTTC
<i>bsg</i>	ENSDARG00000019881	Fw: ATCAAGAGCACCCCAACAA Rv: CACTGGTGCCTTGACTGG
<i>tubb5</i>	ENSDARG00000037997	Fw: CAAACTCACCACCCCCACAT Rv: GCTTGTGAGAGGAGCGAAGC

Chapter 5

Liposome encapsulation of prednisolone phosphate improves its therapeutic ratio in a zebrafish model for inflammation

Yufei Xie, Panagiota Papadopoulou, Björn de Wit, Jan C. d'Engelbronner, Patrick van Hage, Fred Campbell, Alexander Kros, Marcel J.M. Schaaf

Abstract

Glucocorticoids (GCs) are effective anti-inflammatory drugs, but their clinical use is limited by the severity of their side effects. Using liposomes to deliver GCs at inflammatory sites in the body is a promising approach to improve the therapeutic ratio of these drugs. In this study, we demonstrate that zebrafish embryos provide a useful tool to determine the therapeutic effects and possible side effects of liposomal formulations of GCs. We used a wound-induced inflammation model to investigate liposome encapsulation of the GC prednisolone phosphate (PLP). First, we studied the biodistribution of liposomes with different formulations. Our results showed that macrophage-targeting liposomes composed of 20% 1,2-distearoyl-*sn*-glycero-3-phospho-*rac*-(1-glycerol) (DSPG), 50% 1,2-dioleoyl-*sn*-glycero-3-phosphocholine (DOPC) and 30% cholesterol accumulated in macrophages, whereas PEGylated liposomes (with polyethylene glycol (PEG) polymers on their surface) remained in circulation for longer periods of time without being scavenged. Upon laser wounding of the tail, accumulation near the wounding site was observed for both liposomes. Furthermore, encapsulation of PLP in the macrophage-targeting and the PEGylated liposomes increased the potency of its inhibition of the migration of neutrophils towards the wound. In contrast, encapsulation of PLP in either type of liposome reduced its inhibitory effects on tail fin regeneration, and encapsulation in the PEGylated liposome attenuated the activation of glucocorticoid responsive reporter genes throughout the body. In conclusion, using a zebrafish model for inflammation we have shown that encapsulation of PLP in liposomes enhances its anti-inflammatory effects and decreases undesired effects in the rest of the body and the regeneration of the affected tissue.

Introduction

Glucocorticoids (GCs) are a class of steroid hormones secreted by the adrenal gland. Due to their potent anti-inflammatory effects, synthetic GCs are widely prescribed for treating immune-related diseases, such as asthma, rheumatoid arthritis (RA), dermatitis and several autoimmune diseases [1, 2]. Through activation of an intracellular receptor, the glucocorticoid receptor (GR), GCs regulate a wide variety of systems in our body, including the immune system, metabolism, bone formation and central nervous system, leading to side effects such as infectious diseases, diabetes, osteoporosis and depression, which severely limits the clinical use of these widely prescribed anti-inflammatory drugs [3]. Using local administration approaches, such as intra-articular injection, inhalation and topical treatment, these side effects could be alleviated to some extent, but these methods are applicable for only a limited number of diseases [4].

Using nanoparticles to achieve targeted delivery of drugs is a promising approach to increase the specificity of a drug and reduce its side effects since it may enable the use of lower therapeutic doses [5, 6]. There are two major types of targeted delivery approaches: active targeting and passive targeting. Active targeting is generally achieved by modifying the surface of the particles with specific targeting molecules, such as antibodies, peptides, or carbohydrates, which may be recognized by antigens or other molecules on the membranes of specific cells so the drugs can be released at a desired location [6]. The surface of passive targeting nanoparticles is generally not altered with targeting molecules. The targeting could be dependent on the enhanced permeation and retention (EPR) effect which is observed in tumors and inflammatory sites due to the locally increased permeability of the vasculature [7]. The uptake by migratory phagocytes like macrophages which are recruited by an inflamed tissues may also contribute to the targeting. The efficacy and specificity of targeting may be influenced by several physicochemical properties of the nanoparticles, including the size, shape, surface charge, composition and surface modification [8-10].

Liposomes are spherical vesicles composed of lipids and widely used to deliver therapeutic molecules, of which the composition can be manipulated easily [11, 12]. One frequently studied formulation of passive targeting liposomes uses phospholipids linked to a polymer polyethylene glycol (PEG) chain [13, 14]. The PEGylation prevents the liposome from being recognized by serum proteins such as complement proteins, immunoglobulins and non-immune opsonins, thereby avoiding opsonization and clearance, thus, increasing the half-life in the circulation [15]. A lot of efforts have been made to explore PEGylated liposome-encapsulated GCs. One widely investigated formulation is using PEG2000-DSPE, DPPC and cholesterol for liposome assembly, and the water-soluble GC prednisolone phosphate (PLP) as the loaded drug [16, 17]. In a rodent model of RA, the PEGylated liposome-encapsulated PLP remained in the circulation longer than free PLP and accumulated in the inflamed joints, resulting in enhanced therapeutic effects compared to free PLP [16, 18].

Similar results were obtained using other rodent models for inflammation-related diseases such as atherosclerosis [19], multiple sclerosis [13] and cancer [20]. Attempts to improve the therapeutic effects include using different synthetic GCs [21-23], conjugation with targeting molecules [24-27], optimization of formulation [28, 29] and co-treatment with anti-tumor drugs [30]. However, obstacles still exist, such as unwanted off-target accumulation in spleen, liver and kidney [18, 31], a certain level of GCs-induced side effects [22, 23], and an unexpected lack of anti-inflammatory effect when applied clinically [32]. Therefore, novel tools are needed, which can be used for rapid screening of the biodistribution, therapeutic effects and side effects of different liposomal formulations of GC drugs.

Macrophages are critical components of the inflammatory response and represent one of the target cells for the treatment of inflammatory diseases. Macrophage targeting can be achieved by modifying the surface of nanoparticles with targeting molecules such as folate, which can be recognized by overexpressed folic acid receptor (FR) in tumor-associated macrophages [33, 34], or mannose residues, which interact with the mannose receptor mainly present on the surface of macrophages [35, 36], or anti-CD163 antibodies, which target CD163 positive macrophages [37, 38]. Moreover, targeted delivery of GCs to macrophages has also been reported by using inorganic-organic hybrid nanoparticles, which were preferentially taken up by macrophages and showed full therapeutic efficacy in a mouse multiple sclerosis model [39].

Over the last decades, the zebrafish has emerged as a useful *in vivo* model for biomedical research, complementary to rodent models due to several characteristics, such as their short generation time, small size, and optical transparency. In addition, the sequencing of the zebrafish genome [40], the availability of various genetic tools [41] and their well-conserved immune system [42] have contributed to the popularity of this animal model. Due to the similarity of the GC signaling pathway between humans and zebrafish, the zebrafish model is highly suitable for studying the effects and mechanisms of GC action *in vivo*, particularly their anti-inflammatory effects [43-45]. Recently, the zebrafish has been used for studies on liposomal drug delivery. In these studies, zebrafish embryos were utilized to determine the biodistribution of fluorescently labeled liposomes with different formulations and to unravel the mechanisms underlying their uptake in specific cell types [46, 47].

In the present study, we have used the zebrafish embryo as a model system to study the biodistribution of liposomes, and their possible use for improving the therapeutic ratio of GC drugs. A new macrophage-targeting liposome formulation was generated and this liposome was shown to behave differently from a PEGylated liposome, although both of them were shown to accumulate at sites of inflammation. In addition, we demonstrate that the encapsulation of PLP in both the macrophage-targeting and the PEGylated liposomes enhances the anti-inflammatory effects of the GC, whereas it decreases possible adverse effects.

Results

Optimization and characterization of macrophage-targeting liposomes

In order to optimize the formulation of macrophage-targeting liposomes, fluorescently labeled liposome formulations were prepared with different ratios of the anionic phospholipid 1,2-distearoyl-*sn*-glycero-3-phospho-*rac*-(1-glycerol) (DSPG) and cholesterol (10:40%, 15:35%, 20:30%, 25:25%, 30:20%), combined with 50% of the neutrally charged, non-saturated 1,2-dioleoyl-*sn*-glycero-3-

phosphocholine (DOPC). This formulation originates from a marketed liposomal product (AmBisome), which is composed of DSPG, cholesterol and 1,2-distearoyl-*sn*-glycero-3-phosphocholine (DSPC) (ratio 21:26:53), and used for treating fungal infections [48, 49]. In preliminary studies, it was found that replacing the saturated phospholipid DSPC with the unsaturated DOPC, macrophage targeting of the liposome was observed in zebrafish embryos (unpublished data).

The liposomes with different DSPG:cholesterol:DOPC ratios were injected intravenously in 2 days post fertilization (dpf) zebrafish embryos from the *Tg(mpeg1:GFP)* line, in which the macrophages are fluorescently labeled. At 2 hours post injection (hpi), confocal microscopy images were taken to study the biodistribution of the liposomes, and representative images are shown in Figure 1A-F. Using the images, we quantitated the number and percentage of macrophages that contained liposomes. The results show that a higher percentage of DSPG in the liposome formulation increases the macrophage targeting efficiency of the liposomes (Figure 1G,H). Simultaneously, we observed association of liposomes with endothelial cells (ECs) of the posterior cardinal vein (PCV), the caudal vein (CV) and the caudal hematopoietic tissue area (CHT). To quantitate this effect, we determined the ratio between the signal in the region encompassing the CHT and CV and the region dorsally from this area, which showed that increasing the DSPG percentage to 25% enhanced targeting of the liposomes to the region encompassing the CHT and CV (Figure 1I). The uptake of liposomes by cells in this region is considered an off-target accumulation, since the endothelial cells (ECs) in this area have been shown to be a functional equivalent of the liver sinusoidal/scavenger endothelial cells (LSECs) in mammals [47]. The total number of macrophages in the embryonic body is not significantly influenced by the variation in DSPG percentages (Supplementary Figure 1A). After comparing the biodistribution of the different liposomes, the 20% DSPG liposome was considered as the optimal formulation since it displays the highest ratio between macrophage targeting and CHT localization.

To characterize the behavior of the 20% DSPG liposomes in further detail, we injected these liposomes in embryos at different ages (1, 2 and 3 dpf), and imaged their biodistribution two hours after the injection (Figure 2A-F). From the images, we quantified the number and percentage of macrophages that contained liposomes. The macrophage targeting property of the 20% DSPG liposome was observed at all ages. After injection at 1 and 2 dpf, around 64% of the macrophages had taken up liposomes (with a lower absolute number of macrophages at 1 dpf), and at 3 dpf approximately 35% of all macrophages contained liposomes. (Figure 2I-J, Supplementary Figure 1B). For comparison, PEGylated liposomes (formulation: DPPC(62%)/PEG-DSPE(5%)/cholesterol(33%)) were injected in 3 dpf embryos. In contrast to the 20% DSPG liposomes, we observed that PEGylated liposomes remained freely circulating in the vasculature, and were not taken up by macrophages (Figure 2G-H), which was reflected in a significantly lower percentage of the macrophages containing PEGylated liposomes

(approximately 6%, Figure 2I-J). No difference in the total macrophage number was observed between larvae injected with 20% DSPG and PEGylated liposomes at 3 dpf (Supplementary Figure 1B). In addition, liposomes containing PLP behaved similarly to empty liposomes (Supplementary Figure 2).

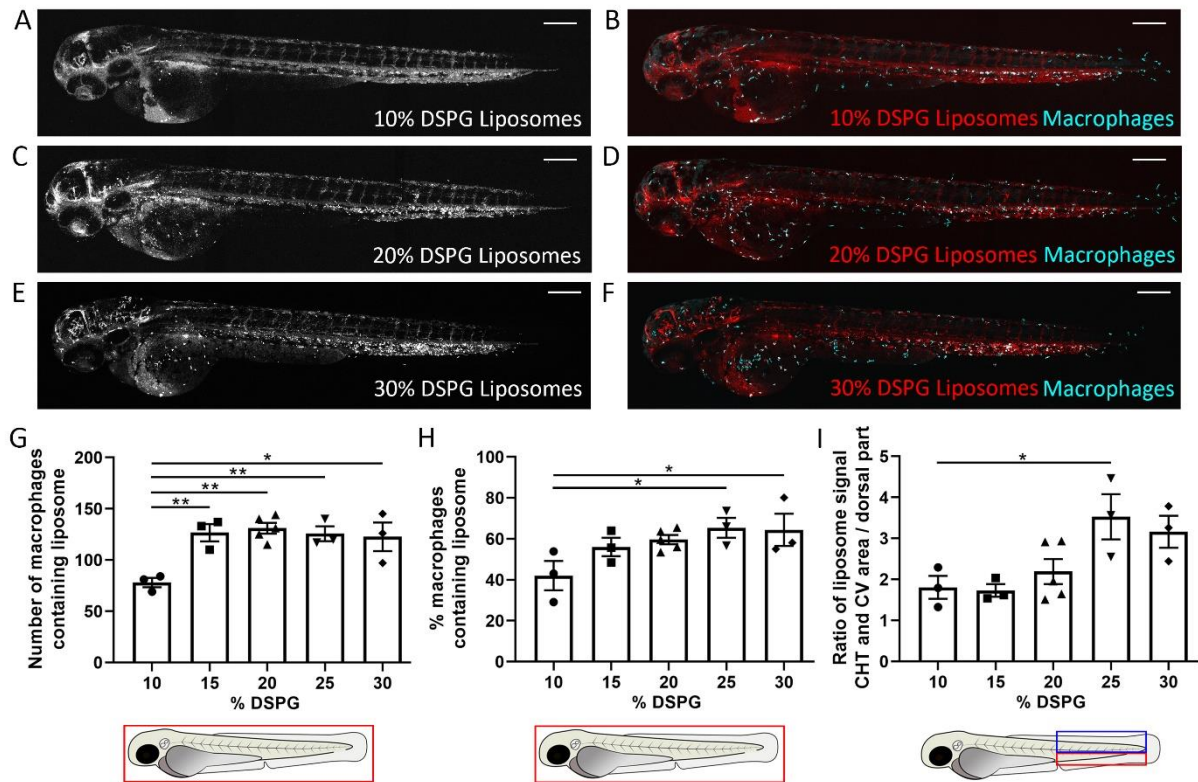


Figure 1. Biodistribution of macrophage-targeting liposomes with different formulations in zebrafish embryos.

A-F. Representative images of *Tg(mpeg1:GFP)* embryos injected with liposomes containing different percentages of DSPG at 2 days post fertilization (dpf). Confocal microscopy images were taken at 2 hours post injection (hpi). Liposomes are shown in red and macrophages in cyan (B,D,F). Scale bar = 200 μ m. G-H. The number (G) and percentage (H) of macrophages containing liposomes quantified in the whole body. A significant difference was observed for the number of macrophages containing liposomes with DSPG percentages of 15% to 30% compared to 10%. For the percentage of macrophages containing liposomes, a significant difference was observed for the 25% and 30% DSPG liposomes compared to the 10% DSPG liposome. I. The ratio between the (fluorescent) signal of liposomes in the area, indicated by the red box, encompassing the caudal vein (CV) and the caudal hematopoietic tissue (CHT) and the signal in the dorsal part of the tail (indicated by the blue box). A significant difference was observed between injection with 25% DSPG liposomes compared to 10% DSPG liposomes. Statistical analysis was performed by one-way ANOVA with Bonferroni's post hoc test. Data shown are the means \pm s.e.m. of 3-5 individual embryos, of which the individual data are indicated. Statistically significant differences between groups are indicated by: * $p < 0.05$; ** $p < 0.01$.

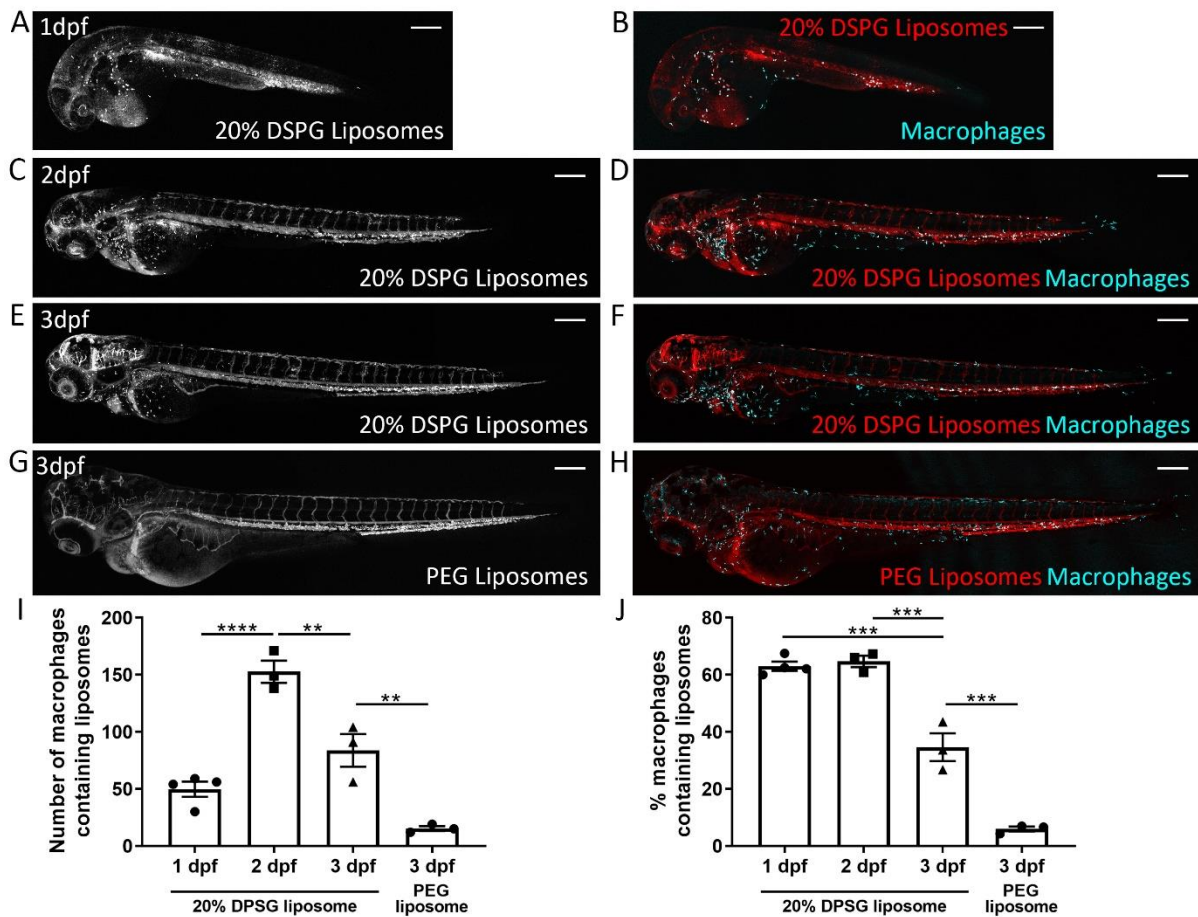


Figure 2. Biodistribution of liposomes in zebrafish embryos at different stages of development. A-H. Representative images of embryos of the *Tg(mpeg1:GFP)* line injected with 20% DSPG liposomes at 1 (A), 2 (B) or 3 dpf (C) or with PEGylated liposomes at 3 dpf (D). Confocal microscopy images were taken at 2 hpi. Liposomes are shown in red and macrophages in cyan (B,D,F,H). Scale bar = 200 μ m. I-J. The number (I) and percentage (J) of macrophages containing liposomes quantified in the whole body of embryos injected with 20% DSPG liposomes at 1, 2 or 3 dpf or with PEGylated liposomes at 3 dpf. Statistical analysis by one-way ANOVA showed a significantly lower number and percentage of macrophages containing liposomes when injected with PEGylated liposomes at 3 dpf, compared to injection with 20% DSPG liposomes. Upon injection with 20% DSPG liposomes, at 1 and 3 dpf significantly lower numbers of macrophages containing liposomes were observed than at 2 dpf. Embryos at 3 dpf showed significantly lower percentages of macrophages containing liposomes compared to embryos at 1 and 2 dpf. Data shown are the means \pm s.e.m. of 3-4 individual embryos, of which the individual data are indicated. Statistically significant differences between groups are indicated by: ** $p < 0.01$; *** $p < 0.001$; **** $p < 0.0001$.

Biodistribution of liposomes upon laser wounding

To study targeting of liposomes towards an inflammatory site, we damaged the tail of 3 dpf embryos from the *Tg(mpeg1:GFP)* line by laser irradiation (Figure 3A), and injected different fluorescently labeled liposomes (20% DSPG or PEGylated) immediately after the laser wounding. Confocal microscopy images were taken at 4 hours post wounding (hpw). In all images, accumulation of macrophages was observed near the wounded area (Figure 3B-E). In the embryos injected with the 20% DSPG liposomes, most of these macrophages that had accumulated near the wounded area contained liposomes (Figure 3B,C). In the embryos injected with PEGylated liposomes, most of the macrophages near the wound site did not contain any liposomes, but accumulation of liposomes was observed in the wounded area with a diffuse pattern (Figure 3D). As a control for the integrity of the vascular system, the polysaccharide dextran (2,000,000 MW) was injected. No accumulation of dextran was observed near the wounded site (Figure 3E), suggesting that the accumulation of the PEGylated liposomes is not caused by local damage to the vascular system but is due to the inflammation-induced change in vesicle permeability. When we quantitated the percentages of macrophages containing liposomes in the area near the laser wound, we again found a very low percentage ($3.2 \pm 2.0\%$) in embryos injected with PEGylated liposomes, and a higher percentage ($39.0 \pm 5.2\%$) in the 20% DSPG liposome injected embryos (Figure 3F).

Effect of PLP and encapsulated PLP on wounding-induced neutrophil migration

Since it has been shown that macrophage migration towards a wounded site is not affected by GC treatment in zebrafish, but that the neutrophil migration is inhibited [50, 51], we used the accumulation of neutrophils at the wounded area as a readout for the anti-inflammatory effect of PLP. For this purpose, we applied laser wounding in 3 dpf embryos from the *Tg(mpx:GFP)* line, in which neutrophils are fluorescently labeled. At different time points after the wounding, fluorescence microscopy images were taken and the neutrophil accumulation in a defined area of the tail was quantitated (Figure 4A-B). The results showed that laser wounding induced a rapid increase in the number of accumulated neutrophils at early time points (from 0 to 4 hpw) and then the number decreased gradually between 4 and 24 after wounding (Supplementary Figure 3). Subsequently, using the number of neutrophils at the site of laser injury at 4 hpw as a readout, we studied the anti-inflammatory effect of free PLP and liposome-encapsulated PLP. Injection of free PLP (0.04, 0.2, 1, 5 and 25 pmol per embryo) resulted in a dose-dependent inhibition of the neutrophil migration, with a significant inhibitory effect observed for the 5 and 25 pmol doses ($23.4 \pm 3.6\%$ and $30.9 \pm 4.2\%$ inhibition respectively) (Figure 4C). Injection of PLP encapsulated in 20% DSPG liposomes (at doses of 0.04, 0.2 and 1 pmol) also inhibited neutrophil migration dose-dependently, and showed a significant inhibition

already at a dose of 0.2 pmol ($21.0 \pm 4.7\%$) (Figure 4D). Injection of PLP encapsulated in PEGylated liposomes resulted in a significant inhibition only at the 1 pmol dose ($21.4 \pm 6.0\%$) (Figure 4E). These results indicate that PLP shows a more potent anti-inflammatory effect when encapsulated in a liposome, with the 20% DSPG liposome showing a slightly higher potency than the PEGylated liposome.

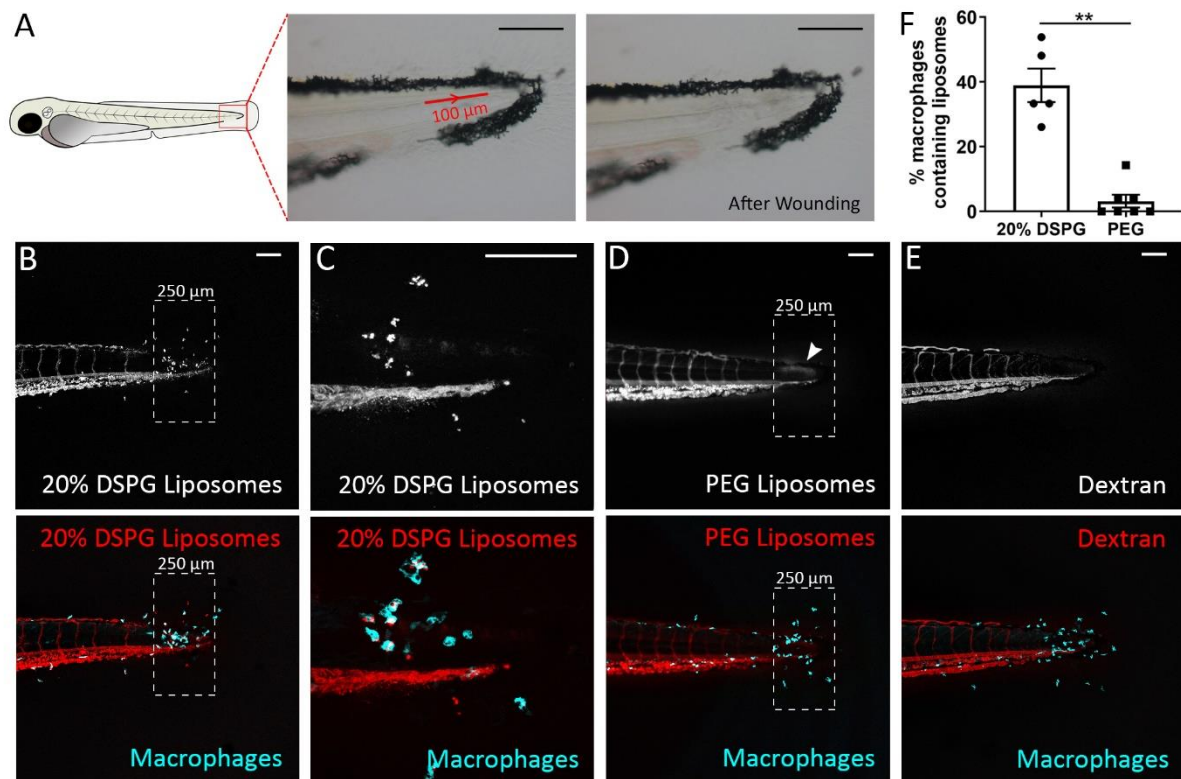


Figure 3. Laser wounding in zebrafish embryos and the subsequent accumulation of liposomes at the wounded site. A. Schematic drawing of a zebrafish embryo at 3 dpf, and brightfield microscopy images showing the position and size of the area exposed to laser irradiation (red line with arrow indicating the direction of laser) and the damaged tissue after the laser wounding procedure. B-E. Representative confocal microscopy images of tail regions from 3 dpf embryos of the *Tg(mpeg1:GFP)* line, subjected to laser wounding and injected with 20% DSPG liposomes (B and C, with C at a higher magnification), PEGylated liposomes (D), or dextran (2,000,000 MW, E). The dashed box indicates the area where damage and accumulation of neutrophils were seen. The white arrowhead indicates the accumulation of PEG liposomes (D). Images were taken at 4 hours post wounding (hpw). The dashed box shows the area of quantification. Liposomes are shown in red and macrophages in cyan. Scale bar = 100 μm . F. The percentage of macrophages containing liposomes in the area near the laser wound (dashed box), in embryos injected with 20% DSPG or PEGylated liposomes. Statistical analysis by two-tailed t-test showed a significantly higher percentage of macrophages containing liposomes upon injection with 20% DSPG liposomes. Data shown are the means \pm s.e.m. of 5-7 individual embryos, of which the individual data are indicated. Statistically significant differences between groups are indicated by: ** $p < 0.01$.

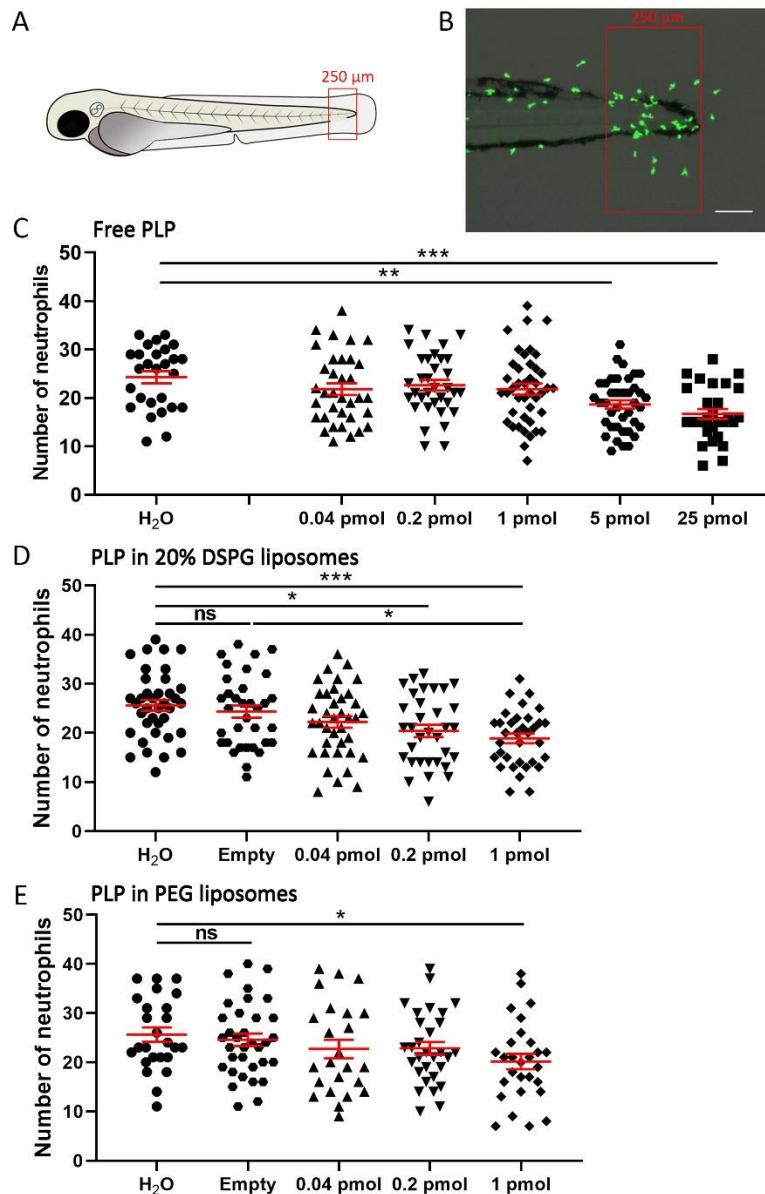


Figure 4. Effect of free and liposome-encapsulated PLP on neutrophil recruitment upon laser wounding.

Tg(mpx:GFP) embryos (at 3 dpf) were subjected to the laser wounding procedure and injected with different doses of free or liposome-encapsulated PLP, and fluorescence microscopy images were taken at 4 hpw. A. Schematic drawing of a zebrafish embryo at 3 dpf indicating the area in which the recruited neutrophils were counted (red box). B. Representative image showing the accumulation of neutrophils (green) near the wound. Scale bar = 100 μm . C-E. The number of neutrophils recruited to the wounded area at 4 hpw are shown after injection of different doses of free PLP (C), PLP encapsulated in 20% DSPG liposomes (D) and PLP encapsulated in PEGylated liposomes (E). H₂O and empty liposomes were injected as control. Statistical analysis was performed by one-way ANOVA with Bonferroni's post hoc test. A significant inhibition of the neutrophil migration was observed when embryos had been injected with 5 or 25 pmol of free PLP, 0.2 or 1 pmol of PLP encapsulated in 20% DSPG liposomes and 1 pmol of PLP encapsulated in PEGylated liposomes. Each data point represents a single embryo and the means \pm s.e.m. of data accumulated from three independent experiments are shown in red. Statistically significant differences between groups are indicated by: ns, non-significant; * $p < 0.05$; ** $p < 0.01$; *** $p < 0.001$.

Effects of PLP and encapsulated PLP on tissue regeneration and transactivation

To develop novel anti-inflammatory GC therapies, it is important to study possible side effects of the treatment as well. In this study, we first investigated the effect of free PLP and encapsulated PLP on tissue regeneration. We performed tail fin amputation on 2 dpf embryos (Figure 5A) and injected the amputated embryos with different doses of free PLP or liposome-encapsulated PLP immediately after the amputation. The length of the regenerated tail fin was measured at 36 hour post amputation (hpa). Free PLP showed a significant inhibitory effect on regeneration at all doses tested (from 0.04 pmol ($3.4\pm 1.0\%$) to 25 pmol ($30.5\pm 3.1\%$)) and this effect was dose-dependent (Figure 5B,E). For PLP encapsulated in 20% DSPG liposomes, a significant inhibition was observed when the injected dose was 1 pmol ($5.7\pm 1.4\%$), but not at lower doses (0.04 pmol and 0.2 pmol) (Figure 5C). When the embryos were injected with PLP encapsulated in PEGylated liposomes, no significant effect of the treatment was observed (Figure 5D). These results indicate that encapsulation of PLP in liposomes decreases the inhibitory effect of PLP on regeneration, showing even an absence of inhibition for the PEGylated liposomes at the doses tested.

Subsequently, we studied the effect of free and liposome-encapsulated PLP on the transactivation of a glucocorticoid response element (GRE)-containing promoter. For this purpose, we used the *Tg(9xGRE-HSV.U123:EGFP)* reporter line, in which the EGFP gene is driven by a GRE-containing promoter. This way, we were able to quantify the systemic induction of the transactivation properties of the Gr by the GC treatment, by quantitating the EGFP signal throughout the embryonic body. Embryos were injected with free PLP and liposome-encapsulated PLP at 3 dpf, and fluorescence microscopy images were taken at 24 hpi. The quantitated EGFP signals showed that both free and liposome-encapsulated PLP induced significant dose-dependent increases in the level of GFP expression (Figure 6). However, for free PLP a significant increase was already observed at a dose of 0.2 pmol ($26.1\pm 2.6\%$), whereas for both the 20% DSPG and the PEGylated liposome-encapsulated treatments a significant increase was only observed for the 1 pmol dose ($44.5\pm 3.4\%$ and $6.2\pm 3.1\%$ respectively). These data demonstrate that liposome encapsulation decreases the potency of PLP to induce the transactivation activity of the Gr throughout the body of zebrafish embryos.

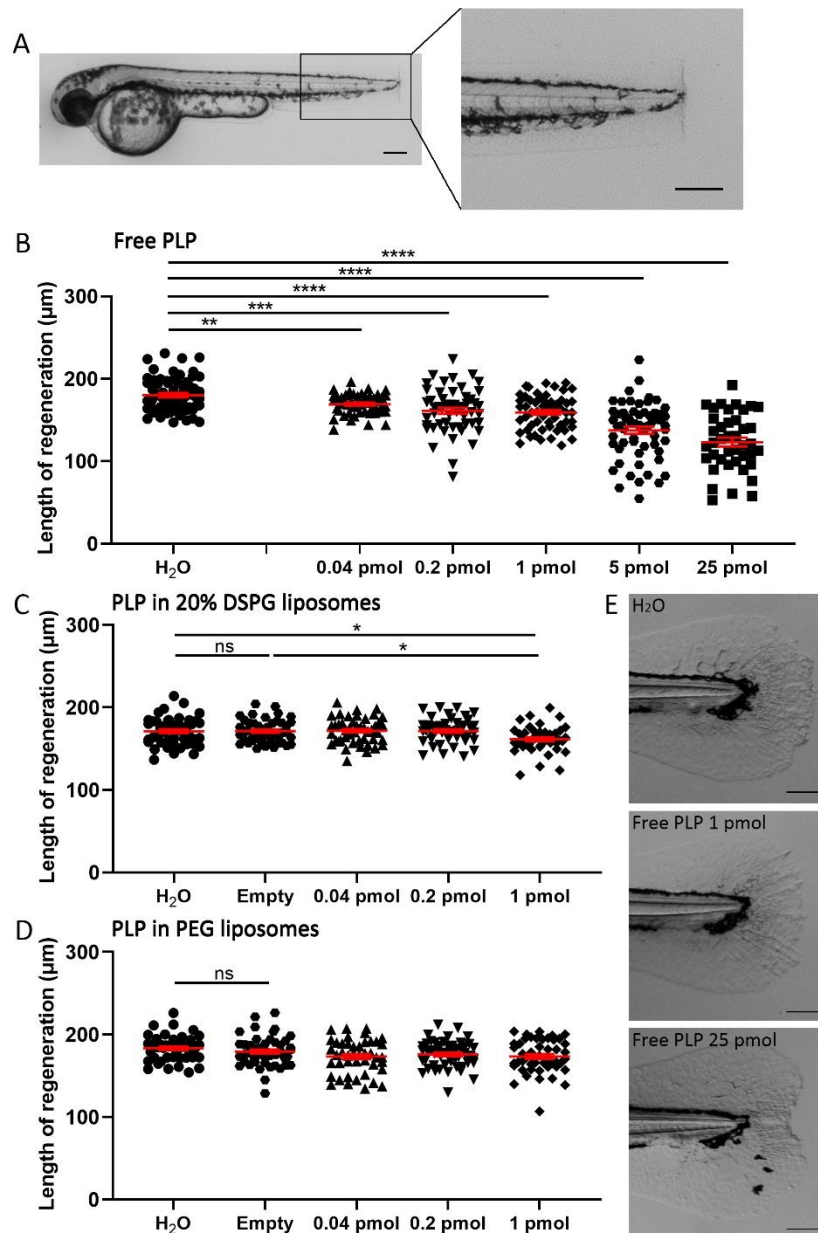


Figure 5. Effect of free and liposome-encapsulated PLP on regeneration of the tail fin after amputation. Embryos (at 2 dpf) were subjected to the tail fin amputation procedure and injected with different doses of free or liposome-encapsulated PLP. **A.** Representative image of a 2dpf zebrafish embryo immediately after amputation, showing the position of the amputated part of the tail fin. Scale bar = 200 µm. **B-D.** The length of the regenerated tail fin, measured at 36 hour post amputation (hpa), are shown after injection of different doses of free PLP (**B**), PLP encapsulated in 20% DSPG liposomes (**C**) and PLP encapsulated in PEGylated liposomes (**D**). H₂O and empty liposomes were injected as control. Statistical analysis was performed by one-way ANOVA with Bonferroni's post hoc test. Significant inhibition of the tail fin regeneration was observed when embryos had been injected with 0.04-25 pmol of free PLP or 1 pmol of PLP encapsulated in 20% DSPG liposomes. No significant inhibition was observed after injection with PLP encapsulated in PEGylated liposomes. Each data point represents a single embryo and the means ± s.e.m. of data accumulated from three independent experiments are shown in red. Statistically significant differences between groups are indicated by: ns, non-significant; * p<0.05; ** p<0.01; *** p<0.001; **** p<0.0001. **E.** Representative images of regenerated tail fins at 36 hpa for embryos injected with H₂O, 1 pmol PLP or 25 pmol PLP. Scale bar = 100 µm.

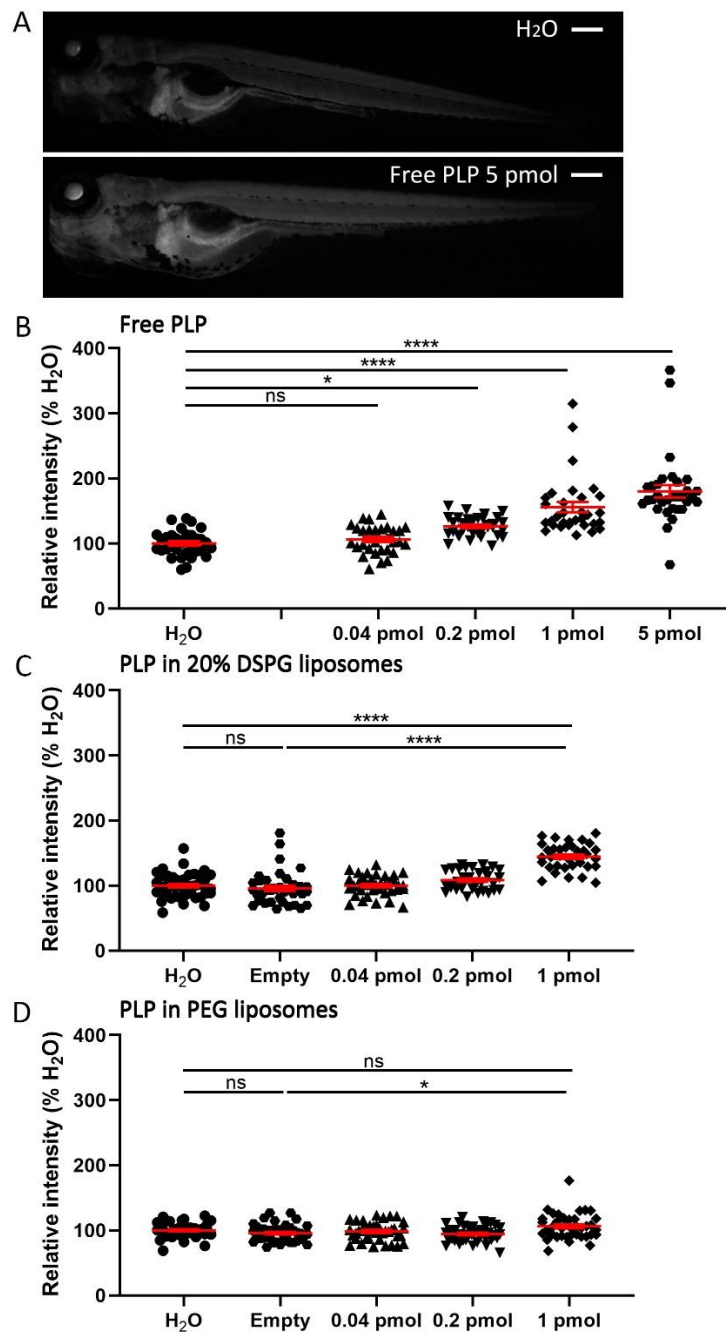


Figure 6. Effect of free and liposome-encapsulated PLP on the systemic Gr transactivation activity. Embryos (3 dpf) of the *Tg(GRE:GFP)* line were injected with free or liposome-encapsulated PLP and fluorescence microscopy images were taken at 24 hpi. A. Representative images of *Tg(GRE:GFP)* embryos injected with H₂O or 5 pmol PLP, showing the GFP signal which is a readout for the transactivation activity of Gr, which is increased after PLP injection. Scale bar = 200 μ m. B-C. The quantified GFP signals in the *Tg(GRE:GFP)* embryos at 24 hpi are shown after injection of different doses of free PLP (B), PLP encapsulated in 20% DSPG liposomes (C) and PLP encapsulated in PEGylated liposomes (D). H₂O and empty liposome were injected as control. Statistical analysis was performed by one-way ANOVA with Bonferroni's post hoc test. Significant increases in the GFP signal were observed when embryos had been injected with 0.2-5 pmol free PLP, and 1 pmol of PLP encapsulated in either 20% DSPG liposomes or in PEGylated liposomes. Each data point represents a single embryo and the means \pm s.e.m. of data accumulated from three independent experiments are shown in red. Statistically significant differences between groups are indicated by: ns, non-significant; * $p < 0.05$; **** $p < 0.0001$.

Finally, we compared all observed effects of the 1 pmol dose of free PLP and PLP encapsulated in 20% DSPG and PEGylated liposomes (Table 1). We used the ratio of the effect on neutrophil migration and the effect on regeneration or transactivation as a readout for the therapeutic ratio of the different PLP formulations. The results showed that when considering the effect on regeneration, encapsulation in 20% DSPG liposomes results in a ratio (4.707) comparable to that observed for PEGylated liposomes (4.040), which both are considerably higher than the ratio observed for free PLP (0.901). For both types of liposome, this difference with free PLP was due to both a larger inhibition of the neutrophil migration and a smaller inhibition of the regeneration. When we determined the ratio between the effect on neutrophil migration and the effect on transactivation, a higher ratio was observed for the PEGylated liposome (3.453) than for the 20% DSPG liposome (0.603), which was only slightly higher than the ratio observed for free PLP (0.177). This difference between the two types of liposomes was due to the fact that PLP in the 20% DSPG liposome had a considerably higher effect on transactivation, comparable to free PLP. In conclusion, our zebrafish model was demonstrated to be a useful model for assessing the therapeutic ratio of novel liposomal GC formulations.

Table 1. Ratio between the therapeutic effect and side effects of 1 pmol PLP treatment

Treatment	Inhibition of neutrophil migration (%) ¹		Inhibition of neutrophil migration (%)	
	Inhibition of regeneration (%)		Increase in transactivation (%)	
Free PLP	0.901	(9.8/10.9)	0.177	(9.8/55.6)
PLP in 20% DSPG liposome	4.707	(26.8/5.7)	0.603	(26.8/44.5)
PLP in PEGylated liposome	4.040	(21.4/5.3)	3.453	(21.4/6.2)

¹All effects are determined as percentage difference relative to the H₂O treatment (absolute values are shown in Figs. 4-6)

Discussion

In the present study, we have used the zebrafish embryo model to study liposomal drug targeting *in vivo*. This model enabled us to investigate the biodistribution of liposomes and to determine the anti-inflammatory effect and possible adverse effects of the glucocorticoid drug PLP encapsulated in liposomes. Our results showed that PEGylated liposomes mainly remained in the vasculature and that liposomes with a novel formulation (20% DSPG, 50% DOPC, 30% cholesterol) were mainly targeted to macrophages. Upon laser wounding, both liposomes accumulated near the wounded site, but the PEGylated liposomes showed a diffuse accumulation and the macrophage-targeting liposomes were localized inside macrophages that had been recruited to the wound. Interestingly, encapsulation of PLP in either liposome resulted in enhancement of the inhibition of neutrophil migration upon laser wounding, whereas the inhibition of tail fin regeneration and the activation of GC-responsive genes throughout the embryonic body was reduced. Thus, using our zebrafish model system we demonstrated that encapsulation of PLP in two different types of increased the anti-inflammatory effects and reduced the side effects of this GC drug.

Our results from confocal microscopy imaging of zebrafish embryos injected with different liposome formulations illustrate the feasibility to visualize and compare the biodistribution of liposomes *in vivo*, adding to previous studies on nanoparticles as a drug delivery system in zebrafish [46, 47, 52, 53]. We have investigated the biodistribution in 3 dpf embryos of the PEG2000-DSPE, DPPC and cholesterol formulation, which is widely studied for delivery of PLP [17, 18, 22, 54]. Our images show that these liposomes are mainly circulating in the vasculature at 2 hours after intravenous injection, and are hardly taken up by macrophages, in agreement with previous reports [46, 52]. For these liposomes, we observed association with endothelial cells (ECs) of the posterior cardinal vein (PCV), the caudal vein (CV) and the CHT. These venous ECs have been shown to function in zebrafish embryos as the equivalent of the liver sinusoidal/scavenger endothelial cells (LSECs) in mammals [47]. The uptake of mainly anionic nanoparticles by these cells was demonstrated to be dependent on the scavenger receptor Stabilin-2 [47]. Clearance of liposomes from the circulation by SECs, especially in the liver, is a critical problem for the application of the liposome drug delivery systems [7, 55], so we suggest to use our zebrafish model system to screen altered formulations of the PEGylated liposome for reduced association with SECs in future studies. In addition to using PEGylated liposomes, we optimized the formulation of macrophage-targeting liposomes by varying the DSPG:cholesterol ratio of a liposome that for the other 50% consisted of DOPC, with the aim to have PLP delivered to sites of inflammation by macrophages recruited to these areas. Our images show that low ratios prevent macrophage uptake and that high ratios induce more targeting to the area that includes CV and CHT, consistent with the finding that these cells preferentially scavenge anionic nanoparticles [47]. The ratio we selected for

further studies showed maximal macrophage targeting without substantial association with venous ECs.

In order to test these liposomes for the delivery of PLP to inflamed tissues, we used laser wounding in the tail of the zebrafish embryo. In previous studies we used tail fin amputation to study anti-inflammatory effects of GCs in zebrafish [51, 56], but for the present study wounding in a better vascularized part of the body seemed a more relevant model system. Both liposomes tested accumulated in the wounded area. The PEGylated liposomes, of which the accumulation is considered to depend on the EPR effect [7, 57], showed a diffuse distribution at the wounded site, whereas the macrophage-targeting liposomes were localized inside the macrophages that had migrated towards the wound. Interestingly, PLP encapsulated in either liposome type was more potent in inhibiting the wounding-induced neutrophil migration compared to free PLP. Thus, using our zebrafish model, we demonstrated an enhanced anti-inflammatory effect of PLP upon encapsulation with a new macrophage-targeting liposome formulation, and upon encapsulation in PEGylated liposomes, similarly to the enhancement observed for this type of liposomes in mammalian models [13, 16-19, 54]. The PEGylated liposome-encapsulated PLP was slightly less potent in suppressing the neutrophil migration than the PLP encapsulated in macrophage-targeting liposomes, which suggests a higher delivery efficiency of liposomes to the inflamed site through macrophage accumulation than through the EPR effect.

In order to improve GC therapies, an important aspect that should be taken into consideration is the severity of the side effects [3]. Therefore, in our study we used two *in vivo* assays to assess possible adverse effects of PLP. First, we determined the inhibition of tissue regeneration upon tail fin amputation. Inhibited wound healing or tissue regeneration is a commonly observed side effect of GC treatment [58], and the regeneration assay had also been used as a readout for side effects of GC drugs in a previous study from our lab [59]. Second, since most side effects of GCs are considered to result from the transactivation of GRE-containing promoters by activated GRs [60], we used a zebrafish reporter line in which the expression of the GFP gene was driven by a GRE-containing promoter and we determined the GFP expression throughout the body of the embryos upon administration of free PLP and encapsulated PLP [61]. The findings from both assays showed that encapsulation in either type of liposome reduced the effects of PLP, suggesting that liposome encapsulation may increase the therapeutic ratio of PLP not only by enhancing the desired anti-inflammatory effects, but also by decreasing the adverse effects. Interestingly, whereas in the tail fin regeneration assay both liposomes showed similar effects, in the GRE:GFP reporter line the macrophage-targeting liposomes showed only a slightly lower induction of the GFP expression than the PEGylated liposomes. This difference may be related to the different pharmacokinetics of the liposomes, since the effect of GCs in the tail fin

regeneration assay depends on their presence during the first hours after amputation [50, 59], whereas the observed effect on GFP expression results from their activity over almost the entire time between the injection and the imaging (24 h).

In conclusion, we present new evidence that zebrafish embryos as an animal model for studies on liposomal encapsulation of GCs are a useful tool in the development of anti-inflammatory GC therapies. Exploiting the transparency of this model, we optimized the formulation of a novel macrophage-targeting liposome and compared its biodistribution with that of a PEGylated liposome, and both liposomes showed accumulation at sites of inflammation. Encapsulation in liposomes enhanced the anti-inflammatory effects of GCs and reduce their adverse effects. These results indicate that liposome encapsulation of GCs is a promising way to increase the therapeutic ratio of these drugs, and that the zebrafish is a valuable model for future preclinical studies aimed at the optimization of liposomal formulations of anti-inflammatory GC drugs.

Materials and methods

Zebrafish lines and maintenance

Zebrafish were maintained and handled according to the guidelines from the Zebrafish Model Organism Database (<http://zfin.org>) and in compliance with the directives of the local animal welfare committee of Leiden University. They were exposed to a 14 hours light and 10 hours dark cycle to maintain circadian rhythmicity. Fertilization was performed by natural spawning at the beginning of the light period. Eggs were collected and raised at 28°C in egg water (60 µg/ml Instant Ocean sea salts and 0.0025% methylene blue). The following fish lines were used in this study: the type (wt) strain AB/TL, the transgenic lines *Tg(mpeg1:eGFP^{gl22})* [62], *Tg(mpx:GFPⁱ¹¹⁴)* [63] and *Tg(9xGCRE-HSV.U123:EGFP^{ia20})* [61].

Liposome preparation

The macrophage targeting liposomes and PEGylated liposomes were formulated in ddH₂O and Phosphate-buffered saline (PBS) respectively at a total lipid concentration of 5 mM [32, 47]. Stock solutions of lipids (in chloroform) were mixed at specific molar ratios, dried and rehydrated in 1 mL ddH₂O. Liposomes with a size of 100 nm were formed through extrusion (Mini-extruder with heating block, Avanti Polar Lipids, Alabaster, US) using the polycarbonate membranes with corresponding pore size, and stored at 4 °C. The macrophage targeting liposomes consisted of DSPG, DOPC and cholesterol, with molar ratios of either 10:50:40, 15:50:35, 20:50:30, 25:50:35 or 30:50:20. The PEGylated liposomes consisted of dipalmitoyl phosphatidyl choline (DPPC), PEG 2000 distearoyl

phosphatidylethanolamine (PEG-DSPE) and cholesterol with a molar ratio of 62:5:33. Prednisolone phosphate (PLP, MedChemExpress) was encapsulated by hydrating the lipid film with an aqueous solution of 50mg/ml PLP. After extrusion the unencapsulated PLP was removed by size exclusion chromatography and the encapsulated amount was determined by the absorbance measured by UV spectrophotometry. Reported amounts of PLP are total amounts in the solution. All liposomes (with or without encapsulated PLP) were prepared freshly before injection.

Injection of drugs

All treatments were given intravenously to the zebrafish embryos. After anesthesia with 0.02% aminobenzoic acid ethyl ester (tricaine, Sigma-Aldrich), 2 or 3 dpf embryos were injected with control solution (water), empty liposomes, different amounts of free PLP or liposome encapsulated PLP in the duct of Cuvier under a Leica M165C stereomicroscope. For free PLP, the injected volume was 1 nl and the concentration of the injected PLP solution (in ddH₂O) varied from 25 mM PLP to 0.04 mM to achieve an injected amount of 25 pmol to 0.04 pmol. For liposome-encapsulated PLP, the injected amount of 1 pmol was achieved by injecting the original liposome solution with a volume calculated based on the concentration determined by UV spectrophotometry. Lower doses were injected using the same volume and a lower concentration of liposomes. As a control for testing the vascular permeability, 1nl of 20 µg/ml dextran was injected (fluorescently labeled with tetramethylrhodamine, 2,000,000 MW, Invitrogen).

Microscopy

For confocal laser scanning microscopy, anesthetized embryos were mounted in 1% low melting agarose in egg water containing 0.02% tricaine on 40 mm glass-bottom dishes (WillCo-dish, WillCo Wells). Images were taken using a Leica TCS SP8 confocal microscope with a 10X (NA 0.4), or 20X (NA 0.75) objective (Figure 1-3, Supplementary Figure 2). For other brightfield and/or fluorescence microscopy imaging, anesthetized embryos were imaged using a Leica M205FA fluorescence stereomicroscope, equipped with a Leica DFC 345FX camera (Figure 4-6).

Laser wounding

Adapted from the method of yolk wounding using laser irradiation in zebrafish embryos described previously [64], we used laser wounding to a region in the tail, since this area is vascularized and the thin tissue allows convenient imaging of accumulated leukocytes. Anesthetized 3 dpf embryos were mounted in 1% low melting agarose in egg water containing 0.02% tricaine on a microscope slide (VWR). A 100 µm long burning wound was created in the tail by laser irradiation with a ZEISS PALM

Microbeam Laser Microdissection system using a 20X objective (NA 0.4) (Figure 3A). Drug treatment by intravenous injection was performed immediately after wounding. The number of recruited neutrophils was determined at 4 hours after wounding.

Regeneration assay

The tails of anesthetized 2dpf embryos were partially amputated with a 1 mm sapphire blade (World Precision Instruments) on 2% agarose-coated Petri dishes under a Leica M165C stereomicroscope (Figure 5A). Drug treatment by intravenous injection was performed immediately after amputation. The length of fin regeneration was determined from microscopic images taken at 36 hpa as previously described [50].

Image analysis

To determine neutrophil migration upon laser wounding, neutrophils were detected based on their fluorescent GFP label, and to quantify the number of recruited neutrophils in the fluorescence microscopy images of the wounded tails, the cells in a defined area of the tail were counted manually (Figure 4A). For the quantitation of the regeneration assay, in the images of the tail fins the length of the regenerated tissue was determined from the center of the original plane of amputation to the tip of the regenerating fin (Figure 5). Quantitation of transactivation of a GRE-containing promoter in the *Tg(9xGRE-HSV.U123:EGFP^{ia20})* was done on images taken at 24hpi, by determining the relative EGFP signal in the embryonic body using the Analyze and Measure tool in the ImageJ software, and determining the value "RawIntDen" (the sum of the values of the pixels in the image) (Figure 6A).

Statistical analysis

Statistical analysis was performed using GraphPad Prism 7 by one-way ANOVA with Bonferroni's post hoc test (Figures 1,2,4-6) or two-tailed t-test (Figure 3F). Significance was accepted at $p < 0.05$.

Acknowledgements

We thank Lukas Wijaya, Olga Snip, Chantal Pont and Dr. Johan Kuiper for their assistance with the Microbeam Laser Microdissection system. We thank the fish facility team, in particular Guus van der Velden, Natasha Montiadi, Ulrike Nehrdich and Ruth van Koppen for zebrafish maintenance. We thank Dr. Graham Lieschke, Dr. Stephen A. Renshaw and Dr. Luisa Dalla Valle for providing transgenic zebrafish lines.

References

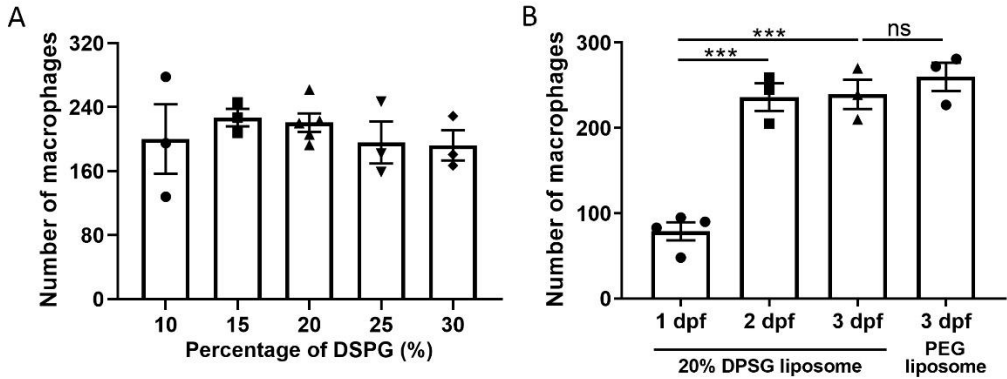
1. Busillo, J.M. and J.A. Cidlowski, *The five Rs of glucocorticoid action during inflammation: ready, reinforce, repress, resolve, and restore*. Trends in Endocrinology & Metabolism, 2013. **24**(3): p. 109-119.
2. Barnes, P.J., *Glucocorticosteroids: current and future directions*. British Journal of Pharmacology, 2011. **163**(1): p. 29-43.
3. Moghadam-Kia, S. and V.P. Werth, *Prevention and treatment of systemic glucocorticoid side effects*. International journal of dermatology, 2010. **49**(3): p. 239-248.
4. Yasir, M. and S. Sonthalia, *Corticosteroid adverse effects*. 2019.
5. Ulbrich, W. and A. Lamprecht, *Targeted drug-delivery approaches by nanoparticulate carriers in the therapy of inflammatory diseases*. Journal of The Royal Society Interface, 2010. **7**(suppl_1): p. S55-S66.
6. Bardania, H., S. Tarvirdipour, and F. Dorkoosh, *Liposome-targeted delivery for highly potent drugs*. Artificial Cells, Nanomedicine, and Biotechnology, 2017. **45**(8): p. 1478-1489.
7. Nehoff, H., et al., *Nanomedicine for drug targeting: strategies beyond the enhanced permeability and retention effect*. International journal of nanomedicine, 2014. **9**: p. 2539.
8. Decuzzi, P., et al., *Size and shape effects in the biodistribution of intravascularly injected particles*. Journal of Controlled Release, 2010. **141**(3): p. 320-327.
9. Taurin, S., H. Nehoff, and K. Greish, *Anticancer nanomedicine and tumor vascular permeability; where is the missing link?* Journal of controlled release, 2012. **164**(3): p. 265-275.
10. Bae, Y.H. and K. Park, *Targeted drug delivery to tumors: myths, reality and possibility*. Journal of controlled release, 2011. **153**(3): p. 198.
11. Voinea, M. and M. Simionescu, *Designing of 'intelligent' liposomes for efficient delivery of drugs*. Journal of cellular and molecular medicine, 2002. **6**(4): p. 465-474.
12. Tiwari, G., et al., *Drug delivery systems: An updated review*. International journal of pharmaceutical investigation, 2012. **2**(1): p. 2.
13. Schmidt, J., et al., *Drug targeting by long - circulating liposomal glucocorticosteroids increases therapeutic efficacy in a model of multiple sclerosis*. Brain, 2003. **126**(8): p. 1895-1904.
14. Grigoletto, A., et al., *Drug and protein delivery by polymer conjugation*. Journal of Drug Delivery Science and Technology, 2016. **32**: p. 132-141.
15. Yan, X., G.L. Scherphof, and J.A. Kamps, *Liposome opsonization*. Journal of liposome research, 2005. **15**(1-2): p. 109-139.
16. Metselaar, J.M., et al., *Complete remission of experimental arthritis by joint targeting of glucocorticoids with long - circulating liposomes*. Arthritis & Rheumatism: Official Journal of the American College of Rheumatology, 2003. **48**(7): p. 2059-2066.
17. Hofkens, W., et al., *Intravenously delivered glucocorticoid liposomes inhibit osteoclast activity and bone erosion in murine antigen-induced arthritis*. Journal of controlled release, 2011. **152**(3): p. 363-369.
18. Metselaar, J.v., et al., *Liposomal targeting of glucocorticoids to synovial lining cells strongly increases therapeutic benefit in collagen type II arthritis*. Annals of the rheumatic diseases, 2004. **63**(4): p. 348-353.
19. Lobatto, M.E., et al., *Multimodal clinical imaging to longitudinally assess a nanomedical anti-inflammatory treatment in experimental atherosclerosis*. Molecular pharmaceutics, 2010. **7**(6): p. 2020-2029.
20. Schiffelers, R.M., et al., *Liposome-encapsulated prednisolone phosphate inhibits growth of established tumors in mice*. Neoplasia, 2005. **7**(2): p. 118-127.
21. Banciu, M., et al., *Liposomal glucocorticoids as tumor-targeted anti-angiogenic nanomedicine in B16 melanoma-bearing mice*. The Journal of steroid biochemistry and molecular biology, 2008. **111**(1-2): p. 101-110.

22. Hofkens, W., et al., *Safety of glucocorticoids can be improved by lower yet still effective dosages of liposomal steroid formulations in murine antigen-induced arthritis: comparison of prednisolone with budesonide*. International journal of pharmaceutics, 2011. **416**(2): p. 493-498.
23. van den Hoven, J.M., et al., *Optimizing the therapeutic index of liposomal glucocorticoids in experimental arthritis*. International journal of pharmaceutics, 2011. **416**(2): p. 471-477.
24. Meka, R.R., et al., *Peptide-targeted liposomal delivery of dexamethasone for arthritis therapy*. Nanomedicine, 2019. **14**(11): p. 1455-1469.
25. Verma, A., et al., *Folate conjugated double liposomes bearing prednisolone and methotrexate for targeting rheumatoid arthritis*. Pharmaceutical Research, 2019. **36**(8): p. 123.
26. Poh, S., et al., *Selective liposome targeting of folate receptor positive immune cells in inflammatory diseases*. Nanomedicine: Nanotechnology, Biology and Medicine, 2018. **14**(3): p. 1033-1043.
27. Gaillard, P.J., et al., *Enhanced brain delivery of liposomal methylprednisolone improved therapeutic efficacy in a model of neuroinflammation*. Journal of controlled release, 2012. **164**(3): p. 364-369.
28. Sylvester, B., et al., *Optimization of prednisolone-loaded long-circulating liposomes via application of Quality by Design (QbD) approach*. Journal of liposome research, 2018. **28**(1): p. 49-61.
29. Lobatto, M.E., et al., *Pharmaceutical development and preclinical evaluation of a GMP-grade anti-inflammatory nanotherapy*. Nanomedicine: nanotechnology, biology and medicine, 2015. **11**(5): p. 1133-1140.
30. Patras, L., et al., *Liposomal prednisolone phosphate potentiates the antitumor activity of liposomal 5-fluorouracil in C26 murine colon carcinoma in vivo*. Cancer biology & therapy, 2017. **18**(8): p. 616-626.
31. Smits, E.A.W., et al., *The availability of drug by liposomal drug delivery : Individual kinetics and tissue distribution of encapsulated and released drug in mice after administration of PEGylated liposomal prednisolone phosphate*. Investigational new drugs, 2019. **37**(5): p. 890-901.
32. van der Valk, F.M., et al., *Prednisolone-containing liposomes accumulate in human atherosclerotic macrophages upon intravenous administration*. Nanomedicine: nanotechnology, biology and medicine, 2015. **11**(5): p. 1039-1046.
33. Turk, M.J., D.J. Waters, and P.S. Low, *Folate-conjugated liposomes preferentially target macrophages associated with ovarian carcinoma*. Cancer letters, 2004. **213**(2): p. 165-172.
34. Tie, Y., et al., *Targeting folate receptor β positive tumor-associated macrophages in lung cancer with a folate-modified liposomal complex*. Signal transduction and targeted therapy, 2020. **5**(1): p. 1-15.
35. Chono, S., et al., *Uptake characteristics of liposomes by rat alveolar macrophages: influence of particle size and surface mannose modification*. Journal of pharmacy and pharmacology, 2007. **59**(1): p. 75-80.
36. Düffels, A., et al., *Synthesis of high -mannose type neoglycolipids: Active targeting of liposomes to macrophages in gene therapy*. Chemistry—A European Journal, 2000. **6**(8): p. 1416-1430.
37. Andersen, M.N., et al., *STAT3 inhibition specifically in human monocytes and macrophages by CD163-targeted corosolic acid-containing liposomes*. Cancer Immunology, Immunotherapy, 2019. **68**(3): p. 489-502.
38. Tentillier, N., et al., *Anti-inflammatory modulation of microglia via CD163-targeted glucocorticoids protects dopaminergic neurons in the 6-OHDA Parkinson's disease model*. Journal of Neuroscience, 2016. **36**(36): p. 9375-9390.
39. Montes-Cobos, E., et al., *Targeted delivery of glucocorticoids to macrophages in a mouse model of multiple sclerosis using inorganic-organic hybrid nanoparticles*. Journal of Controlled Release, 2017. **245**: p. 157-169.

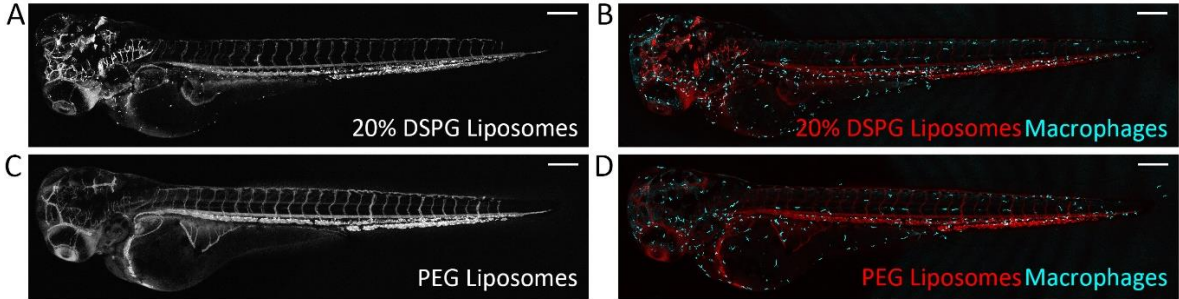
40. Howe, K., et al., *The zebrafish reference genome sequence and its relationship to the human genome*. Nature, 2013. **496**(7446): p. 498-503.
41. Doudna, J.A. and E. Charpentier, *The new frontier of genome engineering with CRISPR-Cas9*. Science, 2014. **346**(6213).
42. Lewis, K.L., N. Del Cid, and D. Traver, *Perspectives on antigen presenting cells in zebrafish*. Developmental & Comparative Immunology, 2014. **46**(1): p. 63-73.
43. Schaaf, M., A. Chatzopoulou, and H. Spaink, *The zebrafish as a model system for glucocorticoid receptor research*. Comparative Biochemistry and Physiology Part A: Molecular & Integrative Physiology, 2009. **153**(1): p. 75-82.
44. Alsop, D. and M.M. Vijayan, *Development of the corticosteroid stress axis and receptor expression in zebrafish*. Am J Physiol Regul Integr Comp Physiol, 2008. **294**(3): p. R711-9.
45. Schaaf, M.J., et al., *Discovery of a functional glucocorticoid receptor beta-isoform in zebrafish*. Endocrinology, 2008. **149**(4): p. 1591-9.
46. Sieber, S., et al., *Zebrafish as a predictive screening model to assess macrophage clearance of liposomes in vivo*. Nanomedicine: Nanotechnology, Biology and Medicine, 2019. **17**: p. 82-93.
47. Campbell, F., et al., *Directing nanoparticle biodistribution through evasion and exploitation of Stab2-dependent nanoparticle uptake*. ACS nano, 2018. **12**(3): p. 2138-2150.
48. Ringdén, O., et al., *Efficacy of amphotericin B encapsulated in liposomes (AmBisome) in the treatment of invasive fungal infections in immunocompromised patients*. J Antimicrob Chemother, 1991. **28 Suppl B**: p. 73-82.
49. Cornely, O.A., et al., *Liposomal amphotericin b as initial therapy for invasive mold infection: a randomized trial comparing a high-loading dose regimen with standard dosing (AmBiLoad Trial)*. Clinical infectious diseases, 2007. **44**(10): p. 1289-1297.
50. Mathew, L.K., et al., *Unraveling tissue regeneration pathways using chemical genetics*. Journal of Biological Chemistry, 2007. **282**(48): p. 35202-35210.
51. Chatzopoulou, A., et al., *Glucocorticoid-induced attenuation of the inflammatory response in zebrafish*. Endocrinology, 2016. **157**(7): p. 2772-2784.
52. Sieber, S., et al., *Zebrafish as an early stage screening tool to study the systemic circulation of nanoparticulate drug delivery systems in vivo*. Journal of Controlled Release, 2017. **264**: p. 180-191.
53. Fenaroli, F., et al., *Nanoparticles as drug delivery system against tuberculosis in zebrafish embryos: direct visualization and treatment*. ACS nano, 2014. **8**(7): p. 7014-7026.
54. Hofkens, W., et al., *Liposomal targeting of prednisolone phosphate to synovial lining macrophages during experimental arthritis inhibits M1 activation but does not favor M2 differentiation*. PloS one, 2013. **8**(2): p. e54016.
55. Immordino, M.L., F. Dosio, and L. Cattel, *Stealth liposomes: review of the basic science, rationale, and clinical applications, existing and potential*. International journal of nanomedicine, 2006. **1**(3): p. 297.
56. Xie, Y., et al., *Glucocorticoids inhibit macrophage differentiation towards a pro-inflammatory phenotype upon wounding without affecting their migration*. Disease models & mechanisms, 2019. **12**(5).
57. Maeda, H., et al., *Tumor vascular permeability and the EPR effect in macromolecular therapeutics: a review*. Journal of controlled release, 2000. **65**(1-2): p. 271-284.
58. Slominski, A.T. and M.A. Zmijewski, *Glucocorticoids inhibit wound healing: novel mechanism of action*. Journal of Investigative Dermatology, 2017. **137**(5): p. 1012-1014.
59. He, M., et al., *Ginsenoside Rg1 Acts as a Selective Glucocorticoid Receptor Agonist with Anti-Inflammatory Action without Affecting Tissue Regeneration in Zebrafish Larvae*. Cells, 2020. **9**(5): p. 1107.
60. Schäcke, H., W.-D. Döcke, and K. Asadullah, *Mechanisms involved in the side effects of glucocorticoids*. Pharmacology & therapeutics, 2002. **96**(1): p. 23-43.

61. Benato, F., et al., *A living biosensor model to dynamically trace glucocorticoid transcriptional activity during development and adult life in zebrafish*. *Molecular and cellular endocrinology*, 2014. **392**(1-2): p. 60-72.
62. Ellett, F., et al., *mpeg1 promoter transgenes direct macrophage-lineage expression in zebrafish*. *Blood*, 2011. **117**(4): p. e49-e56.
63. Renshaw, S.A., et al., *A transgenic zebrafish model of neutrophilic inflammation*. *Blood*, 2006. **108**(13): p. 3976-3978.
64. Redd, M.J., et al., *Imaging macrophage chemotaxis in vivo: studies of microtubule function in zebrafish wound inflammation*. *Cell motility and the cytoskeleton*, 2006. **63**(7): p. 415-422.

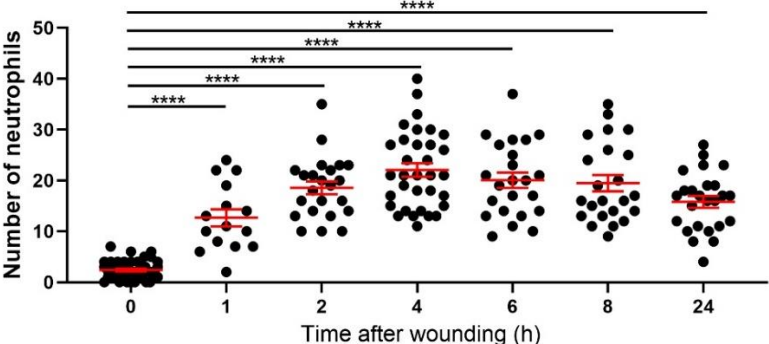
Supplementary material



Supplementary Figure 1. The number of macrophages in the whole body of embryos. *Tg(mpeg1:GFP)* embryos were injected with liposomes containing different percentages of DSPG at 2 days post fertilization (dpf) (A) or 20% DSPG liposomes at 1, 2 and 3 dpf and PEGylated liposomes at 3dpf (B). Confocal microscopy images were taken at 2 hours post injection (hpi) and the number of macrophages over the whole body was quantified. Statistical analysis was performed by one-way ANOVA with Bonferroni’s post hoc test. No significant differences were observed in panel A. In panel B, no significant difference was observed when injected with 20% DSPG liposome and PEG liposome at 3 dpf. Upon injection with 20% DSPG liposomes, at 2 dpf and 3 dpf significantly higher numbers of macrophages were observed than at 1 dpf. Data shown are the means ± s.e.m. of 3-5 individual embryos, of which the individual data are indicated. Statistically significant differences between groups are indicated by: ns, non-significant; *** p<0.001.



Supplementary Figure 2. Biodistribution in zebrafish embryos of liposomes encapsulating PLP. A-B. Representative confocal microscopy images of 3 dpf embryos of the *Tg(mpeg1:GFP)* line injected with 20% DSPG (A) or PEGylated (B) liposomes encapsulating PLP. Images were taken at 2 hpi. Liposomes are shown in red and macrophages in cyan. Scale bar = 200 μm.



Supplementary Figure 3. Number of neutrophils recruited to the wounded area at different time points after laser wounding. Embryos (at 3 dpf) of the *Tg(mpx:GFP)* line were subjected to laser wounding, and fluorescence microscopy images were taken at different time points after the wounding procedure. The number of neutrophils recruited to the wounded area are shown. Statistical analysis was performed by one-way ANOVA with Bonferroni’s post hoc test. Each data point represents a single embryo and the means \pm s.e.m. of data accumulated from three independent experiments are shown in red. Statistically significant differences between groups are indicated by: **** $p < 0.0001$.

Chapter 6

Summary and Discussion

Zebrafish as a model to dissect the effect of glucocorticoids in the immune system

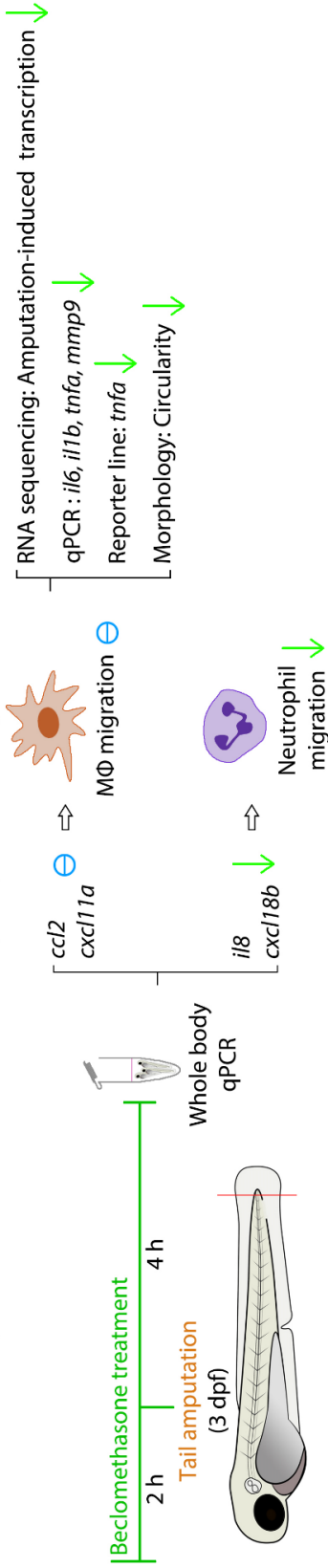
Glucocorticoids (GCs) regulate, through the activation of the glucocorticoid receptor (GR), a wide variety of systems, like the metabolic, reproductive, cardiovascular, nervous and immune system [1-3]. Due to their well-established immunosuppressive effects, GCs are widely prescribed as anti-inflammatory drugs. However, their utilization is severely limited by the occurrence of side effects and drug resistance [4, 5]. Therefore, there is still a major need to investigate the molecular and cellular mechanisms underlying the effects of GCs. These mechanisms appear to be highly complex, since the effects of GCs are cell type- and context-specific and their transcriptional regulatory effects on pro-inflammatory genes are not strictly suppressive [6, 7].

Zebrafish are increasingly used as an *in vivo* model system for studying the immune system, in particular the inflammatory response, for research aimed at the discovery of novel drug targets and for screening of drug libraries [8-10]. The advantages of this model system include its evolutionarily conserved immune system, the accessibility of embryos for genetic manipulation and non-invasive live imaging and the cost-effective maintenance [10-13]. In **Chapter 2**, an overview is presented of how the zebrafish is used as an animal model for inflammatory diseases. Different models are described, and how they are used for research on the mechanisms underlying the inflammatory response and for testing of potential novel anti-inflammatory drugs, in particular GCs. In addition, the structure and function of the zebrafish Gr and the regulation of the secretion of the endogenous GC cortisol are highly similar to the human system [14-17]. This makes the zebrafish a valuable tool to study the complex modulatory effects of GCs on the immune system. In this thesis, we have used this model system to study molecular and cellular mechanisms of GC action on the immune system and to develop a model for *in vivo* screening of the anti-inflammatory effects as well as possible adverse effects of novel GC therapies. For this purpose, we have studied the effect of GCs on leukocyte migration and differentiation during an inflammatory response (**Chapter 3**), how GCs modulate the immune response to a mycobacterial infection (**Chapter 4**), and we have investigated targeting of GCs to inflamed tissue by liposomal delivery (**Chapter 5**). In figure 1, a graphical overview of the experimental chapters is presented.

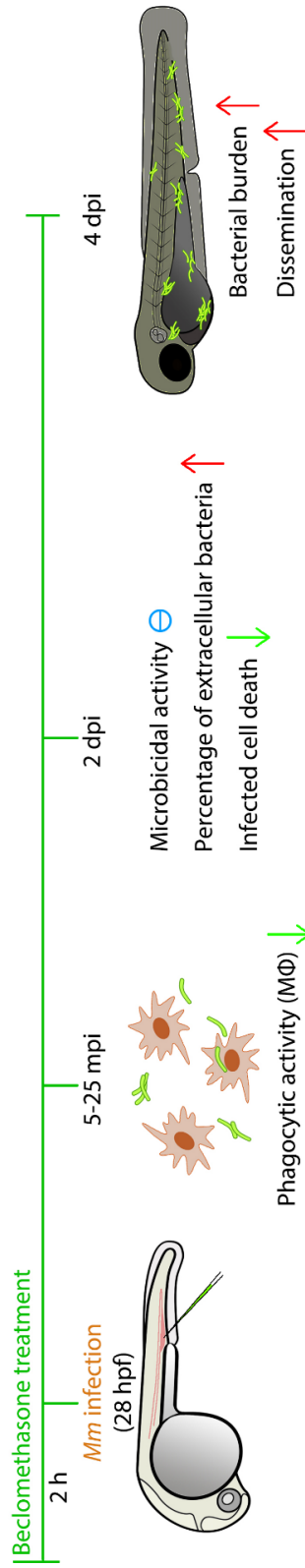
Glucocorticoids inhibit the differentiation of macrophages towards a pro-inflammatory phenotype through transcriptional regulation

In **Chapter 3**, studies are described in which we have used the zebrafish tail fin amputation model as a model for inflammation. In this model, neutrophils and macrophages migrate towards the area that is

Effect of GCs on amputation-induced inflammatory responses (Chapter 3)



Effect of GCs on *Mm* infection (Chapter 4)



Liposome delivery of GCs (Chapter 5)

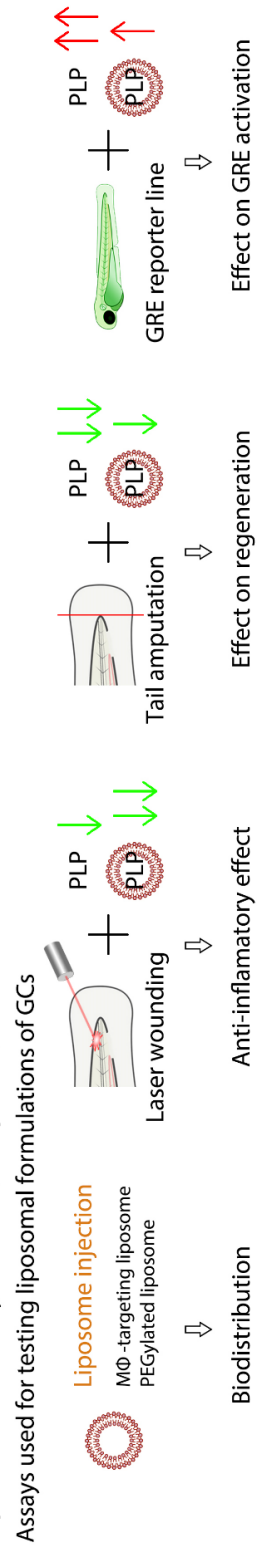


Figure 1. Graphical overview of the experimental chapters

wounded by the amputation. Treatment with the GC beclomethasone inhibits the migration of neutrophils towards the wound. However, the amputation-induced macrophage migration is not decreased by GCs, similar to earlier observations in other studies [18-20]. Our work demonstrated that this difference in the response to GCs is related to the GC-induced decrease in the expression of genes encoding chemoattractants which are involved in neutrophil recruitment such as *Il8* and *Cxcl18b*, whereas the expression of genes encoding chemoattractants involved in macrophage recruitment, such as *Ccl2* and *Cxcl11aa*, is unaffected by the GC treatment. Similar to our results, in a human breast cancer cell line (T47D) GC treatment has no effect on the IL-1-stimulated CCL2 production [21], and no effect of GCs was seen on the IFN- γ -induced CXCL11 production in human lung epithelial cells (A549) [22]. However, in most studies different observations have been made, as GCs have been shown to inhibit inflammation-induced CCL2 levels in humans and rats [23-25]. Moreover, CXCL11 upregulation was inhibited by GCs in isolated human peripheral blood monocytes, IFN- γ - or LPS-stimulated RAW 264.7 macrophages and multiple tissues of endotoxemia mice [26, 27]. These differences between studies suggest that the GC resistance of the *ccl2* and *cxcl11a* transcription observed in our study, which causes the GC insensitivity of the macrophage migration, requires a specific context. The interaction with GR with other transcription factors and various coregulator proteins has been shown to be highly complex and it is often unclear how this results in positive or negative gene regulation [28-32]. In future studies it will be interesting to unravel the molecular factors determining the resistance of the transcription of genes encoding macrophage-specific chemoattractants in our model.

GCs have been shown to strongly inhibit the immune response by inhibiting the transcriptional activity of pro-inflammatory genes and inducing the expression of anti-inflammatory genes [7]. For example, in cultured macrophages, it has been reported that the expression of pro-inflammatory regulators are efficiently suppressed by GC treatment [28, 29, 32, 33]. Similarly, GC treatment attenuates the vast majority of genes induced by tail wounding in zebrafish [19]. To study transcriptional regulation by GCs in macrophages in our model, an RNA sequencing analysis was performed on macrophages isolated from zebrafish larvae. We observed that GC treatment suppresses virtually all amputation-induced changes in gene expression, among which the induction of pro-inflammatory genes. In addition, using the *Tg(tnfa:eGFP-F)* reporter line we showed that the number of macrophages expressing *tnfa* was significantly reduced by GC treatment, and we observed that GCs decreased the percentage of macrophages displaying the typical more rounded morphology that is observed in response to an inflammatory stimulus.

Macrophages display a continuum of phenotypes but two opposite functional phenotypes are often distinguished: a classically activated (M1) phenotype which promotes the inflammatory response, and an alternatively activated (M2) phenotype which is involved in the resolution of inflammation and

wound healing [34, 35]. Our data suggest an inhibitory effect of GC administration on the differentiation of macrophages towards an M1 phenotype. Apparently, GCs allow macrophages to migrate towards a site of inflammation, but prevent them from becoming pro-inflammatory.

It is still unclear whether GCs, in addition to the inhibition of the differentiation to an M1 phenotype, induce an M2 phenotype. A possible approach to study this would be to establish a reporter zebrafish line for the expression of M2 macrophage markers, like *arg2*, *cxc4b*, *tgfb1*, *ccr2*, *vegf*, *irf4*, or *ccl22* [36, 37]. Several such lines are under being generated in laboratories of our collaborators, but not yet available. Therefore, we have analyzed the expression level of several M2 markers in macrophages, but results remained inconclusive because the induction of *arg2* by wounding was not sensitive to GC treatment and the expression of *cxc4b*, *tgfb1* and *ccr2* was not induced by wounding. However, this analysis was based on the whole population of macrophages so specific effects in M2 macrophages may have been hidden. In order to further study the effect of GCs on the macrophage phenotype, an expression analysis of *tnfa*-positive (M1) versus -negative (M2) populations could be performed, or single cell RNA sequencing to discriminate all different subpopulations.

Glucocorticoid treatment exacerbates mycobacterial infection by decreasing macrophage phagocytosis

To study the functional consequences of the observed GC effects on immune cells, in **Chapter 4** we have performed research on how GCs modulate an infection with *Mycobacterium marinum* (*Mm*), which is a species closely related to *Mycobacterium tuberculosis* (*Mtb*), the causative agent of tuberculosis (TB) in humans. Infectious complications are one of the side effects of GC therapy resulting from the compromised immune system [38-40]. Although treatment with GCs is associated with a higher risk of developing TB [41, 42], adjunctive GC therapy has been shown to be beneficial for patients suffering from certain types of TB that are associated with inflammatory complications [43-45].

Mm causes a TB-like infection in zebrafish and other cold-blooded animals naturally [46] and zebrafish larvae are widely used to study host-pathogen interactions underlying TB and to investigate potential host-directed therapeutic strategies [47-49]. We found that GC treatment increased the infection level in zebrafish larvae. This increased *Mm* infection upon GC treatment is related to an inhibited phagocytic activity resulting from a decreased transcription level of phagocytosis-related genes in macrophages. When using another intracellular pathogen, *Salmonella* Typhimurium, the GC-inhibited phagocytic activity of macrophages was also observed. Similarly, it has been reported that GCs inhibit the phagocytosis of several *Escherichia coli* strains by PMA-stimulated human monocyte-derived (THP-

1) macrophages and murine bone marrow-derived macrophages (BMDMs) [50]. In macrophages from rats and rheumatoid arthritis patients, GC treatment also inhibits phagocytosis of carbon particles [51, 52]. However, in some studies GC exposure has been reported to enhance the phagocytosis of apoptotic neutrophils by human blood monocyte-derived macrophages, PMA-stimulated THP-1 macrophages [53-55] and mouse alveolar macrophages [56]. These results suggest that the effects of GCs on macrophage phagocytic capacity could mainly be dependent on the particles they encounter and the tissue environment.

The phagocytic activity of macrophages is essential for eliminating harmful components and maintaining homeostasis during inflammation and infection. In our study, the decreased phagocytic activity of macrophages also resulted in a lower level of macrophage cell death due to the *Mm* infection and exacerbated growth of the extracellular fraction of bacteria. We propose that the increased numbers of extracellular bacteria could traverse endothelial barriers directly and grow more rapidly in a less restrictive environment outside macrophages. These results may explain the increased susceptibility to mycobacterial infections induced by GC treatment. As an adjuvant therapy for severe TB, the beneficial effect of GCs was reported to be observed in a subpopulation of patients with excessive inflammation resulting from specific polymorphisms in the *LTA4H* gene, which was modeled in zebrafish by *Ita4h* knockdown or overexpression [57, 58]. To further explore the interplay between these effects, we may study the effect of GCs in relation to the *Ita4h* polymorphism and the involvement of *Ita4h* expression in changes in phagocytosis and bacterial burden induced by GCs. Investigating the effect of GCs at later stages of *Mm* infection may also help to understand the role of GCs in exacerbation of TB.

Encapsulation of glucocorticoids in liposomes enhances their anti-inflammatory effects and reduces their side effects

Chapter 5 describes studies on the targeting of GCs to inflamed tissue by encapsulating them in liposomes. Targeted delivery of drugs using nanoparticles like liposomes is a promising approach to improve the therapeutic ratio of these drugs, through optimization of their pharmacokinetics [59, 60]. Encapsulation of prednisolone phosphate (PLP) in PEGylated liposomes (which contain phospholipids linked to a polymer polyethylene glycol (PEG) chain) has been shown to increase the therapeutic effects of PLP in several animal models for inflammation-related diseases, such as rheumatoid arthritis [61-64], atherosclerosis [65], multiple sclerosis [66] and cancer [67]. However, the occurrence of side effects [68, 69], unwanted off-target accumulation [62, 70] and unexpected lack of anti-inflammatory effect when applied clinically [71] are still obstacles for the development of liposomal GC drugs. In our study, the targeting of PLP encapsulated in liposomes was visualized in zebrafish larvae in which an

inflammatory response was triggered by laser wounding. In addition, both the anti-inflammatory effects and effects on tissue regeneration after tail fin amputation and the systemic activation of a Gr-responsive reporter gene (as a proxy for possible adverse effects) were determined.

We tested two types of liposomes, a PEGylated liposome which was relatively resistant to scavenging, and a macrophage-targeting liposome. In the zebrafish laser wounding model, we observed liposome accumulation near the wounded area for both liposomes. Our results showed that both liposomes enhanced the inhibitory effect of PLP on wounding-induced neutrophilic migration, and that encapsulation using the macrophage-targeting liposome was even more effective than encapsulation in the PEGylated liposome, probably due an increased accumulation of the liposomes near the wound upon delivery by macrophages. The effect of PLP on tissue regeneration was alleviated by encapsulation in both liposomes, and the activation of a Gr-responsive reporter gene throughout the body of the embryo was only reduced by encapsulation in the PEGylated liposome. This could probably be explained by a slower release of PLP from the PEGylated liposomes, which is protected from scavenging and degradation by the PEG chain, leading to lower concentration of ligands available for Gr activation.

Our results suggest that the zebrafish is a useful model for screening different liposomal formulations, since the (dynamics of the) bio-distribution of the liposomes can be assessed, as well as their therapeutic anti-inflammatory effects and effects on processes such as tissue regeneration, exemplifying the side effects of GCs. Using this model, we showed, as a proof-of-principle, that encapsulation in both PEGylated and macrophage-targeting liposomes increases the therapeutic ratio of PLP treatment. The advantage of using zebrafish includes direct observation on the biodistribution of liposomes and the possibility of high-throughput screening, which may promote solving the problem of unwanted off-target accumulation [62, 70]. In addition, the side effects such as repressed corticosterone level and hyperglycemia [68, 69] could also be assessed using the zebrafish model. In future studies, we therefore recommend using this model for optimization of liposomal formulations, as a first screening model to be used for pre-selection of liposomes before they are tested in rodent models and/or clinical studies.

Conclusions

A broad knowledge of the modulatory effects of GCs in the immune system is necessary for the improvement of anti-inflammatory GC therapeutics. Our work demonstrates a general inhibitory effect of GCs on the pro-inflammatory phenotype and the phagocytic activity of macrophages and illustrates an important role for macrophages as a target for anti-inflammatory GC therapy (**Chapter 3, 4**). Indeed,

specific targeting of GCs to macrophages by encapsulation in liposomes increased the therapeutic efficacy of these drugs, although encapsulation in liposomes that are not scavenged had a similar effect (**Chapter 5**). The work in this thesis has added to our understanding of how GCs modulate the innate immune response upon inflammation and may contribute to the improvement of anti-inflammatory therapies by using different zebrafish models for assays to be used in pre-clinical research.

References

1. Heitzer, M.D., et al., *Glucocorticoid receptor physiology*. Reviews in Endocrine and Metabolic Disorders, 2007. **8**(4): p. 321-330.
2. Revollo, J.R. and J.A. Cidlowski, *Mechanisms generating diversity in glucocorticoid receptor signaling*. Ann N Y Acad Sci, 2009. **1179**: p. 167-78.
3. Ramamoorthy, S. and J.A. Cidlowski, *Exploring the Molecular Mechanisms of Glucocorticoid Receptor Action from Sensitivity to Resistance*. Endocrine development, 2013. **24**: p. 41-56.
4. Barnes, P.J., *Glucocorticosteroids: current and future directions*. British Journal of Pharmacology, 2011. **163**(1): p. 29-43.
5. Moghadam-Kia, S. and V.P. Werth, *Prevention and treatment of systemic glucocorticoid side effects*. International journal of dermatology, 2010. **49**(3): p. 239-248.
6. Baschant, U. and J. Tuckermann, *The role of the glucocorticoid receptor in inflammation and immunity*. The Journal of steroid biochemistry and molecular biology, 2010. **120**(2-3): p. 69-75.
7. Busillo, J.M. and J.A. Cidlowski, *The five Rs of glucocorticoid action during inflammation: ready, reinforce, repress, resolve, and restore*. Trends in Endocrinology & Metabolism, 2013. **24**(3): p. 109-119.
8. Lieschke, G.J. and P.D. Currie, *Animal models of human disease: zebrafish swim into view*. Nat Rev Genet, 2007. **8**(5): p. 353-67.
9. Oehlers, S.H., et al., *A whole animal chemical screen approach to identify modifiers of intestinal neutrophilic inflammation*. Febs j, 2017. **284**(3): p. 402-413.
10. Tavares, B. and S. Santos Lopes, *The Importance of Zebrafish in Biomedical Research*. Acta Medica Portuguesa, 2013. **26**(5): p. 583-592.
11. Lewis, K.L., N. Del Cid, and D. Traver, *Perspectives on antigen presenting cells in zebrafish*. Developmental & Comparative Immunology, 2014. **46**(1): p. 63-73.
12. Jekosch, K., *The zebrafish genome project: sequence analysis and annotation*, in *Methods in Cell Biology*. 2004, Elsevier. p. 225-239.
13. Bennett, C.M., et al., *Myelopoiesis in the zebrafish, Danio rerio*. Blood, The Journal of the American Society of Hematology, 2001. **98**(3): p. 643-651.
14. Stolte, E.H., et al., *Evolution of glucocorticoid receptors with different glucocorticoid sensitivity*. J Endocrinol, 2006. **190**(1): p. 17-28.
15. Chatzopoulou, A., et al., *Transcriptional and metabolic effects of glucocorticoid receptor alpha and beta signaling in zebrafish*. Endocrinology, 2015. **156**(5): p. 1757-69.
16. Schaaf, M.J., et al., *Discovery of a functional glucocorticoid receptor beta-isoform in zebrafish*. Endocrinology, 2008. **149**(4): p. 1591-9.
17. Alsop, D. and M.M. Vijayan, *Development of the corticosteroid stress axis and receptor expression in zebrafish*. American Journal of Physiology - Regulatory, Integrative and Comparative Physiology, 2008. **294**(3): p. R711-R719.
18. Jen, R., S.I. Rennard, and D.D. Sin, *Effects of inhaled corticosteroids on airway inflammation in chronic obstructive pulmonary disease: a systematic review and meta-analysis*. Int J Chron Obstruct Pulmon Dis, 2012. **7**: p. 587-95.

19. Chatzopoulou, A., et al., *Glucocorticoid-Induced Attenuation of the Inflammatory Response in Zebrafish*. *Endocrinology*, 2016. **157**(7): p. 2772-84.
20. Mathew, L.K., et al., *Unraveling tissue regeneration pathways using chemical genetics*. *J Biol Chem*, 2007. **282**(48): p. 35202-10.
21. Kelly, R.W., G.G. Carr, and S.C. Riley, *The Inhibition of Synthesis of a β -Chemokine, Monocyte Chemoattractant Protein-1 (MCP-1) by Progesterone*. *Biochemical and Biophysical Research Communications*, 1997. **239**(2): p. 557-561.
22. O'Connell, D., et al., *IFN-gamma-induced JAK/STAT, but not NF-kappaB, signaling pathway is insensitive to glucocorticoid in airway epithelial cells*. *Am J Physiol Lung Cell Mol Physiol*, 2015. **309**(4): p. L348-59.
23. Kim, J.S., M. Chopp, and S.C. Gautam, *High dose methylprednisolone therapy reduces expression of JE/MCP-1 mRNA and macrophage accumulation in the ischemic rat brain*. *J Neurol Sci*, 1995. **128**(1): p. 28-35.
24. Wada, T., et al., *MIP-1alpha and MCP-1 contribute to crescents and interstitial lesions in human crescentic glomerulonephritis*. *Kidney Int*, 1999. **56**(3): p. 995-1003.
25. Little, A.R., K. Sriram, and J.P. O'Callaghan, *Corticosterone regulates expression of CCL2 in the intact and chemically injured hippocampus*. *Neurosci Lett*, 2006. **399**(1-2): p. 162-6.
26. Ehrchen, J., et al., *Glucocorticoids induce differentiation of a specifically activated, anti-inflammatory subtype of human monocytes*. *Blood*, 2007. **109**(3): p. 1265-1274.
27. Widney, D.P., et al., *The Murine Chemokine CXCL11 (IFN-Inducible T Cell α Chemoattractant) Is an IFN- γ - and Lipopolysaccharide- Inducible Glucocorticoid-Attenuated Response Gene Expressed in Lung and Other Tissues During Endotoxemia*. *The Journal of Immunology*, 2000. **164**(12): p. 6322-6331.
28. Ogawa, S., et al., *Molecular Determinants of Crosstalk between Nuclear Receptors and Toll-like Receptors*. *Cell*, 2005. **122**(5): p. 707-721.
29. Uhlenhaut, N.H., et al., *Insights into Negative Regulation by the Glucocorticoid Receptor from Genome-wide Profiling of Inflammatory Cistromes*. *Molecular Cell*, 2013. **49**(1): p. 158-171.
30. Kuznetsova, T., et al., *Glucocorticoid receptor and nuclear factor kappa-b affect three-dimensional chromatin organization*. *Genome Biology*, 2015. **16**(1): p. 264.
31. Rao, N.A., et al., *Coactivation of GR and NFKB alters the repertoire of their binding sites and target genes*. *Genome Res*, 2011. **21**(9): p. 1404-16.
32. Sacta, M.A., et al., *Gene-specific mechanisms direct glucocorticoid-receptor-driven repression of inflammatory response genes in macrophages*. *Elife*, 2018. **7**.
33. Reichardt, H.M., et al., *Repression of inflammatory responses in the absence of DNA binding by the glucocorticoid receptor*. *The EMBO Journal*, 2001. **20**(24): p. 7168-7173.
34. Mosser, D.M. and J.P. Edwards, *Exploring the full spectrum of macrophage activation*. *Nat Rev Immunol*, 2008. **8**(12): p. 958-69.
35. Martinez, F.O. and S. Gordon, *The M1 and M2 paradigm of macrophage activation: time for reassessment*. *F1000Prime Reports*, 2014. **6**: p. 13.
36. Nguyen-Chi, M., et al., *Identification of polarized macrophage subsets in zebrafish*. *Elife*, 2015. **4**: p. e07288.
37. Saha, S., I.N. Shalova, and S.K. Biswas, *Metabolic regulation of macrophage phenotype and function*. *Immunological Reviews*, 2017. **280**(1): p. 102-111.
38. Dixon, W., et al., *The influence of systemic glucocorticoid therapy upon the risk of non-serious infection in older patients with rheumatoid arthritis: a nested case-control study*. *Annals of the rheumatic diseases*, 2011. **70**(6): p. 956-960.
39. Fardet, L., I. Petersen, and I. Nazareth, *Common Infections in Patients Prescribed Systemic Glucocorticoids in Primary Care: A Population-Based Cohort Study*. *PLoS Med*, 2016. **13**(5): p. e1002024.
40. Caplan, A., et al., *Prevention and management of glucocorticoid-induced side effects: A comprehensive review: A review of glucocorticoid pharmacology and bone health*. *J Am Acad Dermatol*, 2017. **76**(1): p. 1-9.

41. Jick, S.S., et al., *Glucocorticoid use, other associated factors, and the risk of tuberculosis*. *Arthritis Rheum*, 2006. **55**(1): p. 19-26.
42. Kim, H., et al., *Mycobacterium tuberculosis infection in a corticosteroid-treated rheumatic disease patient population*. *Clinical and experimental rheumatology*, 1998. **16**(1): p. 9-13.
43. Singh, S. and K. Tiwari, *Use of corticosteroids in tuberculosis*. *The Journal of Association of Chest Physicians*, 2017. **5**(2): p. 70-75.
44. Wiysonge, C.S., et al., *Interventions for treating tuberculous pericarditis*. *Cochrane Database Syst Rev*, 2017. **9**(9): p. Cd000526.
45. Smego, R.A. and N. Ahmed, *A systematic review of the adjunctive use of systemic corticosteroids for pulmonary tuberculosis*. *Int J Tuberc Lung Dis*, 2003. **7**(3): p. 208-13.
46. Tobin, D.M. and L. Ramakrishnan, *Comparative pathogenesis of Mycobacterium marinum and Mycobacterium tuberculosis*. *Cellular microbiology*, 2008. **10**(5): p. 1027-1039.
47. Meijer, A.H., *Protection and pathology in TB: learning from the zebrafish model*. *Semin Immunopathol*, 2016. **38**(2): p. 261-73.
48. Ramakrishnan, L., *The zebrafish guide to tuberculosis immunity and treatment*. *Cold Spring Harb Symp Quant Biol*, 2013. **78**: p. 179-92.
49. Cronan, M.R. and D.M. Tobin, *Fit for consumption: zebrafish as a model for tuberculosis*. *Disease models & mechanisms*, 2014. **7**(7): p. 777-784.
50. Olivares-Morales, M.J., et al., *Glucocorticoids Impair Phagocytosis and Inflammatory Response Against Crohn's Disease-Associated Adherent-Invasive Escherichia coli*. *Frontiers in Immunology*, 2018. **9**.
51. Jessop, J., B. Vernon-Roberts, and J. Harris, *Effects of gold salts and prednisolone on inflammatory cells. I. Phagocytic activity of macrophages and polymorphs in inflammatory exudates studied by a "skin-window" technique in rheumatoid and control patients*. *Annals of the rheumatic diseases*, 1973. **32**(4): p. 294.
52. Vernon-Roberts, B., J. Jessop, and J. Dore, *Effects of gold salts and prednisolone on inflammatory cells. II. Suppression of inflammation and phagocytosis in the rat*. *Annals of the rheumatic diseases*, 1973. **32**(4): p. 301.
53. McColl, A., et al., *Glucocorticoids induce protein S-dependent phagocytosis of apoptotic neutrophils by human macrophages*. *J Immunol*, 2009. **183**(3): p. 2167-75.
54. Liu, Y., et al., *Glucocorticoids Promote Nonphlogistic Phagocytosis of Apoptotic Leukocytes*. *The Journal of Immunology*, 1999. **162**(6): p. 3639-3646.
55. Zahuczky, G., et al., *Differentiation and Glucocorticoid Regulated Apopto-Phagocytic Gene Expression Patterns in Human Macrophages. Role of Mertk in Enhanced Phagocytosis*. *PLOS ONE*, 2011. **6**(6): p. e21349.
56. McCubbrey, A.L., et al., *Glucocorticoids relieve collectin-driven suppression of apoptotic cell uptake in murine alveolar macrophages through downregulation of SIRPα*. *The Journal of Immunology*, 2012. **189**(1): p. 112-119.
57. Tobin, D.M., et al., *The Ita4h locus modulates susceptibility to mycobacterial infection in zebrafish and humans*. *Cell*, 2010. **140**(5): p. 717-730.
58. Tobin, D.M., et al., *Host genotype-specific therapies can optimize the inflammatory response to mycobacterial infections*. *Cell*, 2012. **148**(3): p. 434-446.
59. Ulbrich, W. and A. Lamprecht, *Targeted drug-delivery approaches by nanoparticulate carriers in the therapy of inflammatory diseases*. *Journal of The Royal Society Interface*, 2010. **7**(suppl_1): p. S55-S66.
60. Bardania, H., S. Tarvirdipour, and F. Dorkoosh, *Liposome-targeted delivery for highly potent drugs*. *Artificial Cells, Nanomedicine, and Biotechnology*, 2017. **45**(8): p. 1478-1489.
61. Metselaar, J.M., et al., *Complete remission of experimental arthritis by joint targeting of glucocorticoids with long - circulating liposomes*. *Arthritis & Rheumatism: Official Journal of the American College of Rheumatology*, 2003. **48**(7): p. 2059-2066.

62. Metselaar, J.v., et al., *Liposomal targeting of glucocorticoids to synovial lining cells strongly increases therapeutic benefit in collagen type II arthritis*. *Annals of the rheumatic diseases*, 2004. **63**(4): p. 348-353.
63. Hofkens, W., et al., *Intravenously delivered glucocorticoid liposomes inhibit osteoclast activity and bone erosion in murine antigen-induced arthritis*. *Journal of controlled release*, 2011. **152**(3): p. 363-369.
64. Hofkens, W., et al., *Liposomal targeting of prednisolone phosphate to synovial lining macrophages during experimental arthritis inhibits M1 activation but does not favor M2 differentiation*. *PloS one*, 2013. **8**(2): p. e54016.
65. Lobatto, M.E., et al., *Multimodal clinical imaging to longitudinally assess a nanomedical anti-inflammatory treatment in experimental atherosclerosis*. *Molecular pharmaceutics*, 2010. **7**(6): p. 2020-2029.
66. Schmidt, J., et al., *Drug targeting by long - circulating liposomal glucocorticosteroids increases therapeutic efficacy in a model of multiple sclerosis*. *Brain*, 2003. **126**(8): p. 1895-1904.
67. Schiffelers, R.M., et al., *Liposome-encapsulated prednisolone phosphate inhibits growth of established tumors in mice*. *Neoplasia*, 2005. **7**(2): p. 118-127.
68. van den Hoven, J.M., et al., *Optimizing the therapeutic index of liposomal glucocorticoids in experimental arthritis*. *International journal of pharmaceutics*, 2011. **416**(2): p. 471-477.
69. Hofkens, W., et al., *Safety of glucocorticoids can be improved by lower yet still effective dosages of liposomal steroid formulations in murine antigen-induced arthritis: comparison of prednisolone with budesonide*. *International journal of pharmaceutics*, 2011. **416**(2): p. 493-498.
70. Smits, E.A.W., et al., *The availability of drug by liposomal drug delivery : Individual kinetics and tissue distribution of encapsulated and released drug in mice after administration of PEGylated liposomal prednisolone phosphate*. *Investigational new drugs*, 2019. **37**(5): p. 890-901.
71. van der Valk, F.M., et al., *Prednisolone-containing liposomes accumulate in human atherosclerotic macrophages upon intravenous administration*. *Nanomedicine: nanotechnology, biology and medicine*, 2015. **11**(5): p. 1039-1046.

Samenvatting

De zebravis als diermodel om de effecten van glucocorticoïden op het immuunsysteem te bestuderen

Glucocorticoïden reguleren, door activering van de glucocorticoïd-receptor (GR), een groot aantal verschillende systemen in ons lichaam, zoals het zenuwstelsel, ons hart- en bloedvatstelsel, en onze stofwisselings-, voortplantings-, en immuunsystemen. Vanwege de welbekende remmende werking op het immuunsysteem worden glucocorticoïden veelvuldig voorgeschreven als ontstekingsremmende geneesmiddelen. Echter, dit gebruik van glucocorticoïden als anti-inflammatoire geneesmiddelen wordt ernstig beperkt doordat ze zware bijwerkingen hebben en er vaak resistentie optreedt. Daarom is het nog steeds noodzakelijk dat er onderzoek wordt gedaan naar de moleculaire en cellulaire mechanismen die ten grondslag liggen aan de effecten van glucocorticoïden. Deze mechanismen blijken bijzonder ingewikkeld te zijn, omdat de effecten van glucocorticoïden afhankelijk zijn van het celtype en de context waarin de cel zich bevindt, en omdat de effecten van glucocorticoïden op de transcriptie van pro-inflammatoire genen niet uitsluitend inhiberend zijn.

De zebravis wordt steeds vaker gebruikt als *in vivo* modelsysteem om het immuunsysteem te bestuderen, vooral de inflammatoire respons, ten behoeve van onderzoek dat gericht is op de ontwikkeling van nieuwe aanknopingspunten voor geneesmiddelen (drug targets) en voor het grootschalig testen van mogelijke nieuwe geneesmiddelen. Het immuunsysteem van de zebravis lijkt zeer op het onze en dit diermodel heeft verschillende voordelen, zoals het gemak waarmee de embryo's genetisch kunnen worden gemanipuleerd en onder de microscoop worden bekeken, en het relatief goedkope onderhoud. In **Hoofdstuk 2** van dit proefschrift wordt een overzicht gegeven van hoe de zebravis wordt gebruikt als diermodel voor ontstekingsziektes. Verschillende modellen worden beschreven en ook wordt geïllustreerd hoe deze modellen worden gebruikt voor onderzoek naar de mechanismen die de inflammatoire respons veroorzaken en voor het testen van mogelijke nieuwe anti-inflammatoire geneesmiddelen, in het bijzonder glucocorticoïden. Eerder onderzoek heeft aangetoond dat de structuur en functie van de zebravis-Gr heel erg lijkt op die van de mens en dat ook de regulatie van de secretie van glucocorticoïden zeer goed vergelijkbaar is met die van de mens. Dit maakt de zebravis een zeer geschikt diermodel om de complexe effecten van glucocorticoïden op het immuunsysteem te bestuderen. In dit proefschrift hebben we de zebravis gebruikt om de moleculaire en cellulaire mechanismen van de werking van glucocorticoïden op het immuunsysteem te bestuderen

en om een model te ontwikkelen om *in vivo* zowel de anti-inflammatoire werking als de bijwerkingen te bestuderen van nieuwe glucocorticoïd-formuleringen. Hiervoor hebben we onderzocht welke effecten glucocorticoïden hebben op de migratie en differentiatie van leukocyten tijdens een inflammatoire respons (**Hoofdstuk 3**), hoe glucocorticoïden de immuunrespons tegen een mycobacteriële infectie beïnvloeden (**Hoofdstuk 4**), en hoe glucocorticoïden specifiek naar ontstoken weefsel kunnen worden vervoerd door middel van liposomen (**Hoofdstuk 5**).

Glucocorticoïden inhiberen de differentiatie van macrofagen naar een pro-inflammatoir fenotype door transcriptie te reguleren

In **Hoofdstuk 3** is onderzoek beschreven waarin we de staartvin van zebravislarven hebben geamputeerd om een ontstekingsreactie op te wekken. In dit ‘staartvinamputatiemodel’ migreren twee typen leukocyten, macrofagen en neutrofielen, naar het weefsel dat is beschadigd door de amputatie. Behandeling met het glucocorticoïd beclomethasone remt de migratie van de neutrofielen naar deze wond. Echter, zoals eerder waargenomen was in studies van onze groep, de migratie van macrofagen wordt niet verminderd door dit glucocorticoïd. Verdere experimenten toonden aan dat het verschil in het effect van glucocorticoïden op de migratie van neutrofielen en macrofagen waarschijnlijk voortkomt uit het feit dat glucocorticoïden wel de expressie verlagen van genen die coderen voor chemokines die betrokken zijn bij het laten migreren van neutrofielen naar de wond (zoals I18 en Cxcl18b), maar niet de expressie beïnvloeden van chemokines die een rol spelen bij de migratie van macrofagen (zoals Ccl2 en Cxcl11aa).

Om te zien of macrofagen werkelijk resistentie tegen glucocorticoïden vertonen in ons model, hebben we een ‘RNAsequencing’ analyse uitgevoerd op macrofagen die we uit de zebravislarven hadden geïsoleerd. De resultaten van dit experiment lieten zien dat behandeling met glucocorticoïden vrijwel alle veranderingen in transcriptie als gevolg van de amputatie in deze cellen blokkeert, waaronder de verhoogde transcriptie van veel pro-inflammatoire genen. Door gebruik te maken van een fluorescente reporter-vislijn konden we aantonen dat het aantal macrofagen waarin het pro-inflammatoire *tnf* gen tot expressie kwam, was verminderd na behandeling met glucocorticoïden. Tenslotte zagen we dat glucocorticoïden ook het percentage verminderde van macrofagen die een ronde morfologie vertonen die kenmerkend is voor deze cellen tijdens een inflammatoire respons. Uit deze resultaten concluderen we dat in ons model glucocorticoïden weliswaar de migratie van macrofagen niet remmen, maar dat ze wel de differentiatie van deze cellen naar een pro-inflammatoir fenotype inhiberen, door vrijwel alle transcriptionele veranderingen in deze cellen tijdens een inflammatoire respons te blokkeren.

Glucocorticoïden verergeren een mycobacteriële infectie door de fagocytose-activiteit van macrofagen te verminderen

Om de functionele consequenties van de waargenomen effecten van glucocorticoïden op immuuncellen te bestuderen, hebben we in **Hoofdstuk 4** onderzoek verricht naar hoe glucocorticoïden een infectie beïnvloeden met *Mycobacterium marinum* (*Mm*), een bacteriesoort die verwant is aan *Mycobacterium tuberculosis* (*Mtb*), de bacterie die verantwoordelijk is voor tuberculose bij mensen. *Mm* veroorzaakt een tuberculose-achtige infectie in zebra vis en zebra vislarven worden daarom veel gebruikt om de interacties tussen gastheer en pathogeen bij tuberculose te bestuderen en om onderzoek te doen dat gericht is op het ontwikkelen van mogelijke nieuwe therapeutische strategieën. Een verhoogde kans op infecties is een belangrijke bijwerking van behandeling met glucocorticoïden, als gevolg van het onderdrukte immuunsysteem, en het is bekend dat glucocorticoïden de kans op het krijgen van tuberculose verhogen.

Wij vonden dat het glucocorticoïd beclomethasone het infectieniveau van *Mm* in zebra vislarven verhoogde. Deze verhoogde infectiegraad ging samen met een verminderde fagocytose-activiteit van de macrofagen, als gevolg van een verminderde transcriptie van fagocytose-gerelateerde genen in deze cellen. Ook toen we een andere intracellulaire bacterie gebruikten voor de infectie, *Salmonella* Typhimurium, zagen we een verminderde fagocytose door macrofagen na behandeling met glucocorticoïden. Ten slotte resulteerde de verminderde fagocytose van *Mm* in minder celdood van de macrofagen en in een grotere extracellulaire bacteriepopulatie. De conclusie van dit werk is dat glucocorticoïden bacteriële infecties kunnen verergeren door de fagocytose van de bacteriën door macrofagen te inhiberen. Dit doen ze door te interfereren met de transcriptie van genen die coderen voor eiwitten die bij fagocytose zijn betrokken. Deze resultaten zouden een mechanistische verklaring kunnen vormen voor het feit dat behandeling met glucocorticoïden de vatbaarheid voor tuberculose verhoogt.

Liposomale formulering van glucocorticoïden versterkt hun anti-inflammatoire effect en vermindert de bijwerkingen

Hoofdstuk 5 beschrijft experimenten waarin we hebben bestudeerd hoe we glucocorticoïden specifiek in het ontstoken weefsel terecht kunnen laten komen. In onze studie hebben we het glucocorticoïd prednisolone phosphate (PLP) in liposomen verpakt en bekeken hoe het dan wordt getransporteerd in zebra vislarven waarin met behulp van een laser een verwonding is aangebracht. Daarnaast hebben we zowel de anti-inflammatoire werking van PLP gemeten als de effecten op het herstel van weefsel na een amputatie en de activering van een glucocorticoïd-gevoelig reporter-gen (als indicator voor

mogelijke bijwerkingen). We hebben twee typen liposomen getest: een gePEGyleerd liposoom, dat relatief ongevoelig is voor opname door fagocyterende cellen, en een liposoom dat juist heel gevoelig is voor fagocytose door macrofagen.

Beide soorten liposomen vonden we in verhoogde concentratie aanwezig in het gebied waar de wond zich bevond, enkele uren nadat we die wond met de laser hadden aangebracht. Onze resultaten lieten verder zien dat beide soorten liposomen het effect van PLP op de migratie van neutrofielen naar de wond versterken, waarbij het soort liposoom dat gevoelig is voor fagocytose door macrofagen zelfs iets effectiever was dan de gePEGyleerde liposomen. PLP remt normaalgesproken het herstel van weefsel na amputatie van de staartvin, maar beide liposomale formuleringen verminderden dit effect van PLP. Tenslotte werd de activering van het glucocorticoïd-gevoelige reporter-gen door PLP alleen verminderd door de gePEGyleerde liposomale formulering. Deze resultaten laten zien dat de zebavis een zeer geschikt model is om een groot aantal verschillende liposomale formuleringen van glucocorticoïden te testen, omdat niet alleen de (dynamiek van de) verdeling in het lichaam kan worden vastgesteld, maar ook de therapeutische anti-inflammatoire effecten en de manier waarop processen als herstel van weefsel na een verwonding worden beïnvloed, die exemplarisch zijn voor de bijwerkingen van glucocorticoïden. Als 'proof-of-principle' hebben we laten zien dat zowel een gePEGyleerde liposomale formulering als een formulering die gevoelig is voor fagocytose door macrofagen, de therapeutische ratio van PLP verhoogt.

Conclusies

Een brede kennis omtrent de effecten van glucocorticoïden op het immuunsysteem is noodzakelijk om anti-inflammatoire behandelingen met glucocorticoïden te kunnen verbeteren. Ons werk laat een algemeen inhiberend effect zien van glucocorticoïden op het pro-inflammatoire fenotype van macrofagen en op de fagocytose-activiteit van deze cellen. Deze resultaten laten zien dat macrofagen een belangrijk doelwit zijn van anti-inflammatoire glucocorticoïden (**Hoofdstuk 3 en 4**). In overeenstemming met dit idee werd de therapeutische ratio van glucocorticoïden verhoogd, wanneer we ze specifiek lieten opnemen door macrofagen door ze in te pakken in bepaalde liposomen. Daarbij dient wel te worden vermeld dat inpakken in liposomen die niet gevoelig waren voor fagocytose een vergelijkbaar effect had (**Hoofdstuk 5**). Het werk dat beschreven is in dit proefschrift heeft ons begrip vergroot van hoe glucocorticoïden de immunrespons beïnvloeden tijdens een inflammatoire respons, waarbij gebruik gemaakt werd van de zebavis als diermodel. Deze kennis en de ontwikkelde modellen kunnen een bijdrage leveren aan het preklinische onderzoek dat gericht is op de ontwikkeling van nieuwe anti-inflammatoire geneesmiddelen.

Curriculum vitae

Yufei Xie was born on November 17th 1990 in Pingxiang, Jiangxi, China. After graduating from Pingxiang High School in 2009, she started a Bachelor's program in Biology at the Faculty of Life Science of Beijing Normal University (BNU). In 2013, she obtained her BSc degree and started to pursue a Master's degree at the same faculty of BNU. During this period, she performed a research project on the immunological and anti-tumor effects of monomeric compounds extracted from Chinese medicinal herbs. After completion of her MSc degree in 2016, Yufei was awarded a scholarship from the China Scholarship Council (CSC) to carry out a PhD research project at the Institute of Biology of Leiden University under the supervision of Dr. Marcel J.M. Schaaf and Prof. Dr. Annemarie H. Meijer. In this project, she used zebrafish as a model for inflammation to investigate the effect of glucocorticoids on the innate immune system, resulting in the work presented in this thesis.

List of Publications

He, M., Huang, X., Liu, S., Guo, C., Xie, Y., Meijer, A.H., & Wang, M. (2018). The difference between white and red ginseng: variations in ginsenosides and immunomodulation. *Planta Medica*, 84(12/13), 845-854.

Xie, Y., Tolmeijer, S., Oskam, J.M., Tonkens, T., Meijer, A.H., & Schaaf, M.J.M. (2019). Glucocorticoids inhibit macrophage differentiation towards a pro-inflammatory phenotype upon wounding without affecting their migration. *Disease models & mechanisms*, 12(5), dmm037887.

He, M., Halima, M., Xie, Y., Schaaf, M.J.M., Meijer, A.H., & Wang, M. (2020). Ginsenoside Rg1 acts as a selective glucocorticoid receptor agonist with anti-inflammatory action without affecting tissue regeneration in zebrafish larvae. *Cells*, 9(5), 1107.

Xie, Y., Meijer, A.H. & Schaaf, M.J.M. (2020). Glucocorticoid treatment exacerbates mycobacterial infection by reducing the phagocytic capacity of macrophages. *bioRxiv* doi: 10.1101/2020.06.19.161653.

Xie, Y., Meijer, A.H. & Schaaf, M.J.M. Modeling inflammation in zebrafish for the development of anti-inflammatory drugs. *Submitted*.

Xie, Y., Papadopoulou, P., D'Engelbronner, J.C., De Wit, B., Van Hage, P., Campbell, F., Meijer, A.H. & Schaaf, M.J.M. Liposome encapsulation of prednisolone phosphate improves its therapeutic ratio in a zebrafish model for inflammation. *Manuscript in preparation*.